IMPACT OF LAND COVER, LAND USE AND CLIMATE CHANGE ON THE HYDROLOGICAL REGIMES OF THE MARA RIVER BASIN

BY

ISAAC ONGONG'A AYUYO

C80/51921/2017

A thesis submitted in fulfillment of the requirements for the degree of Doctor of Philosophy (PhD) in Environmental Planning and Management in the Department of Earth and Climate Sciences of the University of Nairobi.

December 2021

DECLARATION

This thesis is my original work and has not been presented for examination in any other university.

02/12/2021

Isaac Ongong'a Ayuyo Date

This thesis has been submitted for examination with our approval as University Supervisors.

2nd December 2021

Date

George Okoye Krhoda

Department of Earth and Climate Sciences

University of Nairobi.

3/12/2021

Dr. Stellah Mukhovi Date

Department of Earth and Climate Sciences

University of Nairobi.

DEDICATION

To God without whom I could not have done this piece of work and to my late parents- Jabes Ayuyo Wandoi and Phoebe Ayuyo who inculcated in me the seed of academic excellence but whom, by the will of God did not live to witness this occasion.

ACKNOWLEDGEMENT

The success of this PhD work required the contributions of various individuals and institutions. My sincere acknowledgement therefore goes to those individuals and institutions whose contributions propelled this study to successful completion. My particular gratitude goes to the University of Nairobi for sponsorship through fee waiver that enabled me undertake the study.

I owe much to my Supervisors Prof. George O. Krhoda and Dr. Stella M. Mukhovi of the Department of Earth and Climate Sciences, whose invaluable guidance, suggestions, criticisms and encouragements during the course of this study and thesis writing brought me to successful end. My heartfelt appreciation goes to the Department of Earth and Climate Sciences for all the support I received including the use of the departmental library and GIS laboratory. Special thanks go to Dr. Boniface Wambua for the commendable support he accorded me in my academic work while serving as Chairman in the former Department of Geography and Environmental Studies.

Many thanks go to the following organizations and Institutions: The Regional Centre for Mapping of Resources for Development (RCMRD), the Kenya Meteorological Service (KMS), the Water Resources Authority (WRA), the Tanzania Meteorological Agency, the Tanzania Water Resources Management, and the Management of the Global Weather Databases, Kenya National Bureau of Statistics (KNBS) and Tanzania National Bureau of Statistics (TNBS). Others are Survey of Kenya and, Food and Agriculture Organization for their invaluable data without which, this study could not have been a success. My unreserved appreciation goes to National Commission for Science, Technology and Innovation (NACOSTI) for furnishing me with a research permit. Equally, I wish to thank various libraries and internet sources including the University of Nairobi Library services for their books, journals and articles that I used in the process of doing my work.

I wish to make special mention to these individuals: Dr. Isaiah Ang'iro Nyandega and Prof. Alfred Owuor Opere of the Department of Earth and Climate Sciences for their exemplary guidance especially in the study specificity and methodology as well as

introducing and guiding me through the use of SWAT model. My sincere appreciation goes to Mr. Clifford Otieno Okembo of ESRI-Eastern Africa for his assistance in the laborious Remote Sensing and GIS work and as my very able Field Assistant. The same hearty thanks go to Mr. Gibson Tott of Eldoret for his rigorous analyses on the SPSS platform.

Many thanks go to Messrs. James Wanjohi and Laurence Nganga of Regional Centre for Mapping of Resources for Development (RCMRD), for designing the necessary scripts for extraction of climate data from satellite sources and mapping the land cover types respectively. Messrs. Oliver Onyango and Clifford Omondi Okech for running the SWAT hydrologic Model and Nicholas Mwakavi for Cartographic work in the Departmental GIS Laboratory. I acknowledge every person who contributed in one way or another towards this noble course and yet, not mentioned individually due to lack of space. Finally yet importantly, I wish to appreciate most sincerely, my dear wife Christine Khabele, children and the entire family for their moral support, prayers and encouragement that carried me through to this successful end. Above all, I give thanks to God Almighty, for His abundant grace and love that guided me throughout the study period.

ABSTRACT

The Mara river basin is a serene sub-catchment of Lake Victoria basin and a part of the upper catchments of the Nile Basin. Importantly, it is a lifeline to the internationally renowned Mara - Serengeti ecosystem and a rich mix of physiography, indigenous cultures and land use practices. The need for more land for the rapidly growing population in the basin has resulted in the excision of large parts of the forests that were formerly preserved, and encroachment to other fragile ecosystems, which has affected the flow volumes of Mara River. Little information exists on how variation in the human activities owing to climate change is affecting the hydrology of the basin. Lack of such information hampers the ability of the various resources managers to formulate a comprehensive ecosystems management strategy that would provide for sustainable livelihoods. This study focuses on the nature, extent and rate of change in land cover, land use and climatic scenarios and their impacts on hydrological regimes in Mara River Basin. Land cover dynamics were analyzed from dry weather Landsat TM and ETM+ images for 1984, 1995, 2003, 2011 and 2016 under ENVI 5.0 and ArcGIS 10.4 software environment. Thematic maps comprising eight land cover/use types were created from the imageries using unsupervised land cover classification technique and FAO land use classes. Time series analysis of the thematic maps was done using post classification visual and area comparisons and overlay operations with significance of change tested at α=0.05 using Chi-Square test statistic. Trends in the simulated long-term daily records of maximum and minimum air temperature, rainfall and river discharge from global weather geoportal were analyzed by use of Mann-Kendall test statistic and Student t statistic, testing level of significance at α =0.05. The study analyzed the past land cover, land use and climate scenarios and modelled future variations with respect to the Mara hydrological regimes (flow volumes). SWAT hydrological model was to simulate the land cover/use and climate scenarios and the river discharge. The simulated data from global weather databases used in the simulation exercise because of lack of complete and consistent hydro-climatic data in the basin. The simulated and observed datasets were however, calibrated and validated for reliability and suitability of use and gave a strong correlation, which meant that, the simulated datasets were good enough for use in the study. The SWAT output data analyzed through the Multiple Regression

and Correlation model. The analysis of land cover scenarios revealed significant changes in which, forestland, shrub land and grassland are all decreasing in spatial coverage while cropland and built-up areas are spatially increasing at accelerated rates with wetlands, water bodies and bare land not having definite trends. Thus, between 1984 and 2016, forestland, shrub land and grassland reduced by 1.37%, 6.61% and 2.99% respectively while cropland and built-up area increased by 10.22% and 0.06% respectively. The analyses of historical data revealed that the climate of the area has progressively become warmer and drier from the 1980s with air temperature indicating gradual upward trends while rainfall and river flow volumes indicate a decline in their trends. When tested at $\alpha = 0.05$, however, neither the mean monthly nor annual rainfall values recorded significant change. The rains in the Mara are bimodal with the main rainy season experienced between March and May while the second rains come from September to November. The study detected a shifting trend in rainfall in the basin with the usually wet months (MAM and SON) becoming relatively dry while the dry months (DJF and JJA) are becoming relatively wet. On the other hand, the mean monthly maximum and minimum air temperature recorded significant increments in some months while the mean annual values had none at $\alpha = 0.05$. The trends in land cover, land use and climate expected to continue beyond 2030 with serious impact on the Mara water resources and therefore livelihoods and environmental services. Conservation of this former pristine basin is a critical matter that addressed by both governments of Kenya and Tanzania respectively. This study provides useful methods and information that can apply broadly to inform medium and long-term planning of water resources management not only in the Mara River Basin but also in other basins in and outside Kenya. The results should be incorporated in the mainstream economic strategies and implementation of the National Water Master Plan, 2030.

TABLE OF CONTENTS

LIST OF FIGURES

LIST OF PLATES

LIST OF TABLES

ABBREVIATIONS AND ACRONYMS

ASALS	Arid and Semi-Arid Lands
DDP	District Development Plan
DRSRS	Department of Resource Surveys and Remote Sensing
EAC	East African Community
EMCA	Environmental Management and Coordination Act
ETM	Enhanced Thematic Mapper
FAO	Food and Agriculture Organization
GIS	Geographic Information Systems
GPS	Global Positioning Systems
IPCC	Intergovernmental Panel on Climate Change
KFWG	Kenya Forest Working Group
KIFCON	Kenya Indigenous Forest Conservation Programme
KWS	Kenya Wildlife Service
LCLU	Land Cover and Land Use
MEMR	Ministry of Environment and Mineral Resources
MFRS	Mau Forest Rehabilitation Secretariat
NEMA	National Environmental Management Authority
RCMRD	Regional Centre Mapping of Resources for Development
RS	Remote Sensing
SOK	Survey of Kenya

SPSS	Statistical Package for Social Sciences
SWAT	Soil and Water Assessment Tool
TM	Thematic Mapper
UN	United Nations
UNEP	United Nations Environment Programme
UNFCCC	United Nations Framework Convention on Climate Change
UTM	United Transverse Mercator
WRI	World Resource Institute
WRA	Water Resources Authority
WWF	World Wide Fund for Nature

CHAPTER ONE: INTRODUCTION

1.1 Background

Land cover, land use and climate change are the main causes of changes in the global environment and global ecology with direct contribution to changes in both local environment and forest ecosystem services (Schroter *et al.,* 2005; Hansen *et al.,* 2001). Land use is expressed by the human actions practiced in a physical environment for socio-economic wellbeing (FAO, 2010) and therefore is dynamic and has changed over time with increase in population resulting in variations of the elements of the hydrological cycle (Tracy and Scott, 2013). Changes in land use that lead to reduction in forest cover and general environmental quality such as urbanization, rural settlement, infrastructural development and farming have negative impact on the rainfall, temperature and humidity and therefore may modify the climate of a given area (UNFCCC, 2011; IPCC, 2007). This is because loss in forest cover even though it tends to increase storms, surface runoff and soil erosion; it also minimizes evapo-transpiration, infiltration into the ground water and base stream flow (Mango *et al.,* 2011).

Multiple human-induced global changes in land cover (especially forest), land use, climate and in the natural components of the environment are complex and are interacting in the context of a multi-system including the forest ecosystem, land system and climate system (Zhuo *et al.,* 2017). These changes are modifying the atmospheric composition as well as the earth's landscape with complex impacts on the forest ecosystem and therefore implications on surface water yields (Dai *et al*., 2016; Foley *et al*., 2005; Karl and Trenberth, 2003). For example, agricultural activities contribute to climate change by releasing greenhouse gases (GHGs) such as carbon dioxide and methane into the atmosphere while deforestation also reduces the forests ability to sequester carbon. IPCC, (2001) had estimated that agriculture, forestry and other land use changes would contribute between 20 and 25% of the annual global emissions by 2010. Climate change impacts land use practices as land users adapt to the changing climatic conditions such as planting early maturing seeds, introducing new crop varieties and changing from one land use practice to another. Understanding how the two scenarios interact with the other systems in the natural environment is therefore

critical for sustainable natural resources management and utilization. Little information exists on the inter-linkage between land cover/land use change and climate change in the Mara catchment basin wise, with implications on the Mara River flow volumes.
Kenya in general and the Mara river basin particularly, is experiencing general decrease in rainfall with increase in air temperature, droughts and floods (GoK, 2010). The Mara River basin has also witnessed remarkable increase in both urban growth and rural settlements as well as mechanized and irrigation agriculture which is interfering with the pastures, wildlife migratory routes and water supply within the basin (Mati *et al.,* 2005). The population is largely of small-scale farmers and pastoralists with 23% in Kenya and 20% in Tanzania (WREM International Inc., 2008). The need for economic development to improve the peoples' living standards is likely to increase the socio-economic activities in the basin with implications on the Mara water resources (Mati *et al.,* 2005). The Mara River basin is found within the Mau forest complex and Serengeti savanna, which offer many economic activities and environmental services that therefore require equitable planning for sustainable development.

Determining the relationship between land cover, land use and climate change with flow regimes of the Mara River is crucial in sustainable management of the water resources in the Upper Catchment of the Nile River system. This is very important because Mara is a water sensitive basin with all its surface water supply coming from the Mara River except during the rainy seasons. Water scarcity not- withstanding, however, the basin supports various economic sectors and systems that highly depend on the availability, distribution, quantity and supply of surface water. They include settlements, industries, agricultural activities, sanitation, infrastructure, transportation and service sector as well as world-renowned conservation areas. River volume flows in the basin are a factor of climate variability and human interventions. Changes in hydrological regimes are likely to impact on climate over a surface area and variability in the climate condition of a surface area directly affects the hydrologic regime as reflected in the availability of surface water resource and its distribution.

The competition between economic activities and environmental services has resulted in degradation such as deforestation, soil erosion and high sediment loads (Ayuyo, 2012; Mango *et al.,* 2011). These challenges have additionally caused changes in land use practices with deforestation in the upper catchment to give way to crop farming and

livestock rearing. The pastoral areas have also witnessed mechanized agriculture, which have also affected the wildlife migration routes (NEMA, 2004; Melesse *et al.*, 2008). The environmental degradation due to unplanned land use practices in the Mara river basin is threatening the entire ecosystem to extinction. Presently, the Mara ecosystem lacks a comprehensive ecosystems management strategy that would provide for sustainable livelihoods despite the linkage that exists between climate change and sustainable development (IPCC, 2007; NEMA, 2004). Although the relationships in the land cover, land use and climate systems are in the public domain, little information exists on how the trio collectively and/or individually impacts the hydrological regimes, especially of the Mara River basin. This is the main gap in knowledge the study set out to investigate. It has since, established the inter-linkages, collective and individual contributions to the variations in the Mara hydrological regimes, both now and in the future.

Understanding the linkages between land cover, land use and climate changes in relation to Mara River flow reveals the nature, extent and rate of change in land cover and land use types as well as the variations in rainfall and temperature that have occurred in the Mara River basin over time which is currently less known. This study therefore provides important information that can assist in the formulation of comprehensive ecosystems management policies and regulations for sustainable resources utilization in the basin and beyond. The worked-out climate scenarios and the projected potential implications on the Mara water balance are critical for ensuring peace within the Nile basin.

1.2 Research Questions

Specific questions addressed were:

1. What are the nature, extent and rate of change in land cover and land use types that have occurred in the Mara river basin between 1983 and 2014?
2. Have there been significant spatio-temporal variations in rainfall, temperature and river flows in the Mara river basin between 1983 and 2014?
3. How well does the simulated river flow relate to changes in land cover/land use and climate in the Mara River basin?

4. Are changes in land cover/land use and climate good measures of river flow conditions in the Mara Basin?

1.3 Objectives of the Study

The overall objective was to determine the impact of land cover, land use and climate change on the hydrological regimes of the transboundary Mara River basin. The Mara River basin flows in Kenya and Tanzania and it forms part of River Nile headwaters.

The specific objectives were:

1. To determine the nature, extent and rate of change in land cover and land use types in the Mara river basin in the period between 1983 and 2014.
2. To determine the spatio-temporal variations in rainfall, temperature and river flows in the Mara Basin in the period between 1983 and 2014.
3. To establish the relationship between river flow volumes and changes in land cover, land use and climate in the Mara Basin in the period between 1983 and 2014.
4. To generate river flow sensitivity indices under different land cover, land use and climate scenarios in the Mara Basin in the period between 1983 and 2014.

1.4 Research Hypotheses

The general study hypothesis is that changes in land use do not affect climate patterns in the Mara basin and therefore have no effect on the Mara river flow regimes.

The specific null hypotheses for the study were:

H_0: Land use practices have not significantly changed over the study period in the Mara River Basin in the period between 1983 and 2014.

H_1: Alternative

H_0: There have been no significant spatio-temporal variations in rainfall, temperature and river flows in the Mara river basin in the period between 1983 and 2014.

H_1: Alternative

H_0: There is no significant relationship between the simulated river flows and changes in land cover/ use and climate in the Mara River Basin, between 1983 and 2014.

H_1: Alternative

H_0: Changes in land cover/land use and climate are not a good measure of river flow conditions in the Mara River Basin in the period between 1983 and 2014.

1.5 Assumptions

The study assumptions were:

Remote Sensing data gives accurate representation on land cover and land use conditions in the Mara River Basin over the study duration.

The observed and simulated hydro-meteorological data available have similar statistical characteristics and influence on water yields in the Mara River Basin.

The modified land cover/land use classification is the best fit of the SWAT land cover/land use classification and the same is true with the modified soil classification.

1.6 Justification of the Study

A comprehensive ecosystems management strategy to guard against unsustainable utilization of Mara river basin resources is required. Understanding the nature, extent and rate of change in land cover and land use types such as forests to grasslands, forests to farmlands, grassland to farmland or grassland to urban settlement in the Mara River basin is critical in formulating sustainable ecosystems management strategy. This is because, changes in land cover/ land use is a major driving force in habitat modification with long lasting consequences on livelihoods, biodiversity and river flow volumes (Ayuyo, 2012). Since human activities in the Mara have interfered with protected forests and other fragile ecosystems (Mango *et al.*, 2011; Dessu and Melesse, 2012; Oruma *et al.*, 2017), a clear understanding of their negative impacts on various economic sectors including the biodiversity is required. The plan to rehabilitate the Mau forest complex will benefit from the present study since it provides such kind of information.

Mara River basin is an important conservation area situated within the fastest growing Counties of Narok and Bomet as well as a growing eco-region of northern Tanzania (WREM International, 2008). With the current population growth rate of about 2.7% in

the Kenyan and Tanzanian sides (TNBS, 2012; KNBS, 2009; WREM International, 2008) that adds directly to both rural and urban population numbers and expansion, more resources are needed to improve quality of human life and to achieve economic development. Human activities aimed at improving the socio-economic status of this populace are likely to result in land use types with economic opportunities for the local population but at the expense of the ecological functions and environmental quality.

Geographical Information Systems (GIS), The Soil and Water Assessment Tool (SWAT) Model and statistical analysis tools were used because they provide opportunities for developing integrated databases that give clear information for informed decision-making. This study fills the gap in knowledge that is required in combating climate change, creating jobs and wealth as well as ensuring water and food security in the region. The study is invaluable for developing a comprehensive ecosystems management strategy that would promote sustainability and environmental equity within the Mara River basin and in the surrounding areas.

1.7 Scope and Limitations of the Study

The current study emphasizes river basin characteristics in terms of topography, soils, climate, ground cover and human practices as key factors in Mara River basin's hydrological regimes. The study covers the period between 1983 and 2014, a duration that is within the climatologists recommended minimum period of 30 years for investigating climate change implications on a surface area including water resources. The study projects the future land cover/use along with climatic projections for forty-seven years (up to 2030) in order to understand the present and future conditions of the Mara water resources and its implications on achieving Kenya Vision 2030.

The Sustainable management of the river systems and their waters requires an understanding of the system's inter-linkages and responses to anthropogenic and natural conditions, specifically with regard to river flow volumes, water quality and availability in time and space. To accomplish the above tasks, the study used long-term daily records of the observed and simulated hydro-meteorological datasets and river flow records for the period between 1983 and 2014. Simulated records were used in SWAT model simulation to solve the problem of missing hydro-meteorological records

while the observed records from selected stations were used for calibration and validation of the simulated datasets.

The land cover and land use classification was based on dry seasons (less than 20% cloud cover) temporal Landsat imageries for 1984, 1995, 2003, 2011 and 2016 procured through RCMRD from the European Space Agency's geoportal. FAO land cover/land use and Soils for Eastern African were used to have the land cover/use types and soils in the Mara conform to those of SWAT for simulation purposes. Digital Elevation Model from the USA Geological Survey Global Visualization portal was used for delineating the study area and generating flow direction and accumulation.

The study was limited in a number of ways: As a transboundary resource; there were administrative challenges in data acquisition due to different laws, policies and rules; the basin had few and unevenly distributed weather stations with none falling under the WMO's Global Telecommunication System (GTS) stations network. In fact, only 16 out of 36 stations were operational and represented a density network of one gauge per approximately 840 km^2. This was far much below the WMO's recommendation of one gauge per approximately 100 km^2 (WMO, 2009). The large size and remoteness of the basin added to the difficulties in acquiring field data in terms of time and money required; most of the weather and river gauging stations were either faulty or vandalized and that rendered them useless while others were swept away by floods. According to information gathered from the Meteorological Officers found at some of the facilities, repair work or replacement of damaged gauges took time and this resulted in long periods without data collected as was observed in the study area.

Lack of funds and poor management of water resources including the often-than-not, lack of trained gauge readers was mentioned as some of the reasons for incomplete and or inconsistent record keeping in some of the weather and river gauging stations. Global weather data was used in the simulation processes to resolve the transboundary problems in data acquisition, the fewness and uneven distribution of the stations in the basin.

1.8 Operational Definitions

Aquifer: Refers to a geological formation that contains adequate saturated permeable rock, rock fractures or material to produce notable amount of water to boreholes or springs.

Base flow: It is a portion of a river or stream flow derived from water discharged from the ground. It's therefore part of the stream flow derived from the natural groundwater discharge into a channel like lake or spring.

Calibration: This implies assessing and modifying a measurement tool for preciseness and reliability thus obliterate or lessen partiality in the readings recorded for a number of continual values.

Change Detection: This implies, observing an object or event at different times and establishing the difference in its state (Singh, 1989).

Climate: The average weather conditions or numerical representation with regard to mean and variability of relevant quantities over a long period, stretching from months to thousands or millions of years (IPCC, 2007).

Climate Change: Natural and/or human induced changes in climatic conditions over time (IPCC, 2007).

Climate Change Scenario: The terrestrial variations in climate state which include rainfall or temperature over a stipulated period or study years compared with a later period (IPCC, 2007).

Conversion: The process of changing or replacing a land cover type by another one (Turner *et al*., 1995).

Deforestation: Replacement of forest by any other land cover type. Deforestation may come because of converting forestland into farmland or settlement, among many other uses (UNEP, 2005).

Flow Regimes: Are a range of stream flows with similar bed forms, flow resistance, and means of transporting sediment.

Gauging Station: It's a designated site used by hydrologists and environmental scientists in monitoring streams, lakes, rivers, canals or reservoirs.

Geographic Information Systems: Computerized database systems used for capturing, storing, retrieving, and analyzing spatial data to generate spatial information

Geo-referencing: A process of assigning the map coordinates to the imageries to enable the details on the images to have same ground coordinates as the map.

High Flow: The generally high river discharge during rainy seasons

Hydrological Regime: The alternation in conditions and features of a body of water depending on seasons thus habitually replicated in time and space.

Land Cover: Refers to the tangible material on the ground, which may consist of water bodies, trees, grass, built-up areas or bare ground.

Land Cover Change: Refers to alteration or total change in ground material or cover because of man's intervention on the landscape (IPCC, 2000).

Land Use: How human activities on the ground such as farm activities, urban development, grazing, timber harvesting, mining and conservation (IPCC, 2000).

Land Use Change: The variation in human activities on land that sometimes changes the vegetation on the ground. Change from forestry to agriculture, urban or bare surface are a few of such activities. (IPCC, 2000).

Land Use Change Scenario: Spatio-temporal variations on the surface like land initially under forest changes into farm land or bare land and will be used so in order to compute changes in river flows (IPCC, 2000).

Low Flow: River discharge during dry spells

Recharge: A process by which an aquifer is refilled with water from rain, stream, swamp and lake as it gets into the soil.

River Basin: Also referred to as Catchment area; a land section where water accumulates before flowing to a river which is the only outlet to other bodies of water such as lakes.

River Regime: Describes the variability in a river's outflow over an annual period in regards to features of rainfall, temperature, evapo-transpiration and watershed

Simulation: Creating particular set of conditions artificially in order study or experience something that could exist in reality.

Supervised Image Classification: A user identifies sample areas of an image known as training sites, which have characteristics of the required type of land cover (Lillesand and Kiefer, 1999).

Training Sites: Areas of known land cover categories that appear homogeneous on the imageries and direct classification software in classifying other images (Lillesand and Kiefer, 1999).

Trans-boundary: Refers to a river shared between two or more regions or countries.

Unsupervised Image Classification: This is where the processing tool operates without user intervention i.e. It distinguishes the image pixel by considering and separating reflectance values into classes or clusters.

Validation: Refers to evaluation and affirmation of a measure or step as to whether it is accurate and capable of giving reliable results.

Water Abstraction: Refers to drawing out water from a natural source for utilization in various ways.

Water Balance: Refers to an equilibrium created between supply and usage of water by a water system within the airspace and on land over a length of time.

Wetland: Refers to a section of land covered by water either seasonal or permanent thus resulting in an ecosystem.

CHAPTER TWO: LITERATURE REVIEW AND CONCEPTUAL FRAMEWORK

2.1 Introduction

This study investigated Mara river hydrological processes and river flow regimes with respect to changing land cover, land use types and climate variability and change. The literature review is structured such that, it starts the first objective in section 2.2 and objective 2 in section 2.3, in that order with subsections in each section. The review is from global to regional, to national and lastly to the study area. The exercise involved review of books and published technical reports and journals and therefore, showed the trends and techniques used previously in similar studies, that is, in land cover, land use, climate and river flow related studies and this helped in identifying gaps for this study.

2.2 Nature, Extent and Rate of Change in Land Cover and Land Use

This first section of our literature review addresses the first objective in trying to understand how human actions have changed over time and space and how such changes have affected different systems and sub systems. This is because human induced changes in the global ecology and global environment have been mentioned as the main cause of globally recognized problems to humanity (Zhuo *et al.,* 2017).

2.2.1 Land Cover and Land Use Change - causes and characteristics

Noe, (2003) reports that, land use changes are complex with the process emanating from deliberate alterations of the land cover in which, anthropogenic and environmental factors interact to influence hydrological processes and land use patterns. Temporal and spatial factors in the human and biophysical dimensions largely lead to land use change (LUCID, 2004; Lambin *et al.,* 2002; Bronstert *et al.,* 2002). Additionally, among all factors that influence hydrological processes and systems, human-induced land use changes are the main factors (Dams, 2007).

Human instigated land use changes are as old as humankind itself is, since human actions have continuously altered the earth's surface due to intensified efforts by man to improve food production and general wellbeing (Kareiva *et. al*., 2007; Turner *et al*., 1993)). Land use changes have been highlighted as a major direct driver to variations in the ecosystems and the services thereof (Vitousek *et al*., 1997). Many studies

however report that, ecosystem changes are a function of different interrelated direct drivers of which land use and climatic changes are among the major ones (Reyers *et al*., 2009). These direct drivers are in turn, influenced by indirect drivers such as population and economic dynamics (see e.g. Reyers *et al*., 2009; IPCC, 2007).

Deforestation of the tropical forests as land use changes escalate is still an on-going practice in the 21st century with Africa as the most affected continent largely due to rapid increase in population and over-reliance on forest products for socio-economic wellbeing (IPCC, 2007; FAO, 2005). A study on change detection on land cover/land use of Kenya's major water towers reported that 8,266 hectares of forest cover destroyed in the Mau, Cherangani and Mt Elgon forests in 2003 alone with Mau losing a total of 7,084 hectares (UNEP, KWS and KFWG, 2005).

Studies report that the Mau forest complex had its closed canopy decreased by 6.2% and area under vegetation cover by 8.6% while cropland, settlements and bare ground had an increase of 71% between 1973 and 1986 with an on-going trend (Ayuyo, 2012). Mango *et al*., (2011) reported rapid alterations in land use practices in the Mara River basin with far-reaching consequences on the climate patterns and therefore, the Mara river flow regimes. Mutie *et al.,* (2006) found out that forests, rangelands and water bodies reduced between 1973 and 2000. The reduction in forest cover relate to logging for timber, tea farming and settlement while rangeland was devoted to agriculture (Serneels *et al.,* 2001). The above changes resulted in areas under tea and open forest, agriculture, and wetlands increasing by more than 200% each.

The spatio-temporal patterns and land fragmentation which occurred in the Mara basin over the study period were analysed with a belief that the findings of this study would assist in revealing the effects that changes in abiotic resources had on biodiversity especially animals in the conservation areas and socio-economic activities such as farming, livestock rearing and tourism. This belief is further reinforced by the fact that changes in land use that reduced forest cover resulted in reduced rainfall and low evapotranspiration rates; increased surface run-off and therefore increased flood events, erosion and siltation of water resources (Rwigi, 2014; Ayuyo, 2012). The ultimate end of the above scenario would be a degraded environment culminating in poor land productivity, low water supply which is also of low quality with further implications

on socio-economic activities and animal life. In formulating policies geared towards sustainable socio-economic activities including tourism in the Mara, focus must be on vegetation and human activities, applying change detection analysis with validation as addressed by the first specific objective in this study.

2.2.2 Trends in Land Cover and Land Use Change

Goldewijk, (2001) carried-out a study to estimate global patterns of land use changes between 1700 – 2000 and found out that cropland had changed from 136 million hectares between 1700 and 1799 to 412 million hectares for the period between 1800 and 1899. It further increased to 658 million hectares between 1900 and 1990. During the same periods, conversion to pasture was 418, 1013 and 1496 million hectares respectively. This process resulted in accelerated deforestation of the tropical rain forests. Lambin and Geist, (2006) concurred with Goldewijk in their study carried out on change in ground vegetation and activities (elements, they say, exist as local processes with global implications on climate systems), when they reported that major global land use changes took place between 1700 and 1990. They found out that, cropland increased from about 3.5 million km^2 to 16.5 million km^2 while forestland previously 53 million km^2, declined to 43.5 million $km^{2.}$ Reports by IPCC, (2007) and FAO, (2005) reveal that deforestation of the tropical forest is still an on-going practice in the 21st century with Africa as the most affected continent. The high level of deforestation in Africa is attributed to increased pressure on forestland by the rapid increase in population characterized by high poverty levels and therefore, over-reliance on forest products for a living.

Studies in Kenya on land cover/land use change in various parts of the country, especially water towers agree with the above sentiments. A joint study by UNEP, KWS, and KFWG (2005) on land use/land cover change detection covering Kenya's five water towers, found-out that a total of 8,266 hectares of forest cover in the Mau, Cherangani and Mt Elgon forests was destroyed in 2003 alone, with Mau losing 7,084 hectares. Ayuyo, (2012) in his study of 'Geospatial Analysis of Land Use/Land Cover Change in Mau Forest Complex', reported that, closed canopy reduced by 6.2% between 1973 and 1986 with the rest of other vegetation cover reducing by 8.6%. During the same period, cropland, settlement and bare ground increased by 71% and the trend continued with time and increase in population.

Mara river basin has attracted many researchers including Mango *et al.*, (2011) all of whom agree, the region is rapidly changing in terms of activities accompanied with far-reaching consequences on the climate patterns and therefore, the Mara river flow regimes. Mutie *et al.,* (2006), for example, in their study on how change in land use affect Mara river flows between 1973 and 2000 found-out that, forests, rangelands and water bodies had a total reduction of 184% at the expense of agricultural land, tea, open forests and wetlands which increased by over 200% each during the same period. These changes are a threat to continued provision of the critical Mara basin transboundary services including the Mara flows and the periodical migration of the wildebeests. Little information exists on the tendency and magnitude of change along the Mara at basin scale. The scenario is quite an impediment to understanding the implications of such changes for climatic conditions, socio-economic activities and Mara flow regimes - for any proactive or affirmative action to be taken to achieve sustainability in the Mara ecosystem. In light of the above, this study adopted the catchment approach, which integrated and analyzed the interdependence of the various processes and activities in the water sensitive Mara basin.

2.2.3 The Role of Forests and their Impact on Water Resources

The forests are useful in several ways including being source of renewable energy, providing environmental services that include maintaining biodiversity, protecting water and land resources, as well as playing a major role in alleviating climate change (Jacobs *et al*, 2007). Increasing areas of world forests, which occupy about 20 per cent (FAO, 2006) of the total land area, would be important primarily for soil, water and environmental conservation. Locally, forests reduce soil erosion, sedimentation, filtering water pollutants through infiltration and forest litter, regulating water yields, moderating flood events and enhancing precipitation and mitigating salinity thus protecting water resources (GoK, 2010b; Homdee, *et al*., 2010) which is insufficient to human needs.

The United Nations International Year of Fresh Water (2003) emphasized on quality and sufficient amount of water at the right place and time. Forests trap radiation in their multilayered canopies resulting in a net warming of the ecosystem **(**GoK, 2010b). This warming generates more thermal turbulence above the forest cover which favours the formation of clouds and hence rainfall over and close to the forest areas.

Evapotranspiration from the forests adds to the existing atmospheric moisture thus enhancing cloud formation. Forests influence water availability from surface water, rivers, streams, and other surface water bodies (IPCC, 2007; FAO, 2008) through evapo-transpiration.

When rainfall reaches the forest floor, it distributes into various components that include surface runoff, interflow, ground water recharge, continental evaporation, and plant intake. In this regard, forests moderate as well as regulate hydrology of river catchments since they influence how the net rainfall is distributed into the various stream flow components. Along streams and rivers, forests provide a shading effect thereby reducing water temperatures and hence loss through evaporation. As catchment land cover, protected and well managed forests tend to increase the hydrological safety of a water catchment area and thereby leading to water being one of the most important products of the forested watershed (FAO, 2008; UNEP 2005)

2.2.4 Impact of Land Cover and Land Use Change

This subsection reviews work done on the impact, implication and effects of land cover and land use change on climate elements because the effects of the two are intertwined. That is to say, land use practices cause climate variability and change while land uses are also influenced by climate variability and change. It looks at how changes in land cover and land use types impact or affect climate of a region.

2.2.4.1 Land Cover and Land Use Change and Climate Variability

Control and alteration of the natural environment by humans have results in characteristics relating to hydrological cycle as well as atmospheric composition. In the atmosphere, human activities are responsible for increased atmospheric nitrogen and carbon dioxide accumulations that result in greenhouse effect. Factors such as land use, ozone depletion and deforestation have far-reaching consequences on climate conditions and the water balance (Houghton *et al.,* 2012; Houghton, 1995). According to Turner *et al.,* (1995), conversion of forests to cropland leads to release in carbon dioxide equivalent to 30% of total amount got during combustion of fossil fuel. The Amazon rainforest faced increased deforestation between 1991 and 2004 with a loss in forest cover of 27,423 km² in 2004 alone. Although the deforestation rate in this ecosystem slowed down since 2004 and only increased between 2008 and 2013, the

rest of the forests are diminishing (Michael, 2006). Reduction in forest cover in the Amazon forest resulted in reduced precipitation as well as decreased evapotranspiration and this led to alteration of the regional climate (Miles *et al*., 2004; Michael, 2006).

Turner et al., (1993) adds that conversion of forestland or grassland into cropland results in much more release of carbon dioxide in humid regions than in the tropical zone (Turner *et al*., 1993) thus, affects both the rate of discharge, runoff as well as surface radiation balance especially in the absence of land cover (Davey *et al*., 2005). Loss of forests contribute 6% to 12% of global carbon dioxide per annum (Turner *et al*., 1995). Although these studies have not been conclusive, climatic changes could cause significant shifts in human practices on land (Miles *et al*., 2004) in the form of continual human adaptation to sustain livelihoods. Land use change therefore, interacts with climate through positive feedback landscape processes, including cultivation on riverine, grassland and draining of swamps as man strives to fulfil his needs. The current study separated the effects of land use change from those of climate change on river discharge. These inter-linkages established between land activities and climate dynamics on the flow of river Mara regimes may enhanced effective development of land use policies that would support sustainable water allocation in the basin. This study demonstrates that adaptation to climate change has in part, been responsible for land use change as livelihoods face threats from hunger and deficit in fuel wood.

Studies on forest cover change within the water towers of Kenya revealed wanton deforestation and general environmental degradation that has been associated with increased temperatures, reduction in rainfall and increased frequencies of droughts and flooding events (Akotsi *et al*., 2004). UNEP, (2005) reports that more than 61,000 hectares were excised from the protected forests in the Mau Complex in 2001 for settlement and farming. Actions that reduce forest cover, promote carbon dioxide accumulation in the atmosphere since their role as carbon sinks is either reduced or eliminated (Houghton *et al.,* 2012). Agricultural activities elevate the amount of gases in the atmosphere that result in greenhouse effect. The excision of parts of the Mau forest complex together with the general degradation thereof have led to microclimate modification within and in the surrounding regions. This is a scenario witnessed in many river basins as anthropological factors set in. In the study by Gereta *et al.,* (2002) that mapped water availability and use in the Mara, it was reported that, the water in

the lower portion of the basin dry up during dry seasons, form shallow pools which dry out completely during severe droughts, which appear to be cyclic after every seven years.

2.2.4.2 River Flow Regimes and Land Cover and Land Use Change

Runoff process within a catchment varies with time and space, influenced by climatic and human factors. As an illustration, water droplet that falls from precipitation takes a long time and space to reach the main stream. Various factors influence the speed at which the drop travels and reaches the stream. These factors include land cover, rainfall intensity, soil type and geomorphological aspects of the catchment According to Vitousek (1997), human induced ground cover and ground activity changes have transformed at least one-fourth to a third of ice-free surface to different types of precipitation. Watersheds have also undergone drastic changes with most of the vegetation cover cleared for grazing and arable land. Piao *et al.,* (2007) argues that effects of land use changes to surface runoff is beyond climate change and that strongest effect has been felt in the tropical regions as evidenced by the decline in forest cover of the Amazon rain forest (Chaves *et al.,* 2008).

Changes in land use impact significantly on a river basin runoff (Zeng *et al*., 1999) through the interactions of land cover, soil and rainfall characteristics. Forests are rain formation areas and do capture much rainfall through interception, storage and soil infiltration. At the same time, even more water escapes through transpiration from trees and swamps especially in sub-humid areas (Hough, 1986). Land use change alters the equilibrium between rainfall, evapotranspiration and consequentially, the runoff (Lambin *et al.,* 2003).

Grassland and cultivated areas allow less infiltration compared to forested areas because of the loss of litter that accumulates to form humus. Increased overland flow carry sediments from tilled land and bare grounds thus, reducing soil thickness where additional carbon sequestration should occur. Changes in land use activities around the Mara just like any catchment have dramatic effects on the basin's response to rainfall and storms (Zheng *et al*., 2008). Changing forestland to other land use types may increase high flows or floods or diminish the low flows (Lin *et al*., 2007). Deforestation is important in the flooding equation because it enhances sediment runoff. Secondly, it

allows the unimpeded raindrops to impact on bare ground as they seal the soil pores and cause heavy erosion and quick overland flow.

Deforestation also contributes to flooding through channel reduction due to deposition of the sediments eroded in the uplands on the riverbeds, thus reducing the river's capacity to carry water without flooding (Lin, *et al*., 2007). The Africa's Sahelian droughts of the 1960s and 1980s had linkage with human-induced climate changes (Wang *et al*., 2004). Evidence of increasing or decreasing flow regime are attributable to changes in human activities and or in climate (Mutie *et al*., 2006; Hoffman, 2007; Melesse *et al.,* 2008). Climate change scenarios demonstrate divergences between rainfall regions thus could vary a long a river profile (Nepal *et al.,* 2014). Humi *et al.* (2005) noted that reduced forest cover coupled with increased farming activities had resulted in increased soil degradation and surface runoff on the Ethiopian highlands while reducing streamflow in the Blue Nile basin. Rientjes *et al.,* (2011) further noting a reduction in forest by an estimated 70% in 1971 through 2000 in Upper Gilgel Abbay catchment of the Blue Nile basin.

Most studies in the Mara and elsewhere (see Foody, 2001) tend to attribute changes in river flow regimes to changes in land use activities without considering climate related implications. Other research (including Mango *et al.,* 2011) have addressed influence of land use alongside climate change on water yielding capacity by considering one part of the basin and not whole, the upper catchment. Such studies fail to capture the upstream-downstream inter-relationships in terms of hydrological processes and interdependence of the hydraulic characteristics of the channel, which influence water yields. In the absence of such information, no informed policy formulation and regulations for sustainable water resources management can be prepared. Mati *et al.,* (2008) looked at response of changes on ground cover in Mara basin, observed that in less than a couple of decades, there was a significant increase in runoff. This is mainly the effect of deforestation, which also results in very low base flows (Hoffman, 2007; Mwania (2014). This study closed these gaps by considering the entire basin and establishing the inter-linkages between changes related to land cover/use and those related to climate as far as Mara water balance is concerned.

2.3 Spatio Temporal Variations in Rainfall, Temperature and River Flows

This section looks at work by researchers covering distribution of weather and climate elements over time and space. Specifically, it reviews work on long-term variations and change in climate and river flow volumes, using the weather elements of temperature and rainfall as well as changes recorded in river flow volumes, in the Mara River basin, which are an attribute of changes in rainfall and temperature.

2.3.1 Climate Variability and Change- Causes and Characteristics

Climate change refers to intensified events and catastrophe that relate to climate variability such as droughts and floods. It is a function of a complex interaction between the components of a climate system, which comprise the atmosphere, oceans and seas as well as land and vegetation cover (IPCC 2001). The interactive responses by any of these components of climate system to external energy sources (mainly solar radiation and human induced) determine the background conditions that govern the world's weather and climate patterns (Wilson *et al.,* 2009). Although solar radiation is the main source of energy contributing to changes in climate patterns, human induced changes in the composition of the atmosphere and the land surface is such a significant source of energy to the climate system. This is because the induced changes modify the likely effects of solar radiation by altering the energy balance between the incoming solar radiation and outgoing terrestrial radiation (UNEP, 2009b).

The nature and extent of surface water and vegetation cover, which form part of the feedback processes within the global climate system have implications on the climate patterns as well (Wilson *et al*.,, 2009). According to Le Treut *et al*, (2007), the earth surface absorbs about two thirds of the solar energy reaching the top of the atmosphere with the rest reflected back to space as long wave radiation. The absorbed energy warms both the atmosphere and the earth's surface and therefore for the earth to balance the incoming solar radiation it must radiate the same amount of energy back to space, through the long wave radiation (IPCC, 2001). The energy balance initiative of the earth is however, interfered with through the accumulation of human induced greenhouse gases in the atmosphere. This is because these gases allow the incoming short wave radiation to pass through but not the outgoing long wave radiation which is instead,

redirected back to the surface, causing more warming on the earth surface and in the atmosphere alike (IPCC, 2013; IPCC, 2007).

Long term changes in the global and regional climate patterns have been experienced over time in terms of increased global temperatures (indicating climate change) which have been attributed to shift in the energy balance basically due to anthropogenic factors (IPCC, 2007). A report by FAO, (2008), warns that climate change will have a significant effect on hydrology and water resources manifested in increased catastrophes such as floods, droughts and landslides, which may result from changes in forest cover. Human beings contribute to global climate change by altering the composition of the greenhouse gases in the atmosphere and to the regional climate by changing the surface albedo through socio-economic activities that alter the earth's vegetation cover (Forster *et al*, 2007; UNEP/IVM, 1998).

IPCC (2007), states that since pre-industrial times there has been a positive trend in the concentrations of greenhouse gases in the atmosphere, attributed to increased human activities on the earth surface. The changes in the atmosphere have altered the energy balance of the climate system the effects of which, are being experienced in increased temperatures, reduced rainfall and increased frequencies of severe and extreme events such as droughts and floods (Dessu *et al.,* 2014). Studies reveal Africa is one of the world's most vulnerable regions to climate change implications due to high poverty levels and over-reliance on natural resources and rain-fed agriculture in pursuit of socio-economic development (WWF, 2002; IPCC 2001; WRI, 1996). Studies report that Africa's climate is already warmer than it was 100 years ago with an upward trend, based on the predictions of the future greenhouse gases (GHG) triggered climate changes (Christensen *et al.,* 2007).

During the 20th century, the continent of Africa warmed at the rate of 0.05ºC per decade with most warming experienced from the month of June to November compared with the period from December to May (Hulme *et al.,* 2001). In Africa, five warmest years on record had all occurred by 2000 with 1988 and 1995 recording the highest temperatures that superseded by 2000 temperature values. Globally however, periods of rapid warming were observed between 1910s and 1930s and the period after the 1970s (IPCC, 2001; Herrero *et al.,* 2010). Climate variability and change have and will

continue to exert significant impact on the water resources in the whole world. The main hydrological processes including stream flow volume, evapotranspiration, soil moisture, water temperature, occurrence and magnitude of runoff as well as the frequency and gravity of floods will all influence environmental conditions.

The IPCC, (2007) predicts that the continent of Africa will bear the largest burden of climate change given its vulnerability to the main drivers of the phenomenon that largely include anthropogenic activities. Therefore, developing an understanding of watersheds' hydrological response to land use and land cover (physical), and climate related (rainfall and temperature) changes is critical to the planning and management of water resources (Awotwi *et al.,* 2015). Climate change is expected to continue into the future with a potential acceleration over the rest of the 21st century due to human induced greenhouse gases emission (IPCC, 2007). The severe droughts that have occurred in most parts of Kenya in the past few decades are a testimony of the fact that Kenya is already vulnerable to climate change impacts (UNEP, 2009; PELUM -Kenya, 2010).

The need to protect the natural flow regimes in the watersheds is critical to the earth scientists (Zang *et al.,* 2012). The best that can be done in the emanating scenario is to have a detailed regional climate change predictions framework which can be used to formulate sustainable laws, policies and regulations that can support adaptive, mitigating and coping strategies aimed at sustainable natural resources utilization. Not much is in the offing to have such predictions in the study area and this is a deterrent to the implementation of necessary mitigations, adaptations and coping strategies that would result in sustainable natural resources utilization and continued provision of ecosystem services. This study came up with climate change scenarios together with detailed projections for the Mara basin in particular and for East African region in general due to similar physiographic characteristics and location within the tropic. The results of these changes and predictions were required in the analysis of the present and future impacts of climate change on the Mara River hydrological regimes.

2.3.2 Trends in Climate Variability and Change

A study by Schneider *et al.,* (2013) that investigated the response of river flow regimes to climate change scenarios in Europe, reported that climate change would modify the

flow regimes through alterations in precipitation, temperature and snow cover. The period between 1900 and 2005 showed rise in precipitation in northern parts of Europe, the eastern sections of North and South America, northern and central parts of Asia and, parts of Central and Eastern Africa (IPCC, 2007). Areas across the Mediterranean, African Sahel and southern regions of Asia had decline over the same period (IPCC, 2007). Predictions in precipitation strongly indicate possibility of increment in the higher latitudes and decline around the sub-tropical regions. Additionally, concentration of greenhouse gases is projected to increase and will have severe impacts on global climate systems during the 21st century more than any other time in history (McCarthy *et al.,* 2001; WWF, 2002; IPCC, 2007).

Most parts of Africa have experienced marked increase in temperature during the 1960s with a mean warming of about 0.7°C across the globe over the 20th century. During the same period, mean annual temperature in Kenya increased by 1^{o}C with an upward projection as climate change implications continue to bite (IPCC, 2013; UNEP, 2009). The severity of extreme events are increasing while rainfall is decreasing in amounts and reliability that is affecting agricultural production in most parts of the country given that, two-thirds of Kenya is rangeland (GoK, 2010). This study investigated changes in climatic conditions and tried to establish the relationships in trends of climate change, land cover/land use and river flow volumes.

2.3.3 Impact of Climate Change on Water Resources

FAO, (2008) warned that climate change would have significant effect on hydrology and water resources which would manifest itself in increased catastrophes such as floods, droughts and landslides, all of which may be influenced by changes in forest cover. Geun *et al.* (2016) looked at climate change and its impact on Lake Malar water levels from 2000 and projected to 2100 and found out that, the lake water level increased by 50 cm and would even increase more because of global warming. Looking at similar debate, anthropogenic factors top the list as the major cause to changes in climate systems (Dai *et al.,* 2016). According to the reports by most studies, climate change has adversely affected the hydrological cycles and forest ecosystems in all their composition of species and communities such as type of trees and abundance, tree biomass, productiveness, distribution, constitution as well as hydrological regimes (Chen *et al*., 2014; Michaletz *et al*., 2014; Dai *et al*., 2016).

Changes in forest biomass is one of the notable indicators in assessing forest quality thus applied in many studies seeking to determine ecological responses of forests to anthropogenic disturbances and climate change and the consequent effect on the hydrological regimes. Many studies including Zhuo *et al*. (2017) report that, climate change impacts on forest ecosystem have to be investigated well beyond the baseline climate study period of thirty years. In most cases, the impacts of climate change manifest in extreme events such as droughts and floods, which usually culminate in the deaths of livestock, crop failures, destruction of property and loss of lives (Schneider *et al.,* 2013). These extreme events hinder economic development and therefore, are a hindrance to poverty eradication efforts. Unfortunately, there is limited literature and knowledge of such extreme events in Africa that would help avert disaster by providing early warning indicators (KNMI, 2006). Other effects of climate change such as rising temperature and changes in precipitation are undeniably clear with impacts already affecting ecosystems, biodiversity and peoples' livelihoods (IPCC, 2007).

High temperatures and variations in rainfall, whether too much or little, have far reaching consequences on lifeforms, food security, economic activities, physical infrastructure, natural resources and the general environment with wanton implications on national and global security ((Schneider, *et al.,* (2013; O'Keeffe, *et al.,* 2007). Climate change is set to exacerbate occurrence of climate related disasters including droughts and floods. Future projections of the impacts suggest worsening situations with continued rise in temperatures while precipitation becomes more unpredictable.

Predictions from existing climate scenarios report that the driest regions of the world will become even drier (UNESCO, 2006) hence, signaling the risk of persistent droughts in many parts of Africa. East African climate is already experiencing large variability in rainfall and occurrence of extreme events such as droughts and floods (Nganga, 2006). Many studies report the East African region to have suffered from both deficient and excess rainfall implications in the past few decades. They include increased drought events and erratic rains, which led to incidences of flooding more often than not (Chen *et al.,* 2014; Webster *et al.,* 1999). According to Shongwe *et al.,* (2009), the number of reported cases of hydro-meteorological disasters in the East African region have increased steadily to the present since 1980s with floods as the main cause of disaster.

According to most studies on issues related to climate change, developing countries are the most affected with Sub-Saharan Africa most disadvantaged. In the tropical agro-ecological zones and worst, the semi-arid areas, there is a significant reduction in crop yields, a big source of fear in Africa since her large areas of marginal agriculture may be forced out of production due aridity (IPCC, 2013). It is projected that sub-Saharan Africa will experience about 33% loss in crop productivity between 2060 and by 2080, resulting in a negative net balance in change in crop-production, with estimated net losses of about 12% of its current production (Parry *et al*, 1999).

Although climate change mostly seen in a negative perspective as having adverse effects, some studies have depicted climate change as a key contributor to changes in forest cover (Gustafson *et al.*, 2010; Thompson *et al.*, 2011). However, land use changes would have effects that are more adverse and therefore offset the positive effects brought about by climate change. Gustafson *et al.*, (2010) studied south-central Siberia and found out that climate change effects were less than effects of land use changes and disturbances (Zhuo *et al*., 2017).

The GoK, (2011) states that Kenya is susceptible to issues of climate variability as it relies on agriculture as the main livelihood for a nation that has high poverty level. According to the government report, 80% of farmers in Kenya depend on rain-fed agriculture and therefore, any reduction in rainfall makes most people vulnerable and food insecure due to climate change impacts (GoK, 2011). Because climate and land use change implications on the environment are intertwined, the study set to establish how the two affect one another and how they individually and collectively impact the Mara River flows regimes, especially in the sub basins. It went further to look at the projected implications for sustainable utilization of the Mara basin resources. Not much of this kind of information exists at the sub basins, save some information existing at basin scale. Another important fact to note is that, a good number of studies of this kind have been carried-out in the headwaters only and therefore, do not reflect the situation in the basin. The outcome of this study is therefore very important to the policy makers to formulate policies and regulations that would promote informed decisions in the management of transboundary Mara River basin resources.

2.3.4 Climate Change Scenarios

Climate change scenario is a representation of the difference between possible future climate scenario, based on climate projections resulting from responses of the climate system to scenario of greenhouse gases and aerosols emission (attributed to social-economic and technological developments) as simulated by climate models, and the baseline climate (Wilson *et al*, 2009; Jones *et al*, 2004). It describes what the future global climatic condition is likely to be, based on coherent and internally consistent set of assumptions concerning the driving forces and their key relationships (Miller and Yates, 2005). Such scenarios have been constructed and explicitly used in the investigation of the potential impacts of anthropogenic climate change.

There is more than enough evidence that human activities have influenced climate in different regions globally and that this influence will increase in the future and lead to albeit, unknown climate scenarios (Mitchell *et al*, 1999). In fact, it is important to establish possible future scenarios of climate change attributed to anthropogenic factors (land use change and greenhouse gases emission) since this is the only way to assess the socio-economic and ecological implications for climate change. This would help in the formulation of policies and regulations aimed at making informed decisions on the necessary adaptive and mitigating measures to put in place.

2.3.5 Modelling Climate Change

Climate modeling employs the use of computer models of climate system to simulate interactions of the earth's components of climate system and their response to solar radiation (Jones *et al*, 2004). Climate models are thus, fundamental research tools for understanding and predicting both natural and anthropogenic changes in the earth's climate (Rummukainen, 2010; Wilby and Miller, 2009). Current climate models suggest a future increasing rates of occurrence and strength of floods and droughts, the effects of which, are already being felt by the rural communities in developing countries (Porter *et al*. 2014; Coe and Stern 2011; Bernstein *et al.* 2007) due to inadequate data that can aid informed decision-making.

The Atmosphere-Ocean General Circulation Models (AOGCMs) simulate climate changes under a range of future greenhouse gas emission scenarios and act as primary tools for future climate assessments. According to IPCC (2001 and 2007), general

circulation models for reducing climate change occurrences are driven through specific complex dynamic systems such as the socio-economic projections, various air concentrates of the key gases that absorb and emit radiant energy and related effects, therefore their future evolution are highly uncertain. Understanding the uncertainties in models of climate is necessary in analyzing climate change, which includes modelling of climate, evaluation of impacts, mitigation and adaptation.

Global Climate Models (GCMs) have been used to provide useful climate change projections at large spatial scale, but their projections at the regional and local scales are still limited especially in developing countries (Zang *et al.*, 2012; Omondi, 2010). Many current climate change studies in developing regions are however, currently based on global models driven scenarios. Several attempts to use statistical, dynamical or hybrid downscaling methods to derive regional climate change scenarios have been in the offing (IPCC, 2007). Such attempts include the Coordinated Downscaling Experiments (CORDEX) - (Yu *et al*, 2014) project and the Couple Model Inter-comparison (CMIP5) project which attempt to provide the downscaled analysis of various GCMs.

The need to understand changes and predict future climate has led to the use of Regional Climate Models (RCMs) for climate studies and future climate projections. The RCMs provide better information than their large-scale global parent models but their use in the regional climate analysis is, however, still limited and mostly relies on the global parent models. Nonetheless, regional climate and hydrological models have been used to assess the influence of climate change on water resources especially in the Mara River Basin, the Blue Nile Basin of Ethiopia and the Volta Catchment in Ghana (Mango *et al.*, 2010; Awotwi *et al.*, 2015).

Climate analysis using the Regional model indicated that Kenya is likely to experience average rise in annual temperature of between 1°C and 5°C in the period between 2020 and 2100. During the same period, the long and short rainy seasons are likely to become wetter, particularly in the short rains from October to December (Anyah *et al*, 2007). Global Climate Models predict increases in rainfall in northern Kenya by 40% by the end of 21st century while the regional model suggests that there may be greater rainfall in the West. This study however, did not use climate modelling in trying to understand

hydrological responses to changes in land cover, land use and climate in the Mara basin, since its application was not within the scope of this study. Instead, hydrological modelling, using SWAT was applied to address objectives 3 and 4, which required creating a simulation of the river flow and generating river flow sensitivity indices under different land cover/land use and climate scenarios respectively, in the Mara River Basin.

2.4 Hydrological Modelling

Hydrological model is a simplified, conceptual representation of a part of the hydrological cycle that aims at representing the physical processes that control the transformation of rainfall, as an input to runoff and river flow as the outputs (Droogers *et al,* 2006). Physical processes that are behind the nature and characteristics of runoffs and river flows in a basin are the topographical, meteorological, hydrological, land cover/land use and soils parameters. In the words of Mutua, (1986), hydrological models relate river flow to the above parameters, whose main use is to predict hydrological dynamics and to understand the hydrological processes that are ongoing in a catchment. The most important climatological predictors for climate change required for the calibration and validation of hydrological models are temperature and precipitation (Akhtar *et al,* 2009). These climatological inputs are obtainable either from in-situ records or from simulations of regional climate models such as PRECIS (Rwigi, 2014).

This study examines the interrelationships in land cover, land use, climate (especially rainfall and air temperature) and river flow in the Mara River basin, a trans-boundary system whose upper catchment is in South West Mau forest, the largest of the 22 blocks (UNEP, 2009a) forming the Mau Forest Complex in Kenya. The study specifically examines how river flows and hence surface water yields vary under different land cover/land use and climate scenarios over time. The extent of variations in the river flow volumes looked at in terms of changes in the mean as a central value. In order to achieve this, a physically based hydrological model, the Soil and Watershed Assessment Tool (SWAT) applied. SWAT extensively described in Neitsch *et al* (2011); Winchell *et al* (2010) and Arnold *et al* (1998).

2.4.1 The SWAT Model

The Soil and Watershed Assessment Tool (SWAT), developed by Arnold *et al*., (1998) is a conceptual continuous time model. In its initial development, the model was to be used by water resources managers to assess the impacts of management on water supplies, sediments and agricultural chemical yields in large and complex watersheds with varying soils, land use and management conditions over long periods of time. Presently, the model is also being used to estimate impacts of climate change and land use management on water resources. In the words of Arnold *et al.,* (1998), SWAT is a basin scale hydrologic model that is computationally efficient, allows considerable spatial detail, requires readily available inputs, is continuous time model that operates on a daily time step at basin scale level, is capable of simulating land management scenarios, and gives reasonable results (Arnold *et al* 1998). This study focused mainly on the simulation of the hydrology process.

Variables for inputs in SWAT include relevant information about topography, soils, weather, vegetation and land management practices in the watershed within which the physical processes associated with water movement are modelled. SWAT model includes procedures to describe how precipitation, temperature, carbon dioxide concentration and humidity affect evaporation, runoff generation and plant growth among others and this makes it suitable for use in the investigation of climate change impacts (Abbaspour *et al,* 2009). SWAT model has the ability to replicate hydrologic and pollutant loads at a variety of spatial scales on an annual and monthly basis as contained in numerous studies involving the application of the model (see Faramarzi *et al,* 2009; Gassman *et al,* 2007; Schuol *et al,* 2008; Githui, 2008).

SWAT is also capable of performing continuous, long-term simulations for watersheds with various sub-basins and different topography, soils, weather, land uses and crops, among others (Neitsch *et al,* 2011). The model simulates the weather, surface runoffs, return flow, evapotranspiration, in-percolation, ground water flows, transmission loss, pond and reservoir storage, crop growth and irrigation among others. In doing so, the model first delineates the watershed into a number of sub-basins and Hydrological Response Units (HRUs) for efficient simulation of the components. This is particularly important where different parts of the watershed are under different land uses and soils so there are different impacts on the catchment hydrology (Neitsch *et al,* 2011). The

model caters for spatial disparity in a basin by considering information from the DEM, soil, and land cover/land use maps (Schuol *et al,* 2008).

SWAT allows hydrology, weather, sedimentation, soil temperature, and agricultural management among other physical processes in the watershed to be simulated (Arnold *et al,* (1998). SWAT is integrated with Geographical Information Systems (GIS) software in order to facilitate and improve the efficiency in the analyses of the impacts of different watershed management scenarios on water yields (Van Griensven *et al,* 2012). The interface of Arc SWAT and ArcGIS allows the model to preserve the spatial nature of the topography, land use, soils databases, and by so doing, preserves the distributed nature of the model parameters (Neitsch *et al,* 2011). This improves SWAT's effectiveness in developing input data files from GIS coverage (Neitsch *et al,* 2011). The model is also very flexible in its operations and all these virtues have popularized its use in simulating a variety of watershed problems as stated above (Van Griensven, *et al,* 2012). This study applies the ArcSWAT2012 under ArcGIS10.4 environment to perform the simulations, calibration and validation to eliminate or minimize the errors in the results.

Taking into account the differences in land use and soils in different parts of the watershed is important because they impact differently on the catchment hydrology (Neitsch *et al,* 2011). The simulated bulk water yield consists of surface runoff (SURQ), groundwater flow (GWQ), percolation (PERCO) and lateral flow (LATQ). The model is designed in such a way that it is capable of independently separating the components for easier evaluation of the catchment's relative response to each of the individual components. The spatial variables and morphometric parameters of the catchment including land cover and soils influence the flow of liquids into the respective components (Wagesho, 2014; Malutta and Kobiyama, 2011).

2.4.2 Watershed Delineation

SWAT model uses the Digital Elevation Model (DEM) data for automatic delineation of the area of interest under ArcGIS environment. Delineation is usually done to establish the general watershed attributes over the basin such as land area and stream network that are known to control a diversity of physical processes at the watershed level (Arnold *et al,* 2011). The model sets the parameters used at default values but the

model users can change them where it is important to do so. The operation is however, done within certain limits, especially to give a better reflection of the characteristics of the catchment being studied.

2.4.3 Sub-Basins

Sub-basins are generated during watershed delineation exercise and their number depends on the basin's land area and topography. The sub-basins are spatially related to one another with each of them occupying specific geographical location within the watershed. Every sub-basin delineated contains at least one area with unique soil-land use-slope combination called Hydrological Response Unit (HRU), a main channel and a tributary channel. Input data for each sub-basin is organized into climate parameters, groundwater, the main channel draining the sub-basin and HRUs. The next sub-section presents a brief discussion of the HRUs.

2.4.3.1 Hydrological Response Units (HRUs)

HRUs are land areas lumped together within sub-basins comprising unique land cover, soil, slope, and management combinations. They allow the SWAT model to capture the diversity of land use and soils within each sub-basin. Unlike the sub-basins, HRUs are not geographically located; rather they represent the total area in the sub-basin with a particular land use, management system, soil and slope characteristics (Winchell *et al,* 2010; Arnold *et al,* 1998). Though HRUs may be scattered all over the sub-basin, SWAT lumps all of them together to form one HRU for each of the sub-basins delineated.

The SWAT simulates the overall hydrologic balance for each HRU, including canopy interception of precipitation, partitioning of precipitation, snowmelt water and irrigation water between surface runoff and infiltration, redistribution of water within the soil profile, evapotranspiration, lateral sub-surface flow from the soil profile and return flow from shallow aquifers. The next step is to aggregate all the above at the sub-basin level followed by routing to the associated reach and catchment outlet through the channel network to obtain the total runoff and water yields for the whole watershed (Faramarzi *et al,* 2009; Abbaspour *et al,* 2009). The above procedure increases the accuracy and gives a much better physical description of the catchment's water balance (Winchell *et al,* 2010).

SWAT model has two options available within its components used to determine the HRUs distribution. The HRUs distribution for each sub-basin can thus be determined as single or multiple HRUs. As explained by Winchell *et al,* (2010), a single HRU for a sub-basin uses the dominant land use category, soil type, and slope class within the sub-basin to simulate the HRU. On the part of multiple HRU, the user has the option to specify a threshold level for the land use, soil and slope datasets used to determine the number of HRUs in each of the sub-basin. These thresholds are usually based either on a percentage of an area or on absolute area.

This study selected the Multiple HRU option and applied the percentage area threshold due to its robustness. The purpose of the thresholds is to eliminate minor land uses, soil types, and slopes in each sub-basin. In this study, 5% land use, 20% soil type, and 30% slope class threshold settings used to define the HRU in each of the sub-basin in the Mara catchment. The thresholds set percentages of the total sub-basin area that land use, soil type and slope class must cover for them to qualify to be included as part of the HRUs in the sub-basin.

2.4.3.2 Main Channels

During hydrological simulations in SWAT, each sub-basin is associated with the main channel in the watershed area. Runoffs from the sub-basins enter the channel network of the watershed in the associated main segments. There are two types of surface flows in a catchment namely: overland flow and channel flow. The processes modeled by SWAT in the main channel of the watershed include the movement of water, sediment, agricultural chemicals and other constituents in the stream network including in-stream nutrient cycling and in-stream pesticide transformation (Winchell *et al,* 2010). This study focused on the movement of water in the Mara River channel and the resulting implications from the same due to changes in land cover, land use and climate over time.

2.4.3.3 Canopy Storage

Plant canopy affects infiltration, surface runoff and evapotranspiration quite significantly. This is because, during a rainfall event, the canopy traps a portion of the rainfall and denies the chance to reach the surface. The density of the plant cover dictates the magnitude of the plant canopy influence on these hydrological processes.

This means that, any human activity that interferes with this density also influences the hydrology of the watershed area (Neitsch *et al,* 2011). Such impacts have been witnessed in the Mara basin where the forest cover in the upper catchment has reduced over the last twenty-five years due to conversion to agricultural land (Mutie *et al.,* 2006 and Mango *et al.,* 2010). SWAT calculates surface runoff using the Soil Conservation Service (SCS) curve number method, canopy interception is lumped in the term for initial abstraction. The amount of water stored in the canopy varies from day to day as a function of Leaf Area Index (LAI) and atmospheric humidity. This study in part, desired to establish how reduction in forest cover (land cover) and therefore plant canopy has affected the hydrology of the Mara basin.

2.4.3.4 Potential Evapotranspiration

The amount of Potential Evapotranspiration (PET) is a function of a combination of several parameters including solar radiation, prevailing conditions of the sky and wind speed, among others. A number of methods and approaches have applied to estimating PET, three of which are incorporated in the SWAT model. These are the Penman-Monteith, the Priestly-Taylor and the Hargreaves methods (Neitsch *et al,* 2011). They differ in the number of inputs required for the calculation of PET. The inputs for Penman-Monteith are solar radiation, air temperature, relative humidity and wind speed. The Priestly-Taylor method requires solar radiation, air temperature and relative humidity while the Hargreaves method uses temperature only as the input required to calculate the PET. Penman-Monteith method employed in this study because of its robustness in terms of the inputs (Neitsch *et al,* 2011).

2.4.3.5 Surface Run-off

Surface runoff is a function of many variables including rainfall intensity and duration, soil type, soil moisture content, land use practices, land cover and slope. It occurs when the rate of water application to the ground surface exceeds the rate of infiltration (Yang *et al.,* 2013). Considering the numerous variables governing the generation of surface runoff, lumped conceptual models are useful approaches of its analysis and prediction. Among the conceptual models developed for the analysis and prediction of surface runoff, the Curve Number (CN) method is one of the most widely accepted (Neitsch *et al,* 2011). SWAT provides two options of estimating runoff; SCS curve number

procedure, and the Green and Ampt infiltration method. The SCS curve number procedure is popularly used because of its simplicity, stability, predictability and the fact that, it relies on a mere two parameters.

Another quality is its responsiveness to major runoff thereby producing watershed properties (Neitsch *et al,* 2011; Ponce and Hawkins, 1996). Soil Conservation Service CN varies with soil absorbent, activities on land, and pre-existing moisture levels (Neitsch *et al,* 2011). Lower values of the curve number indicate low runoff potential while higher values indicate probability of high runoff thus lower CN indicate that the soil is more porous as opposed to higher CN (Ponce and Hawkins, 1996

2.4.3.6 Sub-Surface Flow

Water that enters the soil through infiltration may move in three different pathways that are important in this study; removal from the soil by plant uptake and evaporation, percolation past the bottom of the soil profile to become aquifer recharge, and lateral flow that contributes to stream flow. Of the three pathways, plant uptake of water removes most of the water entering the soil profile (Neitsch *et al,* 2011). Therefore, any change in plant cover in a watershed will alter its hydrology. Understanding these pathways is very important in a study of this nature where impact of changes of vegetation cover on hydrology is investigated within such a basin as Mara whose upper catchment including the Mau Escarpment has faced heavy deforestation in the last three decades (Mango *et al.,* 2011). The amount of water held by the soil and made available to traverse the above pathways is a function of the soil structure that determines the drainage characteristics of the soil.

The soil water content can range from zero for oven-dried soil to a maximum value possible when the soil is at its maximum saturation (Neitsch *et al,* 2011). Saturated water flow is driven by the gravity while unsaturated flow is influenced by the gradient created by the adjacent areas of high and low water content (Neitsch *et al,* 2011). (Neitsch *et al,* 2011). Saturated water is directly replicated Soil and Water Assessment Tool. SWAT models the bypass flow, the vertical movement of free water along macrospores and cracks through unsaturated soil horizons by calculating the crack volume of the soil matrix for each day of simulation. Infiltration and run-off values are calculated when it rains by use of a number of techniques such as the SCS curve number

method. The generated run-off on a rainy day enters the cracks and macro-pores from which, a volume of water equivalent to the total crack and macrospore volume for the soil profile may enter the profile as bypass flow (Neitsch *et al*, 2011).

2.4.4 SWAT Input Data Requirements

The Digital Elevation Model (DEM), land cover, soil types and climate data comprising the daily precipitation, maximum and minimum temperatures, solar radiation, wind speed, and relative humidity are among the data requirements in running the SWAT model. SWAT uses the DEM for automatic delineation of catchments, generation of sub-basins and stream network under ArcGIS environment. The model then uses the sub-basins, land cover and soils within the basin to obtain the HRUs.

Due to flexibility in operating the SWAT model, meteorological data at one or more locations in the basin provide sufficient information to run the SWAT model (Droogers *et al*, 2006). The weather generator within the SWAT model generates a set of daily weather data for each sub-basin. The generated data are for the purposes of filling in the missing data if any, in the observed records and as inputs in simulating stream flow under different land cover/land use types and climate scenarios. The precipitation generator component within the SWAT model's weather generator uses a first order Markov Chain model to define a day as wet or dry by comparing a random number generated by the model to the monthly wet-dry probabilities input by the user. Skewed distribution or modified exponential distribution curves show the amount of precipitation for days marked as wet (Neitsch *et al*, 2011).

Both maximum and minimum air temperatures and solar radiation are generated from a normal distribution where a continuity equation is incorporated into the generator to take account of temperature and radiation variations caused by dry and rainy conditions. The maximum air temperature and solar radiation are usually adjusted downward when simulating rainy conditions and upwards when simulating dry conditions so as to make the long term generated values for the average monthly maximum temperatures and solar radiation agree with input averages (Neitsch *et al*, 2011). In order to generate the daily mean wind speeds from the mean monthly wind speeds data, a modified exponential equation is used. The relative humidity model on its part uses a triangular distribution to simulate the daily average relative humidity from the monthly means.

Just like in the case of temperature and radiation, the mean daily relative humidity is adjusted to account for wet and dry day effects (Neitsch *et al*, 2011).

The SWAT model simulation outputs are separated into stream flow output and land based results. The stream flow outputs include the water quality and volume aspects for every stream in the basin. The land-based results vary, comprising all the components of the hydrological cycle as well as the erosion, pollutants, nutrients, and crop growth. These types of information are given per a sub-basin as well as per HRU (Neitsch *et al*, 2011).

Water balance is the driving force behind all sorts of problems worth studying using the SWAT model in a watershed. Hydrological simulations of a watershed by the SWAT model is organized into two main divisions namely: the land phase and the water routing phase of the hydrologic cycle (Figure 2.1). The land phase majorly controls the water movement over the land surface and therefore determines the amount of water that is eventually routed in the channel network of the watershed on to the outlet (Neitsch *et al*, 2011).

Vegetation canopy in a vegetated area intercept and hold some rainwater, denying it the chance to reach the soil, at least for a while, before joining the rest that fall directly onto the soil. When the rainwater reaches the soil surface, it first infiltrates into the soil until the soil shocked before generating overland flow or surface runoff. The surface runoff moves quickly based on the topography of the area towards the stream channel thereby contributing to short-term stream responses. The water that infiltrates into the soil profile has a retention period, depending on the soil type and water table, before making its way back to the surface water system via underground paths or to the atmosphere through evapotranspiration.

The land phase of the hydrological cycle controls the amount of water that goes into and out of the system. Precipitation component, a climatic event, controls the amount of water that goes into the system. For this to be so, the rainwater has to naturally or otherwise be distributed over and moved along the land with great accuracy. This greatly depends on the condition of the land surface that is determined by the land cover (Neitsch *et al*, 2011). The land cover thus, controls the amount of water that goes out of the system.

2.4.5 SWAT Model Calibration and Validation

Before the SWAT model simulation outputs and the analyses results can be used in decision-making processes, it is necessary to first calibrate and validate the model to reduce the uncertainties in the model simulations. This is done following a two-step procedure namely the model sensitivity analysis followed by the model parameter calibration and validation (Winchell *et al,* 2010).

2.4.5.1 Sensitivity Analysis

Model calibration is quite a complex and tiresome exercise due to the large number of model input parameters involved in the hydrological models such as the SWAT. It is therefore important to carryout sensitivity analysis before model calibration and validation exercise conducted in order to identify and rank the parameters based on their magnitude of influence on the hydrological responses in the catchment (Moriasi *et al,* 2007; Gassman *et al,* 2007). SWAT model employs two types of sensitivity analysis namely; local sensitivity analysis and global sensitivity analysis. In the local sensitivity analysis, the output responses identified by sequentially varying each of the model input parameters by a certain fraction while holding all the other parameters at their nominal values. This process is also known as One-factor-at-a-Time (OAT) method. The global sensitivity analysis on the other hand considers all the model parameters together and simultaneously perturbs them and then investigates their interactions and impacts on the model output (Glavan and Pintar, 2012; Veith and Ghebremichael, 2009; Griensven, 2005).

The sensitivity analysis method used in SWAT combines both local and global sensitivity analyses by using the Latin Hypercube and One-factor-at-a-Time (LH-OAT) sampling where the LH samples are used as the initial points for an OAT design. The LH generates the distribution of the plausible collections of parameter values from a multi-dimensional distribution and hence forms the initial points for an OAT design (Liew and Veith, 2010; Griensven, 2005). The LH simulation is based on Monte Carlo simulation and uses stratified sampling for efficient estimation of the model outputs. The parameter distribution in the LH simulations is divided into *N* ranges each with a probability of occurrence of *1/N* where each of the ranges is sampled once for purposes

of generating random numbers. The random combinations of the model parameters are used to run the model *N* times in order to cover the *N* range (Griensven, 2005).

The OAT method integrates local and global sensitivity methods. One parameter only changed for each model run to attribute the changes in the output to the changed input parameter. For *n* model parameters, *n*+1 model runs are necessary in order to obtain the effect of each of the parameters. Since the result of the influence of a parameter may depend on the values chosen for the remaining parameters, the process repeated for several sets of input parameters. The final effect is the mean of all the partial effects and their variance that is used as a measure of the uniformity of the effects (Ghebremichael, 2009; Griensven, 2005).

The combination of LH and OAT methods ensures that the full range of all parameters have been sampled for an OAT design; that is a robust and efficient sensitivity analysis method. With m intervals in the LH method and p parameters, a total of m(p+1) model runs are necessary. The SWAT sensitivity analysis tool automatically performs sensitivity analysis both with and without observed data by varying the values of each model parameter within a specified range. Depending on the parameter, changes are made by any of the three methods; multiplying the values by a certain percentage, adding part of the value to the base value, or replacing the base value with a new value (Neitsch et al, 2011; Winchell *et al,* 2010; Glavan and Pintar, 2012; Veith and Ghebremichael, 2009; Griensven, 2005). The results of the sensitivity analysis are parameters arranged in ranks where the parameter with the maximum effect in catchment response is assigned rank 1. A parameter with a global rank of 1 is categorized as ‘very important’, Rank 2-6 as ‘important’ (Glavan and Pintar, 2012).

2.4.5.2 Calibration and Validation

One of the most common applications of the SWAT model is to evaluate the impacts of climate change and different land management practices on stream flow. The model is first calibrated and validated for the existing conditions before it performs the impacts studies (Arnold *et al,* 2012). Calibration is an effort to better parameterize a model to a given set of local conditions, thus reducing the model prediction uncertainty. Calibration process involves adjusting the model input parameters by comparing model outputs for a given set of assumed conditions with observed data for the same

conditions. Validation is the process of proving that a given site specific model is capable of making sufficiently accurate simulations. It involves running the calibrated model using a different set of data other than that used in calibration and comparing outputs to observed data (Arnold *et al,* 2012). There are three key steps in model calibration and validation. The first step entails the selection of a portion of observed data followed by running the model at different values of known input parameters and then comparing the output with observed data until fit to observation is good. The last step involves applying the model with calibrated parameters to the remaining portion of the observed data (Arnold *et al,* 2011).

Both automatic and manual calibration options are available in SWAT model (Arnold *et al,* 2012; Winchell *et al,* 2010). The automated calibration scheme, in-built in the SWAT2012, is used to calibrate the model by assigning appropriate lower and upper bounds of parameter values before initiating the process (Moriasi *et al,* 2007, Liew *et al,* 2005). The scheme executes up to several thousand model runs to find the optimum parameter values (Gassman *et al,* 2007) under the assumption that all error variance is contained within the simulated values while the observed values are free of error (Moriasi *et al,* 2007). The model input parameters are adjusted within acceptable ranges (Arnold *et al,* 2012; Neitsch *et al,* 2011; Gassman *et al,* 2007) until acceptable agreement between the simulated and observed values of stream flow is achieved (Glavan and Pintar, 2012; Krause *et al,* 2005).

As already confirmed by other studies (Van Griensven *et al,* 2012), projected impacts of climate change on stream flow are associated with large uncertainties that arise from the climate model, statistical post processing scheme and the hydrological model (Bosshard *et al,* 2013). Using properly distributed datasets for calibration and validation of hydrological models can be a determinant factor in reducing these uncertainties (Bosshard *et al,* 2013). The uncertainties can be reduced further by carrying out a thorough assessment of errors in the data used in the modeling. Presently, the two main factors that are limiting further improvements in the accuracy of model simulations and predictions are the quality of the data used and the scaling of the information at the resolution required by the particular application (Blasone, 2007).

From the foregoing review, none of the studies has specifically focused on the stream flow at the river basin level in relation to changes in climate and land use, especially in the Mara. PRECIS RCM products were only used to project future climate scenarios and no attempt was made to use the products to determine the impacts of climate change on stream flow (Omondi 2010; Sabiiti, 2008). The products of SWAT hydrological model used to determine the impacts of land cover, land use and climate change on stream flow in the Mara River basin. This study sought to establish the 'Impact of land cover, land use and climate change on the hydrological regimes of the Mara River basin for the period from 1983 to 2016.

2.4.6 SWAT Model Application

Over the past few decade, worldwide application of SWAT model have expanded, triggered by the needs of various government agencies, especially in the European Union and the United States of America to have direct assessments of the effects of climate change and anthropogenic factors on the water resources. Other studies have been exploratory, assessing the capabilities and potential applications of the SWAT model in the future (Gassman, *et al.,* 2007).

Arnold and Allen, (1996) used data measured from three Illinois watersheds of sizes between 122 and 246 km^2, to validate groundwater flows and recharge, evapotranspiration rates and surface runoff. Santhi *et al.,* (2006), conducted wide stream flow validations for two watersheds in Texas covering over 4,000 km^2. Arnold *et al.,* (1999) assessed sediment yield data and streamflow in the Texas Gulf basin whose drainage area ranges from 2,253 to 304,260 km^2. Approximately 1,000 stream monitoring gauges provided streamflow data from 1960 to 1989, which was used to calibrate and validate the model in this study. The results showed a 5% increase in predicted average monthly streamflow for three major river basins measuring between 20,593 and 108,788km^2 compared to the measured flows, where standard deviations between measured and predicted were within 2 percent.

Across the vast sub-continent of U.S.A, annual runoff and ET were validated as part of the Hydrologic Unit Model for the U.S.A (HUMUS) modelling system. A GIS linked SWAT model was used to simulate 10 years of monthly streamflow without calibration (Rosenthal *et al.* 1995). It was found out that, although SWAT model underrated the

adverse events, it produced accurate stream flows in the overall. In 1996, Bingner simulated ten years runoff for a watershed in northern Mississippi using the SWAT model in which, the model produced significant results in the daily and annual simulation of runoff from multiple sub-basins except those of a wooded sub basin. The SWAT model was successfully used in Central Texas to simulate flows, sediment, and nutrient loadings on a 9,000-km^2 watershed in order to locate potential water quality monitoring sites. Van Liew *et al*., (2003) assessed SWAT's ability to predict streamflow under varying climatic conditions for three nested sub- watersheds in the 610 km^2, Little Washita River experimental watershed in South Western Oklahoma. Their findings revealed that SWAT model could sufficiently simulate runoff for dry, average, and wet climatic conditions in one sub-watershed, after adjustment for relatively wet years in at least two of the sub-watersheds.

In Africa, SWAT model applications are found in various fields in the Nile basin (within which the area of study falls) and many other river basins especially those that require direct assessments of anthropogenic climate change, and other influences on a wide range of water resources (Ndomba *et al,* 2008; Setegn *et al,* 2008). In Sub – Saharan Africa, several case studies using the SWAT model have been applied successfully (Maliehe and Mulungu, 2017; Gabiri *et al*., 2019). For instance, Awotwi *et al*. (2015) used SWAT model to assess the impact of land cover and climate change on water balance components of the White Volta, which suggested that changes in rainfall lead to a corresponding change in all the water balance components. According to Guug *et al*., (2020), the SWAT model was successfully applied in the Sherigu catchment of Ghana and Southern Burkina Faso, where it provided detailed results of the hydrological processes. The model performed satisfactorily with acceptable statistical value of Nash-Sutcliffe (NSE > 0.7) and a correlation coefficient (R^2 > 0.7). The results provided a remarkable understanding of water availability in the catchment, particularly the percolation tank and surface runoff, which is key water use budget in a basin.

In a study conducted in a small watershed in South Africa, Govender and Everson, (2005) reported a comparatively strong streamflow simulation results. The findings in this study also showed that, SWAT model performed better over drier years compared to wet years. The however reported that, the model was unable to sufficiently simulate

the growth of Mexican Weeping Pine as a result of inaccurate accounting of observed increased ET rates in mature plantations. Qi and Grunwald, (2005) noted that most studies have calibrated and validated SWAT model at the drainage outlet of a watershed. Based on this, Qi and Grunwald, (2005) calibrated and validated SWAT model at the drainage outlet of four sub watersheds and found that, spatially distributed calibration and validation influenced hydrologic patterns in the sub watersheds.

In Kenya, the SWAT hydrological modelling has been used in a number of river basins to study the hydrological responses to changes in land use types and climatic conditions. Jayakrishnan *et al.,* (2005) used the SWAT to model the hydrology of River Sondu as part of assessment of the impacts of modern technology on the smallholder dairy industry. Sang, (2005) applied SWAT model to evaluate the impact of changes in land use, climate and reservoir storage in the Nyando basin. Jacobs *et al.,* (2007) applied the Soil and Water Analysis Tool Model to evaluate the ecological effects of reforestation in the higher elevations of the upper Tana basin as part of mitigation of economic damage studies. Githui, (2008) used the SWAT model in the Nzoia river basin as part of the assessment of impacts of environmental change studies.

Mango *et al.,* (2011) applied the SWAT model to investigate the response of the headwater hydrology of the Mara River to scenarios of continued deforestation and projected climate change. In all these studies, it was established that SWAT model produced outstanding results in the simulation of stream flow with changes in land use and climate scenarios. SWAT was also found to be suitable for assessing the impacts of land use and climate change on flooding. Additional advantages of SWAT model stem from the fact that it is provided freely in the market, has good technical support systems to use many databases at one go while at the same time it can use any available data (Gassman *et al.,* 2007). The SWAT interfaces with ArcGIS through Arc SWAT and this enhances overlay operations that promote change detection analyses (Winchell *et al.,* 2013). In the current study, the SWAT model was used to assess the impacts of land cover, land use and climate change on the hydrological regimes of the Mara River basin within the Mau forest complex, Kenya/Tanzania.

2.5 Research Gaps

Modelling the hydrological responses to changes in land use and climate in the Mara River basin has attracted many researcher in the recent times due to increased human induced climate change implications in the former pristine basin. A summary of some of the studies done in the basin include Mutie *et al*., (2006) evaluating land use change effects on river flow using USGS geospatial stream flow model in Mara River basin on Kenyan side. Mutie *et al*., (2006) found out that changes in land use in the Mara is resulting in low base flows and high peak flows. Mati *et al*, (2008), on the other hand, looked at impacts of land use/cover changes of the hydrology of the trans-boundary Mara River, and covered the entire basin. Among other things, they also reported increased incidences in peak flows with low base flows during wet and dry periods respectively.

Mango *et al*., (2010) Modeled the Effect of Land Use and Climate Change Scenarios on the Water Flux of the Upper Mara River Flow, Kenya. Mango et *al*., (2011) Land use and climate change impacts on the hydrology of the upper Mara River Basin, Kenya: results of a modeling study to support better resource management. The two studies reported well on the variations on river flows in the upper Mara River. Thus, the reported high peak and low base flows were due to deforestation in the headwaters. The studies on the upper Mara were based on the fact that, determining the hydrological responses to land use, rainfall and air temperature changes for the whole basin would give inaccurate representation due to the large spatial extent and the variability in topography, land cover/ land use, soils and climate of the basin. This study found out some problem with this argument because it did not recognize the upstream-downstream linkages in river basins that, events that occur in the upper part of the basin have direct influence downstream and that issues arising downstream may sometimes be addressed through interventions upstream. Effect of the water users in the rangelands and lower reaches on the flow volumes, for example, through abstraction were also not considered.

Dessu and Melesse, (2012) through modelling the rainfall and runoff using SWAT Model also reported similar conditions about river flow volumes in the Mara River basin, which are attributed to the degradation of the Mara through irrational land use practices and poor management of water resources. Other studies including Oruma *et*

al., (2017) have reported similar cases on the Mara River flow volumes despite the many study recommendations that have been put at the disposal of the policy makers to help them know best on how to formulate policies and regulations for sustainable water resources utilization in the Mara Basin.

The complex nature of the upstream – downstream linkages including the spatial heterogeneity in terms of topography, land uses and climate, together with the different manifestations of change, not only in the upstream but in the entire basin calls for the need for a multi-sectorial and basin-wide approach to water resources management. Changes within a basin differ in space and time, due to the above factors and therefore impacts of land cover, land use and climate on the Mara hydrology would better be understood when looked at according to sub basins. This is because different land use practices in the sub basins would lead to changes in rainfall and flow volumes due to changes in evapotranspiration rates, surface flow, infiltration, percolation and ground water reservoirs in the sub basins. Not many studies have been conducted at sub basins level for this kind of knowledge. Ochieng' and Kimaro, (2018) did a study in the sub basins in Mara but with a different objective, to compare performance of satellite derived rainfall estimates with the measured values.

This study closed the gaps stated above by conducting basin wide study on the hydrological responses to changes in land cover, land use and climate scenarios in the basin with emphasis on the sub basin characteristics of rainfall, surface flow, ground water, percolation and evapotranspiration as predictor variables in the river flow volumes.

2.6 Conceptual Framework

The linkages of land cover, land use and climate change and the Mara flow regimes over time were examined. The main linkages are through the Mara river basin hydrological cycle. Rainfall, temperature and evapo-transpiration constitute the major inputs into the basin. These climatic elements generate the river flow regimes. Since there have been changes in rainfall, temperature and evapo-transpiration, it is expected that stream flow is impacted as well. However, land cover land use and soil characteristics attenuate the flows of the Mara River. The implications of land

cover/land use categories and climate change may influence each other and generate stream flow of various magnitudes and variability.

From Figure 2.1, the conceptual framework, both vegetation cover, ground exploitation as well as climatic patterns are dynamic because of physical and anthropogenic factors. In most cases, changes in land use result in changes in the land cover which may have either positive or negative implications on the physical environment. Deforestation in any landscape or in a water catchment that comes with changes in land use practices result in reduced stream flows and general water supply due to reduction in rainfall since forests have direct input in rain formation. Removal of forests also leads to accumulation of greenhouse gases in the atmosphere, a process that encourages climate change over time that is witnessed in many countries, regions or areas in the form of reduced rainfall, high temperatures and increased droughts and floods events.

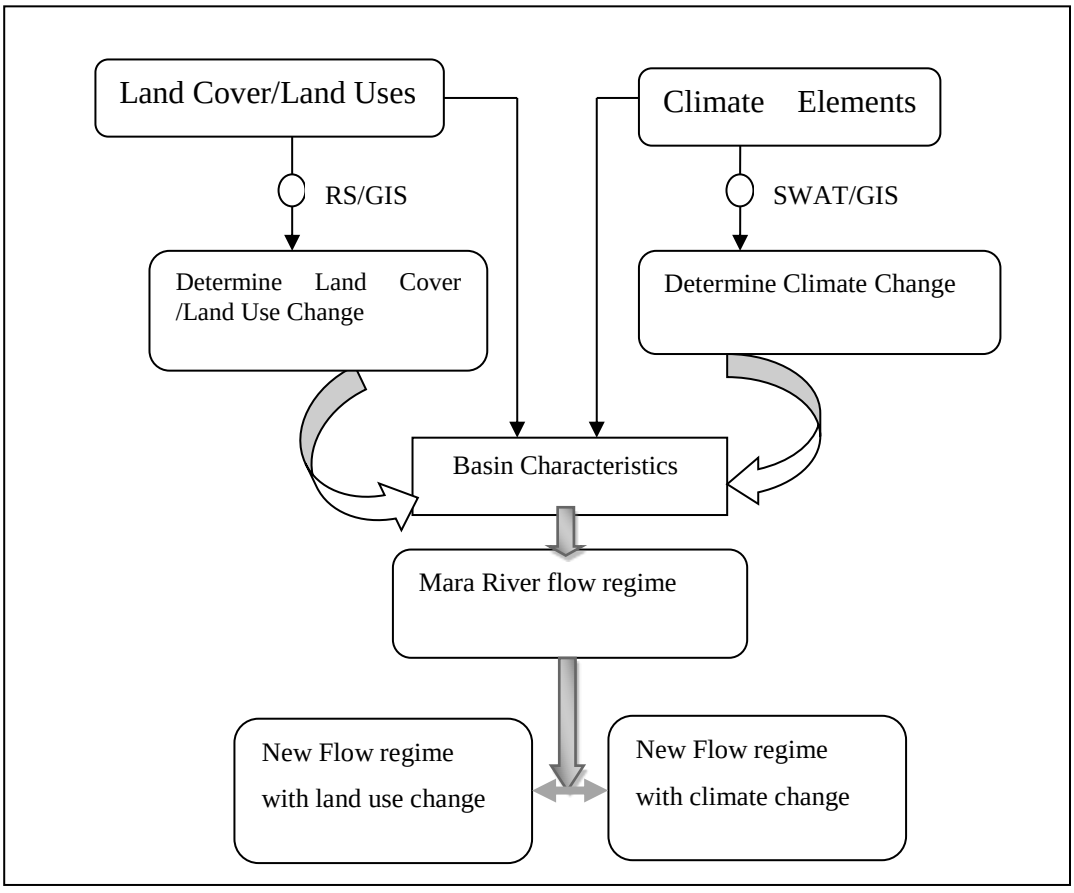

Figure 2.1: Conceptual Framework (Source: Researcher, 2017)

The changes in climate conditions may cause further changes in land use as people try to cope, adapt and mitigate climate change impacts. The process is bound to continue (cyclic in nature) as the two direct drivers of change continue to influence one another. These intervening factors alter the basin characteristics in that, exposing soil increases surface runoff, soil erosion and evaporation. Increase in temperatures and reduction in rainfall result in high evapo-transpiration and drought events. These conditions interfere with both the surface and underground water reserves and therefore have direct input into the water balance equation reflected in the variations in flow regimes characterized by reduced base flows and increased high flows following erratic rains. More variations in flowing patterns of the river are likely to occur as human activities together with climate conditions continue to be dynamic, obviously with negative implications on the water balance and general water supply.

CHAPTER THREE: DESCRIPTION OF THE STUDY AREA

3.1 Introduction

There are four primary basin characteristics affecting different aspects of stream flow hydrographs and therefore control the amount of water draining into a river network (Arnold *et al*., 1998). They include the factors that affect run-off response time (topography and size), factors that affect sub-surface base flow (geology and soils), those that affect water abstraction and run-off volumes (land cover/land use), and finally, those that affect the amount of rain water arriving in the basin (climate). These features and others basin characteristics are hereby presented.

3.2 Location and Size

The Mara river basin is a transboundary resource linking the two East African countries of Kenya and Tanzania and is situated on longitudes 33°47′ E and 35°47′E, and latitudes 0°38′ S and 1°52′S with a length of about 395 km. (Figure 3.1)

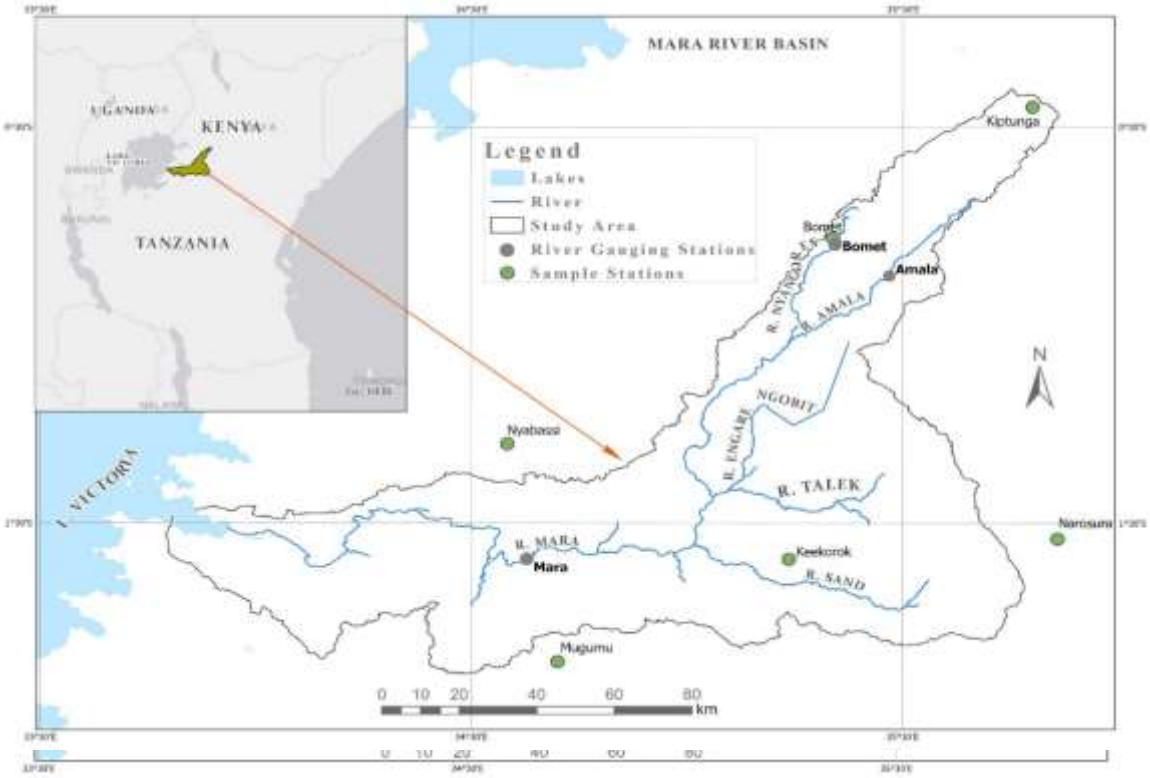

Figure 3.1: Location of Mara River Basin astride Kenya and Tanzania (Source: WREM International, 2008)

It drains a surface area of 13,750 km^2 of which, 8,941 km^2 (65%) is found in Kenya while 4,809 km^2 (35%) is found in Tanzania. The basin originates from the Napuiyapui Swamp in Mau Escarpment. It traverses Nakuru, Bomet and Narok Counties in Kenya and Ngoro Ngoro, Serengeti, Tarime and Musoma Rural Districts in Tanzania.

3.3 Geology and Soils

De Pauw (1984) reported that the lower reaches of the Mara River Basin, especially in Tanzania are made up of horizontal layers of young grey to darker shades of volcanic rock linked to metamorphic stones of pre-Cambrian rock origin. De Pauw, (1984) classifies the soils within the Mara basin into three namely: (1) Granite granodiorite foliated gneisses and magnetite found in Tarime's Northern highlands, Serengeti and Musoma districts. (2) Volcanic rocks of alkaline origin in the Southern highlands of Serengeti and Bunda districts, and (3) Meta-volcanic soils found mainly in Serengeti and some regions of Bunda and Musoma districts. Majule, (2010) adds that these soils are suitable for agricultural activities.

The Kenyan side of the basin is comprised mainly of Cambisols on the upper and middle zones whereas the bottom zones have Vertisols (Davies 1996). The Cambisols are good for agriculture because they are physically firm, permeable, have high hydraulic reservation with medium to elevated prolificacy. The Vertisols are dark clay and good in water retention, though they need special agricultural methods for more productivity (Mati, 2008). The underlying bedrock are of metamorphic origin (Lamprey, 2004) whereas upper catchments, which were formerly made of dense forests are now open forests on steep slopes.

The deforestation in the headwaters together with other activities degrading the environment have resulted in increased runoffs and soil erosion. Figure 3.2 shows the soils in the Mara River Basin. The highlands of Kenya have Andosols of volcanic origin and therefore, are deep, rich and well drained. These properties make them suitable for agriculture. With poor vegetation cover however, Andosols will erode very easily. The middle and lower regions are dominated Nitisols accompanied by other soils including the Planosols, Fluvisols, Leptosols, Phaeozems and Vertisols.

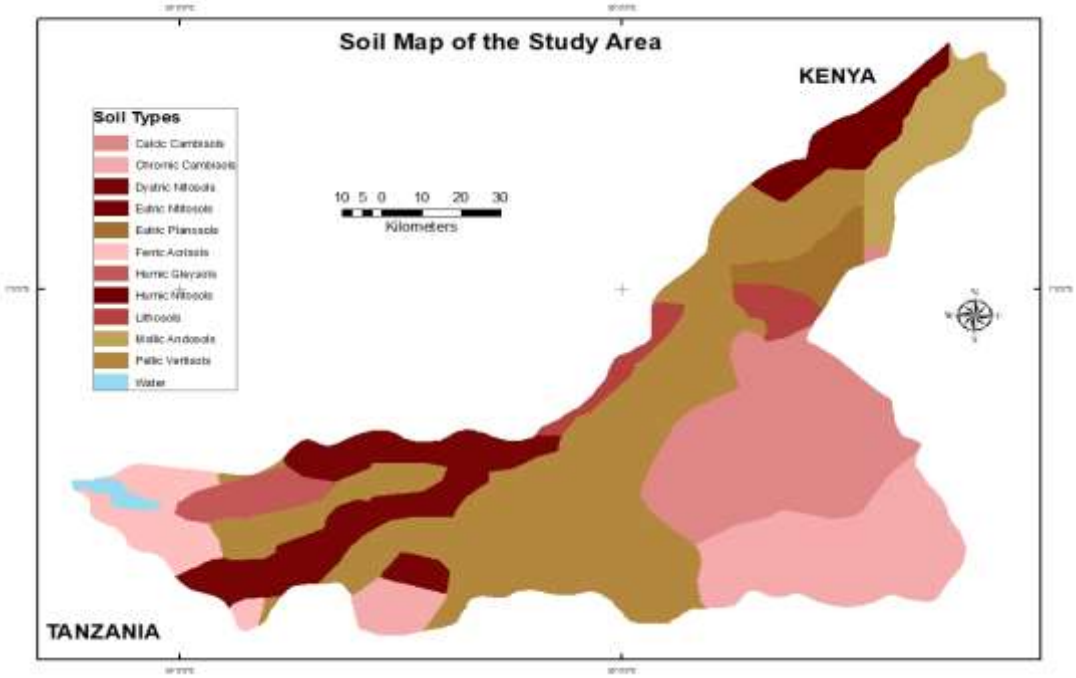

Figure 3.2: Soils in the Mara River basin (Source: Researcher, 2018)

Planosols, Vertisols and Phaeozems are common in the lowlands of Tanzania and Kenya. Generally, Planosols and Vertisols are poorly drainage and are prone to flooding and waterlogging during wet seasons. Understanding the soil properties in the basin is important because soil influences the rate of infiltration and runoff, topography and land cover being constant.

3.4 Topography and Drainage

At the source, the Mara River stands at an altitude of about 3057m and drains into Lake Victoria at an elevation of 1,106m (Figure. 3.3). This physiography consists of the Mau Escarpment to its north, Soit Ololo Escarpment to the west, Loita and Sannia plains to the east and southeast. Different land cover, land use, soils and topography, rainfall, temperature, evapotranspiration and water yields characterize the basin. All these factors have both individual and collective roles they play in the geography of the Mara basin and are therefore key to the planning, management and utilization of basin's resources especially water and land use practices. It is at Musoma in the northeastern side of Tanzania that the Mara River enters Lake Victoria. Its climate regime such as rainfall, temperature, river runoff, floods and droughts are dependent upon geographical location within the basin and the physiographic characteristics.

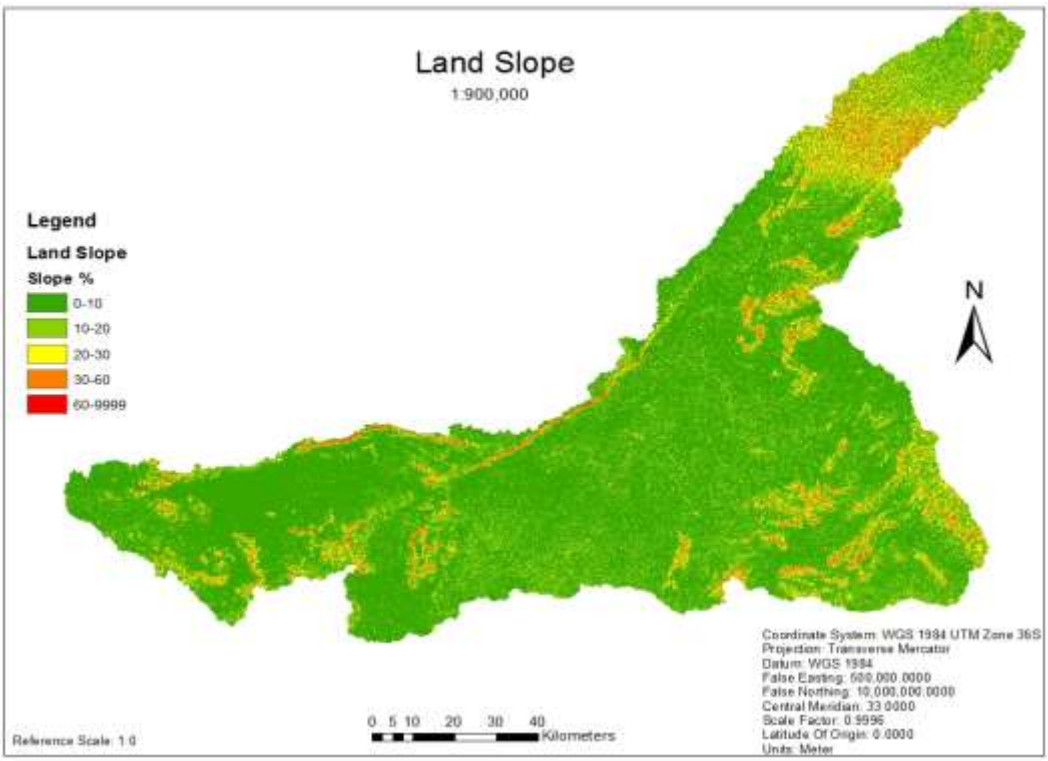

Figure 3.3: Slope of the Mara River Basin (Source: Researcher, 2018)

Five tributaries on the Kenyan side drain the basin including Amala and Nyangores that form the Mara River headwaters as they originate from the western Mau forest (Figure 3.4). The other rivers are River Talek, joining the Mara in the Maasai Mara Game Reserve from Loita plains; Engare Engito from the Ilmotyookoit and Soyet ridges; lastly, Sand river, joining the Mara at the Kenya-Tanzania border in the Serengeti plains. The Mara is joined by rivers Mori, Kenyo, Tambora and Nyambire (Mutie et al., 2006), among others on the Tanzanian side before it enters the Mosirori (Mara) Swamp on its way to Lake Victoria where its drains off at Musoma Bay.

The basin has 27 sub basins (Figure 3.5) and, with the variations already mentioned, do experience different runoffs, infiltration, erosion, droughts and flooding events. Understanding the topography of the Mara basin is necessary for this study because topography determines the run-off response time and the amount of rainwater that infiltrates into the soil. The drainage network indicates the nature of the basin's water

supply. River basins with steep gradients respond quickly to rainfall events, normally with flashy run-offs as opposed to the basins with gentle slopes.

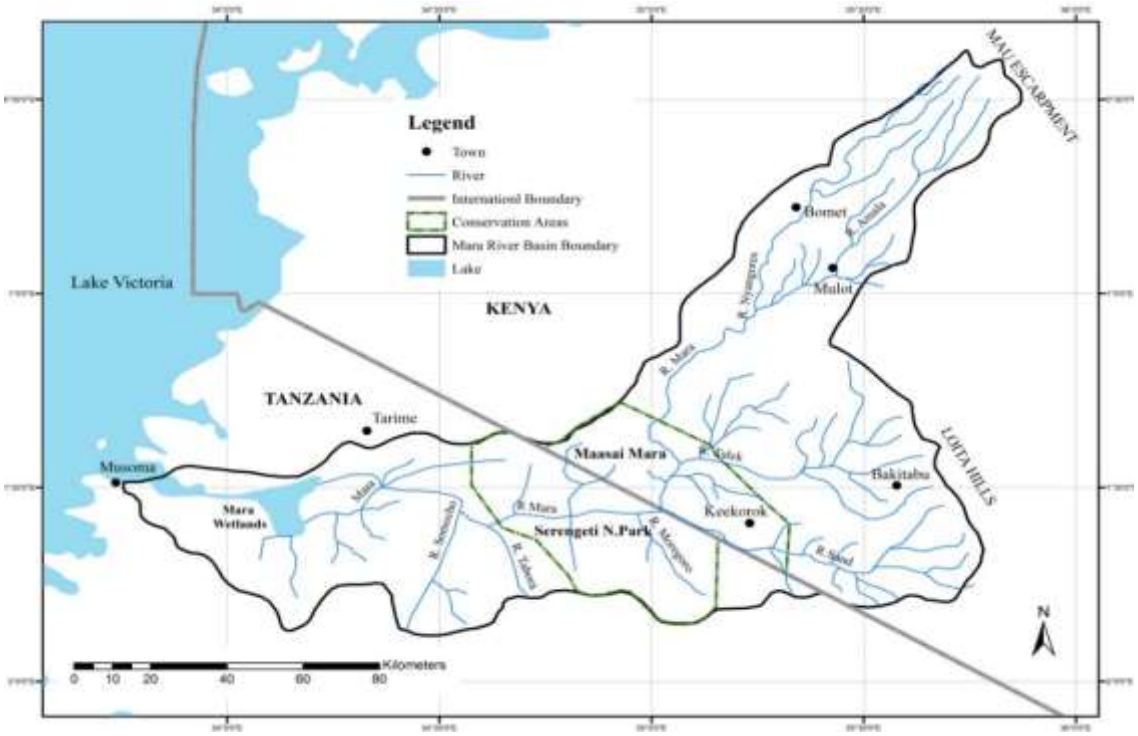

Figure 3.4: Mara River Drainage System. Source: (LVSB, 2015)

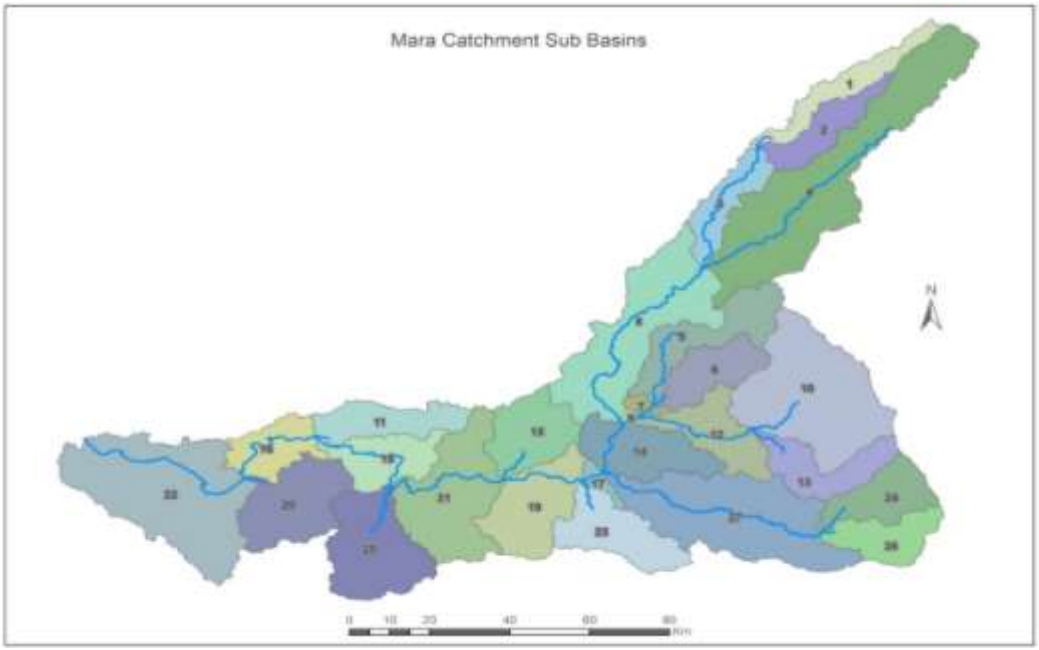

Figure 3.5: Sub-basins of the Mara River Basin (Source: Researcher, 2018)

Plate 3.1: Aerial View of the Mara River (Source: WREM International, 2008)

Plate 3.1 is an aerial view of Mara River basin. From the view, the basin is made of thicket, bushes and open areas, characteristic of a rangeland. The river is therefore prone to siltation and faces a lot of evaporation due to high temperatures.

3.5 Climate

The climate of Mara River basin is influenced largely by the movement of the Inter-Tropical Convergence Zone (ITCZ) air mass, modified by the local topography and the proximity of Lake Victoria, Atlantic and Indian oceans. Inter-Tropical Convergence zone is characterized by low and medium level convergences, usually marked by a line of thunderstorms and showers in most cases. It marks the boundary between the two inter-hemispheric monsoon wind systems over the region. Omeny *et al*., (2008) report that the ITCZ is the main synoptic scale system that affects the intensity, distribution and migration of seasonal rainfall over the Eastern Africa region.

Studies have established that, airstreams from the north and southern parts of the globe generally converge at ITCZ. Above Africa however, this general scenario is broken since the ITCZ breaks into two spatial components referred to as the zonal and the meridional components. This occurs over the central parts of Africa largely accredited to the contiguous geographic trenches, that is, Rift Valley and the row of high mountain summits of the East African region (Okoola, 1996). The zonal component of the ITCZ

is a zone of convergence between the NE and SW monsoons while the meridional component is a quasi-permanent low over the Central African region. The meridional component of ITCZ oscillates East to West and contrariwise. Most eastern stretch occurs in July and August when the arm is located above Kenya's Rift Valley highlands (Rwigi, 2014).

The eastern extent of the meridional arm of the ITCZ enhances the penetration of westerly winds further eastwards giving rise to enhanced June-July-August (JJA) rainfall over the western side of Kenya, including the Mara River basin from the Atlantic Ocean, the Congo basin, and Lake Victoria (Kiangi *et al*, 1981). The third rainfall peak observed in the western parts of Kenya during the JJA season are due to the movement of these air masses (Okoola, 1996). The zonal component of the ITCZ migrates north and south of the equator following the seasonal match of the sun with a time lag of about one month. It traverses the Mara catchment area twice a year bringing with it the long rains during the March-April-May (MAM) season and the short rains during the September-October-November (SON) season.

The Atlantic and Indian Oceans are the major sources of moisture for the East African region and therefore greatly influence the regional climate through interactions associated with Oceanic and atmospheric circulations (Nyakwanda *et al*, 2009). The above normal rainfall over the upper catchment is associated with the low-level circulation patterns dominated by easterly inflows from the Indian Ocean and westerly inflows from the Atlantic Ocean and the Congo basin. Lake Victoria trough induces a mesoscale circulation with a strong diurnal cycle over the lake basin region. The existence of a large water body (Lake Victoria) brings about a thermal contrast between the land and the water surfaces. This thermal contrast initiates local circulations that include land-sea breezes.

The temperature contrasts between the lake and the land during the day and night, resulting in a land breeze during the day and a sea breeze during the night. The Lake Victoria basin experiences rainfall throughout the year due to land-sea breeze interaction, enhanced during the three rainfall seasons (Sabiiti, 2008). Figure 3.6 is Hydrological Cycle of the Mara River basin derived from the SWAT simulation output. It clearly shows among other things, the average annual values for precipitation,

evapotranspiration, potential evapotranspiration, surface flow, percolation, lateral flow, return flow and revap from shallow aquifer. The difference between the averages in rainfall and potential evapotranspiration is very small, meaning that, the basin is a rainfall deficient area.

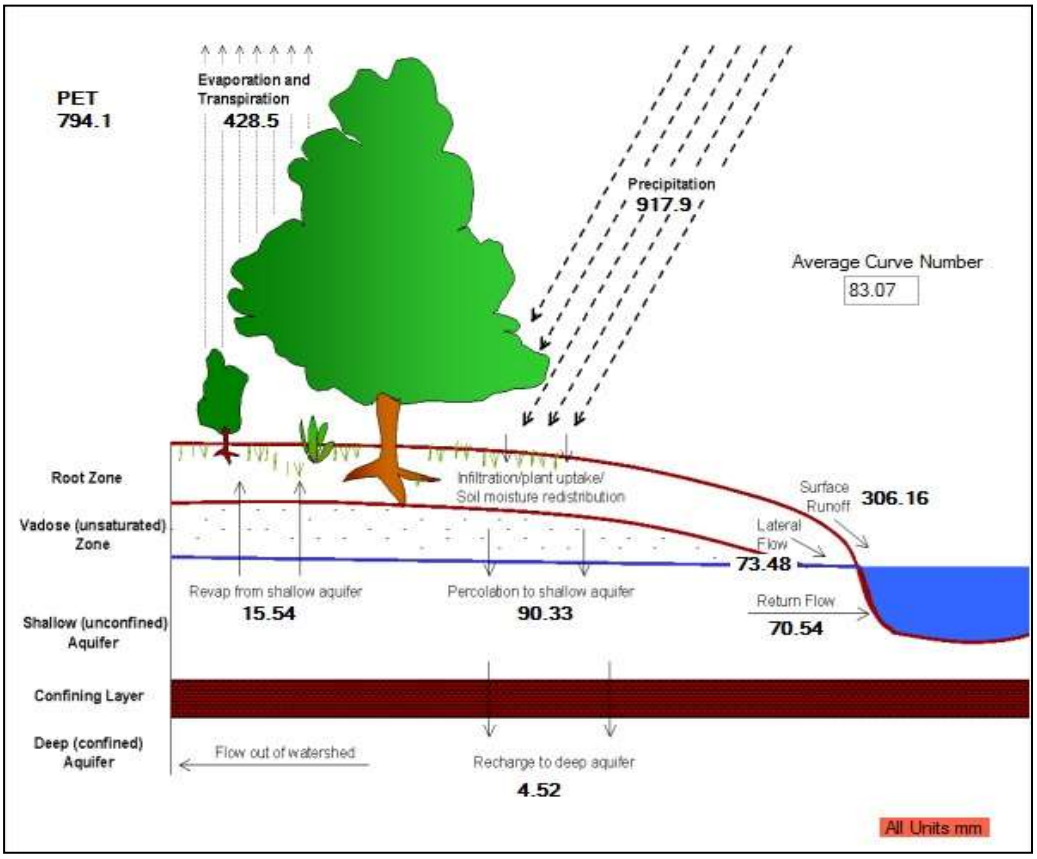

Figure 3.6: Hydrological Cycle (Source: Researcher, 2017)

Unlike in the higher latitudes where climatic patterns are marked by high seasonal variability in temperatures, precipitation and evapotranspiration, among others, the climatic parameter with the highest variability within the tropics is rainfall. This is because seasonal temperature changes are relatively small within the tropics compared to the rainfall due to the insignificant seasonal changes in the solar radiation. The warmest month is normally February while July in the coldest, with an average range of about 10˚C between the warmest and the coldest months (Ahrens, 2009).

3.5.1 Temperature

The mean temperature of the Mara River Basin is 25^{o}C and temperature increases with decrease in altitude such that the forested upper parts are the coolest; the central parts generally cold while middle rangelands are hot with the lower plains including the Loita

area being the hottest (WREM International, 2008). The basin experiences 27-28^{o}C as the average maximum temperatures throughout the year with a lowest of 16^{o}C on hot months (i.e. October to March) and 13^{o}C during the cooler months (i.e. May to August)

3.5.2 Rainfall

The Mara River basin has two rainy seasons a year, influenced by the relief and the occasional motion of ITCZ as explained under section 3.5. The rainy seasons occur over March - May with April as its, peak while the short rains are experiences over September - November. The timing of the rainfall vary according to the location of a place within the basin (Krhoda, 2001). Many studies attribute these variations to human activities on the landscape, especially the deforestation in the Mau forest complex. According to Climatologists however, yearly differences result from solar and global climate indicators related to shifts in Pacific Ocean circulation. These are a cause and effects of world climate change, which may cause floods and dry spells.

Understanding the precipitation characteristics in the Mara is important because it is a key contributor to fresh water resources followed by ground water seasonality (Awotwi *et al.*, 2015). The Mau Escarpment experiences high annual rainfall of about 1,000 to 1,750 mm yearly, mid sections experience about 900 to 1,000mm whereas lower areas near Loita hills, Musoma and Mugumu have about 700-850 mm per year. The region experiences variations in rain in space and time thus regions of Lake Victoria Basin (LVB) have varied rain across the year (LVBC, 2013).

3.5.3 Evapotranspiration

Evapotranspiration in the Mara River Basin has been high, averaging about 71% because of the high temperatures associated with savannah grassland. Evidently, however, evapotranspiration is on the decline (Figure 3.7) despite an upward trend in temperature. The declining trends in evapotranspiration is due to deforestation and general decline in vegetation cover, whose continued trend may impact badly on the Mara basin rainfall amounts and distributions because reduction in evapotranspiration interferes with the linkage between the terrestrial hydrological cycle and the atmosphere. Vegetation cover in the Mara is therefore very important in the hydrology of the basin in including the absorption and retention of water beneath the surface, which sustains the River Mara annual flow especially during dry periods.

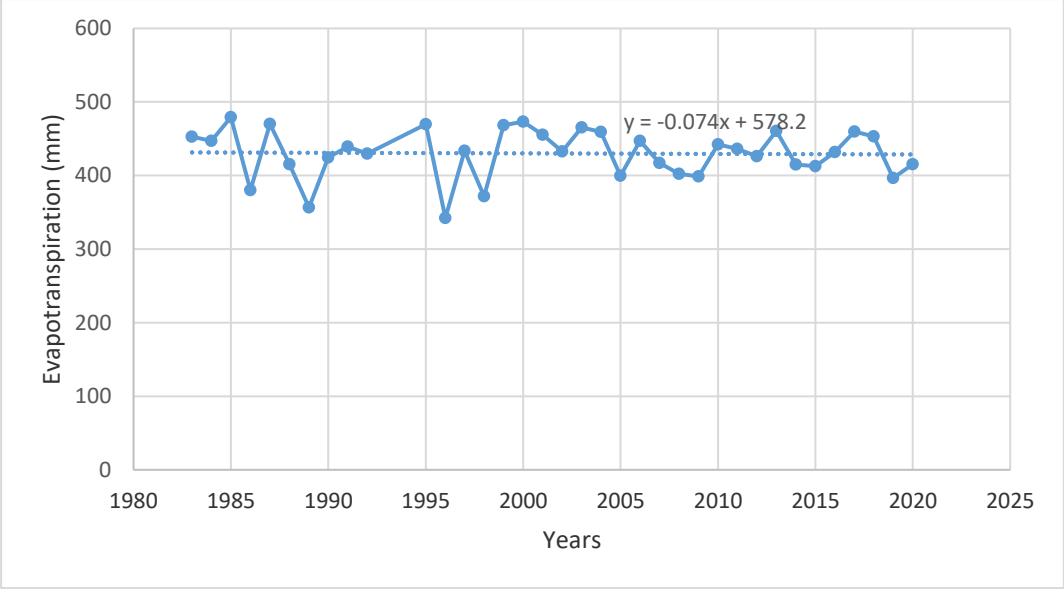

Figure 3.7: Annual Trends in Evapotranspiration. (Source: GoK, 2010)

3.6 Lakes and Wetlands

Africa's largest freshwater lake and the second largest in the world, Lake Victoria form the lower part of the Mara River basin because, this is where it pours about 5% of all the water the lake receives from the rest of the rivers (WREM International, 2008). Importantly, Mara basin is within the Lake Victoria's 194,000km^2 drainage basin, which stretches to Rwanda and Burundi. The 68,800km^2 Victoria water is a portioned amongst Kenya, Tanzania and Uganda in the ratios of 6%, 43% and 51% respectively. Lake Victoria is rich in various species of fish is main source of proteins for both local consumption and the far off markets in parts of Kenya and for export, therefore earning Kenya foreign exchange. The lake offers employment opportunities to anglers, fish traders, and other activities associated with fisheries and fish products. The lake is a resource of aquatic biodiversity and offers transportation, recreation and climate regulation functions (LVBC, 2010).

The Lake's catchment area has huge rain potential and therefore, key in agricultural activities and industrial sectors. Lake Victoria has high yearly evapotranspiration due to high temperatures and almost balances the annual rainfall over the lake. The contributions of the various rivers draining into the lake are very significant in ensuring a balance in the many systems in the basin. The lake in turn aids in hydrologic process of the river basins and in particular, the Mara catchment area by moderating its rainfall patterns. Plate 3.2 shows part of Lake Victoria at Musoma Bay in Tanzania.

Plate 3.2: Musoma Bay on Lake Victoria (Source: Researcher, 2018)

Wetlands are a common feature in the basin, mainly in the lower parts with the largest, Masurura being in the lower reaches just before Mara River drains into Lake Victoria at Musoma Bay in Tanzania (Plate 3.2). Masurura is usually full to its capacity during rainy seasons owing to excessive back flow as lake water stretches to approximately 45 km offshore and retreating to its least coverage in rainless seasons (Mati *et al*, 2007). The Enapuiyapui swamp is part of the upper catchment, found within the Mau Escarpment and source of Amala river because it feeds Amala via Nyabuiyabui stream.

Plate 3.3: Masurura Swamp in the lower reaches (Source: Researcher, 2019)

Enapuiyapui swamp is rich in biological resources of great importance to the local communities made of the Maasai and the Ogiek together with the immigrant farmers. These wetland ecosystems provide very important environmental goods and services, which include storage of water and water filtration among other gains. The encroachment on these wetlands by an ever-increasing population over the past few years is a threat not only to the important economic and ecological functions they provide but also to their very existence. Immigrant farmers affect Enapuiyapui swamp in the upper catchment more through logging and use of farm implements: it has declined a lot in its areal coverage, vegetation cover and water quality (WREM International, 2008; Mango *et al.*, 2011).

3.7 Agro-Ecological Zones

Agro-ecologically, the Mara River basin falls under the high, middle and low potential regions. Olenguruone of Nakuru County and Mau Narok Divisions in Molo Sub-county with an altitude of about 2,400 metres has high rainfall averaging about 1,270 mm annually (Table 3.1). Tea, potatoes and pyrethrum are the main crops grown in this zone with dairy cattle and sheep as the main livestock reared. Bomet County lies 900 - 1,850 metres above sea level and has moderate to high rainfall of about 1,100-1,500 millimeters per annum. It supports large-scale wheat farming and subsistence maize and beans farming.

Lower stretches of Narok Sub-county encompass the savannah grassland, lies between 1,500 and 2,100 metres of altitude, occupies around 1510 km^2 and hosts the Maasai Mara Game Reserve. This zone has a number of ranches that serve as dispersal areas for wildlife and large-scale wheat production with farms exceeding 10,000 hectares in size is a major agricultural activity in the Sub-county. The Trans Mara Sub-county, also in Narok County is within 900-2,500 metres above sea level and lies in the medium and low rainfall zones with annual average rainfall of 930.9 mm.

Table 3.1: Agro-Ecological Zones of the Mara River Basin

Zones	Agricultural Potential	Crops Grown	Rainfall (mm)	Altitude (mm)
I	High	Tea, pyrethrum, Irish potatoes, dairy cattle and sheep	Above 1300	Over 2,400
II	High- medium	Mixed e.g. wheat, maize and beans	1150 - 1300	1,800 - 2400
III	Medium	Livestock, wheat, wildlife	1000 - 1150	1,500 - 1800
V	Medium-Low	Cassava, maize, sweet potatoes and beans	600 - 1000	1,200 - 1500
VI	Low		Below 600	1000 - 1200

Source: WREM International, 2008.

The high potential areas are generally above 2400m of altitude and rainfall above 1300mm per year. The area is located in the Mau escarpment of the Mau forest complex and comprise of the Kiptunga, Keringet and Molo forests. Forestry, tea, dairy cattle and sheet are key features in this zone. The high to medium zone occupies areas around Bomet, Mau Narok and around Loita hills. Mixed agriculture including maize, wheat and beans are the main crops in this zone. These two zones lie on the Kenyan side of the basin with a bit of high to medium zone in Ngoro Ngoro in Tanzania. (Figure 3.8). The medium zone with rainfall ranging from 1000 - 1150mm occupies the ranches and areas around Loita hills in Narok County, lower part of Bomet, upper parts of Tarime District and the southern Serengeti in Tanzania. The zone has reasonable potential for crop farming and that is why wheat farmers have invaded the ranches. The zone supports livestock and wheat as well as wildlife.

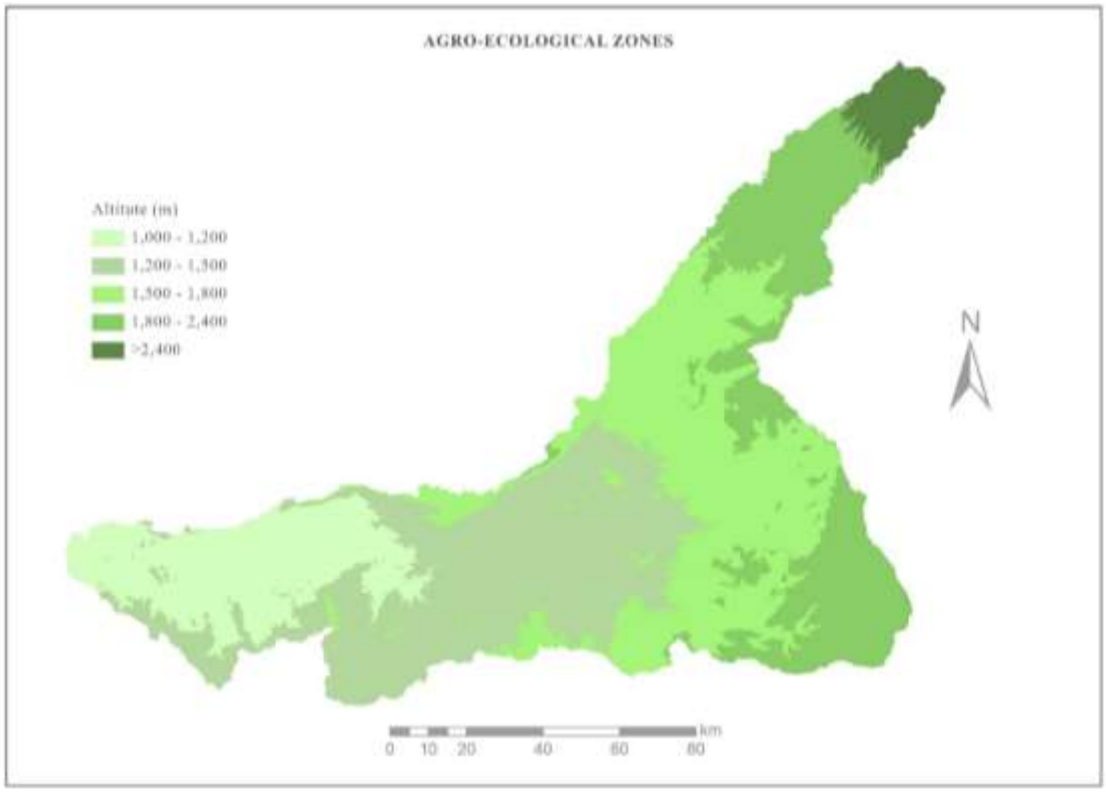

Figure 3.8: Agro-Ecological Zones of the Mara River basin (WREM International, 2008)

Tanzania's side of the Mara is covered mainly by the low and middle potential zones with only a few areas under high potential zones. The altitudes range from around 1000 to 1500 metres above sea level, mainly along the narrow strip off the lakeshore covering a distance of about 10 to 15 km. It covers the rural districts of Tarime and Musoma. The area has an average of 900mm of rain per annum. Tarime and Musoma as of the year 2003 had an estimated populace of 958,000 persons, Soils here are infertile but population pressure and alternative economic activities such as fishing have influenced farming activities in this place. The stable food crop in this zone covering about 35% of cropland is cassava and potatoes.

The staple crops grown for food in this region are maize, sorghum, finger millet, groundnuts and other leguminous crops with cotton as the major cash crop. The middle regions of Musoma, Tarime and Serengeti districts stretch from lakeshore into the highlands with an annual rainfall ranging between 900-1,250 mm, which is highly variable and increases with altitude. The cash crops in this zone are cotton and chickpeas. The apex region rests within Tarime's confines exclusively with an annual average rainfall exceeding 1500 mm and is bimodal in nature. Main cash crops in this

zone are coffee, sorghum and tobacco while cassava and maize are for food with cattle rearing as the main livestock in this zone.

3.8 Biodiversity

The River Mara Basin has a lot of diversity in its plants and animals. At the Mau escarpment, there is closed canopy forest, giving way to open forests in parts of Olenguruone and Maasai Mau (due to human interventions) to the plains including Loita plains to scanty forests, shrubs and thorny bushes of savannah grassland. Plate 3.4 shows some vegetation and impala found in the Mara triangle. The spongy and

Plate 3.4: Some plants and animals in the Mara Triangle of the Basin (Fieldwork, 2019)

Swamps are common in the catchment area though largely on the alluvial plains. Forest formations: *Aningeria-strombosia-Drypetes*, *Albizia-Neoboutonia-Polyscias*, along with mixed podo (*Podocarpus falcatus*) are found on western part of the Mau. *Aningesia-Strombosia-Drypetes* is reserved for forests found on western side of Kenya's Rift valley and occupies considerable part of the Mau forest.

The Mara system holds a large number of wildlife including Buffaloes, Elephants, Leopards, and Hyenas, Bongo, Yellow-backed Duiker, Golden cat, Giant forest hog, Colobus monkey and Impala. Some of the animals are of international conservation concern. The forests also host a rich variety of birds that represent the richest montane avifauna in Eastern Africa. Understanding the biodiversity of the Mara River basin is important because their conservation is key to sustainable tourism industry in the basin since it is critical in revenue generation in Kenya and Tanzania respectively.

3.9 Socio-Economic Activities in the Mara Basin

River Mara basin contributes immensely to Kenya's economy alongside that of Tanzania. It enables realization of socio-economic and environmental activities in these regions. Both the rural and urban population rely on Mara River for drinking water, irrigation agriculture, livestock rearing, fishing, wildlife conservation, tourist attraction, and industrial and mining activities. The Mara cuts across Kenya's Maasai Mara Reserve and Tanzania's Serengeti National thus attracting tourists and bio-diversification.

Mara Monograph report and many other studies on the Mara catchment have given detailed discussions of the opportunities, the concerns, obstacles and challenges that are ongoing in the basin due to human interventions (Mango *et al.*, 2011; WREM International, 2008). Such information enhances the perception and understanding of the various stakeholders of the need to conserve the critical Mara water resources in order to continue with its trans-boundary lifeline functions for the good of the populace and biodiversity whose lives depend not only on the mere existence of the Mara River but in sufficient water supply. The sub-sections below give an elaborate account of the various social and economic activities found on the Mara region.

3.9.1 Population

The Mara River basin has experienced high human population and livestock growth rates over the past three decades as more people, mainly agriculturalists who migrated from the neighbouring communities into the basin, especially into the areas that were largely under pastoral activities (WREM International, 2008). The Mara area Master Plan, (2006-2036) places the annual growth rates at 3.3 %, 2.7% and 2.3% for Narok South, Bomet and Trans Mara Sub-counties respectively while the overall rate was estimated at 2.4% (KNBS, 2009) and 2.5% for the Mara region districts of Tarime, Musoma, Serengeti and Ngoro Ngoro (TNBS, 2002).

In 2008, the Mara's population on the Kenyan side was 1,112,060 persons with Bomet leading in number of persons (Table 3.2) owing to high agricultural productivity (WREM International, 2008). According to the KNBS report (KNBS 2009), the Kenyan side of the basin had a total population of 1,481,366 spread at about 96 individuals per square kilometer. Tanzania's 2012 national head count indicated a total

Table 3.2: Population Size and Density in Mara Basin, Kenya.

SUB-COUNTY	Area (Km^2)	1999		2002		2008		2009	
		Pop.	Dens.	Pop.	Dens.	Pop.	Dens.	Pop.	Dens.
Narok S.	9650	223,725	23	250, 646	26	310, 388	32	355,114	37
Bomet	1882	382,794	203	417, 868	222	488,089	259	397,104	211
Trans-Mara	2846	170,591	60	87,459	31	100,100	35	182,070	64
Molo	1101	157,207	143	173,830	158	213,484	194	676, 991	615

Source: D. D. Plans, (2002-2008) - Narok, Trans Mara, Bomet and Nakuru and KNBS, 2009).

population of 1,287,547 people in Mara catchment zone spread at 83 individuals per square kilometer (TNBS, 2012). Bomet and Musoma, the largest towns within the basin lead in population at about 500 individuals per square kilometer. (LVBC, 2013). Lower reaches and some parts of middle zones are generally dry thus have sparse population. According to the KNBS report (KNBS 2009), the Kenyan side of the basin had a total population of 1,481,366 spread at about 96 individuals per square kilometer.

Table 3.3: Population Size and Density in Mara Basin, Tanzania.

DISTRICT	AREA (Km^2)	1988		2002		2012	
		Population	Density	Population	Density	Population	Density
Musoma Rural	1957	248,268	127	330,953	169	443,597	227
Tarime	3885	333,888	86	492,798	127	581,425	150
Serengeti	10942	111710	10	176,609	16	262,525	24

Source: Mara Region Social-Economic Profile, 2002 and TNBS, (2012).

Tanzania's 2012 National head count indicated a total population of 1,287,547 people in Mara catchment zone spread at 83 individuals per square kilometer (TNBS, 2012). Bomet and Musoma, the largest towns within the basin lead in population at about 500

individuals per square kilometer. (LVBC, 2013). Lower reaches and some parts of middle zones are generally dry and therefore have sparse population.

3.9.2 Land Cover and Land Use

Different types of vegetation and human practices characterize the Mara catchment area. The main cover types include forests, grassland, shrub land, wetland, cropland, water bodies and built-up areas while land use practices include farming, fishing, mining, plumbing and conservation of flora and fauna especially the forests and the wild life in the Maasai Mara- Serengeti ecosystem. The high influx of people in the basin has notable changes in land use practices leading to clearance of vegetation including forests for agricultural activities and construction of homes. Vegetation cover and human practices affect hydrologic abstractions as well as runoff volumes through canopy interception, evaporation and evapotranspiration dynamics (Rwigi, 2014).

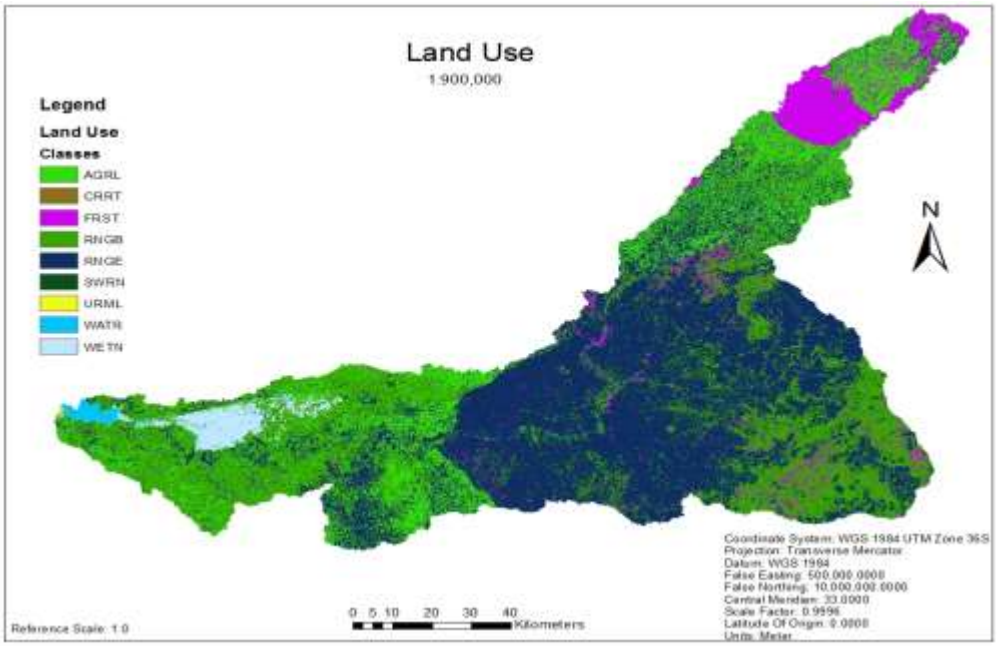

Figure 3.9: Land use types in Mara River Basin (Source: Researcher, 2018)

Thus, land use changes, especially those that result in reduction of forest cover and abstraction of water have had negative impacts on the hydrology of the Mara River basin. These impacts include faster run-offs with less infiltration and less ground recharge with reduced base flows. Increased flash floods and landslides in hilly areas also characterize the basin with increased sediment loads in rivers and lakes with increased drought frequencies and drying up of streams (WREM International, 2008). This study carried-out an elaborate evaluation of changes in land cover and land use in

the Mara River basin to establish the nature, extent, rate and magnitude of change and investigated the impacts of the changes on the Mara River Hydrological Regimes. The information was useful in establishing interventions to curb the undesirable human-induced trends that, if not regulated may impact negatively on basin's water resources availability and therefore, a deterrent to socio-economic development of the basin (Mutie *et al.*, 2006; Melesse *et al*., 2007; Mango *et al.*, 2011; Mwania, 2014).

3.9.3 Agriculture and Livestock Rearing

The populace in the Mara region rely on agriculture, which accounts for more than 80% of their occupation and livelihood. Relief of the area influences agricultural activities within the basin that is divided into four segments, for that purpose. These include the Mau forest complex, which is the source of the Mara River and lies between 2400-2900 metres above sea level and covers an area of about 82,410 hectares. The average rainfall per year witnessed ranges between 1400-1800 mm. Tea and dairy farming are a major agricultural activity in the area (O'Keeffe, 2007). A part from the Mau escarpment forests, the basin has a few plantation forests for timber and tea.

The second segment lies below the Mau forest complex with the protected South West Mau Reserve to the west. This area has an altitude that varies from 1600 - 2000 metres above sea level and characterized by large-scale farms of wheat, barley, maize, dairy cattle and sheep rearing with tea as the main cash crop. Eastern parts of the Mau forest and parts of Trans-Mara Sub-county have small to medium scale farms (5 to 20 hectares) of maize, beans, and potatoes. The third section ranges from an altitude of 1500 and 2100 metres in altitude, houses the Maasai Mara-Serengeti ecosystem, and covers about 1,510 km^2. This is a marginal area characterized by low and unreliable rainfall but very significant in supporting livestock production in the ranches and wildlife conservation in the Maasai Mara-Serengeti ecosystem (Gathanju, 2009).

The last section lies on the Tanzanian part of the basin and is mainly comprised of livestock farming. High population density characterizes this part of the basin that hosts about 20% of Tanzania's livestock- cattle, sheep and goats. Small scale mixed agriculture including the growing of maize, beans, and millet. The Mara Swamp (also known as Masurura swamp) which is an extensive wetland found within this section,

occupying the lower zones of the basin with papyrus farming and fish harvesting as key profit ventures.

Livestock keeping especially pastoralism by the Maasai community entail cattle, goats and sheep rearing as well as poultry farming. Other animals include pigs and rabbits keeping. About 90% of the livestock farming is on a small scale while some are pastoralists and mixed farmers. The animals are good sources of revenue through their sale and sale of the various products like meat and milk among others. Additionally, they provide help in cultivation with their excrement being good source of manure. The cattle are a source of recognition in the society as it also links people to their traditional practices and cultural values.

Maasai as an example, associate cattle to wealth and honor. They are also a medium for payment of dowry and the number of animals given out for dowry earns such marriages the respect and value in the society. Parts of the basin on the Kenyan side have some large-scale dairy farming and sheep rearing. The dominant breed kept by the local communities is the small East African Zebu and the Maasai type because they are resistant to most of the diseases and drought. Some group ranches keep the Boran and Saiwal breeds of livestock.

3.9.4 Fishing

Fishing and fish related activities are another sector that contributors to the socio-economic wellbeing of the populace in the Mara basin. Fishing is an important source of nourishment plus income generation to improve living standards mainly for Musoma district, which borders the shores of Lake Victoria. Most fishing activities take place in Lake Victoria and the Mara Swamp (wetland) as well as in fishponds within the district. The distribution of fish produced in the basin is through three channels namely: local consumption, sale to the fish processing plants for value addition before exportation and selling in the markets in the neighbouring districts (LVBC, 2012). There are two fish processing factories in Musoma town where the fish is processed, packed and distributed to local and international markets.

Proceeds after the sale of fish, especially the Nile perch to the processing plants form the main source of income from fishing. Tanzanians consumes more fish than Kenyans do because communities like the Maasai who live in the basin consider eating of fish

an interdiction since they believe in eating meat from cows. A part from Lake Victoria offering a good fishing ground, the Mara wetland (Masurura swamp) offers a significant fishing ground. Catfish and lungfish survive generally in low oxygenated zones thus live in swamps. Aquaculture is a common practice on the Kenya side than on Tanzania with fish hatcheries being a feature on Kenyan side only (WREM International, 2008).

3.9.5 Tourism

Tourist attraction is an important income generating activity, contributes about 12 and 16% of gross domestic products for Kenya and Tanzania respectively. Mara ecosystem is famous globally as a wildlife sanctuary with the most robust and variety of animals. The Maasai Mara Game Reserve in Kenya and the Serengeti National Park in Tanzania are part of the Mara. Their rich mix of and large wildlife population attract a number of tourists each year from all over the world in the Mara ecosystem (Gathanju**,** 2009). The Mara's Serengeti Park in Tanzania has cultural, scientific and historic site with international conservancy activities undertaken to preserve the site. The park extends to about 14,763km^2 and hosts large number of animals and a variety of birds. Of all the twelve parks under the management of TANAPA, it attracts the largest number of tourists accounting to up to 40% of Tanzania's tourism. Tanzanian government has reported that the revenues generated by the park are at steady increment of around 12% annually.

The Maasai Mara National Reserve covers an area of 1,523 km^2 and together with the adjoining pastoral group ranches, forms an area with limitation of activities within the region only to wildlife conservation and tourist attraction centre. Birds' population in the Maasai Mara ecosystem is half the bird species found in Kenya i.e. 50%. It is a home to nine bird species which are threatened with extinction globally and because of this, it was declared by RAMSAR as 'an Important Bird Area' which must be conserved in the East Africa region. As far way back in1987, tourism sector remains Kenya's main source of foreign exchange with 18% of all the tourists visiting the Kenyan Mara area and generating 8% of gross tourist revenues. Tourist related services such as sale of traditional artefacts and crafts to the tourists is a source of revenue to the populace in tourists' attraction areas.

3.9.6 Forest and Forest Products

The forests found in the Mara catchment area help to sustain lives of the population around the area. They support various human activities including game hunting, bees hunting for honey, farming, animal grazing, and wood as a source of energy and fuel, charcoal generation, as well as herbal medication from various plants. They also use grasses and vines in weaving baskets and roofing of houses. Industries also get raw materials from forest e.g. timber industry, pulp industry and paper manufacturing plants. Last and importantly, it is a habitat for both plants and animals that attract tourists thus offer huge source of revenue and foreign exchange.

The Mara River basin forests fall into two namely: the upper and lower most zones respectively. The overlying Mau section encompasses Bomet County and four sub-counties including Molo, Narok North, Narok South and Trans Mara in Kenya. The management of the forests in the Mara basin fall in four different jurisdictions. The first block is Maasai Mau Forest that occupies about 45,794 hectares of land. Second is the gazetted, Ol Pusimoru Forest Reserve managed by the Kenya Forest Service (KFS) and lying on 36,832 hectares. The third one is South West Mau forest, approximately 81,000 hectares in size, a gazetted forest reserve and managed by KFS. Lastly, the Trans Mara Forest Reserve also gazetted, stands on about 35,270 hectares and managed by Kenya Forest Service.

Narok North Sub-County has the largest section of Mau region, which is significantly important as a watershed of other rivers. It is equally of regional significance, being the source of trans-boundary rivers flowing into Lakes Victoria and Natron. It is renowned for variety of plants and animals. It also supports livelihoods for the large populace found around the region. Tanzania hosts the bottommost sections of the drainage area with several forests including Kyanyari, Kyarano, Bwiregi, Nyabasi, Mogabiri and Tarime. The gazetted forests have a total area of about 3,092 hectares.

3.9.7 Mining and Quarrying

Mara River is rich in mineral resources such as gold mines, slates and sand. The Buhemba area of Musoma District and Nyamongo area of Tarime District in the lower Mara have two large open-pits for gold mining that are a source of livelihood to many families. Other potential mineral resources include kaolin, limestone and gemstones.

The mines have attracted business communities and professionally skilled people in various areas including service providers. Mining related activities are disrupting the usual land uses and at the same time, have high demands on water resources. These conditions can have long-term environmental despoliation.

Plate 3.5: Buhemba and Nyamongo mining sites (Landsat ETM+, 2016)

CHAPTER FOUR: RESEARCH METHODOLOGY

4.1 Introduction

Research methodology is a systematical approach to solving problems in a scientific research. Methods and principles applied in realizing study objectives are presented. This chapter 4 is broken into several sections. Sections (i) Research Design (ii) Data Types and Sources (iii) Target Population and Sample Size (iv)Data Collection. Data Collection Instruments is in section (v), Pilot Survey Sampling Procedure in is presented in section (vi), Data Processing in (vii) Land Cover Classification in (viii). Land Cover Map Accuracy Assessment, Determination of Trends in Land Cover and Land Use, Determination of Trends in Rainfall, Temperature and River Discharge, Hydrological Modelling, and Analysis of Impacts on River Flow Volumes are presented in the rest of the chapter 4.

4.2 Research Design

This study used multistage, spatially distributed sample survey design to determine the impacts of land cover, land use and climate change on the Mara River hydrological regimes. Inputs in this study design included both qualitative and quantitative in-situ measurements, field observations and secondary data from existing databases. The watershed of the Mara River constituted spatial platform used to integrate all datasets required in the impact simulation and defined by the digital elevation model sourced from ARSTAR 30 metres resolution system. The delineated watershed shapefiles were used to specify the land cover, land use, hydrography and climate limits, respectively of the Mara River basin based on satellite imageries on land cover/land use and soils spatial data to define the hydrological response units (HRUs).

The HRUs together with weather information (observed and simulated) were used to create variable tables required in simulating the impacts on flow regimes. The simulated outcomes were calibrated using in-situ measurements of rainfall to reduce uncertainties in the model outputs and analysis results. Land cover types and position in the basin guided the selection of ground-truthing points, for validating the simulated and observed data. The resulting simulated flow regimes applied in determining the relationship between the Mara flows and the land cover/land use and climate in the

watershed. The estimations of the relationships were arrived at using geo-statistical technique of spatial autocorrelation.

4.3 Data Types and Sources

To determine the impacts of land cover, land use and climate change on the Mara River flow regimes there was need for information on the terrain, land cover types, land uses, soil types, river flows, topographical maps and weather. Most of the datasets used were secondary since the study was mainly spatial in approach (Table 4.1). Secondary data included the downloaded Digital Elevation Model (DEM), satellite imageries and global weather data (including precipitation, temperature, wind speed, relative humidity and solar radiation) for the Mara River basin. The other sets of secondary included the observed long-term daily rainfall and temperature records for six (6) weather stations. They were Kiptunga forest, (-0.45^{o}S, 35.80^{o}E); Bomet Water Supply, (-0.45^{o}S, 35.46^{o}E); Keekorok Game Lodge, (-1.58^{o}S, 35^{o}E); Narosura Chief's Camp, -1.50^{o}S, 3.80^{o}E; Nyabassi, -1.35^{o}S, 34.57^{o}E and Mugumu Primary School, -1.87^{o}S, 34.72^{o}E. The observed long-term daily river flow records for Amala, Nyangores and Mara gauging stations, located at -0.90^{o}S, 35.44^{o}E; -0.79^{o}S, 35.35^{o}E and -1.23^{o}S, 35.04^{o}E respectively. Others were the soils data, land use and topographical maps at 1:50,000 for Mara River basin. The datasets were from different sources including various geoportals.

The Digital Elevation Model (DEM) was from ARSTAR 30-metre resolution system and downloaded from the United States Geological Survey Global Visualization (USGSGLOVIS) website. The DEM was used to delineate the Mara watershed and to provide spatial platform to integrate all the datasets required in the impact simulation. Climate data used in the simulation exercise was from the global weather data records as opposed to the use of observed data. The use of satellite-based estimates was necessitated by the fact that, Mara River basin is found within the basins that are poorly gauged and have incomplete historical climate and runoff records that cannot perform well in the discharge model..

Table 4.1: Data Type and Sources

Study Variables	Data Type	Data Source	Date of Data
Satellite Imageries:			
1. Landsat 5 TM 2. Landsat 5 TM 3. Landsat 7 ETM+ 4. Landsat 7 ETM+ 5. Landsat 8 ETM+	Secondary each at 30mx30m spatial resolution	From archives of European Space Agencies and secured through Nairobi based RCMRD. For land cover and land use mapping.	15/11/84 18/12/95 10/02/03 13/02/11 25/01/16
Digital Elevation Model (DEM)	Secondary (spatial)	United States Geological Survey Global Visualization (USGSGLOVIS). ARSTAR 30m resolution system. Used for basin delineation and as a platform to integrate the various datasets	16/01/15
Weather input data: - Including precipitation, surface flow, ground water, lateral flow, water yield and evapotranspiration.	Secondary	Global Weather data website. For simulation of land cover/land use and climate scenarios with river flows to generate the desired basin characteristics for this study.	1983 - 2016
Observed Hydro-meteorological Data: 1. Long-term daily records of rainfall. 2. Long-term daily records of minimum & maximum temperature. 3. Long-term daily records of river discharge.	Secondary	Water Resources Authority, (WRA) NHIF Building and Kenya Meteorological Service, (KMS), both in Nairobi. Others were Meteorological Agency, Ubongo Plaza, Dar-es-Salaam and Water resources Management Authority in Dodoma. Used in calibration and validation exercise to check the accuracy of the SWAT simulation exercise to reduce margin of error in the analysis.	1983 - 2014 1983 - 2014 1983 - 2014
Land Cover and Land Use Data	Secondary (spatial)	Food and Agricultural database for East Africa. Used to reclassify the land cover and land use maps from the images, according to SWAT format.	2003
Soils Data	Secondary (spatial)	Food and Agricultural database for Eastern Africa. It is an input in ArcSWAT simulation exercise. It is important in influencing percolation and overland flow volumes in an area.	2003

Topographical Maps at 1:50,000	Secondary (spatial)	Survey of Kenya Field Headquarter, Ruaraka Nairobi. For geo-referencing the imageries, DEM & FAO datasets	2005
Books, journals and statistical abstracts	Secondary	Institutional libraries, internet and other available sources	Various dates and periods
Population data from Kenya and Tanzania Population & Housing Census Reports.	Secondary	National Bureau of Statistics and other appropriate libraries	KNBS, 2009, TNBS, 2012, development plans, etc.
Ground Truthing & coordinates	Primary	Field Survey: to validate the thematic maps from Landsat imageries	2018
Photographs	Primary	Field Survey: Captured important details for inclusion in the thesis.	2018 and 2019

The observed long-term daily records of rainfall and temperature were from Kenya Meteorological Service (KMS) Headquarters at Dagoretti Corner for and were calibration and validation exercises to check for the consistency and accuracy of the simulation results. The observed long-term records of river discharge obtained from the Water Resources Authority (WRA) Headquarters at NHIF Building in Nairobi were for simulation using change scenarios of land cover/use and climate. The land use and soil maps for the Mara River basin were extracted from the Food and Agricultural Organization (FAO) databases for East Africa. The land use data was for reclassification of the land cover and land use classes got from the Mara basin satellite imageries since they were not in conformity with the SWAT Model formats used in the simulation exercise.

Soils data was a requirement as an input in the ArcSWAT simulation exercise since soil influences the amount of water that percolates into the soil and or drains overland. The Satellite imageries were from the geoportal of the European Space Agencies and procured through the Nairobi based Regional Centre for Mapping of Resources for Development (RCMRD). These images were used for the classification and production of the thematic land cover/land use maps required to determine the trends, nature, magnitude and rates of change in land cover and land use types within the Mara River

basin. The topographical maps of the study area at 1:50,000 were from Survey of Kenya Field Headquarters in Ruaraka, Nairobi and were used to geo-reference the Satellite imageries before image classification exercise.

In order to evaluate the nature, extent and rate of change in land cover and land use types, the study used cloud-free satellite images of the Mara catchment for the years 1984, 1995, 2003, 2011 and 2016. The study could not use equal interval in the satellite data used because those that were available were noisy or unclear and therefore not suitable for the task. The Landsat sensors used were as follows; - Landsat 5 Thematic Mapper (TM) images at Band 2 (Green: 0.52 –0.60 μm), Band 3 (Red: 0.63- 0.69μm) and Band 4 (the NIR: 0.76 – 0.90μm) for the years 1984 and 1995. Landsat 7, Enhanced Thematic Mapper Plus (ETM+) images at the same bands were used for the years 2003 and 2011 and Landsat 8, also ETM+ but with extra sensor facilities, (Operation Land Imager and Thermal Infrared Sensor) was used for the year 2016.

Figure 4.1 shows the Landsat grid scene coverage for the Mara River basin. Three grid scenes cover the basin namely: P169R060, P169R061 and P170R061. Landsat imagery was appropriate for this exercise since it has a band combination of Red, Green and Near Infra-Red that facilitates easy delineation of the various vegetation categories, the built up areas, the water bodies as well as the bare surfaces. Its spatial resolution of 30-

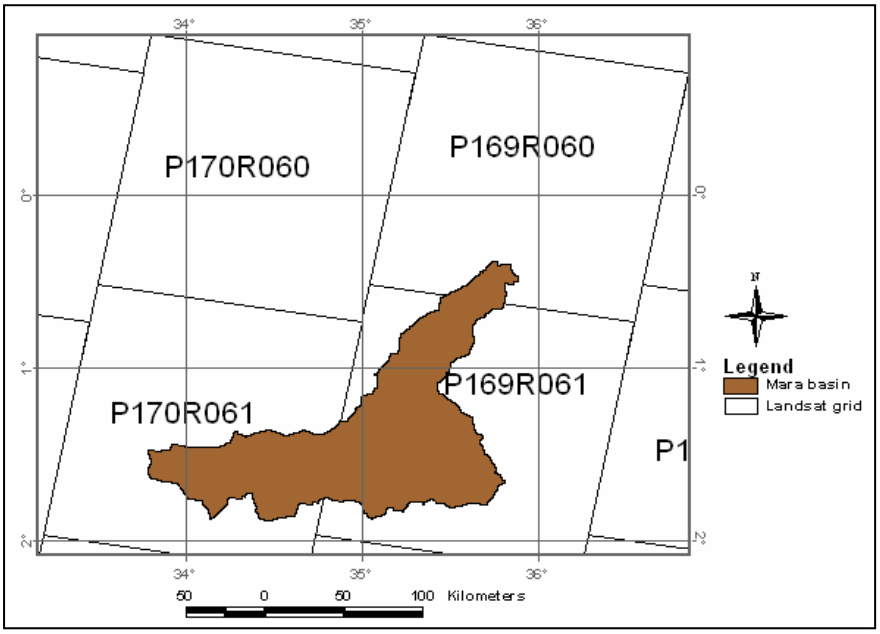

Figure 4.1: Landsat grid scene coverage for Mara River basin (Source: Mutie, *et al.*, 2006)

metre pixel and seven band radiometric resolutions make it suitable for land cover classification and, with its instantaneous field of view of 15 degrees and a swath width of 185 km (Jensen, 2005); it covers large areas and therefore many features within one scene.

The Landsat sensors TM, ETM and ETM+ respectively, are an improvement of each other in terms of spatial resolutions and spectral bands. The choice of the sensors was made on this basis. Table 4.2 shows the specific Landsat series used for each year of study together with the image scene identity. Each grid scene has three scene identities.

Table 4.2: Image scene identification used in cover classification

Year	**Landsat series**	**Image Scene ID used**
2016	Landsat 8	lc81690602016047lgn00
		lc81690612016047lgn00
		lc81700612016054lgn00
2011	Landsat 7	lt71690602011017mlk00
		lt71690612011017mlk00
		lt71700612011184mlk01
2003	Landsat7	le71690602003067sgs00
		le71690612003067sgs00
		le71700612003138asn00
1995	Landsat 5	lt51690601995037xxx01
		lt51690611995037xxx01
		lt51700611995092xxx02
1984	Landsat 5	lt51690601984183xxx09
		lt51690611984183xxx09
		lt51700611984254aaa01

Ground truthing points covering different types of ground cover meant for validating the thematic maps got from the image classification exercise of the satellites, procured from the field. These included the GPS coordinates of the selected temperature, rainfall and river flow recording stations and photography of the various landscapes and features relevant to this study.

4.4 Target Population and Sample Size

Various target population groups formed part of this study, including all the land use types, all the weather stations (both operational and non-operational) and all the river gauging stations along the Mara River system and all soils in the basin. Each variable

had its own unique way of evaluation for inclusion in the sample. The land cover and land use analyses depended on imagery data sampled from all Landsat imageries of the Mara of same duration as the study. Images used were for dry seasons and only one month was included for each year of study – imagery target population. From this target population, samples were drawn depending on level of cloudiness (at least <20%), sensor, target object and month and therefore the intervals used for the various datasets were different. For the whole Mara basin, each month of the study period had three imageries forming a scene as shown in Figure 4.1. The sum total of the imageries for this study period on different intervals for 1984, 1995, 2003, 2011 and 2016 was therefore 15 from which, analyses scenes were created to get a total 5 scenes for the duration of study. All the weather stations in the Mara catchment (operational and non-operational) formed the target population (tables 4.3 and 4.4) for the samples for climate variability and change assessments using the SWAT hydrological model and other statistical techniques. Tables 4.3 and 4.4 show all the weather stations ever operated

Table 4.3: The Weather Stations in the Mara River Basin, Kenya

S/No	Code	Station Name	Location		Altitude (m)	Period of Recording	
			Lat.	Long.		Start	End
1	9035067	Kiboroni F. Co. Molo	-0.416	35.683	2697	1959	1977
2	9035079	Tenwek Mission	-0.750	35.366	2012	1959	2001
3	9035085	Olenguruone D.O.s	-0.583	35.683	2743	1959	2004
4	9035126	P.B.K. Olenguruone	-0.583	35.683	2591	2001	2006
5	9035227	Bomet D.O.s Office	-0.783	35.333	1951	1959	1992
6	9035228	Kiptunga Forest	-0.450	35.800	2957	1961	2006
7	9035241	Baraget Forest	-0,416	35.733	2865	1961	1997
8	9035265	Bomet Water Supply	-0.783	35.350	1951	1966	2006
9	9035284	Mulot Police post	-0.933	35.433	1829	1973	1997
10	9035302	Nyangores Forest	-0.700	35.433	2219	1979	2006
11	9035303	Nairotia Forest	-0.766	35.533	2310	1979	2006

12	9035324	Keringet Forest	-0.483	35.633	2560	1984	1999
13	9135008	Kaboron G. Mission	-1.000	35.233	1646	1960	1985
14	9135010	Aitong Hydromet	-1.183	35.250	1829	1960	1992
15	9135013	Keekorok Game Lodge	-1.583	35.233	1602	1965	1996
16	9135022	Africa Gos. Naikara	-1.550	35.633	2462	1967	1999
17	9135025	Ilkerin Integral D.P.	-1.783	35.700	2195	1973	1999
18	9135026	Governor's Camp	-1.283	35.033	1585	1973	2004
19	9135035	Kichwa Tem. Camp	-1.233	35.016	1887	1987	2002

Source: WREM International, 2008.

Climate variability analysis used both in-situ and simulated long-term daily weather records; temperature rainfall and discharge (observed) surface flow, ground water, percolation, water yield and evapotranspiration (simulated) respectively depending on climatologically acceptable radius plus consistency of recording and therefore, constituted the climate data population. Only stations with daily climate records ≥30 years formed the climate data target population. Since the climate inputs were essential in estimating river discharge in the Mara watershed, the discharge data were also for the period ≥30 years from the river gauging stations of the watershed for Nyangores, Amala and Mara rivers.

The in-situ measurements for rainfall, temperature and river flows were for determining the trends in each of them and for calibrating the simulated spatial climate data retrieved from the global weather database for the period 1983-2013 to reduce error margins. In estimation of the flow direction and flow accumulation, the study generated terrain information on the Mara watershed from a single Landsat ETM+, DEM grid, soils data, and then compared with the SWAT model.

Table 4.4: The Weather Stations in the Mara River Basin, Tanzania

S/No	Code	Station Name	Location		Altitude (m)	Period of Recording	
			Lat.	Long.		Start	End
1	09133000	Musoma Met	-1.50	33.80	1147	1921	2007
2	09133001	Busegwe Mission	-1.70	33.93	1219	1940	1990
3	09133002	Shirati Mission	-1.13	33.98	1158	1902	1990
4	09133004	Nyabangi	-1.55	33.87	1158	1949	2004
5	09133007	Kiabakari Prison	-1.77	33.85	1219	1954	1990
6	09133011	Lukuba Island	-1.40	33.70		1975	1989
7	09133018	Nyambono Pri. Sch.	-1.88	33.68		1977	1989
8	09134000	Tarime Agriculture	-1.37	34.38	1524	1933	1978
9	09134008	Nyabassi (Nyarero)	-1.35	34.57	1829	1943	1990
10	09134014	Bwiregi Pri. Sch.	-1.40	34.63	1799	1952	1976
11	09134016	Kisaka Nguruime	-1.57	34.47	1219	1952	1979
12	09134026	Tarime Hydromet.	-1.33	34.33	1280	1969	1989
13	09134029	Buhemba Tr. Centre	-1.77	34.08	1448	1969	2007
14	09134031	Nyiboko Pr. Sch.	-1.50	34.55		1970	1984
15	09134033	Mugumu Pri Sch.	-1.87	34.72		1970	2007
16	09134044	Geitasamu Pri Sch.	-1.73	34.62		1980	1989
17	09234005	Seronera	-2.33	34.92	1540	1960	1990

Source: WREM International, 2008.

4.5 Data Collection

The study relied on secondary data mostly and therefore, majority of the data were in digital form (soft copy), received through emails and flash disks from various organizations (Table 4.1). Collection of primary data happed during the ground truthing exercise and the main fieldwork and data included selected ground truthing points, digital photographs and field notebook records. The following subsections present the various data collection approaches in the study

4.5.1 Pilot Survey

The pilot survey was for purposes of familiarising with the study area in terms of size, physiography, biodiversity, the weather patterns and location of the institutions

earmarked for subsequent engagements during the actual field operations. The identification of the study target variables including the weather and river gauging stations (both operational and non-operational), land cover/land use types and soils in the study area took place during this survey. The sampled weather and river gauging stations plus the land cover/use types - (ground truthing points) for validating the spatial land cover classes developed from the image classification exercise were identified and coordinates recorded, Plate 4.1 shows the Researcher in the field.

Plate 4.1: Researcher at the Amala River RGS

The survey was necessary for testing the data collection instruments such as the functionality and accuracy of the handheld GPS receivers and the Digicam, among the other instruments. Pilot survey estimated the duration, cost of field operations, and identified the challenges to the fieldwork. The view was to finding ways and means of overcoming the challenges i.e., based on the physiography, size of the study area, conservation (protected) areas, hindrances in transportation and weather patterns. Importantly, pilot survey helped in locating the actual positions of some of the sampled weather and river gauging stations and recording their coordinates for validating the coordinates from the data sources. Picking the coordinates of some of the sampled ground truthing points, based on the various land cover and land use types for validating the land cover classes obtained during the image classification exercise also took place during the pilot survey before the actual fieldwork. Photography of some important

features in the basin for the purposes of this study as well as writing down some details thereof took place.

4.5.2 Data Collection Instruments

A combination of information gathering equipment were utilized including digital cameras, handheld Global Positioning Systems (GPS), laptops, field notebooks and pens, portable hard disks, floppy disks and internet. The cameras were for taking take field photographs during reconnaissance survey and in the actual fieldwork. The handheld GPS receivers were for picking and recording coordinates of sampled weather and river gauging stations, the ground truthing points and the various land cover/land use types that were for validating the land cover classes from the imageries. The computers and laptops were for capturing various datasets, through keyboards and scanners and for enhancing the online retrieval and downloading of data from various geoportals and e-mail services. Hard copies such as topographical maps at 1:50,000 were loaded into the computer environment through Computer Scanners, for further processing and manipulation. Field notebooks, data sheets and pens were for recording information in the field that were relevant to the study objectives.

Internet sources were for securing data from various geoportal databases including the global weather database website, the United States Geological Survey Global Visualization (USGSGLOVIS) database website for DEM, the geoportal of the European Space Agencies for satellite imageries, and FAO geospatial websites for Africa for the land use and soils data. Portable hard disks, flash disks and CDs were to store the downloaded datasets including the global weather data comprising precipitation, surface water, ground water, evapotranspiration, lateral flow, surface flow, potential evapotranspiration and water yields. They were also for retrieving and storing satellite imageries procured from RCMRD and the in-situ rainfall, temperature and river flow measurements secured from the computer databases of Water Resources Authority (WRA) and the Kenya Meteorological Services (KMS) through emails.

4.5.3 Sampling Technique

Sampling technique is the process of selecting a sample that is as representative of the total population as possible in order to produce a miniature cross-section, a survey

called ‘sample survey’ (Kothari *et al.,* 2019). In this study, Multistage and purposive sampling techniques applied as explained in the following sub-sections.

4.5.3.1 Multistage Sampling

This is sampling procedure applied when the population from which a sample is to be drawn does not constitute a homogeneous group based on their geographical affiliation rather than some social characteristics like in the case of stratified sampling (Kothari and Garg, 2019; Lucy, 1996). Under multistage sampling therefore, the population is a portioned into a number of geographically non-overlapping sub-populations or strata. Each stratum has common characteristics such as relief, agro-ecological or climatic zones and soil types, which are some of the factors that influence rainfall characteristics and river flow volumes within a watershed and therefore fits well for use in this study. The choice of Mara River basin out of the five river basins that drain into Lake Victoria from the Mau forest complex for study was purposive. The choice was based on the premise that, the Mara is by large, a water deficient basin and yet has important transboundary, ecological and socio-economic functions that must be sustainable in the end.

The transboundary functions are that, it discharges about 5% of the water that drains into Lake Victoria and therefore important for the River Nile’s survival. Secondly, it is a lifeline to the world acclaimed conservation areas of Maasai Mara National Reserve in Kenya and Serengeti National Park in Tanzania. Ecologically, the Mara River basin influences microclimate modification and environmental quality. Finally yet importantly, the Mara waters support a variety of livelihoods such as agriculture, domestic, industrial and urban uses. To get the samples of the various variables, the basin was considered on the basis of the along profile of a river valley namely: the upper, middle and lower zones -based on the unique characteristics in terms of relief, climate and land use, each of which has direct implications on rainfall and river flow volumes.

Sampling of the study variables named in this study were purposively or deliberately done by the researcher based on the characteristics of the variables/population and the study objectives. A deliberate sampling technique is a form of non-probability sampling technique, which involves deliberately selecting particular units of the universe for

constituting a sample, which represents the universe in question (Kothari and Garg, 2019). In each stratum or zone, purposive sampling applied in selecting the temperature, rainfall and river gauging stations guided by their location and distribution within the basin and along the river profile. Only those weather and river gauging stations that had operated for over thirty years and had consistent records such as Bomet water supply, Keekorok Game Lodge, Narosura Met, Kiptunga forest, Nyabassi, Mugumu School, Amala, Nyangores and Mara qualified for inclusion in the sample. The records from these stations were used for calibration and validation of the simulated variables like water yields.

Sampling of ground truthing points were purposive, guided by land cover type and location in the basin. The ground truthing points were used to geo-reference the imageries and validate the classified land cover/land use categories and check the accuracy in the unsupervised classification. The Amala and Nyangores gauging stations are located in the headwaters and to that effect, the only two permanent rivers supplying Mara River with water all the year round. The soils at the selected river gauging stations were part of input data for simulating the river flows against the various land use and climate scenarios.

4.6 Data Processing and Quality Control

Hydro-meteorological and Spatial datasets obtained from data collection agencies were processed and subjected to quality control assessments that involved sorting, summarizing, aggregating and validating the raw datasets. The aim was to obtain the required data in the desired format and to ensure the cleanliness and usefulness of the datasets. The foregoing subsections give details of the operations performed on observed hydro-meteorological and spatial data from the area of study and the steps taken to ensure that their quality were uncompromised.

4.6.1 Digital Elevation Model (DEM)

Digital Elevation Model of 30-metre resolution for terrain derived from USGSGLOVIS online site was projected and clipped to fit in the Mara River Catchment using data transformation WGS 84 UTM zone 36 and saved as mara__fill_pr. The delineated Mara Basin DEM was necessary to account for water distribution and accumulation in the soil with respect to the area's topology. In order to map the topography in a more logical

manner to cater for all the minor differences in gradient, the basin was a portioned into five categories of slopes. This helped in quantifying the surface water storage, calculating the drainage network, density and the relationships thereof to the soil permeability, land use types and relief. The relationships established were compared with availability and distribution of hydrological resources in and across the slope of the area under study (Figure 4.2).

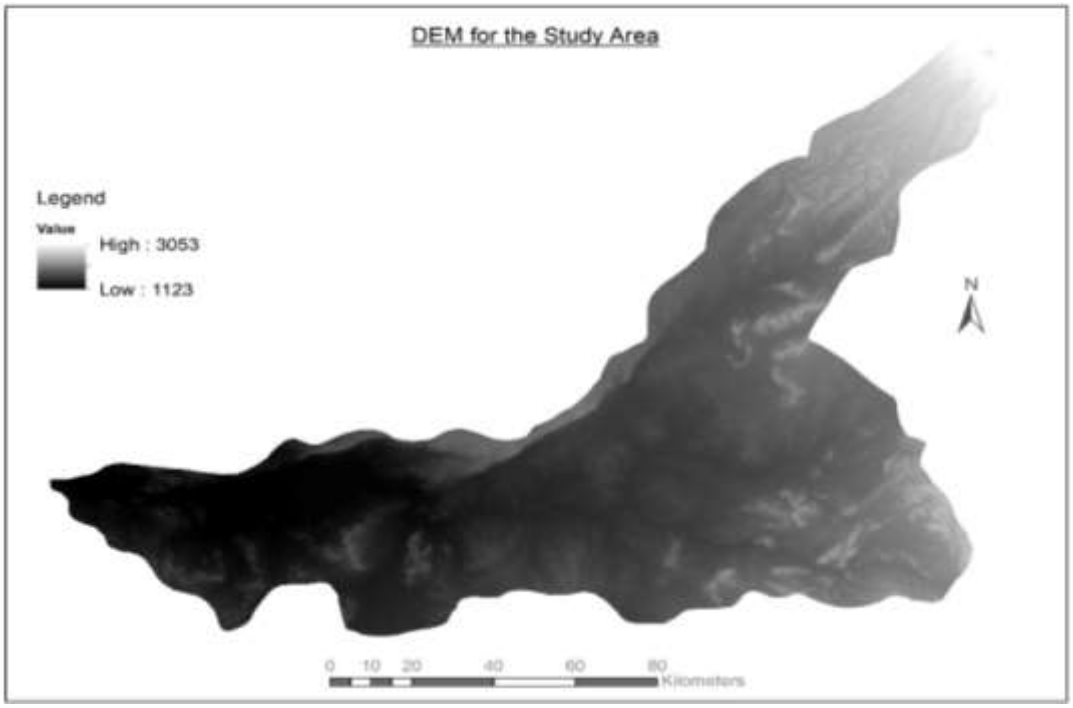

Figure 4.2: Digital Elevation Model of the. Source: US Geological Survey, 2017)

4.6.2 Image Processing

The image processing procedures used in this study are shown in Figure 4.3, a flowchart illustrating the stages involved in the preparation and analysis of land cover and land use dynamics in the Mara River basin over the study period. This includes image pre-processing, the design of classification scheme, image classification, accuracy assessment, analysis of the land cover/land use dynamics as well as the comparison of the changes across the years being studied.

The pre-processing procedures to correct for geometric and radiometric errors and comparing the images to per cent reflectance on the images. The images were geo-referenced in decimal degree coordinate system and rectified to correspond to the Clarke 1880 spheroid and the UTM projection. Topographical maps at scale 1: 50,000

covering the entire basin together with the ground truthing coordinates picked were reference data and for accuracy assessment.

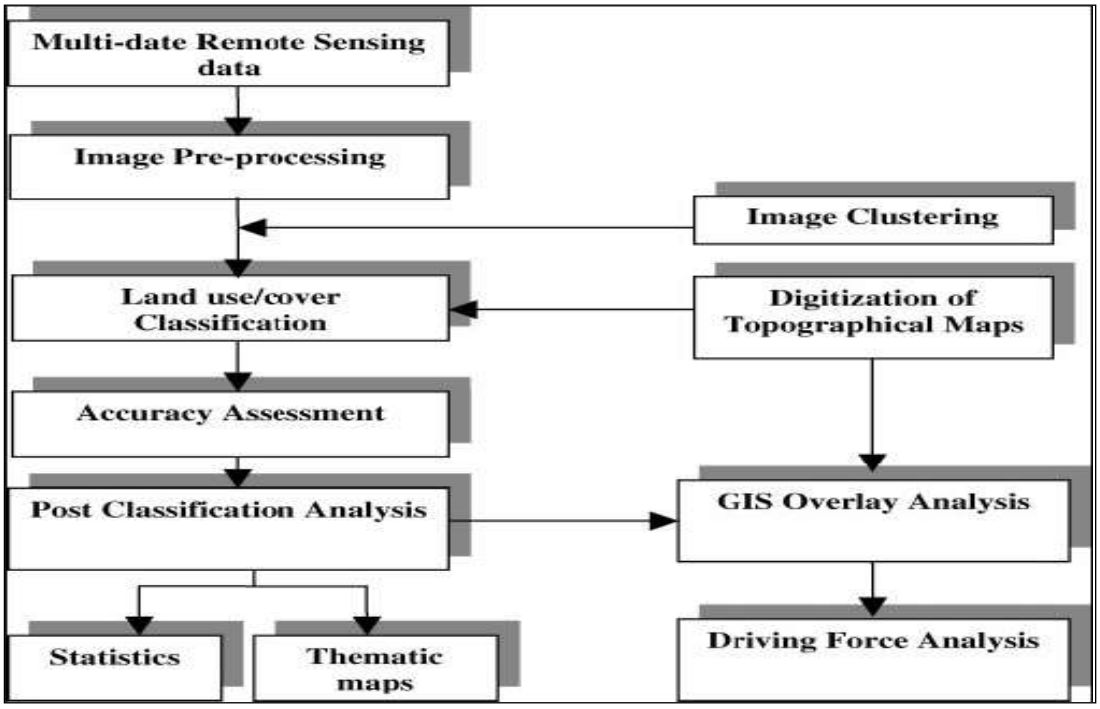

Figure 4.3: Flowchart for the analysis of land cover/land use dynamics (Source: Adopted from Jensen, 1996).

The geo-referencing of the images to correspond with the Clarke 1880 spheroid and the UTM projection was carried out using eleven (11) ground truthing points distributed within the basin (Table 4.5 and Figure 4.4) together with the tie-points in line with the number of image classification classes. Tie-points were the points whose geographical coordinates were derived from the 1:50,000 topographical maps covering the study area. On-screen digitisation using second-order polynomial transformation was carried out in order to rectify (geo-reference) the images to the topographical map coordinates.

The process resulted in a Root Mean Square (RMS) error of less than half a pixel. The images were further re-sampled to a pixel size of 30m by 30m using the nearest neighbour method in order to maintain the radiometric properties of the original data. The study employed the use of unsupervised method of Image Classification of which the first step was extracting Area of Interest from year 2016 larger imageries. It was important to do so in order to exclude data beyond the study area since imageries cover very wide areas with lots of data irrelevant to the study at hand. Towards this end, the

geographical coordinates of the study area or the area of interest were extracted from the vectorized map of the same.

Table 4.5: The Ground Truthing Points Used for Validation of the Cover Types

Points	Coordinates		Details
	X (Longitude)^{O}E	Y (Latitude) ^{O}S	
A	35.42416	-0.88472223	Quarry at Kapkimolwa
B	35.346389	-0.7894444	Bomet weather Station
C	33.975278	-1.5275000	Mara River Bridge, Tanzania
D	33.806389	-1.4977778	Musoma Bay
E	34.933333	-1.2616667	Kawai
F	35.126111	-1.1916667	Maasai Mara Reserve
G	35.390243	-1.0997310	Lemek
H	34.522965	-1.4687480	Mara Mines
I	34.618258	-1.7813410	Mugumu Mara
J	35.668839	-1.5983900	Naikarra Market
K	35.697353	-0.4643110	Sachangwan Shopping Centre

Source: (Researcher, 2018)

The coordinates were input in the ArcGIS 10.4 environment using extract by polygon function in the spatial analysis toolbox. The output of this operation is an extract of the study area fully geo-referenced in the coordinate systems in the three image bands. The extracted image of the study area was exported to ENVI 5.0 (remote sensing software) environment from the ArcGIS 10.4 environment in TIFF format. It is important to note that in the process, the exported image became unrectified and therefore another operation performed in the ENVI 5.0 environment to restore the geo-reference properties. The imported image was geo-referenced using tie-points and the geographical coordinate system. This process was repeated for all the remaining images namely images for 1984, 1995, 2003 and 2011.

Upon accomplishing the geo-referencing in the ENVI 5.0 environment, colour separation operation was done on the imageries followed by building of the colour composites of

the imageries using combinations of different bands until the combination, which was closer to the true colour was got. The combination found closer to the true colour within

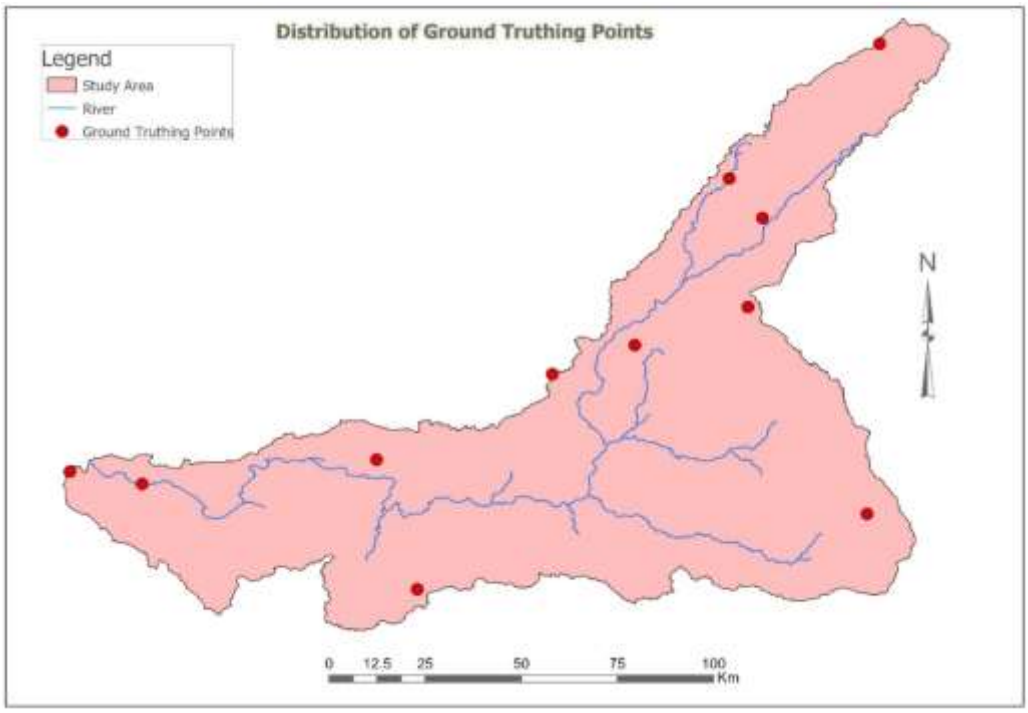

Figure 4.4: Ground Truthing Points for georeferencing, verification and validation

the band combinations under consideration was the band combinations 4-3-2 and thus, was used for the image processing purposes due to the ease with which they aid in visualisation and identification of the image features. The image classification process after establishment of the true colour composites involved the creation of the map list, sample set creation and classification domain creation. These operations necessitated the assignment of the classification schema to the pixels in sample set editor environment.

4.6.3 Hydro-meteorological data

The Hydro-meteorological data for this study were purely from secondary sources, as either measured or simulated. They included the long-term daily rainfall, temperature and river flow measurements from Kenya Meteorological Service (KMS) and Water Resources Authority (WRA). Other measured datasets were from Meteorological Agency, Ubongo Plaza, Dar-es-Salaam and Water Resources Management Authority in Dodoma. The datasets were processed and summarized into monthly, seasonal, annual and long-term mean values and sorted into their respective time series between January 1983 and December 2014. This was to provide a better description of the

climate patterns and the hydrological regime of the area of study. The simulated datasets on the other hand, were from the global weather website, in SWAT format, including precipitation, temperature, wind speed, relative humidity and solar radiation. The observed measurements were in tab-delimited format and therefore were transferred and recorded on excel spreadsheets in months and years from January to December for the years 1983 to 2014.

Due to incomplete records and large data gaps in the hydro-meteorological records in most river basins in the region, including the Mara, it was important to check the quality of these datasets before subjecting them to further analysis. This allowed for making valid inferences from the analysis of observed hydro-meteorological data. Data quality checks entailed careful scrutiny of the observed datasets to ascertain their completeness and consistency. Estimation of the missing data and homogeneity test applied in data quality control checks as explained in the following sub-sections.

4.6.4 Estimation of Missing Data

Continuity of data is a crucial research requirement since incomplete records in hydro-meteorological data may compromise the integrity of the results obtained from the data. Estimating the missing records of the hydro-meteorological datasets in this study was important to drive and calibrate the hydrological model that required continuous data records. Several methods are available in literature for filling in missing records of hydro-meteorological data. They include spatial correlation, weighted arithmetic mean, double mass curve, linear regression, normal ratio, and inverse distance among others. Details of these methods are in Rwigi (2004) and Opere (1998).

In this study, spatial interpolation and regression analysis were used in conjunction with weighted arithmetic mean method to fill in the missing records. The study applied weighted arithmetic mean approach to estimate missing rainfall and temperature values, linear regression was used for estimating the missing discharge values while spatial interpolation was applied in filling the gaps in SWAT model. A brief highlight on the weighted arithmetic mean and linear regression methods is presented in the foregoing sub-sections.

4.6.4.1 Linear Regression

Simple linear regression describes the linear relationship between two variables. The method seeks to summarise the relationship between the two variables by a single straight line (Equation 4.1). The linear relationship is a predictive model of the missing record using the corresponding available record in another station. Regression analysis of data from significantly correlated weather stations was performed to obtain the slope coefficient for the relationship, which was then tested for significance before the model could be applied to estimate the missing values.

$$\hat{Y}_i = a + bX_i \qquad \text{.....4.1}$$

$\hat{Y}_i =$ estimated random variable of the missing record series,

X_i = the available random variable corresponding to the missing record.

a = y – intercept of the regression line

b = the slope of the regression line (Wilks, 2006).

The values of ***a*** and ***b*** are obtained by minimizing the least slope equation (Equation 4.2).

$$\sum_{i=1}^{n}(Y-\hat{Y}i)^2 \text{.....4.2}$$

The significance of the slope was tested at $\propto = 0.05$ level of significance using student t-statistic computed using Equation 4.3

$$t_{cal} = \frac{b}{s(b)} \text{.....4.3}$$

t_{cal} = computed t-statistic

b = slope of the regression line

$s\ (b)$ = standard deviation of the slope

The calculated t-statistic (t_{cal}) was compared with the corresponding tabulated critical value t_{cric} and slope was considered significant whenever$t_{cal} > t_{cric}$. This equation was used also to determine the significance of trends in observed and simulated time series.

4.6.4.2 Weighted Arithmetic Mean Method

The weighted arithmetic mean is a popular technique employed in filling in missing meteorological records (Opere, 1998). In this method, the missing records are estimated using corresponding records of three stations, which are close and correlated to the station with the missing records. The ratio of the normal annual rainfall of the station with missing record to that of the station with data corresponding to the missing record is used as the weighting factor. The missing record is estimated using Equation 4.4.

$$P_X = \frac{1}{3}\left[\frac{N_X}{N_A} + \frac{N_X}{N_B}P_B + \frac{N_X}{N_C}P_C\right] \quad \text{.....4.4}$$

Where:

P_X = estimated missing record; N_X = the normal annual rainfall of the station with missing records; N_A = the normal annual rainfall of station A; P_A = the record in station A that corresponds to the missing record in station X; N_B = the normal annual rainfall of station B; P_B = the record in station B that corresponds to the missing record in station X, N_C = the normal annual rainfall of station C and P_C = the record in station C that corresponds to the missing record in station X.

4.6.5 Land Cover and Land Use Data

Land cover and land use data was from the Africa FAO geoportal database with a spatial resolution of 1km. The land cover/land use map, was clipped to the East Africa environment in general and to the Mara River basin in particular then projected and saved as Landuse_p2shp file. From the FAO land use file, a land use user table (lookup.dbf) file was created to match the SWAT land uses and the land use types in the Mara River basin. The projected land use file was saved as land use project_file folder. Use was made of the historical Mara basin land use maps created from the Landsat-TM, ETM and ETM+ satellite imageries for 1984, 1995, 2003, 2011 and 2016. A modified version of the Anderson *et al.,* (1976) classification schema consisting of eight land cover/land use classes was adopted for this purpose as shown in Table 4.6 on the next page.

Table 4.6: FAO and SWAT land use classes

LC_ Code	Land Cover	SWAT Code	SWAT Land Use	Detail
1	Forestland	43	FRST	Mixed Forest
2	Shrub land	51	RNGB	Range Shrub land
3	Grassland	71	RNGE	Grassland/Herbaceous
4	Cropland	85	AGRL	Generic
5	Wetland	92	WETN	Emergent/Herbaceous Wetlands
6	Water body	11	WATR	Water
7	Built-up area	21	URML	Urban Medium Density
8	Bare land	31	SWRN	Bare Rock

Source: Researcher, 2018

4.6.6 Soils Data

The soils for East Africa were sourced from the Africa FAO soils database, clipped to he East Africa environment and further specifically clipped to the Mara catchment area then projected and saved as soil2pshp file (Table 4.6). For the model to use the soil properties for the basin, a soils user table was generated by transforming the Mara FAO soils to the SWAT soils database format reflecting SWAT soils for the Mara basin (Table 4.7).

Table 4.7: FAO-SWAT Soil Classification Scheme

SNUM	FAO SOILS	SNAM	Soil Type
57	Gh7-2a	Gh7-2a-57	Humic Gleysols
76	I-R-bc	I-R-bc-76	Lithosols
412	Af32-1/2a	Af32-1-2a-412	Ferric Acrisols
440	Bc14-2bc	Bc14-2bc-440	Chromic Cambisols
443	Bc16-2a	Bc16-2a-443	Chromic Cambisols
467	Bk25-2a	Bk25-2a-467	Calcic Cambisols
802	Nd24-2c	Nd24-2c-802	Dystric Nitosols
805	Nd37-2/3ab	Nd37-2-3ab-805	Dystric Nitosols
848	Nh2-2c	Nh2-2c-848	Humic Nitosols

SNUM	FAO SOILS	SNAM	Soil Type
941	Tm10-2bc	Tm10-2bc-941	Mollic Andosols
960	Vp42-2/3a	Vp42-2-3a-960	Pellic Vertisols
970	Vp52-3a	Vp52-3a-970	Pellic Vertisols
977	We4-2a	We4-2a-977	Eutric Planosols
9999	water	WATR	Water

Source: Researcher, 2018

The new soils file was saved as faolookupnew.dbf. The aim was to avoid making errors during the delineation and the creation of HRUs in the process of modelling the watershed. Thus, the various soil types that existed in FAO were matched with SWAT and FAO East Africa soil types.

4.7 Data Analysis

4.7.1 Image Classification and Generation of Land Cover Maps

Image classification involving ISODATA Unsupervised classification approach to land cover classification was applied in which eight land cover types were used namely: forestland, shrub-land, grassland, cropland, wetland, water-bodies, built-up areas and bare-land. Maximum Iteration (MI), a parametric classifier was used to carry out the classification exercise that gave the static quantitative coverage for each cover type for each dataset. Appropriate classification scheme was developed using Landsat imagery of 2016 and a topographical map of 2014 at 1:50,000 since some of the details on the imagery could be identified on the map. During ground truthing, the same details were identified in terms of spectral signatures and coordinates to check on accuracy in the classification schema.

After the signature for each land cover category had been defined, the software used the signatures to classify the rest of the pixels. For every class used, mean values and variances of the DNs were calculated from all the pixels enclosed in each site for each band used to classify them. The images were vectorized under ArcGIS environment and the false colours clipped using ENVI 5.0, ready for full classification. Using the signature developed for every land cover category, the software automatically classified all the remaining pixels and gave them new polygon themes. Field validation and verification were done after preparing the maps to check on the level of accuracy and

to do corrections where necessary before using the maps for trends analysis and production of change detection maps. The classified images were converted from raster to vector format and the total area of each class estimated using geometry tools in ArcGIS software. Temporal land use changes between 1984 and 2016 were determined through post classification area comparison of the static thematic maps and overlay operations of the various land cover maps, specifically: 1984 and 1995; 1995 and 2003; 2003 and 2011; 2011 and 2016, respectively.

After carrying-out the above stated steps and having assigned commensurate number of pixels to various land cover/land use classes, the classified images were processed in the ENVI 5.0 using image-processing operation called classification. The output of this operation is the classified images that were exported to ArcGIS 10.4 software environment for layout design and polygonisation to enable labelling similar to manual image interpretation for the land cover/land use information. The accuracy of the images was assessed through crossing the sample sets and the classified images with accuracies being established using the confusion matrix operation in the ENVI 5.0, environment and accuracy of 90% and above were accepted. However, it is important to note that the variation in the levels of accuracy between the various images used in this type of study would be occasioned by seasonal variations at the time of the image acquisition.

As earlier mentioned, to analyse the land cover/land use changes that had taken place in the successive years, the cross-matrix function for the classified images was used. In this regard, the crossing of the images of years 1984 and 1995, years 1995 and 2003, years 2003 and 2011 as well as years 2011 and 2016 were undertaken. The output tables for the operations were generated to reveal the magnitude of changes in tabular format. The tables were further transformed into histograms using statistics operations in the ENVI 5.0 environment to reveal the percentage changes that had taken place between the successive imageries that were cross tabulated. The raster image of the operation revealed the spatial distribution of the changes. Upon completion of the operations, the land cover/land use classification outputs and the raster images of the detected changes were exported to ArcGIS 10.4 environment and geo-referenced for polygonisation. This process aids in the creation of spatial layouts of the various land cover/land use categories and the visualisation of the detected changes.

The classification process further enabled the calculations of the nature, extent and rate of change in land cover and land use types. The calculations were used to analyse the nature, extent and rate of change in land cover and land use that had occurred in the Mara river basin. It is also important to note that the exportation of the classified images and the change detection raster images to ArcGIS 10.4 environment further enabled the operations such as the maintenance and analysis of the spatial and attribute data, integration of spatial and attribute data as well as the output formatting, notably the overlaying operations among others.

The digitization was done for sets of land cover/land use layers augmented with such base map information like rivers and their tributaries, major roads and selected neighbourhood names as derived from the topographical maps of the study area. The classified images together with the digitized layers were further manipulated in ArcGIS 10.4 environment due to its capability to allow post-classification quantitative comparisons of land cover/land use changes that are clearly presented in the next chapter. The comparisons of land cover/land use statistics are crucial in identifying the percentage, trend and rate of change over the study period as well as for projection into the future scenarios.

A modified version of the Anderson *et al.,* (1976) schema consisting of eight land cover/land use classes was adopted for this study as illustrated by Table 4.8. Some of the factors considered during the design of the classification schema included the major land cover/land use categories found within the study area and the need to consistently discriminate land cover/land use classes irrespective of seasonal variations. This is informed by assertions of scholars such as Olang *et al*., (2011) who noted that there is need to limit the number of schema so as to avoid the spectral confusion, which occurs due to several land cover/land use classes having similar spectral response, which they note is the major cause of inaccuracy in digital image classifications.

Towards this end, spectral reflectance values were assigned to land cover and land use categories outlined in the schema. Where a number of mix pixels arose, spatial and contextual properties of the images were used to resolve the spectral confusion. This involved visual interpretation using the cover classes sampled with the Global Positioning Systems (GPS) during ground truthing meant to augment further

knowledge of spectral as well as spatial content to split the land cover/land use into their correct classes.

Table 4.8: Land Cover/Land Use Classes used in the Study

No	Classes	Description
i	Forestland	Evergreen forests, deciduous forests and mixed forests with closed canopy and little or no under storey vegetation. Others are open forests with undergrowth and regenerated vegetation.
ii	Shrub land	Sparsely distributed scrub with grass cover at the ground. Include acacia mellifera and Lawsonia inermis species and low-lying scrub species, usually less than 1metre.
iii	Grassland	Land largely of grass cover, inhibited by some scattered trees, scrub or thicket. Also called Savannah grassland.
iv	Cropland	Small-scale subsistence farms e.g. maize, tea/coffee farms, horticultural farms, wheat plantations, other agricultural crops.
v	Wetlands	Swampy or boggy land with biodiversity of plants and animals
vi	Water Bodies	Lakes, rivers, natural dams, reservoirs and waste water lagoons
vii	Built-up land	Urban, residential, transportation, communication and utilities, commercial and services, industrial, industrial and commercial complexes
vi	Bare land	Open land, exposed areas, quarries, wasteland and transitional areas

Source: (Modified from Anderson *et al.*, 1976)

4.7.2 Land Cover Map Accuracy Assessment

Image classification was assessed for accuracy to correct any errors and omissions that might have occurred in the classification process. The process included creating and using a classification error matrix to compare the classification results with the ground truthing data obtained during fieldwork (Table 4.9). The error matrix was evaluated by means of Kappa analysis, a discrete multivariate technique that yielded the statistic Ḱ (K_{hat} Coefficient of Agreement) estimate to measure the agreement between the remote sensing-derived classification map and the reference data. The assessment was done by selecting the menu item ***classifier>accuracy assessment*** and then importing the ground truthing coordinates from an Excel file which was already saved in text format. According to Coppin and Bauer (1996), whatever the algorithm used, the spectral image classification always results in accuracies ranging between 50% and 75%, depending on the number of available image registrations, the quality of the ground truth and the

number of considered change classes. In this case, overall classification accuracy is 72.5% and Overall Kappa statistic is 0.7245.

Table 4.9 Accuracy Assessment Results for 2016 Image Classification

Class	Reference totals	Classified totals	Classes Corrected	Producers Accuracy (%)	Users Accuracy (%)
Forestland	5	4	4	72.5	100
Shrub land	5	4	4	71.0	100
Grassland	5	4	4	74.2	100
Cropland	5	3	3	69.9	100
Wetland	5	3	3	73.1	100
Water body	5	4	4	75.0	100
Built-up Area	5	3	3	70.5	100
Bare land	5	2	2	74.0	100
Total	40	27	27		

The Kappa coefficient expresses the proportionate reduction in error generated by a classification process compared with the error of a completely random classification (Coppin and Bauer, 1996).

$$Kappa\ coeffecient = N\frac{\sum_{i=1}^{N} x_{ii} - \sum_{i=1}^{r}(x_{i+} \times x_{+i})}{N^2 - \sum_{i=1}^{r}(x_{i+} \times x_{+i})} \quad \text{..... 4.5}$$

r = number of rows in the error matrix; X_{ii} = number of observations in row I and column I; The diagonal element, X_{i+} = marginal totals of row I; X_{+i} = marginal totals of column I; N = Total number of observations.

The calculated value was scrutinized and found give a good agreement between the remotely derived map and the reference data from the field. The map was therefore linked to the look-up table for the SWAT hydrological modelling procedures.

4.7.3 Determination of Trends in Observed Data

The methods used in this study to analyse the processed data for purposes of meeting the stated specific objectives one and two. Including determination of long-term means, variance, and trend analysis of time series of observed rainfall, temperature, river flow and land cover/land use between 1983 and 2016 are presented here.

4.7.3.1 Time Series Analysis

Time series analysis is a very important tool for hydrological analysis. It is mainly used in building mathematical models to generate synthetic hydrological records, forecasting hydrological events, detecting trends and shifts, cycles and seasonality in hydrological records, and filling in missing records including extension of short hydrological records where necessary (Salas, 1993; Helsel and Hirsch, 2002; Rwigi, 2004). Time series analysis was used in this study to examine the past, present and future trends of hydro-meteorological and land use data. The following subsection presents the methods used to determine the mean, variance and trend sample statistics.

4.7.3.2 Overall Sample Statistics

The overall sample statistics, the mean *($\bar{Y}$)* and the variance *(S^2)* were determined for monthly and annual time series for rainfall, maximum and minimum temperatures, and discharge over the Mara catchment area. For a time series denoted by Y_t, the mean $\bar{Y}$ (Equation 4.6) and variance S^2 (Equation 4.7) were determined.

$$\bar{y} = \left(\frac{1}{N}\right)\sum_{i=1}^{N} y_t \quad \text{.....4.6}$$

$$S^2 = \frac{1}{N-1}\sum_{i=1}^{N}(y_t - \bar{y})^2 \quad \text{.....4.7}$$

$\bar{Y}$ is the sample mean, S^2 is the sample variance, N is the sample size, Y_t is the time series variable. These statistics were used to detect trends in observed and simulated data.

4.7.3.3 Trends Analysis

4.7.3.3.1 Trends in Land Cover and Land Use

Post classification change detection was performed on the thematic maps created from the Landsat imageries to get the spatio-temporal changes in land cover and land use. Post classification change detection is among the most popular technique applied under this kind of analysis (Lunetta and Elvidge, 1999; Chen, 2000; Singh, 1989; Coppin and Bauer, 1996; Pettit *et al.*, 2001). The maps were compared such that, the 1984 map was compared with the 1995, 1995 compared with 2003, and the process continued (Figures 5.1a -5.1e and Table 5.1). Change detection was further done through overlay operations (Section 5.2.3; Figure 5.3a-5.3d) using the unclassified images under ENVI

5.0 environment since this approach gives the software a better chance to get the most appropriate classes than when thematic maps were used in the change detection. The overlay operation produced four overlays or 'from-to', change matrices, each giving the quantities of change in each class in percentage and hectares. The detection of the changes provided the trends, magnitude and rate of change in the various cover types. The study gave an understanding of the implications of human intervention on the Mara basin over the years and the possible influence on the water flow in the Mara River system.

$$Land\ Cover\ Change\ (\%) = \frac{Observed.Change}{Sum\ of\ Area}.x.100 \quad \ldots\ldots\ldots\ldots\ldots\ldots\ldots\ldots\ldots\ldots 4.8$$

The land cover and land use change in percentage was calculated as in Equation 4.8 with positive values indicating increase while negative, a decrease. The spatio-temporal changes in land cover and land use were tested at $\alpha = 0.05$ level of significance using chi-square (χ^2) test, to test the null hypothesis that: 'Land use practices have not significantly changed over the study period in the Mara River basin'. Chi-square (χ^2) is a non-parametric test with a wide application such as determining dependency in categorical data or for comparing theoretical populations and actual or observed data when categories are of significance (Kothari, 2019). Thus, it can be used as a test of goodness of fit to see how well an assumed theoretical distribution (say water yield) fits to the observed data, such as rainfall. In this case, chi-square was used as a test of independence to enable this study to explain whether two attributes - land use and change over time are associated.

To carry out the process, the first task was to calculate the expected frequencies (expected changes in land use) using the actual land cover categories (observed frequencies) before working out the value of χ^2. The observed frequencies and the theoretical or expected frequencies were grouped in the same way and the theoretical distribution adjusted to give the same total frequency as that of observed distribution. Another advantage for using χ^2 is that, it has no rigid assumptions about the underlying distribution of the population. One of the disadvantages of χ^2 and non-parametric test statistics in general is that, they take too long to calculate despite being simple in their outlook (see Appendix V).

χ^2 was calculated as follows:

$$\chi^2 = \sum \frac{(O_{ij}-E_{ij})^2}{E_{ij}} \quad \text{.....4.9}$$

Where, O_{ij} = observed frequency of the cell in ith row and jth column.

E_{ij} = expected frequency of the cell in ith row and jth column

The value obtained (calculated) from the formula was compared with the table value at $\alpha = 0.05$ level of significance and the number of degrees of freedom. When calculated value is greater than the table value, the null hypothesis is rejected and verse versa.

4.7.3.3.2 Trends in Rainfall, Temperature and River Flows

Trends in hydrological data could be due to long-term climatic changes but for studies of this nature, the trends could be due to changes in the catchment as it responds to effective rainfall or flow dynamics due to land use changes that cause reduction in grass, shrubs and forest cover with general environmental degradation. There are many parametric and non-parametric methods of detecting trends. One of the most useful parametric methods of detecting trend is the simple linear regression analysis, which assumes normality of errors, constant variance and true linearity of relationships (Opere, 1998; Helsel and Hirsch, 2002). In this study, trends in temperature, rainfall and river discharge were determined using Mann-Kendall (MK) test, which is a non-parametric statistic. Microsoft Spreadsheet was used to compute ten-year variations in rainfall in the 1980s, 1990s and 2000s.

4.7.3.3.2.1 Mann-Kendall Test

The (MK) test statistic has been widely used in research for detecting trends in hydro-meteorological time series (Opere, 1998; Douglas *et al.,* 2000; Yue *et al.,* 2002b; Cong *et al.,* 2010; Burn *et al.,* 2012; Sang *et al.,* 2014; Chebana *et al.,* 2017; Serinaldi *et al.,* 2018; Wang *et al.,* 2019). MK-test is popular because it has no requirements for homogeneity or prior assumptions on the distribution of the variables (Önöz and Bayazit, 2003; Babar and Ramesh, 2014). It is also less sensitive to abrupt breaks in data, making it suitable for analysis of variables with inconsistent or missing records like hydro-climatic data (Kendall, 1975; Hamed and Ramachandra, 1998; Helsel and Hirsch, 2002; Hamed, 2007; Gao *et al.,* 2018; Dong *et al.,* 2019; Duan *et al.,* 2019).

The limitation of this method however is that, it may not apply to too short trends since the actual scale of change variation may be inaccurate (Wasserstein *et al.*, 2019).

Sense slope estimator

The Sen's slope estimator in MK test statistic was used to determine trends or nature of change in time series such that, a positive slope (+ value) indicate increasing trend and vice over a specified period. Generally, for any given time series, say $\{X_i, i = 1, 2\ldots, n\}$, the null hypothesis ($H_0$) assumes independent distribution while the alternative hypothesis (H_1), existence of a monotonic trend. The strength of the trend or magnitude of change is proportionate to the test statistic S, which is the total Sgn of the whole time series (Equation 4.10).

$$Sgn = (x_j - x_k) = \begin{cases} 1 & if\ x_j > x_k \\ 0 & if\ x_j = x_k \\ -1 & if\ x_j < x_k \end{cases} \quad \ldots\ldots\ldots\ldots\ldots\ldots\ldots\ldots\ldots\ldots\ldots\ldots 4.10$$

is computed as:

$$S = \sum_{i=1}^{n-1} \sum_{j=k+1}^{n} sign(x_j - x_i) \quad \ldots\ldots\ldots\ldots\ldots\ldots\ldots\ldots\ldots\ldots\ldots\ldots\ldots\ldots\ldots\ldots 4.11$$

Where $x_j - x_k$ is the indicator function resulting in the values -1, 0, 1 according to the sign of $x_j - x_k$ where j>k. Assuming that $x_j - x_k = \theta$, the value sign θ is computed as:

$$sign\ \theta = \begin{cases} 1 & if\ \theta > 0 \\ 0 & if\ \theta = 0 \\ -1 & if\ \theta < 0 \end{cases} \quad \ldots\ldots\ldots\ldots\ldots\ldots\ldots\ldots\ldots\ldots\ldots\ldots\ldots\ldots 4.12$$

This computation represents all positive differences minus all negative differences factored in the calculations.

The variance of S is calculate as;

$$var = \frac{1}{18}\left[n(n-1)(2n+5) - \sum_t f_t(f_t - 1)(2f_t + 5)\right] \quad \ldots\ldots\ldots\ldots\ldots\ldots\ldots\ldots\ldots 4.13$$

Where: n = length of data set; t = number of data value in a group of determination

The standard normal deviation (z-statistic) is computed as:

$$z = \begin{cases} (S-1)/se, & S > 0 \\ 0, & S = 0 \\ (S+1)/se, & S < 0 \end{cases} \quad \text{……. ……...…4.14}$$

Where *se* = the square root of *var*.

During the analysis, the trend would be said to be decreasing if Z is negative and the calculated probability is higher than the significance level. Correspondingly, the trend increases with positive Z and computed probability is more than the significance level. There is no trend if computed probability is lower than the significance level.

4.7.3.3.2.2 Microsoft Excel Spreadsheet

Other than using Mann – Kendall test, Microsoft Excel spreadsheet was used with the observed rainfall data from Kiptunga, Bomet, Keekorok, Narosura, Nyabasi and Mugumu rainfall stations to compute the mean monthly averages for the years 1984-2014, categorized into 1980s, 1990s and 2000s data sets and graphs drawn to illustrate the overall trend over the 30 years period.

4.8 Hydrological Modeling

This study used the Soil and Water Assessment Tool (SWAT), hydrological model in modeling the Mara hydrological regimes because of its unique qualities. First, it is a physically based model requiring specific information about the topography, weather, soil properties, vegetation and land use types that it uses as inputs in the simulation of the physical processes associated with the movement of water, transportation of nutrient and sediments as well as crop growth. These variables are important in achieving the objectives of this study. Being a physically based model, the SWAT is good in modeling ungauged watersheds and more importantly, quantifying the impact of alternative input data such as changes in land use and land management practices and changes in climate on water quality and quantity.

Secondly, it uses readily available data and can operate with minimum data and this makes it suitable for use in the Mara River basin, which has insufficient and unreliable hydro-meteorological data. Third, the SWAT model is computationally efficient and is able to run simulations of very large basins with different land management practices

like in the Mara basin without spending much time and money. Finally yet importantly, it is a continuous time step or simply, a long-term yield model, able to simulate long term impacts of land use, land management practices and pollutants accumulations (Neitsch *et al*, 2005). These qualities of the SWAT model enabled the quantification of long-term impacts of land use changes, variations in rainfall and air temperature on the hydrology of the Mara Basin.

Hydrological modelling was done to tackle specific objectives three and four: 'To create a simulation of river flow under different land cover and land use given varying climate scenarios in the Mara basin' and 'To generate river flow sensitivity indices under different land cover, land use and climate scenarios in the Mara basin'. This study examined the correlation in land cover, land use, rainfall, temperature and river flow volumes in the Mara River basin, whose upper catchment consists of protected forests and woodland within the gazetted area of Mau Forest Complex (EAC, 2013). Importantly, the study examined how stream flows and hence, surface water yields vary under different land cover, land use and climate scenarios.

The variations in stream flow over time were quantified in terms of changes in the mean as a central value in SWAT model, extensively described in studies by Neitsch *et al* (2011), Winchell *et al* (2010), and Arnold *et al* (1998). Thus, SWAT hydrological model was used to establish the interrelationship between changes in climate, land cover and land use with their impacts on the Mara River hydrological regimes. This involved simulating the land cover and climate scenarios (rainfall) with the river flow volumes for the period 1983-2013.

4.8.1 SWAT Model Input and Setup

This sub-section presents the requirements for running the SWAT hydrological model including the operational requirements of input data, data preparation, model set up, model application and the simulation options applied in the Mara basin. It also gives a summary of the procedures in setting up the model and its use in simulating the hydrological characteristics of the area of study. The model set up involved using the terrain in the form of Digital Elevation Model (DEM), land use, soil and climate datasets. The model parameterization was derived using the ArcGIS interface with ArcSWAT, which provided a graphical support for the desegregation scheme and hence

supported data handling (Schuol *et al,* 2008). The ArcSWAT interface delineated the basin into sub-basins based on the DEM and the stream network. The Land cover/land use data downloaded from the universal FAO geoportal- land cover database at a spatial resolution of 1km was projected and saved as Landuse_p2shp file.

The land use data were coded and a user table called 'lookup.dbf file' created to match the SWAT land use types with the land uses in Mara River basin. The projected land use file was saved as landuse project_file. The total drainage area was the threshold for delineating the Mara River basin to strike a balance between the resolution of the available data and the practical SWAT project size (Faramarzi *et al,* 2009). The exercise created 27 sub-basins for the whole basin from each of which, the HRUs were generated based on land cover/use, soils and slope thematic layers. The processed climate data were loaded into the SWAT model environment and later, together with the HRUs, simulated to generate the river flows over the study period with a view to understanding the hydrological responses to changes in land use and climate scenarios.

4.8.1.1 Model Data Requirements

The datasets required for SWAT model setup and operation included the Digital Elevation Model **(**DEM), land cover/land use and soil type maps and were projected using ArcGIS 10.4 to the Universal Transverse Mercator (UTM) Zone 36S, the Transverse Mercator Projection zone covering the area of study within the East African framework,. The delineation of the basin employed the use of DEM, which enabled analysis of the drainage patterns on the land surface terrain. The land cover/land use data was reclassified using the SWAT land cover types and a user look up table created for the same to help in the identification of the different land cover and land use types on the map as per the required SWAT format. The soils map of the area of study was reclassified to match the SWAT soil types using the user lookup table created to help overlay the various maps and for spatial change analysis. Other hydro-meteorological datasets incorporated included the rainfall, temperature, river flows, evapotranspiration, wind speed, humidity and solar radiation for the basin.

4.8.1.2 Watershed Delineation

This procedure enables the setting up of boundaries of the basin (study area). The basin boundaries were derived from the Global Digital Elevation Model (DEM) at 30 metres

resolution, which was obtained from the Shuttle Radar Topographic Mission within the USGS site using automated procedures within the watershed delineator an ArcGIS extension within SWAT2012. The basin delineation process started with loading the DEM that helped in calculating sub-basin and reach parameters followed by specifying the critical surface area (Wilson and Weng, 2011) that was used to determine the details of the stream network as well as the size and number of sub-basins in the larger Mara catchment area. The third step involved the review and editing of the stream network points (outlets) to achieve the optimum number of sub-basins, which would help in the calculation of the sub-basin parameters (Zhang *et al.*, 2012).

Automatic delineation of the basin boundary and creation of the stream network enabled the identification of flow points and therefore effective creation of streams and outlets. All the sub-basins and outlets were specified and the sub-basin parameters calculated followed by the generation of the output report to complete the basin boundary delineation. The task that followed was reviewing and editing the stream outlet points to obtain the maximum number of sub-basins and to calculate the sub-basin parameters. The next step involved inputting and overlaying the land cover/land use and soils thematic maps followed by automatic characterization of each sub-basin within the ArcGIS-ArcSWAT interface. All the soil-landuse-slope combinations were differentiated within each sub-basin. These unique areas, called Hydrological Response Units (HRUs) were used as the basis for the water balance calculations (Abbaspour *et al,* 2009; Schuol *et al,* 2008). The ArcSWAT interface enabled automatic parameterization of the stream reaches and the basin geomorphology.

4.8.1.3 Sub-Basin Parameters

Spatial parameterization of the model was performed using the 27 sub-basins created, based on the surface topography such that, all the streams in the entire Mara basin drain through the outlet at Musoma RGS number 09133000. The sub-basins were further sub-divided into a series of Hydrological Response Units (HRUs) based on the uniqueness of the soils, land use types and slope characteristics. Still an automatic process, the parameterization of the stream reaches and the sub-basin geomorphology was performed using the ArcSWAT interface that resulted in the computation of the minimum and maximum elevations plus standard deviation for each sub-basin. A

summary of the elevation types is on Table 4.10 while the detailed one is in Appendix VI.

Table 4.10: Summary Topographic report

Parameter	Height (m)
Minimum Elevation	1,123
Maximum Elevation	3,056
Mean Elevation	1,687.84
Standard Deviation	360.51

Source: Researcher, 2018 (see Appendix VI for details)

4.8.1.4 Hydrological Response Units (HRUs) Analysis

Land use, soil and slope characterization in the Mara basin, and for each of the respective sub-basins was performed within the ArcGIS-ArcSWAT framework or interface using the regional (FAO) land use and soils datasets imported and matched with the SWAT databases. As stated earlier, the slope classification was based on the DEM of the Mara River basin in which the multiple class slopes option was used because of the wide range of slopes in the Mara basin. Land use, soil types and slope class datasets were used to define HRUs for each of the 27 sub-basins. Land use datasets were defined and reclassified into SWAT land cover types. Since the Mara basin is outside the U.S.A, a user look-up table was created by editing the default land cover and land use database in order to reflect the local conditions. The projected land cover and land use data (landuse.dbf file) was added into the SWAT model in order to reclassify the land use in the study area using the prepared land use lookup user table (Landuse lookup.dbf) to match the SWAT land use reclassification.

The soil dataset was also defined and reclassified. From the digital soil FAO soils database for East Africa, the various categories of soils found within the Mara basin were matched with the SWAT soils database to minimize error margins during simulation. After land use and soil datasets were successfully reclassified and the slope class chosen, the land use, soil and slope thematic layers were overlaid to the using the

delineated basin boundary. These layers were used to automatically define the HRUs for each of the 27 sub-basins using preset threshold levels of 10% land use, 20% soil, 30% and 60% slope.

4.8.1.5 Channel Characteristics

In modeling channel flow in a river basin, SWAT model assumes that the main channels have a trapezoidal shape. The user is then required to define the width and depth of the channel when filled to the top of the bank as well as the channel length, slope along the channel length and the Manning's n value for the basin. Further, the model assumes the channel sides to have a 2:1 run-to-rise ratio (Z_{ch}=2) so that the slope of the channel sides is 0.5. The bottom width of the channel is then calculated (Equation 4.15) from the bank full width (Neitsch *et al*, 2011).

$$W_{btm} = W_{bnkfull} - 2.Z_{ch}.depth_{bnkfull} \quad \text{4.15}$$

W_{btm} is the bottom width of the channel (m), $W_{bnkfull}$ is the top width of the channel when filled with water (m), Z_{ch} is the inverse of the channel side slope, *and* $depth_{bnkfull}$ is the depth of water in the channel when filled to the top of the bank (m). By solving Equation 4.16 for a given depth of water in the channel, the width of the channel at the water level was determined.

$$W = W_{btm} + 2.\ Z_{ch}\ .\ depth \quad \text{4.16}$$

W is the width of the channel at the water level (m), W_{btm} is the bottom width of the channel (m), Z_{ch} is the inverse of the channel side slope, *depth* is the depth of water in the channel (m). The volume of water held in the channel at any one time was evaluated by solving Equation 4.17

$$V_{ch} = 1000.\ L_{ch}\ .\ A_{ch} \quad \text{4.17}$$

V_{ch} is the volume of water stored in the channel (m^3), L_{ch} is the channel length (km), A_{ch} is the cross-section area of flow in the channel for a given depth of water (m^2).

4.8.1.6 Climate Component

The climate component of the model was presented in the form of long-term weather data gathered for the entire Mara catchment. The variables used for running the SWAT model consisted mainly of the simulated daily rainfall, maximum and minimum air

temperature, solar radiation, wind speed and relative humidity. The model has an option of using input values of daily weather variables from observed or simulated datasets but can also use internally generated values from the monthly records averaged and summarized over a number of years like in this case that is thirty years (Wilson *et al.*, 2011). Generated climatic data may also be used to fill in gaps in the observed records (Winchell *et al,* 2010). In this case, however, the observed daily rainfall records were used for calibration and validation while spatial interpolation was used to fill in the missing values.

4.8.1.7 Weather Data

The weather variables that were included in the SWAT model that drive the hydrologic water balance are precipitation, air temperature, solar radiation, wind speed and relative humidity (Arnold et al, 1998). The observed daily rainfall, maximum and minimum temperatures were input directly and then simulated internally using the inbuilt weather generator. The model always internally simulates solar radiation, wind speed and relative humidity. In this study, the weather data used in the basin to simulation stream flow were downloaded from the global weather database, already in the SWAT format. Weather stations including Bomet, Kiptunga, Keekorok, Narosura, Nyabassi and Mugumu (Table 4.11) were loaded to the model for the purposes of defining the Weather generator datasets, which were used to generate the various weather parameters for the model. The Creation of SWAT model weather generator database started by providing a table showing the location of the above mentioned local weather generator stations with their code numbers, co-ordinates and elevations within the Mara basin.

A daily rainfall data table was made for each of the rainfall recording stations listed in the location table (Table 4.11). The table was used to record the daily rainfall values in a sequential order for every rainfall gauging station. Temperature data table was also prepared to record the maximum and minimum temperature values for each of the listed temperature recording stations. The table according to Winchell *et al,* 2010) has three columns namely: the date, maximum and minimum temperature columns and could hold a maximum of 150 years of daily temperature data. The other climate datasets including the relative humidity, solar radiation and wind speed were internally generated using the SWAT weather generator.

Every sub-basin had the climate data assigned to it obtained from the closest station. Because different datasets are incorporated in this exercise, the resulting synthetic meteorological data that is finally used introduces some uncertainties in the SWAT simulations (Zhang et al., 2012). The best situation would therefore be to use the long-term measurements or observed datasets. In most cases however, lack of observed time series of adequate length to permit impacts studies and the limited coverage of station networks, and the need for catchment scale response datasets with high spatial and temporal resolutions necessitates use of synthetic data in studies such as this one (Mirus *et al,* 2011).

In a study like this where simulated (synthetic) datasets are used, Calibration and Validation exercises have to be carried out using observed records to ascertain the authenticity and suitability of the simulation results. The quality of the results depended on how well the distribution of the sampled weather stations were done and how the statistics of the observed data described (Brissette *et al,* 2007). Proper description of the statistics of observed data allows for direct use of the synthetic time series datasets with physical models such as the SWAT to model and project climate variability with change events (Brissette *et al,* 2007).

Table 4.11: Weather stations used by the weather generator component of SWAT model

ID	Name	Code Name	Latitude (°S)	Longitude (°E)	Elevation (m)
1	Kiptunga	9035228	-0.45	35.8	
2	Bomet	9035265	-0.783	35.350	1951
3	Narosura	9135026	-1.540	35.859	1585
4	Keekorok	9135013	-1.583	35.233	1602
5	Mugumu	09134033	-1.87	34.72	
6	Nyabassi	09134008	-1.35	34.57	1829

Source: Researcher, 2018

4.8.1.8 Thiessen Polygons

The choice and distribution of the sampled weather stations was based on the use of thiessen polygons to ascertain quality of the results from the analysis of these datasets. The thiessen polygons were created from the shapefiles of the rainfall stations for

spatial proximity analysis in which, the most suitable stations were taken for study. This was to ensure that every part of the basin was covered by a thiessen polygon such that, a particular part of the river network was covered by a particular rainfall station (Figure 4.5). They were chosen such that, two catered for the upper catchment, two for middle and two for the lower reaches of the basin. To do further analysis on the relationships between these rainfall stations and the river flows, the shapefiles of the river outlets were used to make the outlet thiessen polygon (Figure 4.6). This polygon gave information on the topography hence the distribution of the river channels that culminated in the river network and therefore the outlets. The shapefiles of the two-thiessen polygons were then matched to check for spatial association (Figure 4.6). It reveals how the chosen weather (rainfall) stations contributed to the waters that passed through the outlets.

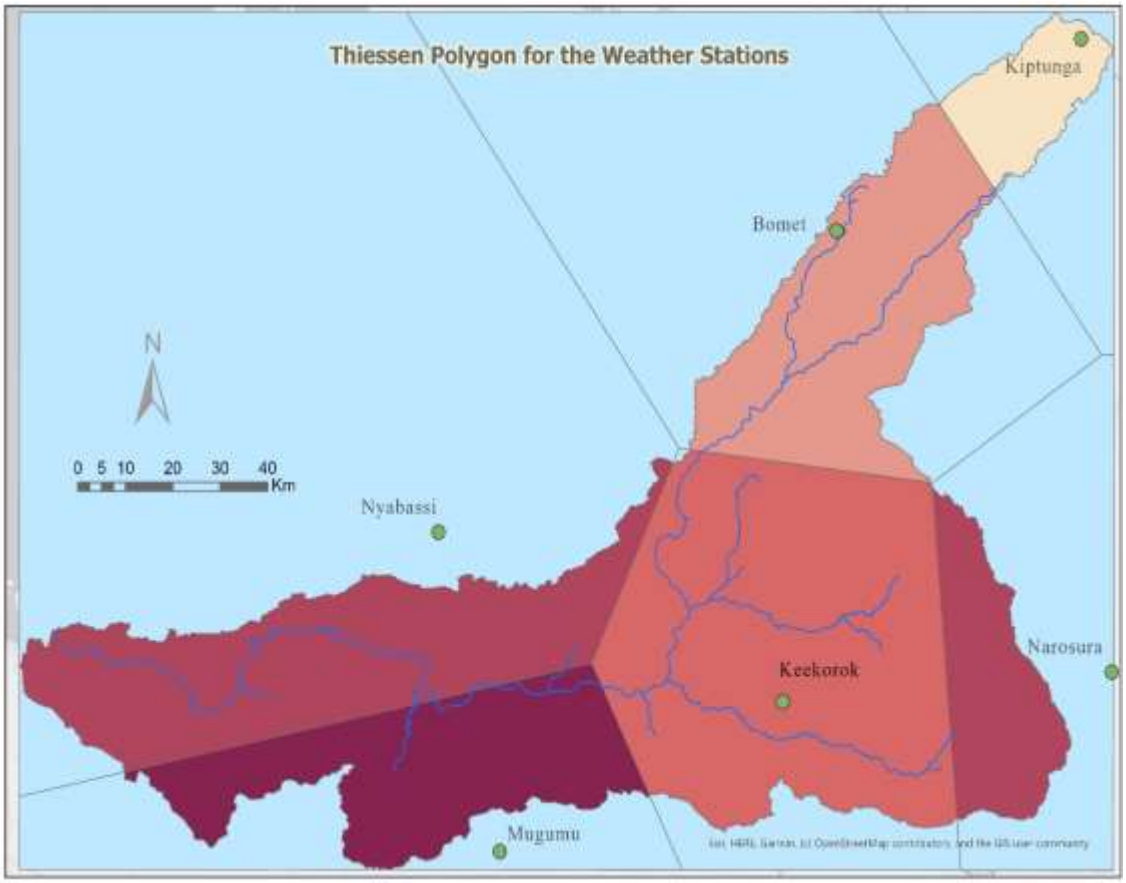

Figure 4.5: Rainfall Stations Thiessen Polygons

To do further analysis on the relationships between these rainfall stations and the river flows, the shapefiles of the river outlets were used to make the outlet thiessen polygon

(Figure 4.6). This polygon gave information on the topography hence the distribution of the river channels that culminated in the river network and therefore the outlets. The shapefiles of the two-thiessen polygons were matched to check for spatial association (Figure 4.6). It revealed how the chosen weather (rainfall) stations contributed to the waters that passed through the outlets.

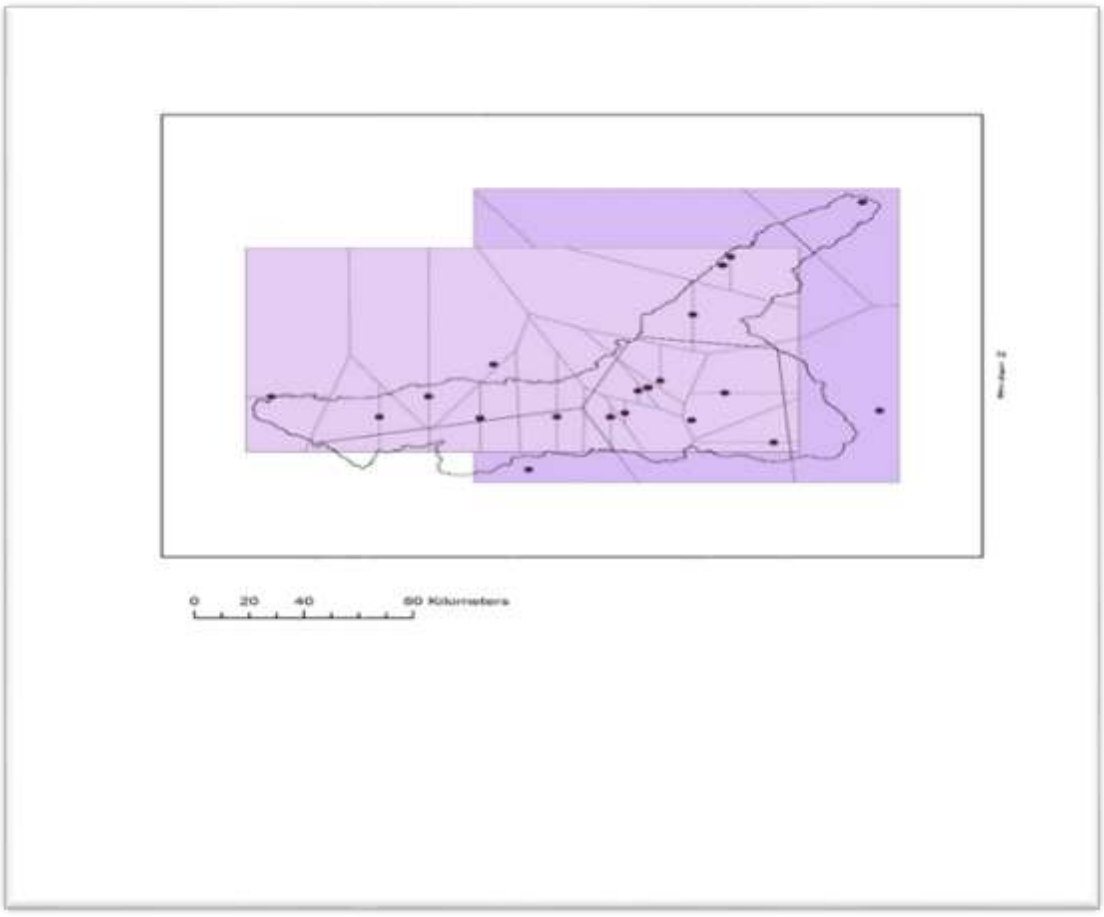

Figure 4.6: Spatial Relationship between Rainfall stations and River outlets

From Figure 4.7, only three outlet points out of a total of thirteen (13) and three out of the six (6) rainfall stations were found to be outside the overlap area. This is an indication of close relationship between rainfall stations and river flows. It shows spatial contributions of the rainfall stations to river outlets and therefore the flow volumes. The created union between the rainfall stations polygon and outlets polygon was subjected to geographically weighted regression (Figure 4.7), which gave standard deviations of between less than 2.5 and more than 2.5. This shows that each rainfall

station has significant contribution of rainfall to the flow volumes in the areas indicated by their polygons.

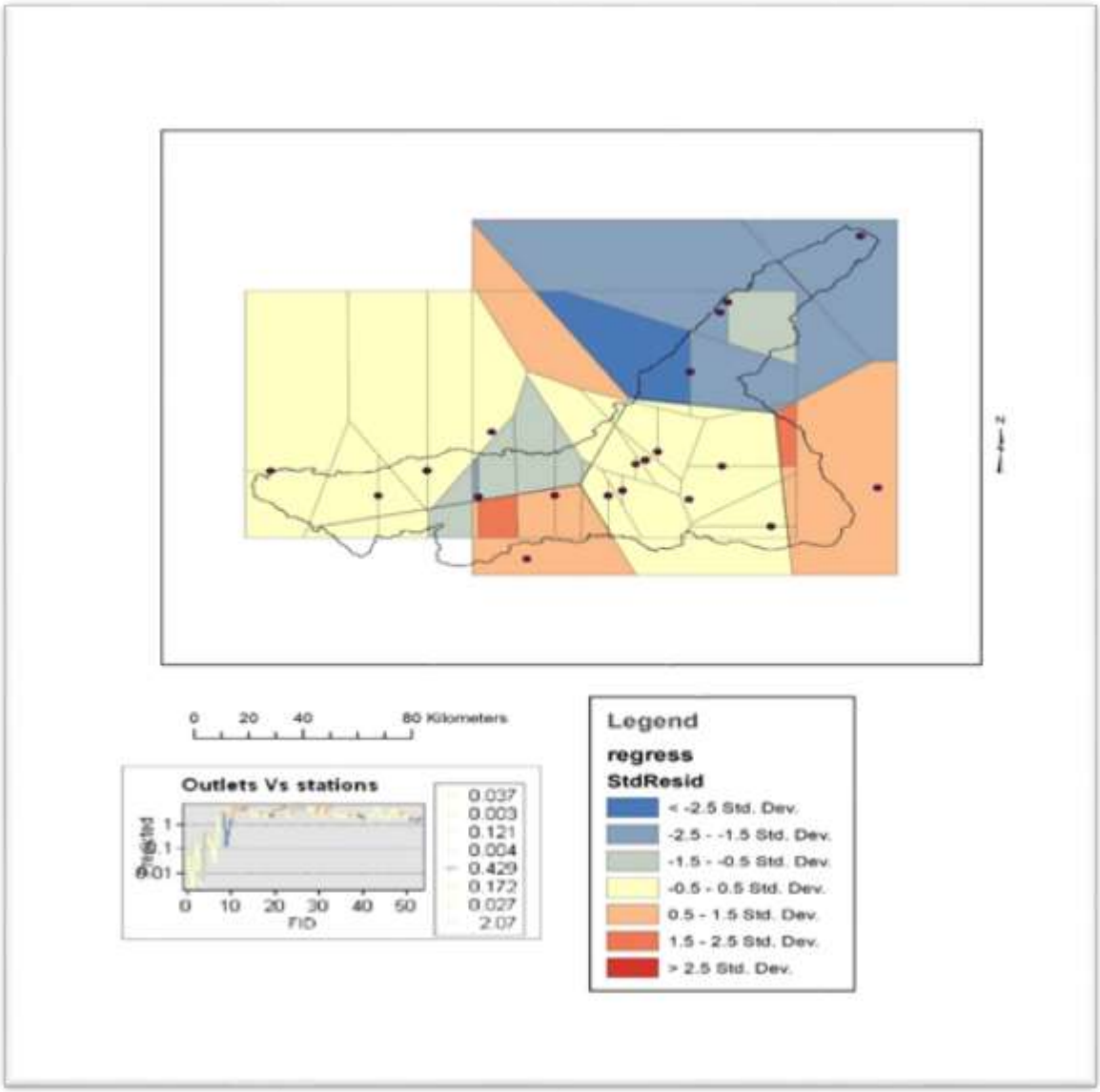

Figure 4.7: Spatial relationship between Rainfall Stations and River Flows in the Mara Basin

4.8.1.9 Rainfall

Rainfall, being the main process through which water enters the land phase component of the hydrological cycle, is one of the most important hydrological processes in the land phase of the cycle. Since rainfall controls the water balance, it is important to have

an accurate simulation of the rainfall amounts and distribution in terms of space and time by the use of SWAT hydrological model. SWAT model can internally generate the amount of rainfall reaching the earth's surface on a given day (Neitsch *et al*, 2011). This may be termed (day R) and can be read from an input file. The occurrence of rain on any given day has a major impact on relative humidity, temperature and solar radiation reaching the surface for that day.

The weather generator component within the SWAT modelling system was first set to generate precipitation for the day independent of the other climatic variables and then computed the distribution of rainfall within the day. Once this was successfully done, maximum and minimum temperatures, solar radiation and relative humidity were then generated based on the presence or absence of rain for the day under consideration while wind speed was independently generated (Neitsch *et al*, 2011). A first order Markov chain-skewed model (Nicks, 1974), inbuilt within the SWAT modeling system, was used to generate (Equation 4.18) daily precipitation for the Mara basin. This was also used (first order Markov chain model) to define the day as dry or wet by comparing a random number ranging from 0.0 to 1.0, generated by the model, to monthly wet-dry probabilities input by the user (Table 4.12).

Table 4.12: SWAT input variables that appertain to the generation of daily rainfall

Variable Name	Definition
PCPSIM	Precipitation unit code: 1-measured, 2-generated
PR_W(1,mon)	$P_i(W/D)$: Probability of a wet day following a dry day in a month
PR_W(2,mon)	$P_i(W/W)$: Probability of a wet day following a wet day in a month
IDIST	Rainfall distribution code: O-skewed, 1-exponential
REXP	*rexp*: Value of the exponent. (required if IDIST=1)
PCPMM (mon)	Average monthly precipitation falling in a month (mm H2O)
PCPD (mon)	Average number. of days of precipitation in a month (μmon = PCPMM/PCPD)
PCPSTD (mon)	δ mon: Standard deviation for daily precipitation in a month (mmH2O)
PCPSKW	gmon: Skew coefficient for daily precipitation in a month

(Source: Neitsch, et al, 2011)

$$R_{day} = \mu_{mon} + 2.\delta_{mon}\{[(SNDday - gmon)\frac{(g_{mon})}{g_{mon}} + 1]^3 - 1\} \quad \text{.....4.18}$$

R_{day} is the amount of rainfall on a given day (mm H20), μ_{mon} is the mean daily rainfall for the month (mm H2O), δ_{mon} is the standard deviation of daily rainfall for the month (mm H2O), SND_{day} is the standard normal deviation calculated for the day, and g_{mon} is the skew coefficient for daily rainfall for the month. Precipitation input parameters include monthly probabilities of receiving precipitation depending on whether the previous day was wet or dry. Given the dry-wet state, the Markov chain-skewed model automatically determined whether precipitation would occur (Arnold *et al,* 1998).

4.8.1.10 Preparation of Rainfall Statistical Parameters

The weather generator component in the SWAT modelling system requires some statistical parameters of daily rainfall as part of the input weather data for use in simulating daily rainfall. These parameters were calculated using the precipitation statistics software (pcpSTAT) written by Liersch (2003). The software uses text files arranged in one column starting with the first day of January of the first year and ending with the last day of December of the last year. Observed and simulated daily rainfall data were arranged together in one column before converting them to text files that were used as input to pcpSTAT. Observed and simulated datasets were arranged such that the first entry coincided with the first day of January of the first year and the last value with the last day of December of the last year (Liersch, 2003). The preparation was done for daily rainfall values of observed rainfall in the period 1983-2013. The outputs from the pcpSTAT included the output file together with two additional files containing a table of total monthly rainfall of each year of the entire period, and a table of average daily rainfall values of each year of the entire period (Liersch, 2003).

4.8.1.11 Solar Radiation and Air Temperature

The SWAT inbuilt weather generator generates maximum and minimum air temperatures as well as solar radiation automatically during SWAT modelling process. The weather generator is incorporated with a continuity equation, which automatically accounts for temperature and radiation variations caused by the dry and wet day conditions in the basin of study. These values were generated from input averages of monthly temperature and solar radiation data (Neitsch *et al*, 2011). Where there are enough rainfall and snow, the average air temperature is usually used to determine

whether precipitation is simulated as rainfall or snowfall. In our case, precipitation was simulated as rainfall since rainfall is the main form of precipitation in the area of study. Maximum and minimum temperature inputs were used in the calculation of the daily soil and water temperatures, which were important in the determination of stream flow rates (Gassman *et al,* 2007). Terrestrial radiation which depends on sunrise, sunset, latitude and solar declination was also calculated (Equation 4.19).

$$H_o = 37.59E_o[\omega T_{SR}Sin\delta Sin\phi + Cos\delta Cos\phi Sin(\omega T_{SR})] \quad \text{.....4.19}$$

H_o is the calculated solar radiation, E_o (dimensionless) is the eccentricity correction factor of the earth's orbit and is given by evaluating Equation 4.20, ω is the earth's angular velocity (rad/h), T_{SR} is the hour of sunrise, δ is the declination angle (rad), and ϕ is the latitude angle (rad).

$$E_o = 1.00011 + 0.034221Cos\Gamma + 0.00128Sin\Gamma + 0.000719Cos2\Gamma + 0.000077Sin2\Gamma \quad \text{.....4.20}$$

Γ is the angle of the day's sun (radians) and is evaluated using Equation 4.21

$$\Gamma = 2\pi (N - 1)/365 \quad \text{.....4.21}$$

N is the number of the day of the year out of the 365 days of the year (Wong and Chow, 2001).

Air temperature was calculated using a sinusoidal function (Equation 4.22) within the model oscillating between maximum and minimum daily air temperatures.

$$T_{hr} = \overline{T}_{av} + (T_{max} - T_{min}) Cos0.2618 (hr - 15) \quad \text{.....4.22}$$

T_{hr} is the surface air temperature at a given hour (˚C), T_{av} is the daily average temperature (˚C); T_{max} is the maximum temperature at a given hour (˚C); and T_{min} is the minimum temperature at a given hour (˚C). Soil temperature in a given layer was calculated (Equation 4.23) using the previous day's soil temperature, the mean annual air temperature, the current day's soil surface temperature and the depth.

$$T_{soil}(z, d_n) = I.Tsoil(z, dn-1) + [1.0-l][df[\overline{T}_{AAir} - T_{ssurf}] + T_{ssurf}] \quad \text{.....4.23}$$

$T_{soil}(z, d_n)$ = soil temperature (˚C) at depth z (mm) below the surface on the day of the year dn; l = lag coefficient that controls the influence of the previous day's temperature

and is set to 0.8 in the SWAT model; $T_{soil\ (z,d_n-1)}$ = previous day's soil temperature (˚C); df = depth factor, which quantifies the influence of the depth below the surface on the soil temperature; T_{AAir} = average annual air temperature (˚C); and T_{ssurf} = soil surface temperature (˚C) (Neitsch *et al*, 2011).

4.8.1.12 Land Phase Component

The land phase of the hydrological cycle comprises two main components: hydrology and routing. The hydrology component of the cycle comprises the flow processes occurring on the land phase of the hydrological cycle. It is based on the soil-water balance equation (Equation 4.24) which forms the basis of hydrological modelling. The main modelling processes of the hydrology component of the SWAT model, which are simulated through the soil water balance equation include surface runoff, infiltration, evaporation, plant water uptake, lateral sub-surface flow, percolation to the shallow and deep aquifers and the base flow (Neitsch *et al*, 2011; Faramarzi *et al*, 2009). In this study, the hydrology component was simulated based on the soil water balance equation suggested by Arnold *et al* (1998).

$$SW_t = SW_o + \sum_{t=1}^{t}\left(R_{day} - Q_{surf} - E_a - W_{seep} - Q_{gw}\right) \quad \text{4.24}$$

Where:

SW_t is the final soil water content (mmH_2O), SW_o is the initial soil water content on day i (mmH_2O), t is the time (days), R_{day} is the amount of rainfall on day i (mmH_2O) and Q_{surf} is the amount of surface runoff on day i (mmH_2O). E_a is the evapotranspiration on day i (mmH_2O), W_{seep} is the amount of water entering the vadoze zone from the soil profile on day i (mmH_2O) and Q_{gw} is the amount of return flow on day i (mmH_2O).

In this study, surface runoff from daily rainfall amounts was modelled using a modified SCS curve number method (Equation 4.25) based on LCLU characteristics, soil hydrologic group and antecedent soil moisture content.

$$Q_{surf} = \frac{\left(R_{day} - 0.2S\right)^2}{R_{day} + 0.8S} \quad R_{day} > 0.2S \quad \text{4.25a}$$

$$Q_{surf} = 0 \qquad R_{day} > 0.2S \quad \text{4.25b}$$

Q_{surf} is the accumulated daily surface runoff (mmH_2O); R_{day} is the daily rainfall depth (mmH_2O); and S is the retention parameter (Abbaspour *et al*, 2009; Schuol *et al*, 2008; Arnold *et al*, 1998).

The retention parameter varies spatially and temporally. The parameter varies spatially among watersheds because soils, land use, management and slope vary; and temporally because of changes in the soil water content (Arnold *et al*, 1998). The parameter is related to the curve number by the SCS equation (Equation 4.26).

$$S = 254\left(\frac{100}{CN} - 1\right) \ldots \quad 4.26$$

CN is the SCS curve number for the given day and ranges from 30 to 100 (Neitsch *et al*, 2011).

4.8.1.13 Time of Concentration

Time of concentration was calculated (Equation 4.27) by summing up the overland flow time and the channel flow time.

$$t_{conc} = t_{ov} + t_{ch} \ldots \quad 4.27$$

t_{conc} = the time of concentration for a sub-basin (hr); t_{ov} = the time of concentration for overland flow (hr) (Equation 4.28); t_{ch} = the time of concentration for channel flow (hr.) (Equation 4.7).

$$t_{ch} = \frac{L_{slp}}{3600.V_{oc}} \ldots \quad 4.28$$

L_{slp} = the sub-basin slope length (m), V_{ov} is the overland flow velocity (ms^{-1}) and 3600 is a unit conversion factor.

$$t_{ch} = \frac{L_c}{3.6.V_c} \ldots \quad 4.29$$

L_c = the average channel length for the sub-basin (km), V_c is the average channel velocity (ms^{-1}), and 3.6 a unit conversion factor.

4.8.1.14 Canopy storage

When SWAT calculates surface runoff using SCS curve number method, canopy interception is lumped in the term for initial abstraction. The maximum amount of water that can be in the canopy storage varies from day to day as a function of leaf area index (LAI) and was computed using Equation 4.30.

$$Can_{day} = Can_{mx}.\frac{LAI}{LAI_{mx}} \quad \text{4.30}$$

Can_{day} is the maximum amount of water that can be trapped in the canopy on a given day, (mmH_2O); Can_{mx} is the maximum amount of water that can be trapped in the canopy when the canopy is fully developed (mmH_2O); LAI is the leaf area index for a given day and LAI_{mx} is the maximum leaf area index for the plant.

4.8.1.15 Sub-Surface Flow

The available soil capacity (AWC) was calculated (Equation 4.31) by subtracting the fraction of the water present at the permanent wilting point (WP) from the fraction of the water present at field capacity (FC).

$$AWC = FC - WP \quad \text{4.31}$$

AWC is the available soil water content, FC is the soil water content at field capacity and WP is the soil water content at the permanent wilting point.

4.8.1.16 Routing Component

The model maintains a continuous water balance and because of this, complex basins are divided into sub-basins to reflect the differences in evapotranspiration for various vegetation, crops and soils. Under such circumstances, the runoff for each sub-basin modelled separately and routed to obtain the total runoff for the basin (Arnold *et al,* 1998). This increases the accuracy of runoff simulation and gives a better physical description of the water balance in a basin. In this study, the modelled runoff from each sub-basin was routed through the river basin to the main basin outlet at Mara Kirumi Bridge RGS 5H3 using the Muskingum method. Manning's equation for uniform flow in a channel (Equations 4.32) was used to calculate the rate and velocity of flow in a channel segment for a given time step.

$$v_{ch} = \frac{R_{ch}^{\frac{2}{3}} slp_{ch}^{\frac{1}{2}}}{n} \qquad \text{4.32}$$

q_{ch} is rate of flow in the channel (m^3/s), A_{ch} is the cross-sectional area of the channel (m^2), R_{ch} is the hydraulic radius for a given depth of flow (m), slp_{ch} is the slope of the channel along the length (m/m), v_{ch} is the flow velocity in the channel (ms^{-1}) and n is the Manning's coefficient for the channel (Neitsch *et al*, 2011).

Muskingum storage method models the storage volume as a combination of wedge and prism storages using equation 4.33 (Neitsch *et al*, 2011).

$$q_{out,2} = C_1 q_{in,2} + C_2 q_{in,1} + C_3 q_{out,1} \qquad \text{4.33}$$

$q_{out,2}$ is the out flow rate at the beginning of the time step 3; $q_{in,2}$ is the
the beginning of the time step 1, $q_{in,1}$ is the inflow rate at the end of the time step 2, $q_{out,1}$ is the outflow rate at the end of the time step 3. Muskingum routing equation (Equation 4.34) was used to route the water in the channel.

$$C_1 = \frac{\Delta t - 2KX}{2K(1-X)+\Delta t} \qquad \text{4.34a}$$

$$C_2 = \frac{\Delta t - 2KX}{2K(1-X)+\Delta t} \qquad \text{4.34b}$$

$$C_3 = \frac{2K(1-X) - \Delta t}{2K(1-X)+\Delta t} \qquad \text{4.34c}$$

C_1, C_2 and C_3 are the routing coefficients and should be confirmed that $C_1 + C_2 + C_3 = 1$, *K* is the storage time constant for the reach and *X* is the weighting factor.

The variable storage method is based on the continuity equation for a given channel reach segment. Importantly, the stored amount of water is the difference between the water input into and output out of the segment. In the foregoing method, one of the options provided for in the SWAT model storage for a given channel segment is based on the continuity Equation 4.35.

$$V_{in} - V_{out} = \Delta V_{stored} \qquad \text{4.35}$$

V_{in} = the volume of inflow (m^3H_2O), V_{out} = the volume of outflow (m^3H_2O), and ΔV_{stored} = the change in the volume of storage during the time-step (m^3H_2O).

4.8.2 SWAT Model Simulation

After a successful SWAT model setup, the starting and ending period was set in the same range with the hydro-meteorological data incorporated into the SWAT system in the MM/DD/YYYY format with an NYSKIP period of three (3) years to give room for model initial condition effect to check for good performance. The model was run on a daily, monthly and yearly time steps for a period of thirty years (1983 -2013) with a future projection to 2030.

4.8.2.1 SWAT Calibration and Validation

Calibration is an effort to better parameterize a model to a given set of local conditions to reduce the model prediction uncertainties. Calibration process involves adjusting the model input parameters by comparing model outputs for a given set of assumed conditions with observed data for the same conditions. The model calibration and validation was done at the sub-basin level using the monthly-observed discharge at Nyangores RGS (1LA03). Calibration was conducted manually using split sample approach following the procedure recommended by Arnold *et al* (2011).

Simulated and corresponding observed monthly discharges from 1986 to 1990 were used to calibrate the model input parameters while those observed from 1991 to 1995 were for validating the model with a warm up period of three years (1983-1985). The predicted uncertainties that were identified were included in the parameter ranges then integrated with the observed data within a high prediction uncertainty range to optimise calibration. The sum of squares method (within SWAT-Cup) was used as the optimization scheme accompanied by visual inspection of monthly hydrographs (Van Liew *et al*, 2005). Results of model validation were used to assess the accuracy or reliability of the model results based on the criteria used (Moriasi et al, 2007).

4.8.2.2 Assessment of Model Performance

There are three popular approaches to evaluating the appropriateness of a hydrological model in a basin: fit-to-observations, fit-to-reality, and fit-to-purpose (Van Griensven, *et al.,* 2012). The fit-to-observations involves the evaluation of performance indicators where the error between the model outputs and observed values for the same variable is computed. The fit-to-reality deals with the evaluation of the extent to which the hydrological processes in the basin are realistically represented by means of the

parameter and mass balance evaluations, and the fit-to-purpose involves evaluation of the extent to which the model is able to tackle the problem. Thus, the calibration statistics involved the objective functions.

In this study, the fit-to-observations criterion, which computes the accuracy of calibrating the simulations with the relevant observations, was adopted. It is the most typical evaluation criterion used to evaluate the performance of hydrological models because of its objectivity and affordability (Liew *et al,* 2005; Krause *et al,* 2005; Moriasi *et al,* 2007; Van Griensven, *et al,* 2012). Moriasi *et al* (2007), recommend the following quantitative statistics for model evaluation based on the fit-to-observation criterion: Coefficient of determination (R^2), Nash-Sutcllife Efficiency (NSE), Percentage Bias (PBIAS), and the ratio of root-mean-square error (RSR) to the standard deviation of the observation data. This is in addition to graphical assessment through hydrographs and percent exceedance probability curves (Krause *et al,* 2005; Moriasi *et al,* 2007; Sexton *et al,* 2010; Van Griensven, *et al,* 2012. The use of any of these statistical techniques is based on the requirement of the calibration.

This calibration exercise was based on the daily time step and both monthly and annual averages. The process went through the Pre-batch, post-batch and finally, SUFI2_Run-batch to successful conclusion. The calibration statistics involved the objectivity functions and affordability for simulated and observed data, slope intercept and the regression coefficient of determination (R^2) and the Nash-Sutcliffe Efficiency. During the calibration and SWAT Run, the basin, HRUs and Sub-basin parameters remained constant for the entire period of simulation to enable the estimation of the coefficient of determination ($R^{2)}$ for discharge and simulated data. In addition to this, Nash-Sutcliffe simulation efficiency (E) was used to gauge the model prediction for the entire period as illustrated herein:

$$R = \sum_i (Q_{.m} - Q_s)_i^2 \times \sum_1 (S_m - S_s) \times \sum_1 (N_m - N_s)_1^2 \quad \text{.....4.36}$$

Where: Q=discharge; N=Number of Observation; M=Measured Data,

S = Simulated Data

$$R^2 = \frac{\left[\sum_1 (Q_{m1} - Q_m)(q_{si} - Q_s)\right]^2}{\sum_1 \left[(M_1 - Q)^2 \sum_1 (Q_{si} - Q_s)\right]^2} \quad \text{.....4.37}$$

R^2 is the Coefficient of determination, which measures the association between observed and simulated discharged values, 1 is the i^{th} measured or simulated data. The coefficient of determination, (R^2) is a number between -1 and 1 that reveals how closely the model-predicted values correspond to the actual observed values as reflected by the values estimated by the trend line (Muthama *et al*, 2008). When R^2 estimates is near to Zero and (E) estimates are less than Zero, then the prediction is not accurate. When the value is one (1), the model prediction is accurate. In this study, the R^2 estimate was found to be accurate thus, its use.

4.9 Impacts Assessment

In this section, the third and fourth specific objectives, 'To create a simulation of river flow under different land cover/land use given varying climate scenarios in the Mara River basin' and 'To generate river flow sensitivity indices under different land cover/land use and climate scenarios in the Mara River basin was addressed. This was done by simulating projected water yields using projected temperature and rainfall as inputs under two main forest cover scenarios: forest cover and built-up area change scenarios and forest conservation scenario (Figure 3.4). The impacts of land cover, land use and climate change on discharge in the Mara River basin were evaluated through multivariate analysis using multiple regression and correlation model with simulated long-term precipitation, temperature and land cover/use as independent variables and simulated water yield as dependent variable between 1983 and 2014 and projected to 2030.

4.9.1 Multiple Regression Model

Multiple Regression and Correlation model (Equation 4.38) was used in this study for impact analysis or to predict the river flow regimes as the dependent variable based on its covariance with the predictor (independent) variables of rainfall, temperature and land cover. The Multiple Correlation and Regression Model was used to generate the river flow sensitivity indices under different land cover/land use and climate scenarios in the Mara Basin (Specific Objective 4). The level of significance was tested at α =

0.05, using Pearson Correlation Coefficient. The Multiple Linear Regression applied in this study was:

$$Y = a + \beta_1 X_1 + \beta_2 X_2 + \beta_3 X_3 + \beta_4 X_4 \ldots + \beta_n X_n + \mathcal{E} \quad \ldots\ldots\ldots\ldots\ldots\ldots\ldots\ldots\ldots\ldots\ldots\ldots\ldots 4.38$$

Where:

Y *is* the value of the dependent variable (Water Yield); a is the Y intercept; β_1, β_2, β_3, β_4, $\cdots$ β_n are the regression coefficients, each representing the amount of change in Y(Water Yield) for one unit of change in the corresponding X value when the other X values are held constant. X_1, X_2, X_3, X_4, $\cdots$ X_n *are* the independent variable (rainfall, land use etc.) and $\acute{\varepsilon}$ is estimated error term or residuals of the regression.

4.9.2 Pearson Coefficient of Correlation

Pearson Coefficient of Correlation (r) was applied in this study to measure the strength of association between water yield, one dependent variable and land cover, land use, rainfall, temperature, surface flow, ground water and percolation as predictor variables. The correlation coefficients are -1 to +1, where values close to zero (0) mean no relation between the variables. The calculation of the correlation coefficient was performed using Equation 4.39 in which x represents the independent variable and y represents the dependent variable. The significance of trends were tested at $\alpha = 0.05$ level of confidence.

$$r = \frac{\sum_{i=1}^{n}(xj - \bar{x})(yj - \bar{y})}{\sqrt{\sum_{i=1}^{n}(xj - \bar{x})^2 (yj - \bar{y})^2}} \quad \ldots\ldots\ldots\ldots\ldots\ldots\ldots\ldots\ldots\ldots\ldots\ldots\ldots 4.39$$

Where:

r is the correlation coefficient and, xj and yj are the jth observations for the two variables, $\bar{x}$ and $\bar{y}$ are arithmetic means of the observations of the two variables and N is the number of observations.

CHAPTER FIVE: RESULTS AND DISCUSSIONS

5.1 Introduction

This chapter presents the results and discussions of this study in five different sections based on the research objectives. (i) The nature, extent and rate of change in land cover and land use types; (ii) The spatio-temporal variations in rainfall, temperature and river flows; (iii) Simulations of river flows under different land cover, land use types given varying climate scenarios; (iv) River Flow Sensitivity Indices Under Different Land Cover Land Use and Climate Scenarios; (v) Impacts on River Flow Volumes.

5.2 Nature, Extent and Rate of Change in Land Cover and Land Use

Results on the nature, extent and rate of change in land cover and land use types in the Mara are discussed under post classification visual comparison, post classification area comparison and trends in land cover and land use categories. Areas of change, the manner of change including changes within and across the cover categories are revealed. The implications of such changes in land cover and land use of Mara water resources and river flow volumes are addressed.

5.2.1 Post Classification Area Comparison between 1984 and 2016

Based on the use of Landsat TM and ETM+ imageries covering the Mara basin for the years 1984, 1995 2003, 2011 and 2016, the land cover classification exercise produced thematic maps for each year as indicated in Figures 5.1a to 5.1e. Each thematic map gives the areal extent of each cover type in hectares and percentages, as shown on Table 5.1 on Page 131. Comparing the values in the table revealed the nature, extent and rate of change in each category for the period 1984 to 2016. In 1984, grassland occupied the largest area, 704169.81 hectares and accounted for 49.13%. Next was shrub land with 496599.12 hectares, which was 34.65% of the total cover types while forestland and cropland followed in that order with albeit lower coverage of 104260.95 hectares and 99529.74 hectares (7.27 and 6.94%) respectively. The other remaining four categories: water bodies, wetlands, bare land and built-up areas covered a mere 28716.48 hectares, which was 2.01% of total coverage (Figure 5.1a and Table 5.1).

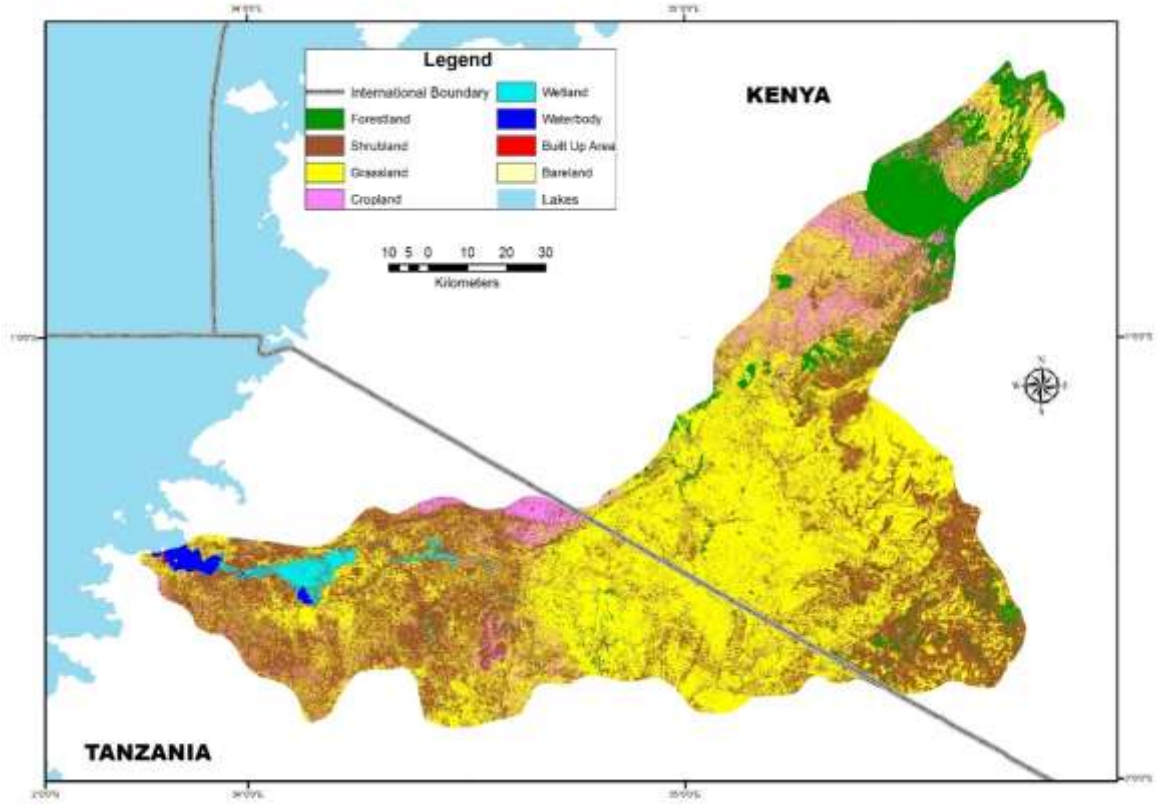

Figure 5.1a: Land cover and land use types in Mara Basin in 1984. (Source: Researcher, 2016)

The Mara River basin is predominantly a rangeland characterized by open grassland and shrubs used for grazing by the pastoral communities and for the wildlife in the conservancies. Crop farming was not a big issue in the basin and that is why it accounted for just 6.94% in 1984 with majority of the farms found in the none-forested, none-pastoral and grazing areas of the basin. The upper catchment around Molo and Bomet had forest plantations and tea, coffee, maize and bean farms.

The lower parts in Tanzania support maize, millet, beans, cassava and sweet potatoes, among others. Forestland in Mara comprised of both closed and open forests in the upper mountain slopes and in the lower reaches and are therefore categorized as either upper or lower catchment forests. Forests in the upper catchment are found within the confines of the Mau complex, specifically those in Bomet County and in the Sub-Counties of Molo, Narok North, Narok South and Trans Mara. The forests in the lower reaches confined entirely on the Tanzanian side.

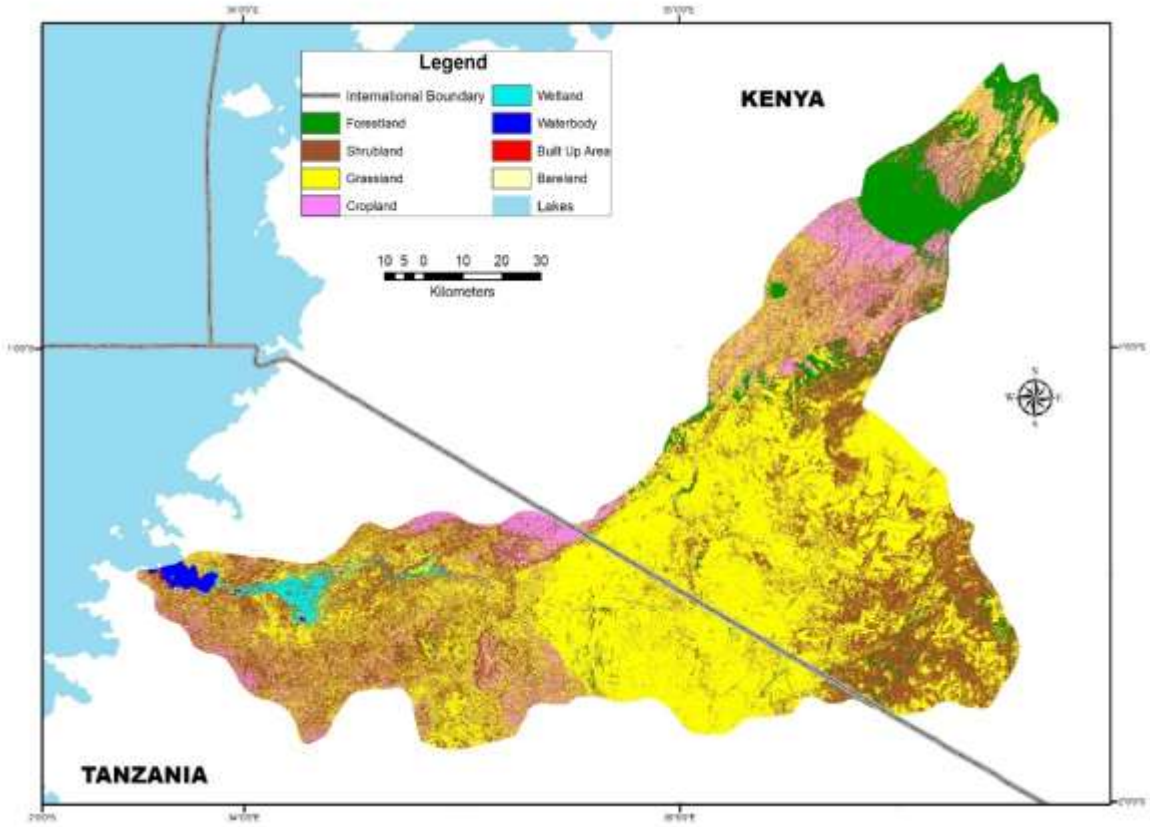

Figure 5.1b: Land cover/ use types in Mara Basin in 1995. (Source: Researcher, 2016)

According to the land cover scenario map of 1995, the area under grassland increased by 1.65% to be 728104.08 hectares (50.78%) while shrub land decreased quite significantly by 3.34% during the same period to stand at 448860.72 hectares, which was 31.31% (Figure. 5.1b). Area under forest registered a decrease of about 0.44% to cover 97959.50 hectares (6.83%) while cropland increased from 99529.74 hectares in 1984 to 134840.54 hectares (9.40%), an increase of 2.46%. During this same period, both wetlands and water bodies decreased in coverage, occupying 13189.24 and 8667.93 (change of 0.31 and 0.04% respectively). On the contrary, built-up area and bare land had slight increments and occupied 565.96 and 1589.94 hectares respectively; accounting for 0.04 and 0.11%, the percentage change in built-up area was minimal.

Importantly, all the land cover categories changed in one way or another (Table 5.1). The table gives overall change in each cover category while the complex change dynamics are covered in the overlay operations in subsection 5.2.3. For example, shrub land, forestland, wetlands and water bodies reduced in favour of cropland, grassland,

built-up areas and bare land all of which increased between 1984 and 1995. It would appear also that the decrease in wetlands and water bodies came about partly due to variations in rainfall and temperature conditions, which might have resulted in some of the wetlands and water bodies drying up at the time of observation or imaging. In 2003, grassland started to witness an ever-decreasing trend in its coverage, joining the shrub land that decreased throughout the study period. Grassland covered 696560.64 down from 704169.81 hectares, a reduction of 2.20% while shrub land occupied 417567.81 hectares, (29.12%) from 31.31% in 1995.

Cropland and built-up areas are the two cover types that increased throughout the study period as population and human interventions increased in the basin (Figure 5.1c). By 2003, cropland occupied 178864.55 hectares, (12.47%), an increase of 3.07%. Forestland witnessed another decrease of 0.84% to stand at 85809.19 hectares (5.98%). During this period, both wetlands and water bodies increased occupying 36225.10 hectares (2.53%) and 17390.83 hectares (1.21%) respectively. These were increases of 1.61% and 0.61% for wetlands and water body. Built-up area was reported to have had a small decrease of 27.4 hectares (about 0.000%), which could have come because of miscalculations in the pixel values and misinterpretation of the rays reflected by the ground surface objects or a few demolitions. Bare land covered 989.66 hectares (0.07%), down from 0.11% in 1995. Grassland, shrub land, forestland consistently gave way to cropland as the main cause of change in land uses in the b asin. Built-up area and infrastructural development such as roads construction, though not classified are also consuming other land cover types, even if bare land hardly changed this period.

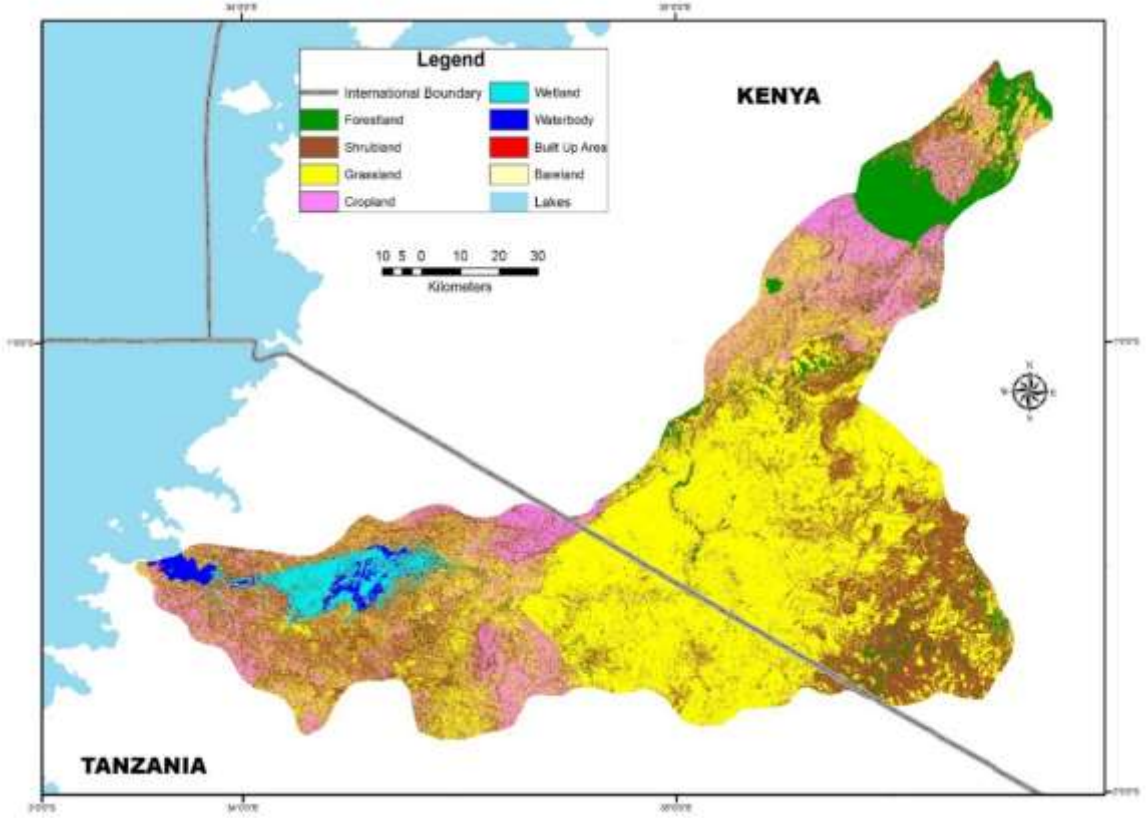

Figure 5.1c: Land cover/ use types in Mara Basin, 2003. Source: Researcher, 2016)

During the classification, areas under large-scale agriculture that resembled grass, especially wheat, might have acquired same class with grass. Cropland with similar cover as grassland at the time of imaging might have given cropland a lower percentage while grassland receiving an unfairly large share for the years under study, given the high rate of increase in human population and therefore, farms and homesteads. The increase in wetlands and water bodies during the same period could have come from flooding events following torrential rains covering the dry swamps, depressions bare land and shrub land in the lower reaches of the basin. With time, some water bodies could have acquire aquatic life forms especially plants and by doing so, converted to wetlands. Forestland especially in the upper catchment were being deforested for timber while some sections were taken over for tea, coffee and maize farming.

In 2011, the area indicated on the map to be under grass was 677281.50 hectares (47.25%) while that of shrub land was 414826.29 hectares (28.94%), a decrease of 1.33% and 0.08% respectively. Cropland stood at 210182.85 hectares (14.66%), an increase of 2.19% with forestland posting an increase for the first and only time.

Forestland occupied 97544.07 hectares (6.81%), an increase of 0.83% from the 2003 coverage while wetlands had 21637.53 hectares, 1.51% and represented a reduction of 1.02% (Fig.5.1d and on table 5.1). The total area under water body in 2011 was 9479.70 hectares (a decrease) and accounted for 0.55% while built-up area occupied 661.14 hectares, translating to 0.05% with bare land having 1728.27 hectares and occupying 0.12%. The Mara basin has continued to witness increased intensity of crop farming, which is consuming forest cover, rangelands and pastoral areas including wildlife migratory corridors thus, threatening the physical and human environment alike.

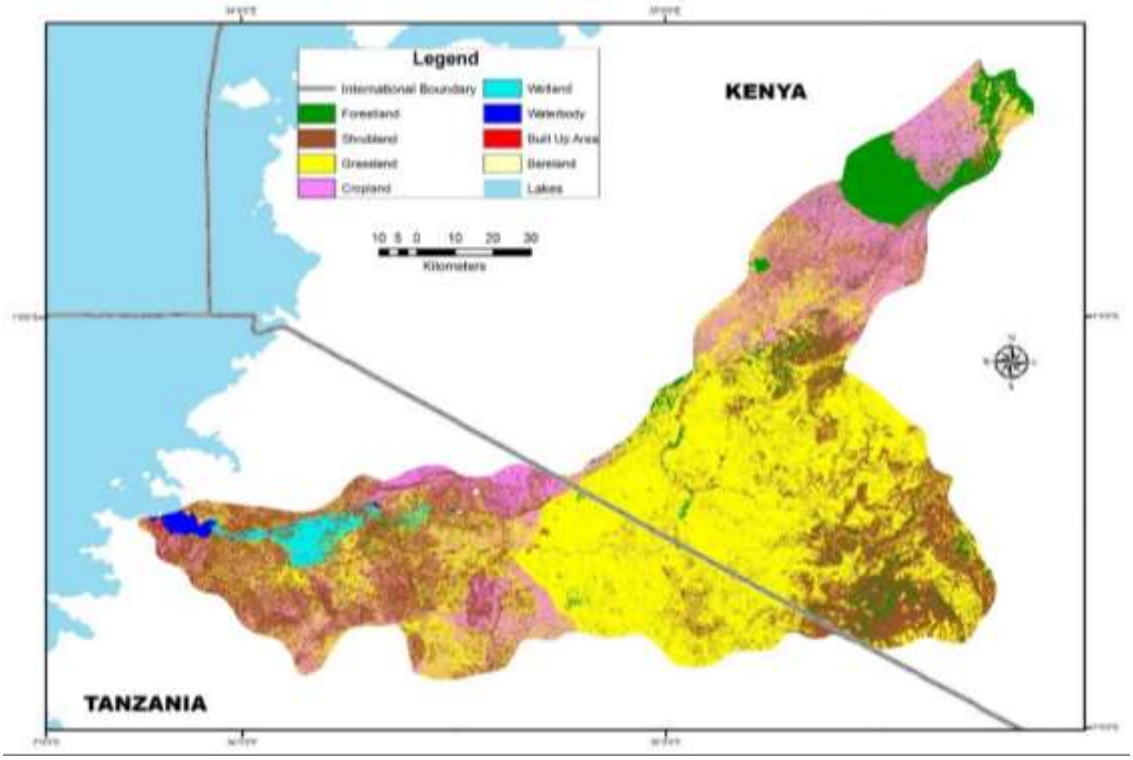

Figure 5.1d: Land cover/ use types in Mara Basin in 2003. (Source: Researcher, 2016)

Other than population pressure in the basin warranting such sporadic changes in land use practices, much of these changes may be attributed to poor governance by the past political regimes especially on matters touching on forest management (UNEP, KFS, KFWG, ENSDA, 2008). Excision of the Maasai Mau in 2001 to settle people is a case at hand, and was in part, the cause of the decrease in the forest cover in 2003. These scenarios are still common with the hotspots of land degradation being adjacent to the protected areas on the Kenyan side with high rate of population growth (WREM International 2008)

On the thematic map of 2016, grassland decreased to 648828.27 hectares (45.27%), shrub land occupied 398843.91 hectares, (27.83%) and those were decreases of 1.98% and 1.11% respectively. Cropland covered 245872.71 hectares, accounting for 17.16% with an increase of 2.5% (Figure 5.1e). Forestland witnessed a slight decrease (of less than 0.00%) and stood at 97414.11 hectares (6.8%), changes attributed to encroachments on forested areas and general degradation of the forest. Both wetlands and water bodies had slight increments of 0.5% and 0.04% to occupy 28823.40 and 10055.16 hectares respectively (2.01% and 0.70%).

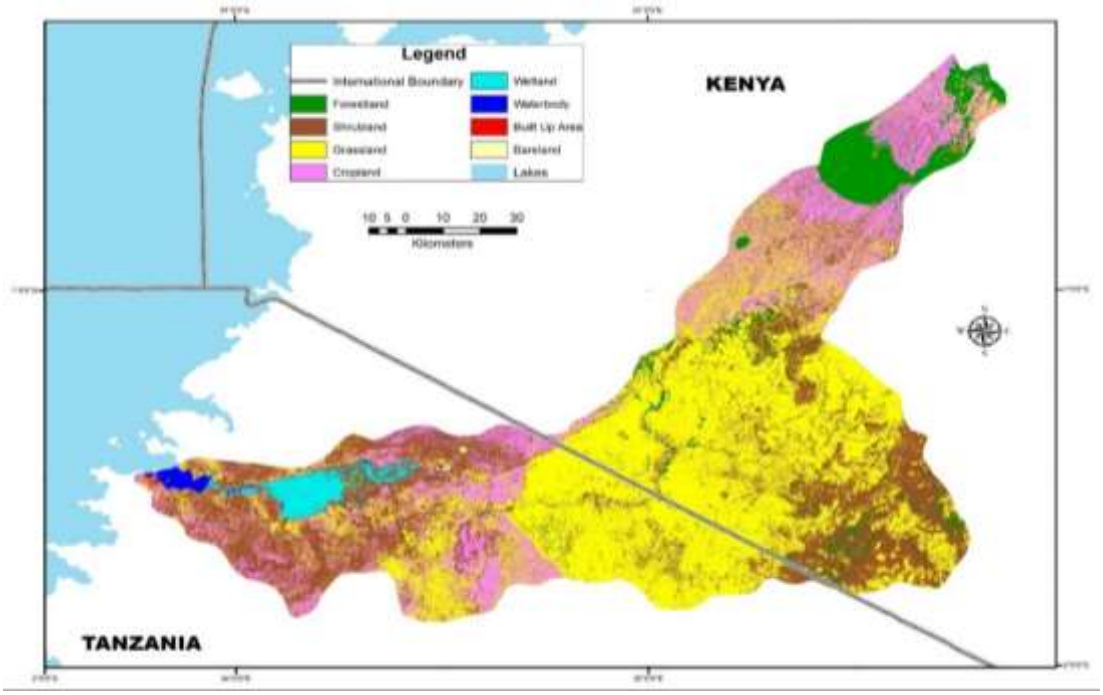

Figure 5.1e: Land cover/ use types in Mara Basin in 2016. (Source: Researcher, 2016)

Built-up areas and bare land increased by 0.04% and 0.03% to occupy 1249.11 and 2149.47 hectares respectively. Some shrubs, grass and farms converted to bare land. Among the fastest growing built-up areas are Bomet town in Bomet County of Kenya and Musuma Town in Musoma District, Tanzania and the point at which the Mara River pours its water into Lake Victoria. Otherwise, there are many upcoming urban centres in both Kenya and Tanzania such as Mulot, Kilgoris and Tarime.

Table 5.1: Land Cover and Land Use Distribution in 1984, 1995, 2003, 2011 and 2016

LCLU TYPE	1984		1995		2003		2011		2016	
	Area_Ha	%	Area_Ha	%	Area_Ha	%	Area_Ha	%	Area_Ha	%
Forestland	104260.95	7.27	97959.50	6.83	85809.19	5.98	97544.07	6.81	97414.11	6.80
Shrub land	496599.12	34.65	448860.72	31.31	417567.81	29.12	414826.3	28.94	398843.91	27.83
Grassland	704169.81	49.13	728104.1	50.78	696560.8	48.58	677281.5	47.25	648828.3	45.27
Cropland	99529.74	6.94	134840.54	9.40	178864.6	12.47	210182.9	14.66	245872.7	17.16
Wetland	17619.03	1.23	13189.24	0.92	36225.10	2.53	21637.53	1.51	28823.40	2.01
Water body	9114.84	0.64	8667.93	0.60	17390.83	1.21	9479.70	0.66	10055.16	0.70
Built. Area	407.25	0.03	565. 96	0.04	379.85	0.03	661.14	0.05	1249.11	0.09
Bare land	1575.36	0.11	1589.94	0.11	989.66	0.07	1728.27	0.12	2149.47	0.15
TOTAL	1,433,276	100	1433777	100	1433787	100	1433341	100	1433236	100

Source: Researcher, 2016

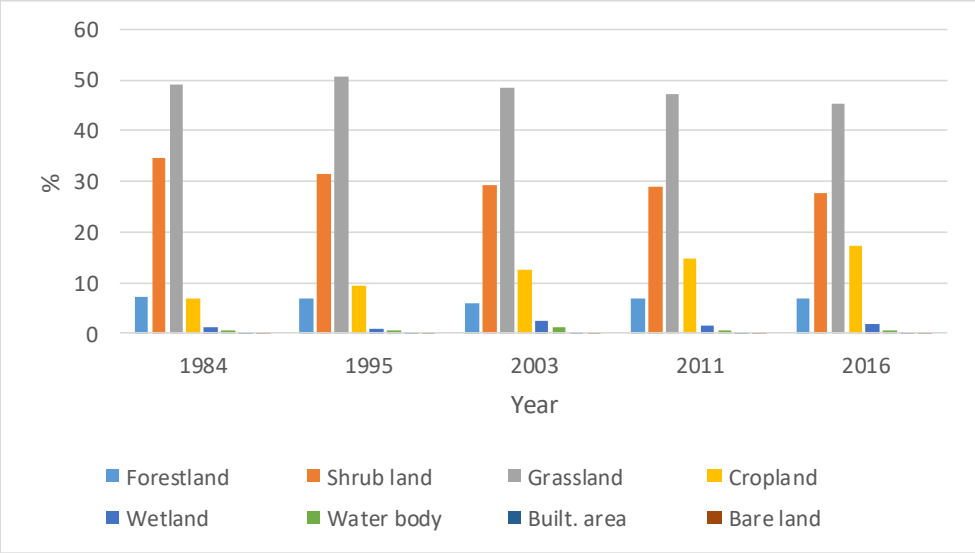

Figure 5.2: Percentage Land Cover Type by Year (1984 – 2016). (Source: Researcher, 2016)

Land cover mapping of the five main forests in Kenya that included Mt. Kenya, the, Mt. Elgon, Mau Complex, the Aberdare Range and the Cherangani Hills conducted between 2003 and 2005, revealed that major destruction of indigenous forests occurred in the Mau complex over that period due to human encroachment on forests (DRSRS, KFWG & Royal Netherlands Embassy, 2006). Four of the forest blocks destroyed in the complex due to encroachment were the Maasai Mau forest (trust forest), which is within the Mara basin and, South West Mau Forest Reserve, Eastern Mau Forest Reserve, and Mt. Londiani Forest Reserve.

Conversion of forestland, grassland and shrub land to cropland and built-up areas which is still ongoing in the Mara will have increased negative implications on the environmental services, ecological functions and livelihoods as they enhance microclimate modification, global warming and climate change. These results agree with other previous studies in the Mara including Mati *et al*., 2005; Mutie *et al*., 2006; Mango *et al*., 2010; Mango *et al*., 2011, Melesse et *al*., 2012; Dessu and Melesse, 2012; Oruma *et al*., 2017, who found out that deforestation and environmental degradation result in reduced base flows and high peak flows observed in the basin.

5.2.2 Post Classification Visual Comparison

Post classification visual comparison was another approach taken to identify and evaluate the areas with more changes in land use practices. Such areas were referred to as hotspots in this study and were found to be in the surrounding of Musoma and Tarime in Tanzania and Bomet and Keringet in Kenya respectively. Thus, from the thematic maps developed from the imageries for 1894, 1995, 2003, 2011 and 2016, areas with more change were identified, delineated and enlarged (Plates 5.1 to 5.4) to enhance visual perception and evaluation of the observed changes. The approach works well in spatial research such as this one in describing changes thereof. It complements the post classification area comparison approach, which cannot be used with ease, to visually discriminate the changes because details are small in map (subsection 5.2.1). The plate 5.1 shows Musoma town and its neighbourhood including the Kitaji dam as the area appears on the Landsat 8 imagery of 2016 and on the maps for 1984, 1995, 2003, 2011 and 2016 that are zoomed out for clarity.

The 1984 map shows a large Musoma town already in existence but without Kitaji dam, meaning that it was not yet in existence in 1984. On the right side of the map is a water body including the point at which, the Mara River pours its waters into Lake Victoria. To the upper left corner are the Lake Victoria waters. Airstrip is shown with some grass-covered area in the neighbourhood while the left side shows industrial, residential and commercial areas. The built-up areas to the right host central business district with open spaces including parks in the built-up area and on the surrounding. The 1995 map shows the Kitaji dam and has the largest coverage of all the maps. This could be because the dam had not stayed for long and therefore had not faced any siltation and eutrophication problems together with inhabitation by aquatic plants. Construction in the open spaces

on the left and parts of the built-up areas continued as shown on the map. The dam is within the built-up area and therefore has high tendency of siltation and pollution.

The 2003 map shows some reduction in the coverage of the dam as indication of siltation, eutrophication, vegetation cover and pollution of the dam. The situation was even worse in 2011 when the dam was at its smallest size. The trend of change in the area covered by the dam from inception to 2016 seems to take a downward trend as human activities in the neighbourhood increased. The 2016 map shows the dam to be a bit wider than what it was in 2011. This could be due to addition of water after some heavy rains or back floods as opposed to cleaning and rehabilitation of the dam, portrayed by the sky blue colour on the edges of the dam, sign of eutrophication. The existing situation in 2016 is that of pollution and general degradation of the dam, although it has more water than in 2011.

Plate 5.2 shows the satellite imagery (Landsat 7) for 2016 and the enlarged thematic maps for 1984, 1995, 2003, 2011 and 2016 covering the Buhemba and Nyamongo Mines and their environs within the Tarime region of Tanzania. The mines in the lower part is the Buhemba while Nyamongo is to the north or upper part. The enlarged maps for 1984 and 1995 have no indication of the Mines and this could mean that, either they were not in existence until after 1995 or they were too small in extent and therefore could not be in the imageries. The dominant features in the area according to the 1984 map were shrubs, grass, wetlands, farms and Tarime town with more farms in 1995, reduced number of wetlands with one becoming larger in the lower left corner. Both mines appear on the 2003 map with the Buhemba Mines larger in coverage than the Nyamongo Mines. This is an indication that, Buhemba Mines became operational much earlier than the Nyamongo Mines, confirmed by the presence of water in the abandoned deeper parts. Within a period of eight years, both the Buhemba and Nyamongo Mines increased more than three times in their coverages (see 2011 map).

The Buhemba Mines increased in extent and depth resulting in an increased area under water. Equally witnessed was the increase in built-up area as more people settled near the mines for business, mining related activities and farming resulting in reduced number of wetlands. The 2016 map shows the largest coverage in both mines while a good part of the grass cover and farms converted to shrubs and built-up areas. This

could be a result of leaving the farms to lie fallow, allowing regeneration of bush and thicket in such areas. The mines have attracted large numbers of people to work in them and to trade in the surrounding, thus the increase in the built-up areas in the neighbourhood of the mines. There is good infrastructure, especially the roads in the area as well as an increase in the number of wetlands that could be due to flooding after excessive rains. The mines are consuming the areas that were under shrubs, grass and cropland while other shrub lands converted to cropland.

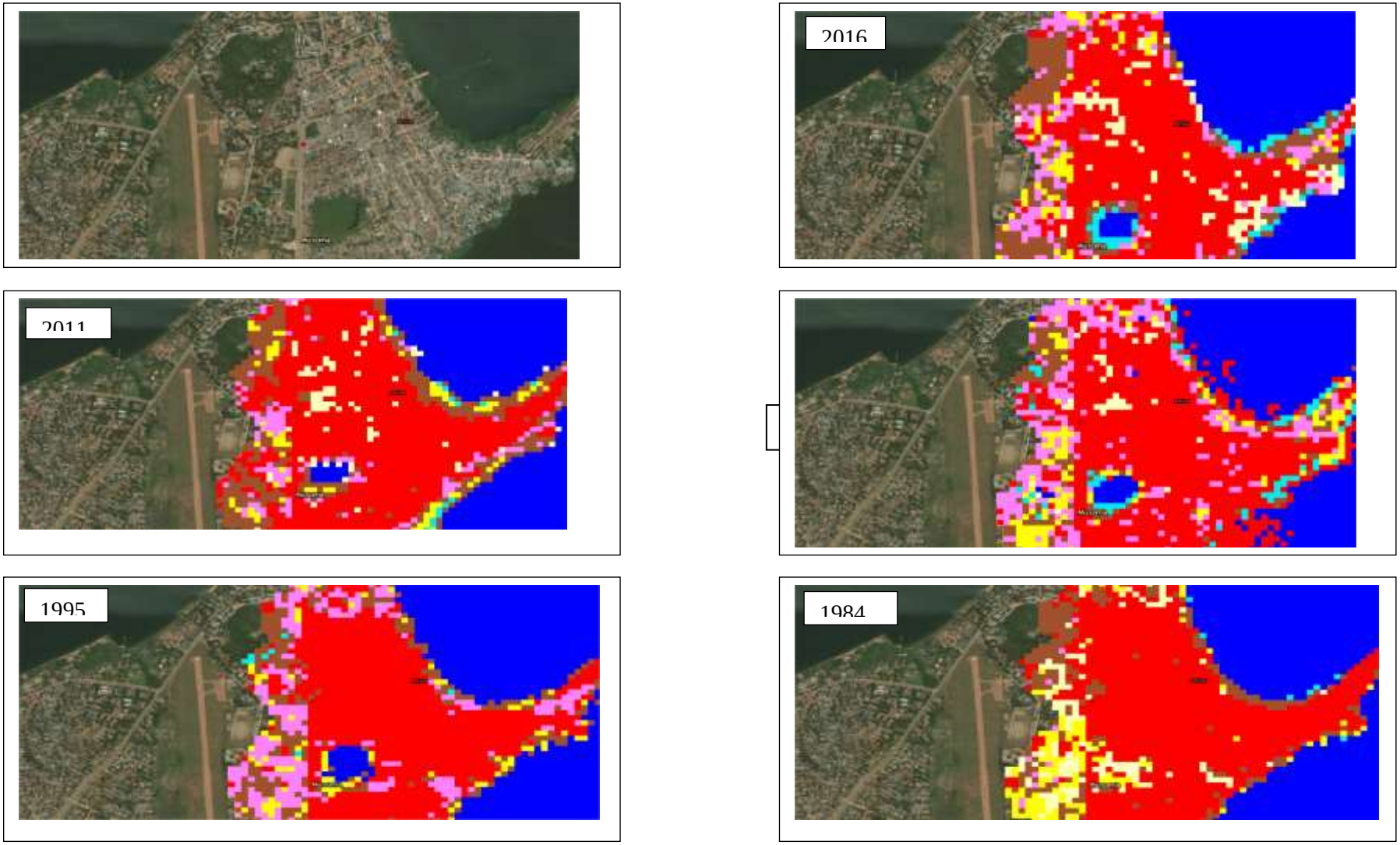

Plate 5.1: Kitaji Dam and part of Musoma Town

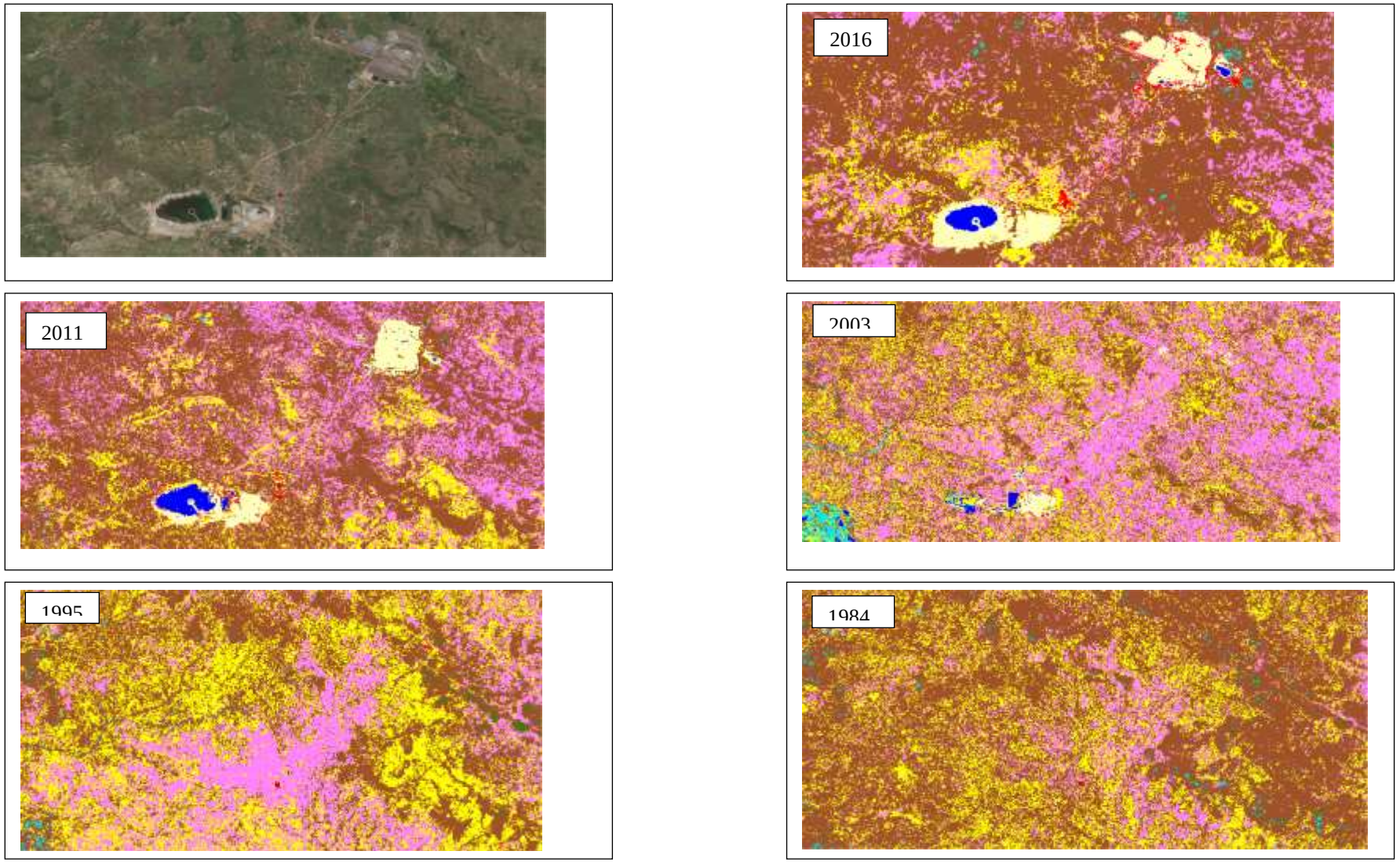

Plate 5.2: Buhemba and Nyamongo Mines in Tarime.

Looking at Bomet town and its environments and comparing the 2016 imagery with the 2016 thematic map and the maps for the other years, the same situations of human interventions observed on the Tanzanian side are again observed. In 1984, Bomet was a very small centre with a few buildings that could not be detected and recorded on the imagery and therefore did not qualify to be a built-up area. The area was largely under grass followed by farms and then shrubs, with forests in some pockets in 1984. By 1995, Bomet had gained a good coverage in extent and number of buildings, thus the area shown on the map, which is not built-up area yet (Plate 5.3). The surrounding had an increase in the area under farms and forests with a reduction in grassland and shrub land. There appears a few water bodies, mainly pools of water in depressions and ponds. By 2003, Bomet town had extensively expanded, hosting a conglomeration of buildings and qualified to be a built-up area. More grassland converted to cropland, built-up area and forestland while some farms laid fallow and converted to shrub land.

In 2011, we see a more expanded Bomet town with more farms in the surrounding as grassland changed to cropland and built-up area. The 2011 map shows water bodies not only around Bomet but also in most parts covered by the map. This could mean that the imagery was taken after some excessive rains that formed pools of water in the surrounding. This can be confirmed by the fact that even the Nyangores river had more water than in the other years. This simply means that the year had an excessive or abnormal rainfall that collected in pools on the surface at the time of imagery scanning. Other than Bomet town, built-up areas developed in the neighbourhood of Bomet as more services came to Bomet attracting more people to the neighbourhood.

The map of 2016 shows even a larger Bomet with a large increase in the built-up areas in the surrounding. It is important to note that Bomet as a town is rapidly expanding and therefore consuming agricultural land in the neighbourhood and this could render the populace food insecure in the near future accompanied by serious environmental degradation. The forests within the Bomet town area and Bomet County in general are due for conservation because they are water towers with microclimate modification abilities thus, keeping the environment healthy. A healthy environment provides

various ecological services and functions as well as supporting livelihoods and socio-economic activities including crop and livestock farming.

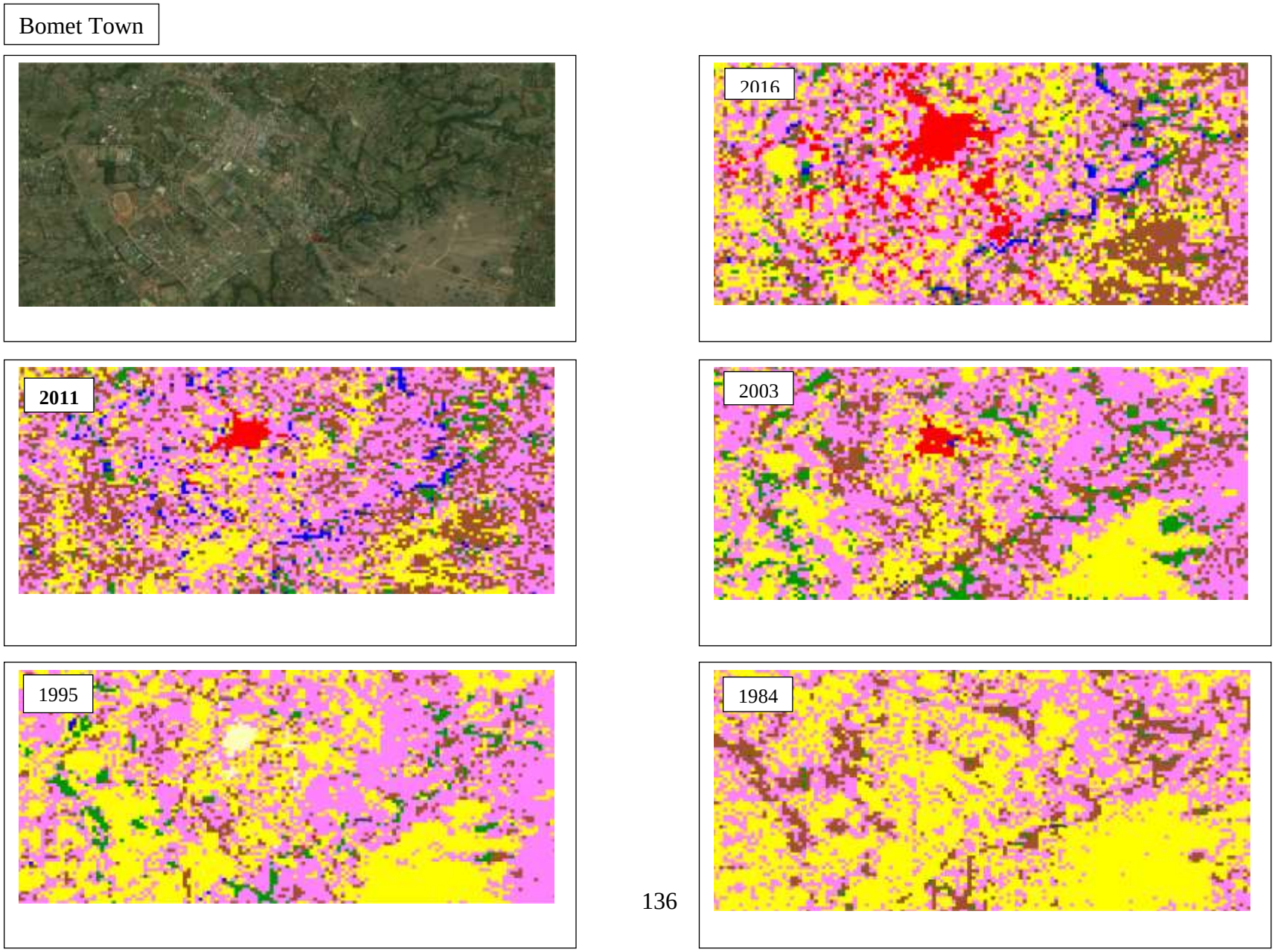

Plate 5.3: Land Use Types around Bomet Town, Kenya.

The map extracts (Plate 5.4) below show part of Kiptunga Forest in the upper catchment of Mara River. Keringet trading centre is an upcoming urban centre in this area. The map for 1984 shows the forest and then, grass as the main cover types with patches of farms, settlements and shrubs. This indicates that not much degradation or deforestation had taken place due to less anthropogenic activities in that environment. The 1995 map of the area however, shows an increase in forest cover and cropland when some grass and shrub lands converted to forest. Some of the grassland and shrub land converted into cropland. Some grass-covered areas also changed to shrubs and vice versa.

As shown on the map of 2003, the forest cover had marked reduction in coverage because of logging and conversion of forestland to cropland, especially tea farms, grazing and settlement areas. During this period, some forested areas changed to shrubs and grass cover while some shrubs changed to grass with some cropland changing to grass and shrubs. The land use map of 2011 indicates that, grassland and cropland increased at the expense of forestland and shrub land. In 2016, shrub land almost disappeared completely, a trend which is also followed by grassland, which is disappearing very fast as they convert into cropland.

The two main features seen on the 2016 map are forests and cropland, although forest cover is on the decline as more of it converts to cropland and built-up areas. The future of Kiptunga forest, the origin of Amala river is threatened and therefore, the very existence of the Amala and, by implication, the Mara River unless proactive infrastructural arrangements aimed at its conservation for sustainability are put in place. The deforestation in Kiptunga and the general Mau Escarpment mean less carbon sinks and more global warming with increased arid like conditions and this would threaten many systems including livelihoods. These are conditions already witnessed more so in the middle and lower parts of the basin.

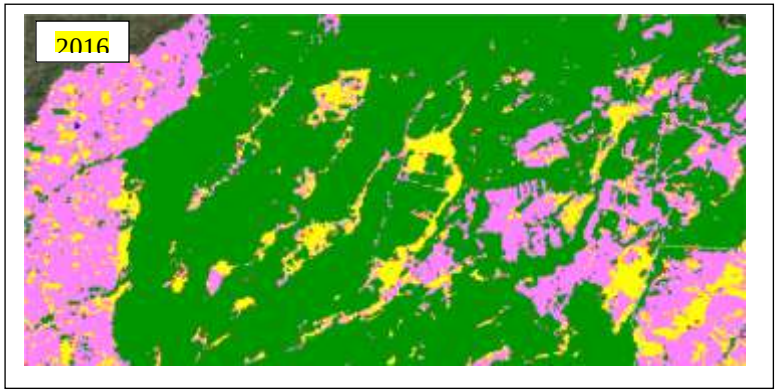

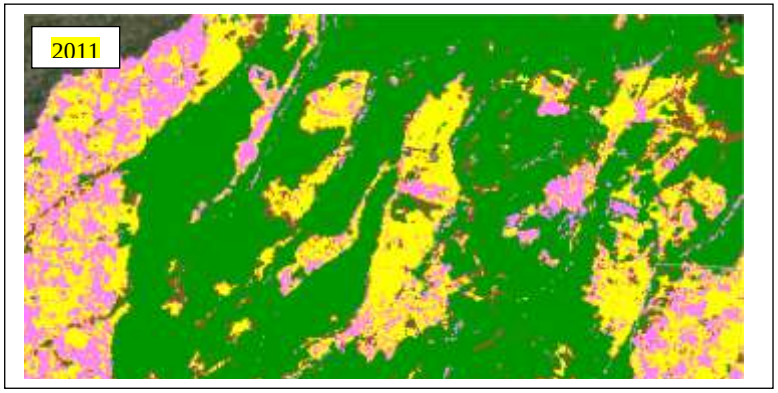

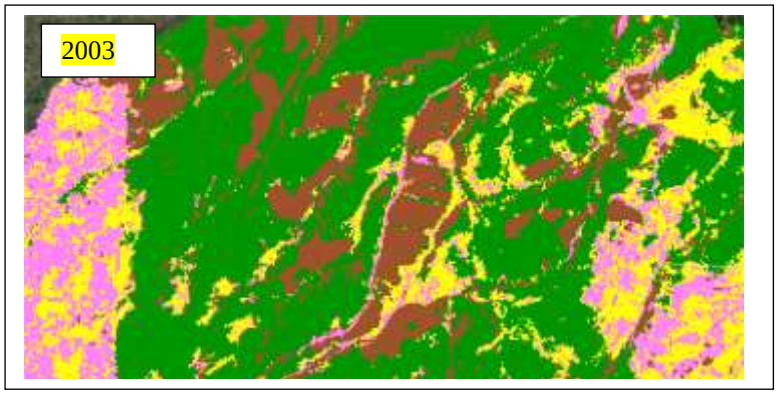

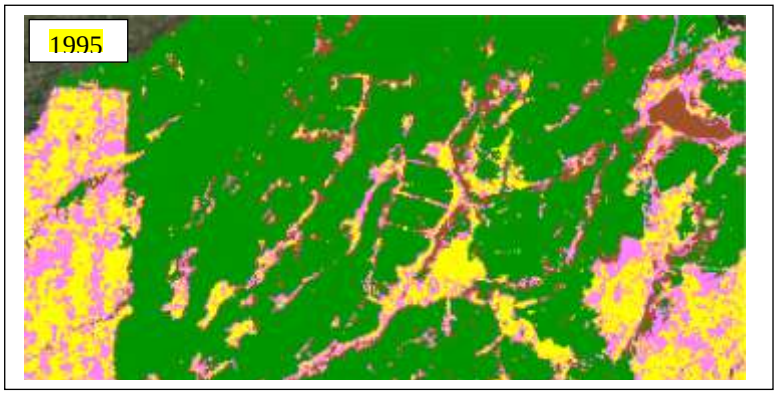

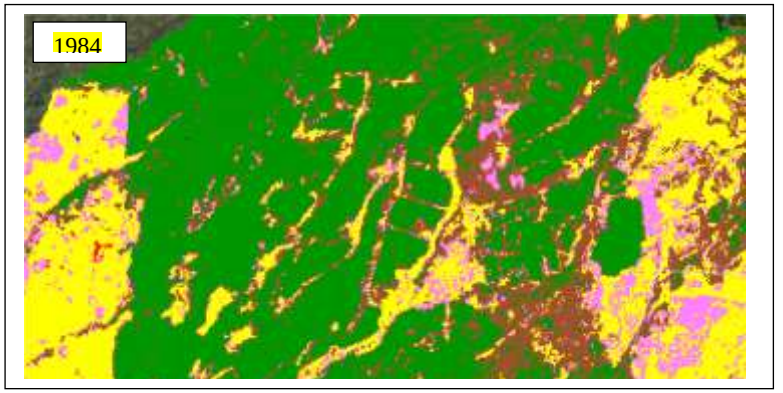

Plate 5.4: Human Activities within Kiptunga Forest, Nakuru

5.2.3 Overlay Operations for Changes within and across Classes

The quantitative spatio-temporal land cover and land use change results were presented through overlay operations of the various false colour land cover imageries produced during cover classification exercise. Overlay operations reveal changes within and cross the classes as well as areas without change over a given period. This simply means that, areas that were under, say, grass at the beginning of a period remained the same at the end of that period. Figures 5.3a, 5.3b, 5.3c and 5.3d are the overlays for the years 1984 and 1995, 1995 and 2003, 2003 and 2011, lastly 2011, and 2016 whose attribute tables are in Appendix IV. The overlays reveal both good and bad changes on the landscape as land use changes and this makes it a good tool for providing quick land use information over large basins or areas that can enhance speedy policy formulation aimed at promoting sustainable natural resources management.

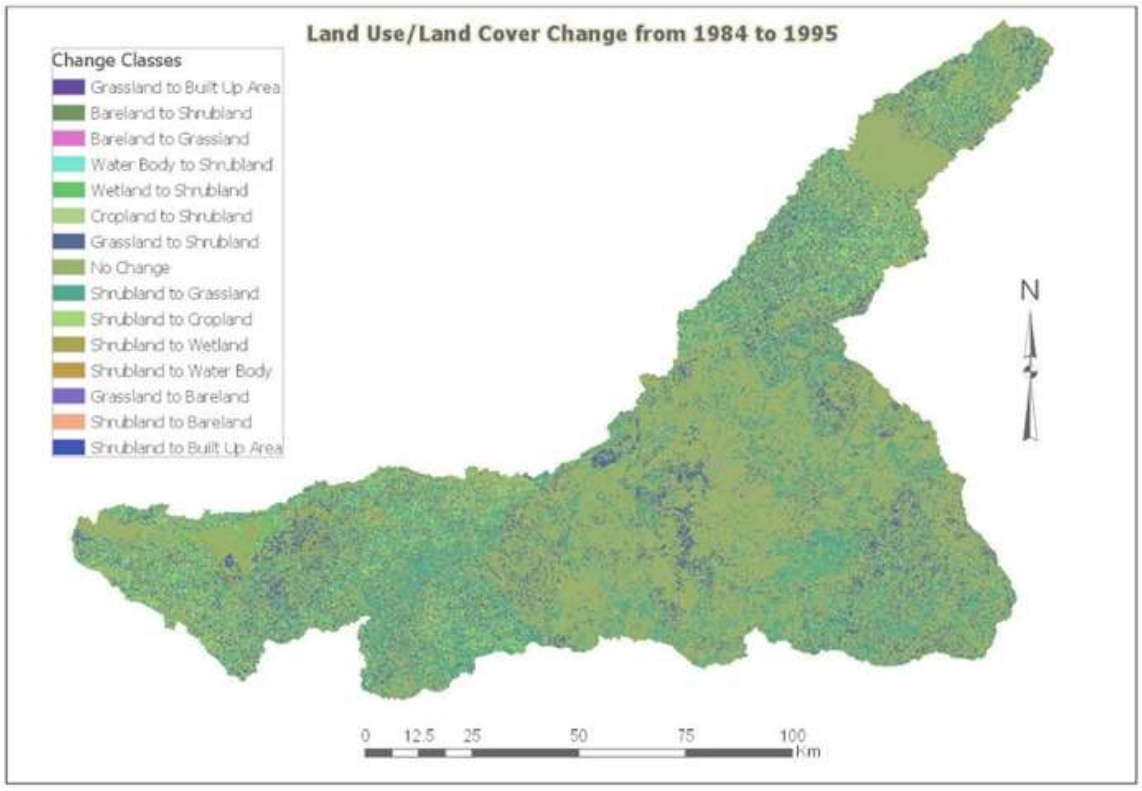

Figure 5.3a: An overlay of 1984 and 1995 Cover Imageries (Source: Researcher, 2017)

From 1984 to 1995, 79.24% of the total coverage did not change to any class with grassland and shrub land forming the greater part of the 20.76% change detected. Specifically grassland and shrub land converted to other cover classes by 9.06% and 6.94% respectively (Figure 5.3a and Table 1 in Appendix IV). Equally, grassland and

shrub lands formed about 85% of the total cover types that had no change, and was expected because the basin is a rangeland. The rest of the cover types changed to other classes as follows: forestland, 0.712%; cropland, 3.82%; wetland, 0.19%; water body 0.019%; built-up area, 0.006% and bare land 0.022% over same period. Notably, grassland was converting at the highest rate followed by shrub land. The about 0.71% change in forestland to other cover types is worth noting because of the role forests play in the physical environment, especially in the Mara. Generally, the conversion of forestland, grassland and shrub land to other types especially cropland and built-up area are impacting the hydrological regimes of Mara River.

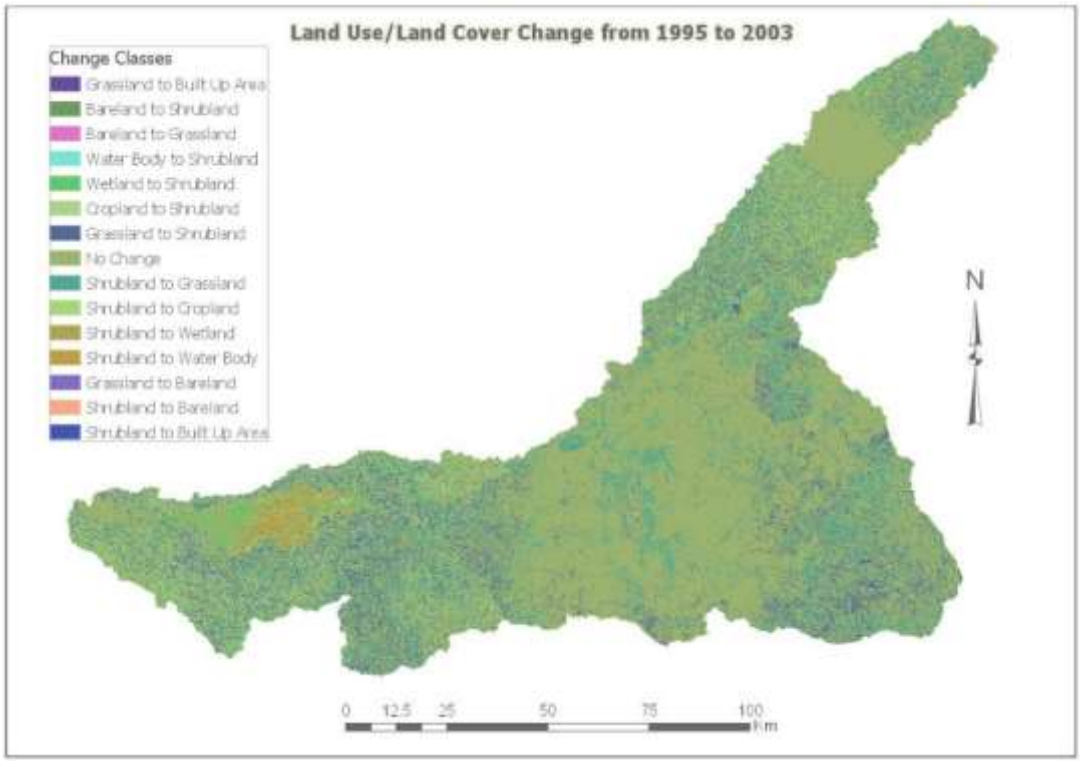

Figure 5.3b: Overlay operations, 1995 and 2003 Cover Imageries (Source: Researcher, 2017)

Between 1995 and 2003, about 80.06% of the total cover remained intact while shrub land and grassland converted by about 6.29 and 6.00% respectively to other cover types. Cropland changed by 4.25%; forestland, 1.08%; wetlands, 1.7% while water body recorded 0.67% change. Built-up and bare land had both changed by less than 0.1% each (Figure 5.3b and Table 2 in Appendix IV). Changes in grassland, shrub land and forestland were of much concern in this study due to their role in Mara River flow volumes. These cover classes are declining at high rates and will compromise the existing systems and sub systems as discussed in subsection 5.2.4, relating to changes

in the Mara hydrographs due to changes in land cover and land uses. The rapidly increasing trends in cropland is worrying because it degrades the natural systems including forests in the water tower that also eliminates its role of carbon sinking and therefore microclimate modification. The degradation of shrub land and grassland reduce their role of supporting wildlife and pastoralism as well as the water bodies with implications on the ecological and environmental functions. The situation is worrying because Mara River basin is a water sensitive region. As discussed in subsection 5.2.1, the trends in wetlands and water bodies are not specific and appear to be a function of seasons and time of the year driven by prevailing conditions based on seasons and specific conditions in a given year. In a way, changes in bare land appear to follow the trends observed in wetlands and water bodies.

During the period from 2003 to 2011, sum of 78.80% of the cover types did not change. Most change was again recorded under shrub land, compared to grassland, f registering 8.08% and 6.38% respectively. Cropland converted by 5.20% to other cover types, including bare land, built-up areas, grassland and shrub land. Over the same period, forestland changed by 1.17%, such a significant change given the percentage occupied by forests in the basin. Forest cover especially in the catchment is very significant since they are water towers. They also regulate temperatures and other whether elements. Reduction in areas under forests, shrubs and grass reduce the rates and amounts of evapotranspiration, especially reduction in forest cover due to reduced leaf cover, hence less moisture goes into the atmosphere resulting in poor rainfall formation and distribution over the Mara. The declining trends in rainfall that are also unreliable in the basin are attributed to changes in land cover and land use practices (example, see Mango *et al.,* 2011). Decrease in the areas under forest and grass cover as well as area under shrubs tend to encourage surface runoff and soil erosion because of reduced infiltration that also results in reduced base flows. Wetlands changed by 0.26%, water body, 0.05%, built-up area, 0.03% and bare land 0.04% with higher changes recorded under wetlands than water bodies because of more encroachments on the wetlands are experienced in the Mara as people try to maximize their gains from the ecosystem (Figure 5.3c and Table 3 in Appendix IV).

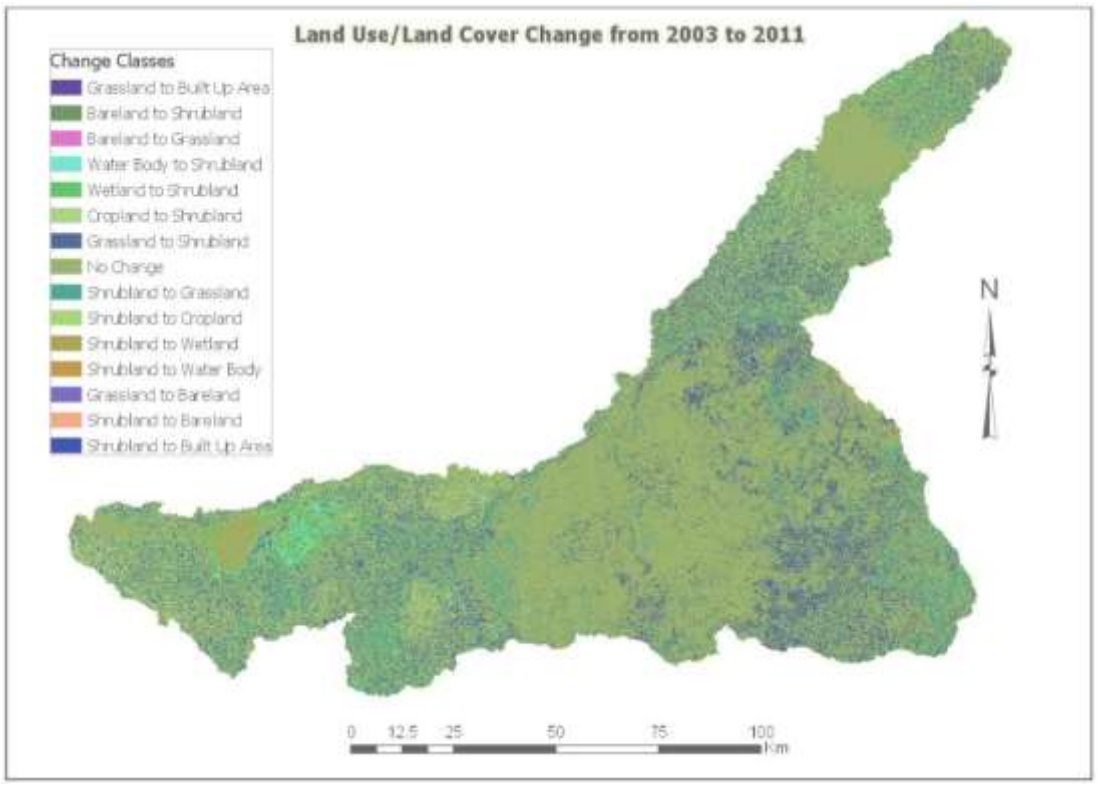

Figure 5.3c: An overlay of 2003 and 2011Cover Imageries (Source: Researcher, 2017)

Between 2011 and 2016, 81.56% of the total cover types never changed with shrub land and grassland converting by 5.98% and 5.15% respectively. Cropland had 5.7% conversion including areas left fallow or abandoned to revert to other none farming activities. Forestland changed by 0.48%, wetlands, 0.63%, water body, 0.06%, built-up area, 0.02 and bare land 0.03%. The overlay operation is very important since it gives a detailed inter and extra changes beyond the classes used in cover classification exercise in a study. This helps much in assessing human activities on the landscape that when relied upon, promote sustainable resources utilization since such changes have different implications on the physical environment (Figure 5.3d and Table 4 in Appendix IV).

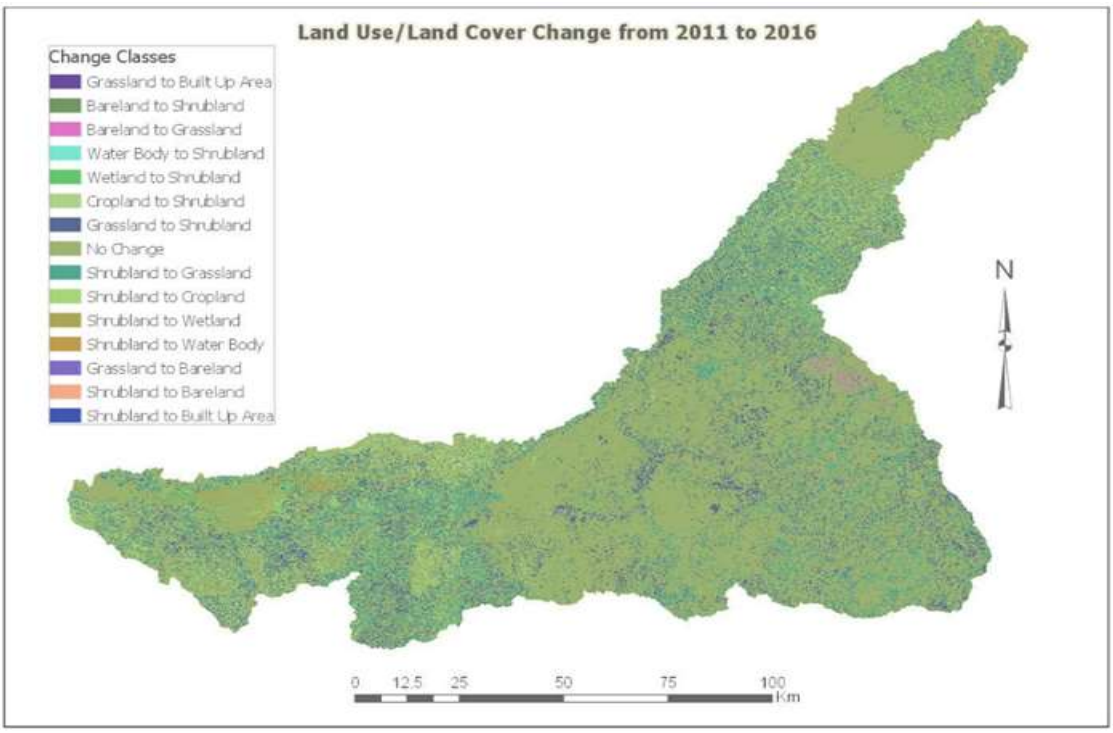

Figure 5.3d: An overlay of 2003 and 2011 Cover Imageries (Source: Researcher, 2017)

From the overlay results, all cover types changed within and across their boundaries with some parts of the same, not changing in the entire period of study. Changes are a function of human interventions and increased with time as human occupation of the basin increased with implications on both the physical and human environment including the Mara River flow volumes. This study discovered that reduction in forestland, grassland and shrub land has resulted in reduced and unreliable rainfall with low base flows and these have their implications on every sector of the economy as reported in the foregoing subsections. These results agree with the previous studies including those by Mutie *et al*., 2006; Mati *et al*., 2008; Mango et *al*., 2011; Dessu *et al*., 2012, Melesse *et al*., 2012; Mwania, 2014; Oruma *et al*., 2017. The reports mention conversion of forests and rangelands to agricultural land as main factors impacting the Mara hydrological regimes witnessed in reduced base flows and high peak flows. Thus, these trends in land use types will have more threaten on the many sectors of the economy and ecosystems alike.

5.2.4 Trends in Land Cover and Land Use Change

Grassland and shrub land are the two major cover types in the Mara River basin because it is a rangeland. The third largest land cover type, cropland is increasing at an alarming rate with the invasion of the basin by farmers from other communities. The pressure on land has forced the farmers to encroach and farm on the grassland and shrub land including the wildlife migratory corridors and fragile ecosystems such as forests and wetlands and this has resulted in tremendous decrease in these cover types and general environmental degradation. Table 5.2 is obtained by comparing values of each land cover type on one thematic map with those of the next thematic map in table 5.1. In effect, Table 5.2 shows the changes in land cover and land use categories over the designated years of study expressed in hectares and as percentages. The positive signs indicate increase while negative values, a decline in the cover types.

Table 5.2: Nature, Trends and Rate of Land Cover Change

Land Cover Types	1984-1995		1995-2003		2003-2011		2011-2016	
	Hectares	%	Hectares	%	Hectares	%	Hectares	%
Forestland	-6301.45	-0.44	-12150.31	-0.85	11734.88	0.83	-129.96	-0.01
Shrub land	-47738.40	-3.34	-31292.91	-2.19	-2741.52	-0.18	-15982.38	-1.11
Grassland	23934.27	1.65	-31543.24	-2.2	-19279.34	-1.33	-28453.23	-1.98
Cropland	35310.80	2.46	44024.01	3.07	31318.30	2.19	35689.86	2.5
Wetland	-4429.79	-0.31	23035.86	1.61	-14587.57	-1.02	7185.87	0.5
Water body	-446.91	-0.04	8722.90	0.61	-7911.13	-0.55	575.46	0.04
Built-up Area	158.71	0.01	-186.11	-0.01	281.29	0.02	587.97	0.04
Bare land	14.58	0.00	-600.28	-0.04	738.61	0.05	421.20	0.03

Source: Researcher, 2017

In this study, shrub land reduced in its extent while cropland and built-up area increased over the study period, hence the negative and positive trends respectively. Grassland and forestland are also on the decline, recording an increase in only one period each (Table 5.2). In essence, the shrub land, grassland and forestland are all reducing in their spatial extent as indicated by the negative signs changing to cropland and built-up areas among others. For a period of 11 years, between 1984 and 1995, forestland reduced by 6301.45 hectares (0.44%, shrub land by 47738.40 hectares (3.34%), wetland by 4429.79 hectares (0.31%) and water body by 446.91 hectares (0.04%), changing mainly

to cropland, grassland and built-up area. Cropland, grassland and built-up area gained by 23934.27 (2.46%), 35310.80 (1.65%) and 158.71 hectares (0.01%) respectively.

These results agree with previous scholars (Mango *et al.*, 2011; Dessu and Melesse, 2012; Oruma *et al.*, 2017) that high population increases and invasion by outsiders including developing agents, and the desire by the government to change the lifestyles of indigenous communities brought numerous conflicts in the use of resources, especially in and around forests and wetlands. The trends in Table 5.2 are alluded to some of these factors while those witnessed in the wetlands and water bodies are attributable to both the human interventions and weather patterns, causing droughts and flooding due to erratic rains.

The 1995-2003, an eight-year period reported close to double the reduction in the area under forest, (12150.31 hectares or 0.85%) with shrub land decreasing by 31543.24 hectares (2.19%) and grassland by 31292.91 hectares (2.2%). These classes changed to cropland and wetland, which recorded major increases of 44024.01 and 23035.86 hectares, accounting for 3.07% and 1.61% respectively. Water body also increased by 8722.90 hectares (0.61%), about a third the increase in wetlands that could partly, be explained by flooding due to excessive rains in the basin covering lower areas including bare lands in low areas as could be seen from the large decrease in bare land. A small decrease in built-up area was recorded, which could be due to miss interpretation of the pixels during image classification exercise.

The period from 2003 to 2011 witnessed changes contained in columns 4 and 5 of Table 5.2. The forest cover increased this time as the only period with an increase, while shrub land and grassland continued to register a decline in their coverage. Wetlands and water bodies had a unique pattern in their variation between 1984 and 2016 recording a decrease in each one of them in one-period followed by an increase in each, over the next period (Table 5.2) to the end of the study. An increase between 1995 and 2003 preceded a decrease in the 2003-2011 period and an increase between 2011 and 2016. Their changes could probably have more to do with the weather patterns than anthropogenic factors. The fact that forestland still encountered a decrease would mean that the management of forest resources in the basin is an issue that has never been adequately addressed.

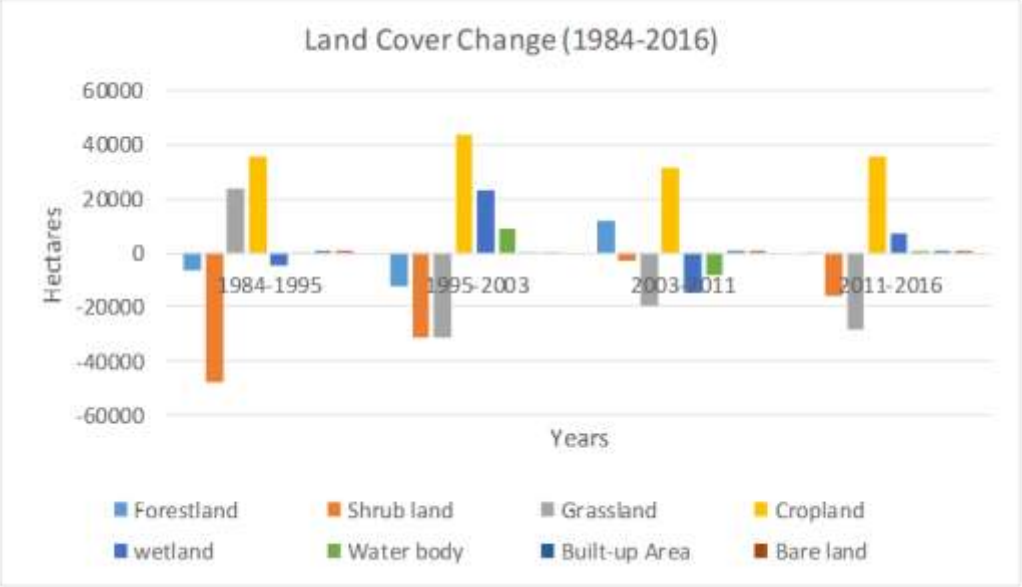

Figure 5.4: Land cover and land use change between 1984 and 2016.

Forests have enormous functions including being water towers, source of renewable energy, providing environmental services such as maintain biodiversity, protection of water and land resources and, alleviating climate change implications as well as improving the aesthetic values of the environment. Decrease in forest cover therefore would result in the contrary to the above with serious impacts on both the physical and cultural landscapes. If this were so in our case, we would have expected a reduction in areas under wetlands and water bodies. The contrary is however the case, more so that forestland decreased in three out of four periods. Figure 5.4 is a graphical presentation of the nature or trends and magnitude in the land cover types between 1984 and 2016.

5.2.5 Annual Trends in Land Cover and Land Use Categories

The results of the annual trends in the various cover types in between the study periods - 1984 to 1995, 1995 to 2003, 2003 to 2011 and, 2011 to 2016 are presented here (Table 5.3). Between 1984 and 1995, forestland decreased by 572.86 hectares, which was 0.04%; shrub land, 4339.85 hectares and 0.30%; wetlands and water bodies decreased by 402.71 and 40.63 hectares and accounted for a reduction of 0.03% and 0.003% respectively. During the same period, grassland increased by 2175.84, cropland, 3210.07, built-up areas, 14.43 and bare land, 14.58 hectares that resulted in increments of 0.15%, 0.22%, 0.001% and less than 0.001% respectively. Between 1995 and 2003, annual decreases occurred in forestland of 0.11%; shrub land, 0.27%; grassland, 0.28%;

built-up area, 0.001% and bare land, 0.005% while increments were observed under cropland, wetlands and water bodies of 0.38, 0.2 and 0.08% respectively. The period from 2003 to 2011 witnessed a slight annual increase in forestland of 0.104% while cropland, built-up area and bare land increased by 0.274, 0.003 and 0.006%, in that order.

Table 5.3: Annual Rates of Change in Land Cover Categories

Land cover types	1984-1995		1995-2003		2003-2011		2011-2016	
	hectares	%	hectares	%	hectares	%	hectares	%
Forestland	-572.86	-0.040	-1518.79	-0.110	1466.86	0.104	-25.99	-0.002
Shrub land	-4339.85	-0.300	-3911.61	-0.270	-342.69	-0.023	-3196.48	-0.222
Grassland	2175.84	0.150	-3942.91	-0.280	-2409.92	-0.170	-5690.65	-0.396
Cropland	3210.07	0.220	8713.21	0.380	3914.79	0.274	7137.97	0.500
Wetlands	-402.71	-0.030	2879.48	0.200	-1823.45	-0.128	1437.17	0.100
Water body	-40.63	-0.003	1090.36	0.080	-988.89	-0.070	115.09	0.008
Builtup Area	14.43	0.001	-23.26	-0.001	35.16	0.003	117.59	0.008
Bare land	14.58	0.000	-75.04	-0.005	92.33	0.006	84.24	0.006

Source: Researcher, 2017

On the other hand, shrub land, grassland, wetlands and water bodies had annual reduction of 0.023, 0.17, 0.128 and 0.07% respectively. During the last period (2011 to 2016), forestland, shrub land and grassland decreased by 0.002, 0.222 and 0.396% annually while the rest had increases of 0.5, 0.008, 0.1, 0.008 and 0.006% for cropland, wetlands, water bodies, built-up area and bare land. The outcome is that forestland, shrub land and grassland are all decreasing in spatial coverage while cropland and built-up areas are spatially increasing at accelerated rates with wetlands, water bodies and bare land not having definite trends.

After establishing the nature, extent, rate and magnitude in land cover and land use change between 1984 and 2016, the null hypothesis 'Land use practices have not significantly changed over the study period in the Mara River basin' was tested at $\alpha = 0.05$ using the Chi-Square test statistic. Using Chi-square at 28 degrees of freedom, the critical table value was $\chi^2 = 41.34$, which was less than the calculated value of 119433.6

(Appendix V). Therefore, we rejected the null hypothesis and accepted the alternative that, the 'land use practices have changed significantly over the study period'.

5.3 Spatio Temporal Variations in Trends in Rainfall, Temperature and River Flow

The results of the trends in the observed hydro-meteorological data are discussed, in addressing the second objective: 'to determine the spatio-temporal variations in precipitation, temperature and river flows in the Mara River basin'. The results are contained in the various tables of the Mann Kendall test statistic, which show nature trends and significance of change in observed monthly, annual and mean monthly rainfall, deviations in the mean monthly rainfall, mean monthly and annual maximum and minimum temperatures as well as trends in monthly and annual river discharge. Pearson correlation coefficient and student t statistic results are also used in indicating significance of change in the variables.

5.3.1 Trends in the Monthly and Annual Rainfall in the Mara Basin

The Mann-Kendall test statistic gives both the nature and strength of change in a variable such that, the z value indicates the nature (a decrease or an increase) while the Sen's slope measures the strength or significance of change (Table 5.4). The results on the monthly and annual rainfall variation between 1984 and 2014 are such that, , five months, including February, March, August, September and December had positive Z values, indicating an increase in rainfall in each of these months for the entire study period. The other seven months namely: January, April, May, June, July, October and November had negative Z values, meaning a reduction in rainfall amounts for these months over the same period. Despite the monthly variations in rainfall between 1984 and 2014, none of the months recorded a significant change when tested at $\alpha = 0.05$ as can be seen from their Sen's slope (Q) less than -0.05 and greater than 0.05. Under such a situation, this study did not have enough reason to reject but instead, accept the null hypothesis 'There have been no significant spatio-temporal variations in monthly rainfall in the Mara basin'.

Table 5.4: MK test for Monthly and Annual Rainfall for the Period 1984 – 2014

Time series	***Test Z***	***Significance α***	**Sen's slope (Q)**
January	-0.99	Not significant	-0.765
February	0.59	‘’	0.396
March	0.87	‘’	0.739
April	-1.39	‘’	-1.745
May	-0.07	‘’	-0.098
June	-0.02	‘’	-0.028
July	-1.84	‘’	-0.333
August	1.14	‘’	0.640
September	1.19	‘’	0.667
October	-0.42	‘’	-0.159
November	-0.20	‘’	-0.273
December	0.12	‘’	0.122
Annual	-0.14	‘’	-0.017

****** trend at α = 0.05*

April had the largest percentage reduction of 1.7% followed by January, 0.77% with June reporting the least value of 0.03%. March, August and September had increases of 0.74, 0.64 and 0.67% respectively. Importantly, April, which is usually the peak of the long rains recorded a remarkable decrease period, which was about three- times the increase observed in March over the study period. This is an indication that the wet months are becoming drier and therefore, the basin is becoming drier over time. The annual trends gave a negative Z value of -0.14 and this indicated a slight reduction in the annual rainfall values as supported by the Sen’s slope of -0.017%, resulting in an annual reduction of about 0.017%/year. As in the case of monthly trends, we again accept the null hypothesis ‘There have been no significant spatio-temporal variations in annual rainfall in the Mara River basin’ over the study period.

In other words, none of the monthly and annual variations in rainfall indicated very different values from the previous month or year over the study period. Although the rainfall in the Mara basin is influenced by altitude and location in the basin as attributes of the Inter-Tropical Convergence Zone (ITCZ), the Lake Victoria basin and the air masses that blow over the Indian and Atlantic Oceans, much of the variations are due to human intervention on the natural environment coupled with the resulting climate change implications. These results agree with Muthoni, *et al.*, (2019) who reported

reductions in annual rainfall amount in central and southern parts of Kenya in their study that analyzed long-term spatial-temporal trends and variability in rainfall over Eastern and Southern Africa. The declining trends in rainfall had resulted in remarkable reductions in the river discharge and this minimizes the water available to the various users in the basin. These changes are impacting the physical and human environment, cases reported by Melesse *et, al.*, 2007 and Mango *et al.*, 2011 in their studies that modelled the impacts of land cover/use and climate change scenarios on the flow volumes of the Mara River.

5.3.2 Monthly Rainfall Characteristics

The results of the analysis of the mean monthly rainfall trends or characteristics from Microsoft spreadsheet are presented for the 1980s, 1990s and 2000s in order to illustrate the overall trend over the 30 years period with 1980s as the base period of reference to climatic variations (Figure 5.5). The basin, according to the results, has bimodal rainfall, just like in most parts in the East African region. The short rains are realized between September and November (SON) while long rains occur in the months of March to May (MAM), April showing the peak. The long rains are generally higher in magnitude than the short rains, being the main rainy season.

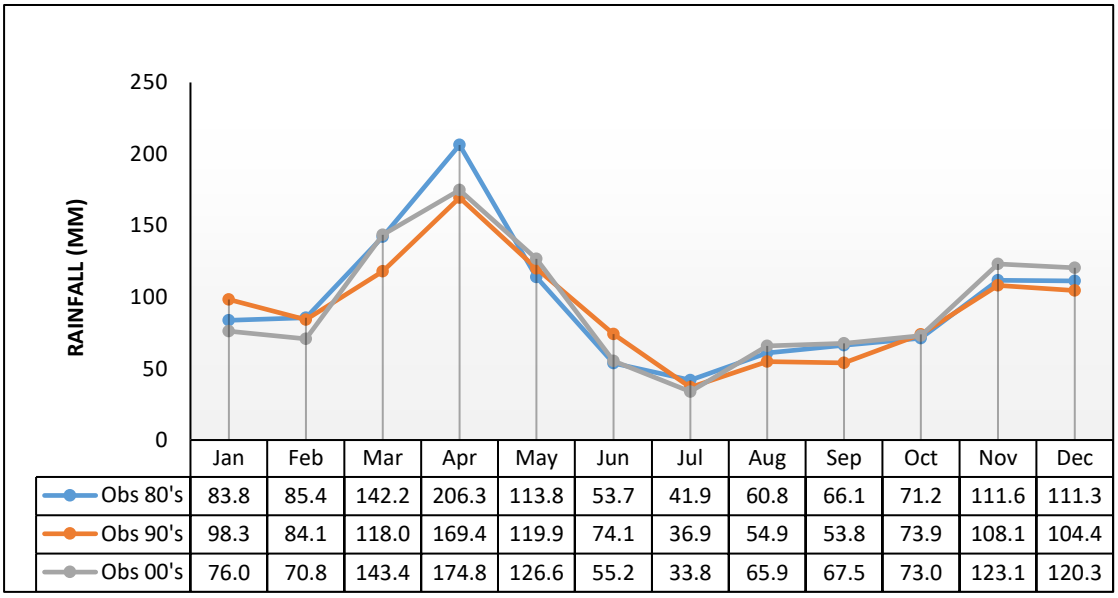

	Jan	Feb	Mar	Apr	May	Jun	Jul	Aug	Sep	Oct	Nov	Dec
Obs 80's	83.8	85.4	142.2	206.3	113.8	53.7	41.9	60.8	66.1	71.2	111.6	111.3
Obs 90's	98.3	84.1	118.0	169.4	119.9	74.1	36.9	54.9	53.8	73.9	108.1	104.4
Obs 00's	76.0	70.8	143.4	174.8	126.6	55.2	33.8	65.9	67.5	73.0	123.1	120.3

Figure 5.5: Monthly rainfall distribution for three climate periods

The results show that the 80s recorded highest rainfall peak during the long rainy season (April) and 2000s during the short rainy season (November). The 1990s had less rainfall

compared to the 1980s and the 2000s, as confirmed from its low records during the peaks in the long rains and short rains (Figure 5.5). The period between June and August is relatively dry compared to the other months with July recording the least amount of rainfall and this is observable in the neighbouring regions generally. Observation from Figure 5.5 is that, the basin is experiencing reduced peak flows during the long rains and increased peak flows in the short rains. The associated variations in rainfall patterns is such that, some of the months that are usually dry are becoming increasingly wetter and the wet months getting increasingly drier. This agrees with Rwigi, (2014) who observed shifts in the Sondu Miriu basin, which also originates from the Mau forest complex. Changes in climatic conditions and human activities are the reasons behind such variations (Mango *et al.,* 2011), especially where all the main cover types are reducing in their extent while temperatures are increasing as observed in this study.

In the 2000s, January and February experienced much reduction in rainfall compared to 1990s that recorded even more than the base year, with November and December recording increase from the base year. The variability in rainfall in the basin could be attributed to the effects of the Indian Ocean monsoon winds, which are easterly air streams in nature and, the large-scale winds from within the Lake Victoria basin, usually laden with thermal energy. Coupled with the low level westerly winds from the Atlantic Ocean, the wind system bring in the Congo air mass which tends to enhance the rainfall in the area including the months that would otherwise be dry (Nyakwanda *et al*, 2009). These airmasses notwithstanding, the human interventions on the basin has been mentioned adversely as a critical source of the many changes seen in the physical and human land scape in the Mara. Being special in its water requirements, the shifts, nonreliability and reduction in rainfall in the basin is impacting livelihoods, conservancies and the general environment, which may put this fragile but important basin out of its functions. It should be noted that reduction in rainfall comes with direct reduction in discharge despite the fact that discharge is very key to almost every sector in the basin.

5.3.3 Monthly Rainfall Percentage Variability

The indicators of changes in rainfall patterns in percentages were given by the difference between the baseline rainfall (1980s) and the 1990s and 2000s rainfall amounts and showed rainfall patterns in the basin in particular and in the surrounding

regions in general (Figure 5.6). The study revealed that there was progressive increase in monthly rainfall between the baseline rainfall (1980s) and 2000s in eight out of twelve months namely –March, May, June, August, September, October, November and December, increments of 1%, 11%, 3%, 8%, 2%, 3%, 10% and 8%. On the other hand, January, February, April and July recorded decreases of 9%, 17%, 15% and 19% respectively. Importantly, the percentage reduction in the four months were higher when compared to the percentage increments in the eight months between 1980s and 2000s. The situation was that, the months of January, February, April and July were quite dry in 2000s compared with the 1980s while the eight months with increasing trends were relatively wet in 2000s as opposed to 1980s. It is therefore improper to conclude that, the 2000s had more rainfall compared to the 1980s, on a mere fact that eight out of twelve registered increment with only four months, decreases. The January, February, April and July of the 2000s were very dry, a condition that tended to counsel the effect of the rather wet months.

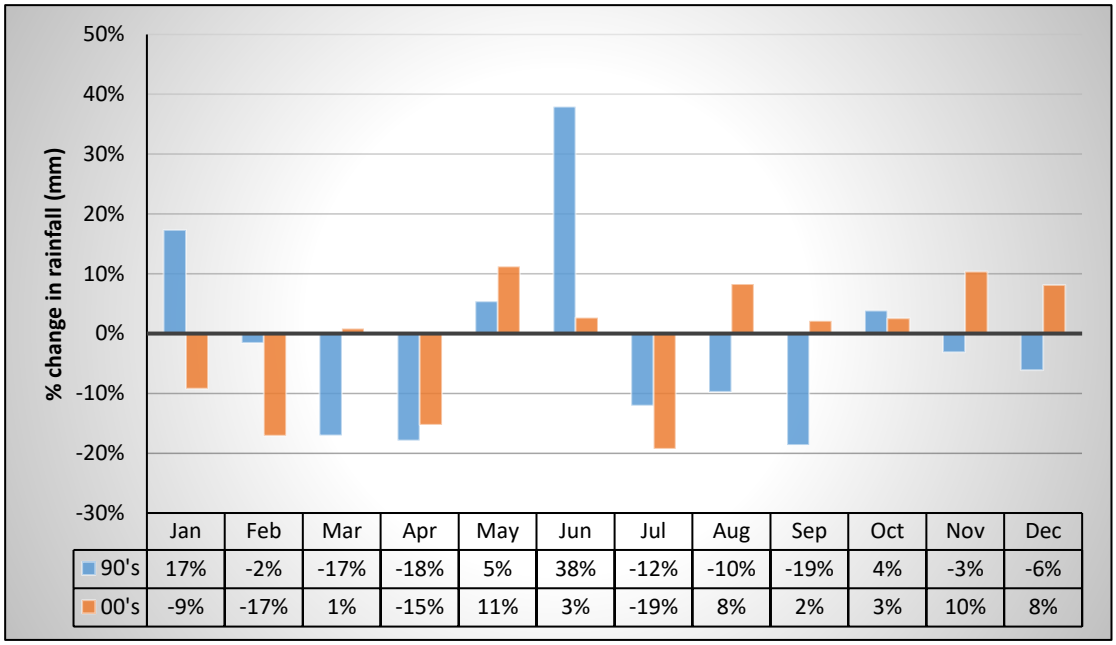

	Jan	Feb	Mar	Apr	May	Jun	Jul	Aug	Sep	Oct	Nov	Dec
90's	17%	-2%	-17%	-18%	5%	38%	-12%	-10%	-19%	4%	-3%	-6%
00's	-9%	-17%	1%	-15%	11%	3%	-19%	8%	2%	3%	10%	8%

Figure 5.6: corresponding percentage changes from the baseline period at Bomet Met. Station

On the other hand, 1990s had its own difference in that, only four months: January, May, June and October recorded monthly increments from 1980s (17%, 5%, 38% and 4%, respectively) with June registering the highest and an extreme increment (38%) that was more than twice the increase in January (17%) while May and October recorded mere 5 and 4% respectively. During the months of February, March, April,

July, August, September, November and December, there were gradual decline in monthly rainfall (2, 17, 18, 12, 10, 3 and 6%) from the baseline to the 1990s. Notably April, the month that usually has the highest peak flows has recorded a declining trend in the two rainfall regimes under study. Coupled with the reduction of 17% in March in the 1990s and a mere increase of 1% in 2000s, the rainfall trends in the basin are actually worrying and therefore corrective interventions are a prerequisite to sustainable utilization of the Mara resources.

Generally, 1990s were drier than the 1980s as indicated by many months that recorded decreases, save for the month of June, which recorded the highest rains over the period. Both the 1990s and 2000s recorded 19% as the maximum reduction in the months of September and July respectively. From the ongoing discussions, the seasonal changes in rainfall like in March, April, among others are indicating shifts in rainfall patterns where the relatively dry months like September, October, November and December are becoming relatively wet while the relatively wet months, March, April and May are becoming relatively drier. Wabwire *et al.,* (2020) found the same trend in their study of spatial and temporal characteristics of rainfall over the Lake Victoria Basin of Kenya.

The shifts and variations in rainfall are a result of altitude, ITCZ dynamics, Lake Victoria basin, the Congo air mass and air masses blowing over the Indian and Atlantic Oceans as modified by human interventions and climate change implications. The month of July has become the driest over the study period, though it falls among the dry months in Mara. This is an indication of declining rainfall trends in the basin save for years with erratic and excessive rains like from mid-October, 2019 to beginning of 2020 and again in the months of March, April and May, 2020, which have been recently witnessed all over Kenya. The changes in monthly rainfall across the two climate regimes have direct impacts on the river discharge in the catchment area and therefore the information gathered can guide on the appropriate adaptive measures across multiple water users.

5.3.4 Trends in the Annual Maximum and Minimum Air Temperatures

The annual trends in Maximum and Minimum air temperature over the study period are contained in linear regression results shown in Figure 5.7, which also explains the variations in the two means over the study period. The two curves and trend lines

indicated a gradual increase in both the mean annual temperatures throughout the study period. Importantly, the basin formerly experienced higher mean annual minimum than mean maximum temperatures in the earlier years up to 2000. For the next four years (up to 2004), both the mean annual temperatures were the same after which, the mean annual maximum temperature become higher than the mean monthly minimum with the gap becoming wider with time, the way it was in the earlier years.

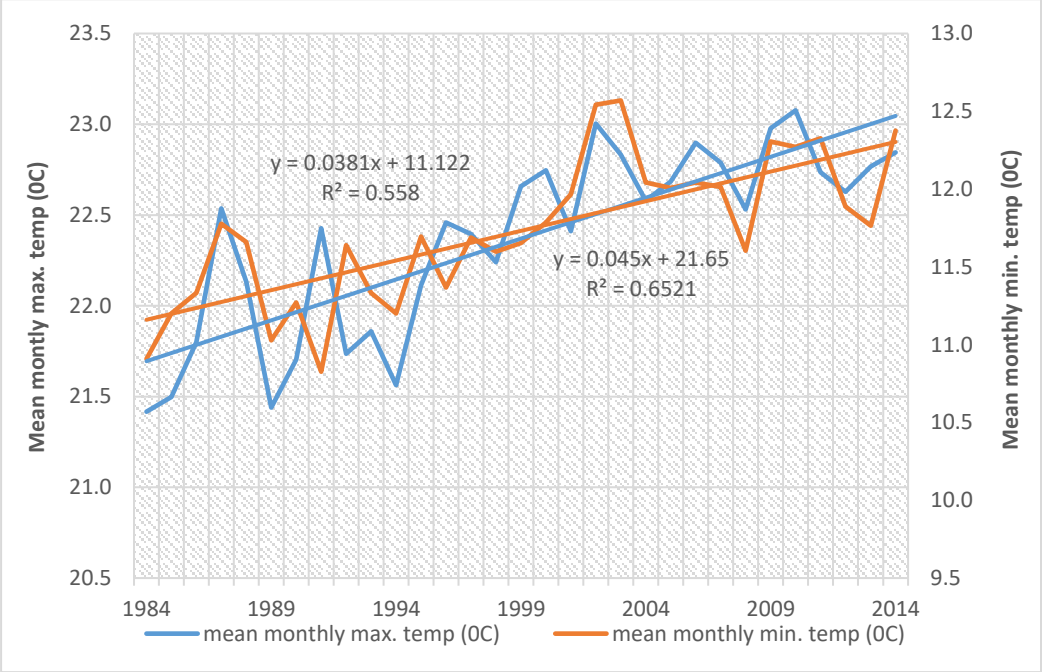

Figure 5.7: Mean Annual Maximum and Minimum Temperatures. (Source: Researcher, 2018).

The trend line equations possessing coefficients of determination, (R^2) of 0.558 for minimum and 0.652 for maximum mean annual values indicate strong positive correlation between increase in the mean annual values and time in years. The curves indicate clearly that, the early years of the study recorded the minimum values in the two mean annual temperatures, with most years recording values below average between 1984 and 1994.

Between 1996 and 2014, the curves shot up with the lower levels of the mean annual minimum and maximum curves following the trend line (average value) while majority were above average with only 2008 and 2013 recording values below average in both

cases. The R^2 values of 0.652 and 0.558 indicate that the changes in mean annual maximum and minimum temperature are statistically significant, causing the already observed increasing frequencies of droughts and incessant cases of erratic rains and flooding events

5.3.5 Trends in Monthly Maximum and Minimum Air Temperature

The Mann Kendall test statistic results of the analysis of trends and associations in mean monthly maximum and minimum temperatures in the Mara River basin are in Table 5.6 in terms of their monthly and annual values between 1984 and 2014. Over the entire study period, the Z values were positive for all the months in the maximum and minimum temperatures. This signifies a general increase in the monthly maximum and minimum temperatures over the study period. When tested at $\alpha = 0.05$, changes in monthly maximum temperatures were found to be statistically significant in the months of January, June, August, September, October and November (6 out of 12 months), leaving half of the year with insignificant changes. Similarly, the changes in the minimum monthly temperatures in eight out of twelve months namely: April, May, June, July, August, September, October and November had significant increments.

Table 5.5: Mann Kendall test for Mean Annual Maximum and Minimum Temperature

	Z test		Sen's slope (Q)	
Month	T. Max temp	T Min temp	Max temp	Min temp
January	2.36*	2.24*	0.050	0.051
February	4.28	3.31	0.070	0.061
March	3.42	3.26	0.053	0.058
April	2.60	2.26*	0.056	0.040
May	3.89	3.74	0.053	0.045
June	2.19*	1.45	0.033	0.024
July	4.18	2.40*	0.060	0.032
August	1.82	2.67	0.036	0.035
September	2.36*	2.42*	0.023	0.039
October	2.45*	1.53	0.035	0.026
November	1.99*	1.87	0.030	0.028
December	3.28	3.06	0.056	0.054
ANNUAL T. max			*0.046*	
ANNUAL T. min			*0.041*	

***** *trend at $\alpha = 0.05$*

In the case of annual trends, the increase in both the maximum and minimum temperatures over the same period were found not to be statistically significant at $\alpha = 0.05$. The Sen's slope signified that the maximum and minimum temperatures increased

by 0.046ºC/year and 0.041ºC/year respectively. For the mean annual maximum and minimum temperatures therefore, we have no reason to reject the null hypothesis that, 'there have been no significant spatio-temporal variations in temperature in the Mara river basin. The increasing trends in the mean temperatures are attributed to human induced climate change implications, including contribution from deforestation and the effect of greenhouse gases. Importantly, both maximum and minimum temperatures are increasing in the basin with monthly maximum and minimum temperatures indicating changes that are statistically significant while the annual trends of change recorded statistically insignificant changes. The basin is faced with gradual increases in the maximum and minimum temperatures that are actually significant in some months while the mean monthly and annual rainfall are both declining on a background of increased human interventions, especially deforestation and mechanized agriculture that utilizes irrigation using the Mara River waters.

The frequent incidences of droughts and flooding events in the basin are a result of the above conditions, which are threatening both the environmental and ecological functions as well as the livelihoods. The variations in rainfall is impacting the peak flows with high peaks during extreme flooding like what has been witnessed in the early part of 2020 not only in Mara but in all parts of Kenya including the marginal lands. Such trends ought to be controlled or mitigated through proactive mechanisms like formulation of ecosystems based approaches to natural resources conservation, especially forests and water bodies. The results of this study show a disconnect in the management and utilization of the same.

5.3.6 Trends in Annual River Flow Volumes

The results of the analysis of the mean annual discharge revealed variability in discharge over the study period. The discharge had a positive and gentle gradient up to 2014 before facing a declining trend, meaning that the discharge was inceasing, albeit insignificantly (R^2 = 0.0002) between 1984 and 2014 Increase in discharge could be due to increase in rainfall which was also found to had increased upto 2015 before showing a decline (Appendix VII). It could also be due to increase in ground water recharge (Figure 5.8). This means that, the increase in discharge had a relation with the increase in rainfall over this period, save for the time lag in rainfall that started to show a decline in 2015 and not 2014 like in the case of discharge. 1990 was the driest year

with rainfall of 600mm and a river discharge of 200m^3. The 2000 was the wettest year, rainfall of about 1350mm and indicated the highest discharge (780m^3).

Between 1992 and 1999, both discharge and rainfall averages were revolving around the mean before reaching a maximum in 2000 followed by a decline which was above average up to 2005. From 2006 to 2014, most years had discharge that were below average, a case witnessed in the trends of rainfall also. The positive slopes between 1984 and 2014 was a blessing in the basin for all the systems and stakeholders that depended on the rainfall amount and discharge or flow volumes. Some of these variations coincided with the El Nino phenomena in the Northern Pacific Ocean while some are linked to the variation in the Indian Ocean temperature, which influence rainfall in East Africa.

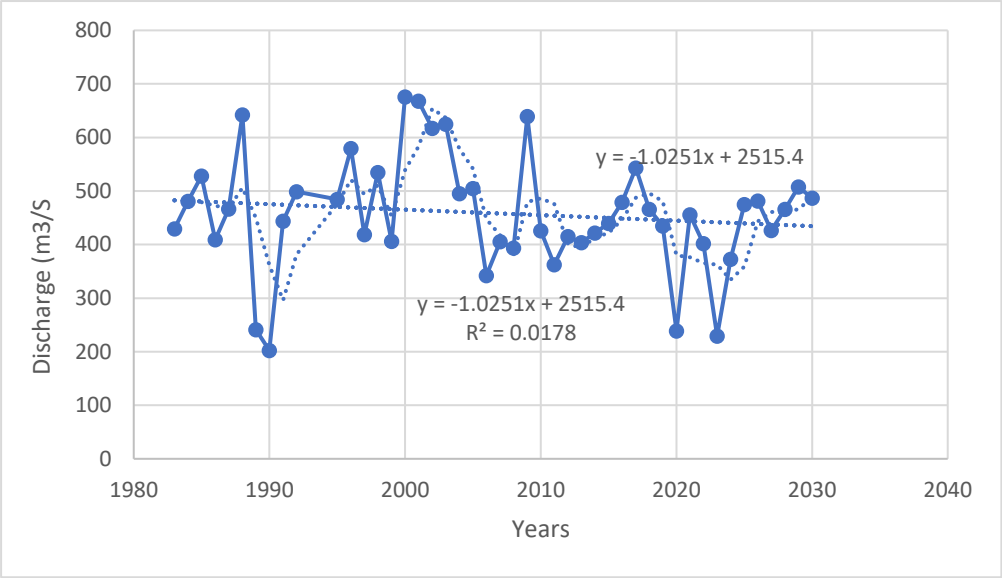

Figure 5.8: Annual trends in observed river discharge (m^3s^{-1}) in the Mara Basin.

The trends in rainfall and discharge indicate that dry and wet years come in clusters of three or more years, usually coinciding with the troughs and peaks of the three-year moving average line (Figure 5.8). Analysis of the hypothesis showed that the variations in discharge are not significant statistically (R^2= 0.0002). We thus, accept the null hypothesis that 'there have been no significant spatio-temporal variations in river flows in the Mara river basin. The river discharge is declining experienced in low base flows and high peak flows but the change in flow volumes from one year to another is however, not statistically significant at $\alpha = 0.05$. These results agree with reports by

many authors including Melesse *et al.*, (2008); *Mango et al., 2011*; *Melesse et al., 2012*; *Dessu et al*., 2014 *Oruma et al., 2017*; who reported declining trends in the Mara flow volumes, especially low base flow and high peak flow from erratic rains.

5.4 Hydrological Modelling

The model calibration process involved sensitivity analysis aimed at determining the most appropriate parameters to calibrate and then use manual calibration to perturb each of the ten most sensitive parameters individually (Table 5.6). The criteria used to calibrate the model were to minimize the difference between simulated and observed values by manually manipulating the sensitive parameters within the ranges allowable in science (Table 5.6).

5.4.1 Model Sensitivity Analysis

The sensitivity analysis ranked the hydrological input parameters that were responsible for the river flow generation in the Mara River basin. The most sensitive parameter was given number 10, last number on the ranking table while the least sensitive got number 1. Table 5.6 indicate the first ten most sensitive SWAT model hydrological input parameters in terms of notable impacts on the model output when changed in the simulation process. These results were obtained by automatically using the sensitivity analysis tool in the SWAT model accompanied by manual calibration for flow input parameters. The results of the sensitivity analysis showed that the most important parameter for river flow generation in the Mara was the Soil Evaporation Coefficient (Esco) and was assigned a global rank 1 while Gw_Revap was the least sensitive and put in number 10.

Table 5.6: Sensitivity analysis results

Rank	Code	Parameter Description	Fault Value	Calibrated Value	Range
1	Esco	Soil evaporation compensation factor	0.93	0.007	0.01–1.0
2	Cn2	initial SCS runoff curve number for moisture condition II	60	50.77	+(-) 25%
3	Sol_Z	Depth from soil surface to the bottom of layer (mm)	110	100	1 - 100
4	Canmx	Maximum canopy storage (mm)	1	Default	
5	Blai	Maximum potential leaf area index		Default	
6	Revapmn	Threshold water level in shallow aquifer for "revap" to occur (mm)	1	0.635	0 – 400
7	Sol_Awc	Available soil water capacity (mm H2O/mm soil)	00.17	0.270	0 - 5
8	Ch_K2	Available soil water capacity (mm H2O/mm soil)	0	0.38	0 - 5
9	Alpha_Bf	Base flow recession factor (days)	0.025	0.022	0. 1–1.0
10	Gw_Revap	Delay time for aquifer recharge (days)	0.03	0.1	0.02- 0.2

SCS runoff curve number for moisture condition II CN2, the depth from the surface to SOL_Z at the bottom is given ranks 2 as the next in importance. Maximum canopy storage (Canmx), maximum potential leaf area index (Blai), and threshold water level in shallow aquifer for "revap" to occur (Revapmn) are moderate in their influence of river flow volumes. Generally, other parameters are less important and can be assigned global ranks ranging from 7 and 42 (Glavan and Pintar, 2012; Ndomba *et al*, 2008**).**

5.4.2 Model Calibration and Validation

The process involved the application of water balance and the modelling of river discharge and rainfall. The model parameters were adjusted to conform to the observed data within the study area basin for a period of study between the year 1983 t0 20134. The SUFI-12 (Abbaspour, 2012) SWAT –Cup programme was applied for parameter optimization. All the uncertainties that were included and mapped into the parameter ranges were integrated with the observed data within a high prediction uncertainty range to optimize calibration. Calibration involved the observed rainfall and river discharge data for Nyangores, Amala, and Mara rivers for the period (1983 to 2014) with an NYSKP of three years (warm up).

The process of calibration for water balance and stream flow was done for average annual conditions, then monthly and finally on daily time step. This began with the Pre batch, post batch and finally SUFI2_Run batch to successful conclusion. The calibration statistics involved objective functions for simulated and observed data, slope intercept and the regression coefficient of determination and the Nash-Sutcliffe Efficiency During SWAT Run, the Watershed, HRU and Sub basin scenarios remained constant during the entire period of simulation and in the process of Calibration to estimate the coefficient of determination R^2 for discharge and simulated data in addition to the Nash-Shcliffe simulation efficiency (E) were applied to gauge the model prediction for the entire Period as illustrated herein;

5.4.3 Suitability in use of simulated and Measured Precipitation

The simulated data from the global weather data were calibrated with the observed hydro-meteorological data from Kiptunga, Bomet and Mugumu weather stations for purposes of establishing the suitability and accuracy in using simulated data in predicting the variations in river flow in the Mara basin. This is a very important information for policy formulation in matters to do with water resources management. The results indicated that, the observed rainfall was generally more than the simulated rainfall except in the years 1992, 2002, 2004 and 1999 (Figure 5.9). The curves are a well representation of the rainfall scenarios in the basin because the two curves have close relation in their variations over the years. Thus, the simulated rainfall variations

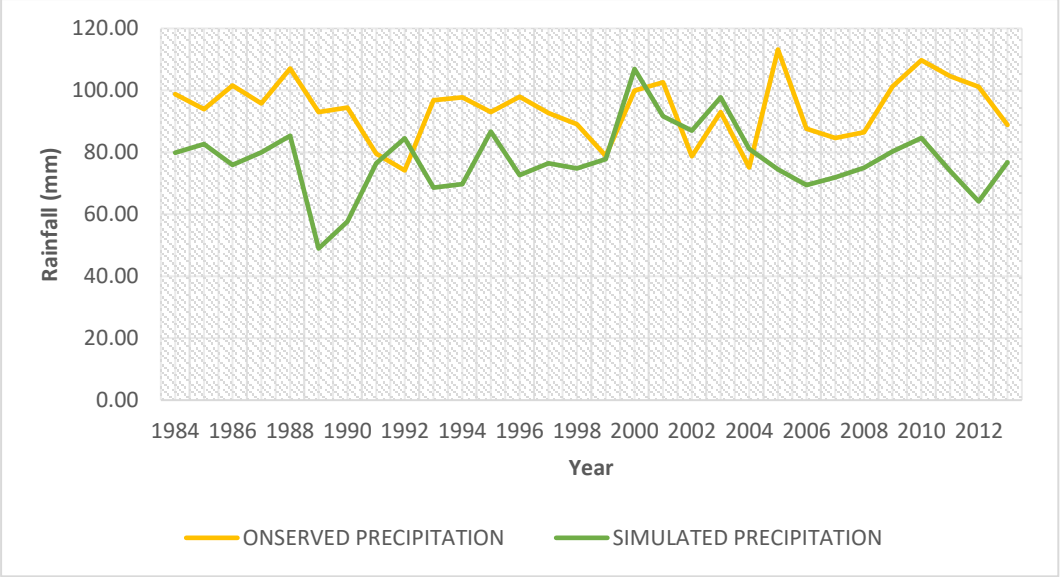

Figure 5.9: Long term Variations in the Observed and Simulated Rainfall

fit well with the variations in the observed rainfall and the significance of the relationship is contained in the student t test statistic (Table 5.7). The variability in rainfall patterns across the entire basin was observed throughout the period of study down to the sub-basins, a fact attributed to relief, presence of Lake Victoria and the prevailing winds that influenced the seasonal climatic pattern. It was established that all the sub basins had a spatial and temporal relationship in terms of rainfall and river discharge, which impacted availability and distribution of water resources in the Mara River basin.

Table 5.7: t-Test: Two-Sample Assuming Unequal Variances

	ONSERVED PRECIPITATION	*SIMULATED PRECIPITATION*
Mean	93.15726	92.07306452
Variance	105.7537	134.064404
Observations	31	31
Hypothesized Mean Difference	0	
df	59	
t Stat	0.389804	
P(T<=t) one-tail	0.349042	
t Critical one-tail	1.671093	
P(T<=t) two-tail	0.698085	
t Critical two-tail	2.000995	

Student t distribution of the difference between means was used to test the significance/association in the two variables at $\alpha = 0.05$ to allow the use of simulated rainfall and generally, simulated data from the global weather data in the simulation process. In other words, it helped in establishing the suitability in using simulated data in the simulation model in predicting the Mara river flows. The mean of the simulated and the observed rainfall values over the study period were tested using two-tail test and 2 degrees of freedom (Table 5.7).

From the t-test output (Table 5.6), the calculated value (P (T <= t) two tail) is 0.698085, which statistically explains a strong positive correlation between observed and simulated rainfall. In addition, since this figure is less than the table value (4.303) at 2 degree of freedom, there is not enough reason to reject the null hypothesis that 'there is no significant difference in the means of the simulated and observed rainfall'. In essence, both the simulated and observed datasets were found reliable in assessing the impacts of climate change on the hydrological regimes of the Mara River basin.

5.5 Distribution of the Sub-Basins Annual Averages

The results of the annual basin characteristics analyzed from the SWAT model output data including the annual precipitation, percolation, surface flows, ground water, actual and potential evapotranspiration and water yields and distributed into the various sub basins to capture the contribution of the variations in soils, land cover, land use and slope, among others, are presented and discussed. Figures 5.10 – 5.13 show all the sub basins within the Mara River basin and are therefore found within the same geographical region and facing effects of climate variability and change in terms of rainfall and temperature in space and time and therefore with variability river discharge. The implications for climate variability and change, specifically on river discharge is compounded by the effects of the rapidly changing land use practices, some of which are taking place on very fragile ecosystems. The results of the delineation and calculation of the basin gave the area of Mara River basin as 1,434,000 Ha or 14340 Km^2. This is not very different from the areas reported by past studies conducted in the Mara River basin.

5.5.1 Average Annual Precipitation

The results of the Mara River basin delineation produced 27 sub basins (Figure 5.10) with varying sub basin characteristics in terms of soils, land use, topography, rainfall, surface flow, evapotranspiration and water yields. According to the SWAT model output results, the basin has total annual rainfall of about 43143.36 mm and an average annual amount of 898.82 mm. Figure 5.10 shows the sub basins' agro-ecological zone /precipitation distribution according to the simulated rainfall records obtained from Bomet, Keekorok, Narosura, Mugumu and Nyabassi. In terms of rainfall distribution, sub basins in the upper catchment and those in the lower forested areas of Mara basin in Tanzania enjoy average annual rainfall of at least 1150 mm (Figure 5.10). The sub basins 1, 2 and 3 covering the Mau Escarpment, Mau Narok and Bomet areas of Kenya and sub basins 11, 15 and 21 in the Nyabassi and Tarime areas of Tanzania are found within the high rainfall areas. Sub basin 4, running down from Kiptunga forest downwards past Mulot is the only sub basin on the Kenyan side that falls within average annual rainfall of 1150-1300 mm.

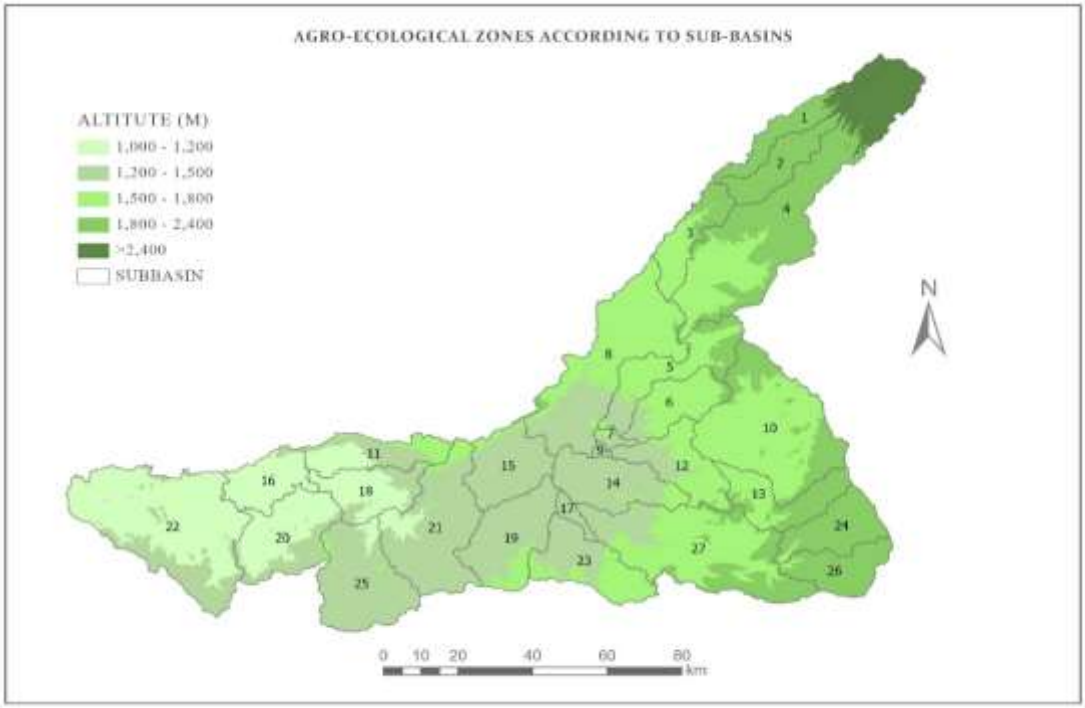

Figure 5.10: Sub-basins Average Annual Precipitation (Source: SWAT Output)

The rest of the sub basins in this class are found in Tanzania and include sub basins 17, 18, 19, 20, 22, 23, and 25. The sub basins with average annual rainfall of between 1000-

1150 mm are mainly found in Kenya and include sub basins 7, 8, 9, 14, and 27. Majority of the sub basins are within the second lowest average annual rainfall zone of between 1000-1150 mm. This area comprises the group ranches in Narok County and the protected areas comprising the Maasai Mara National Reserve of Kenya and the Serengeti National Park in Tanzania. The lower reaches are of plat plains therefore have few sub basins

5.5.2 Average Annual Evapotranspiration

The SWAT simulation and analysis results gave the sum total of Evapotranspiration between 1983 and 2030 in Mara River basin to be 18255.05 mm. with an average annual amount of 380.31mm while the daily maximum and minimum were 62.84mm and 0.7767mm respectively. Evapotranspiration in the Mara basin is generally high because most parts of the basin are in marginal and low-lying areas experiencing high temperatures (Figure 5.11). This fact notwithstanding, areas categorized as high potential such as Bomet and its environments (highland) and the areas near Lake Victoria including the Masurura Swamp have the highest evapotranspiration rates in the Mara basin.

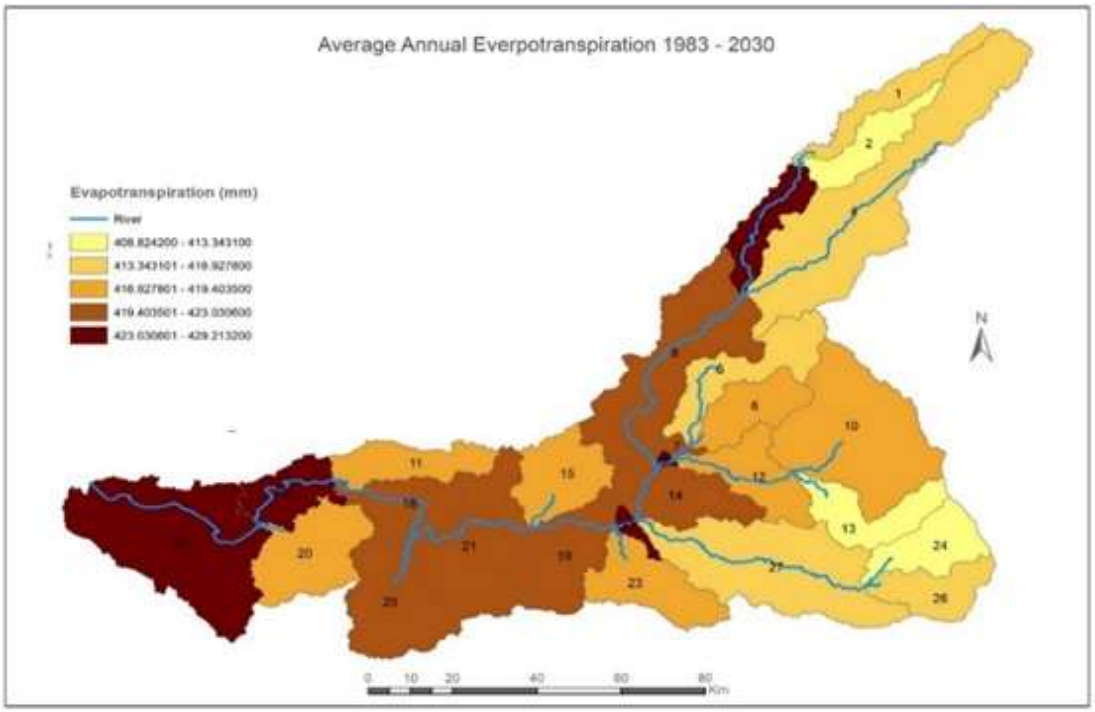

Figure 5.11: Sub basins Average Annual Evapotranspiration (Source: SWAT Output)

The high amount of evapotranspiration in the highlands as indicated above is attributed to the high temperatures in pockets of Bomet, especially in the lower areas surrounded by mountains and the high temperatures around the lake. The parts of Bomet that experience high evapotranspiration also receive high amount of rainfall at the same time, being a high rainfall belt. Evapotranspiration in the basin is however on the decrease, due to anthropogenic factors on the Mara basin, especially clearing and farming on the forested areas and on the rangelands, reducing leaf coverage that would promote evapotranspiration

The consumption of forestland, grassland and shrub land by cropland is leaving behind a degraded environment, increasingly experiencing droughts and flooding events mainly in the lower areas. Thus, in spite the high temperatures in the basin, removal of forest cover is reducing the amount and rate of evapotranspiration, poor formation of precipitation and therefore, reduction in precipitation and water yields. This is a scenario exemplified by the presence of a few water bodies in the basin.

5.5.3 Average Annual Percolation

The results of the sub basins annual percolation averages are not different in any way but vary with soils, topography and rainfall (Figure 5.12). Percolation is a factor of soil

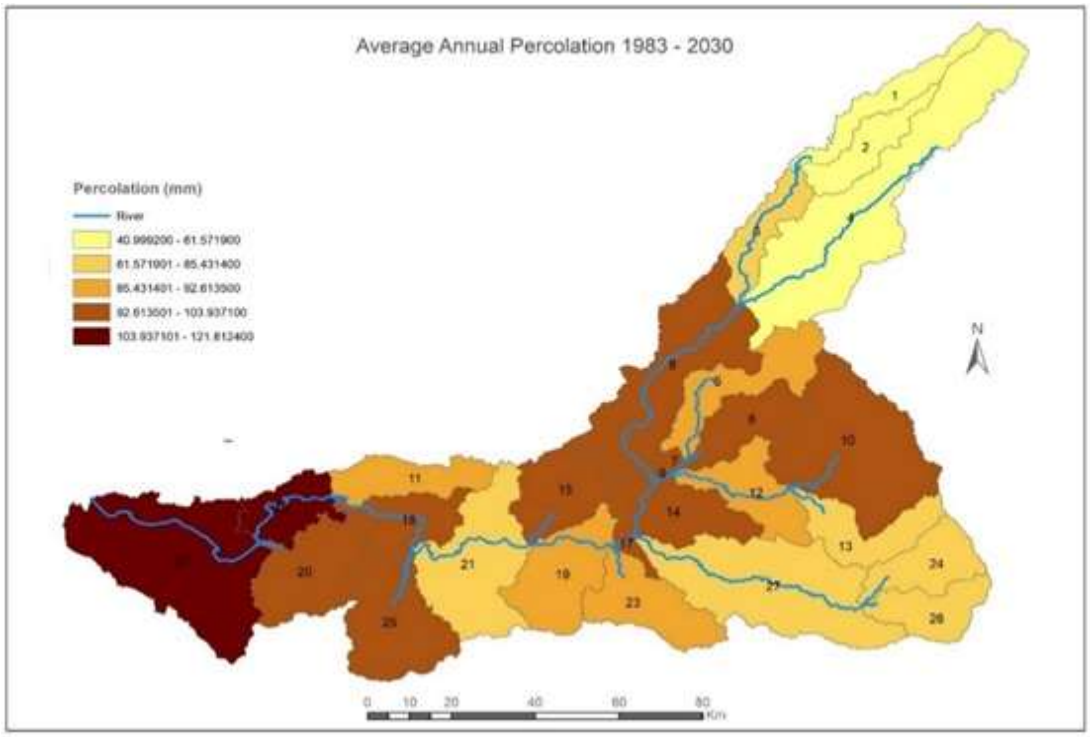

Figure 5.12: Sub basins Average Annual Percolation (Source: SWAT Output)

type in that, compacted soils allow very little if any, water to infiltrate into the soil while loose soils such as sandy soils, allow almost all the available water on the surface to percolate into the soil. According to Figure 5.12, eleven (11) out of the 27 sub basins had the second highest percolation rate of between 92.6 – 103.9 mm and include the sub basin numbers 6, 7, 8, 9, 10, 14, 15, 17, 18, 20 and 25. These sub basins cover the ranches in the Mara Kenya including the Keekorok area, the Maasai Mara National Reserve, parts of the Serengeti and Musoma districts in Tanzania where the soils are quite permeable.

The highest percolation rate (103.91 – 121.8 mm) occurred in only two sub basins (16 and 22), found in the lowest reaches of the basin in Musoma and Tarime Districts. These are the areas neighbouring Lake Victoria including the massive Masurura Wetland and therefore have water saturated soils, this being the lowest topography in the basin. The upper catchment sub basins comprise of areas with least percolation, which attributed to steepness of the slopes. These are sub basins 1, 2, 4, and covering the Kiptunga forest, Keringet, Olenguruone and Maasai Mau forest areas. These sub basins have percolation range of between 40.999 and 61.572 mm. and expected to have more percolation due to good forest cover but because of the slopes, the situation is different since sloppy surfaces promote surface runoff.

Sub basin 3, the Bomet area that also falls within the upper catchment area of the Mara is in one group with sub basins 13, 21, 24, 26 and 27, which are second in percolation rate after sub basins 1, 2 and 4 (61.572 to 85.431 mm). Most of these sub basins are in the middle rangeland areas including areas surrounding the River Sand sub basin and around Mara Mines in the Tarime Area plus parts of Serengeti Park. Percolation ranged between 40 and 122 mm. over the study period and years with low percolation meant either high evapotranspiration, low rainfall or more surface flows compared to percolation due to removal of surface cover and therefore, environmental degradation.

5.5.4 Distribution of the Average Annual Water Yields

The results on the distribution of water yields in the sub basins in the Mara over the 1983 and 2030 period revealed that, the upper catchment (including the Napuiyapui swamp in the Mau Escarpment, Mau Narok and Olenguruone areas) and the lower catchment in the Musoma and Tarime areas (forming the Massive Masurura Swamp),

had the highest water yields. Being catchment and the receiving areas alike, water yields are high in these areas, promoted by low evapotranspiration and low percolation rates (Figure 5.13). The wetland and its environments have good yield because of constant supply from ground water reservoirs, percolation and surface flow in spite of high evapotranspiration, being within the vicinity of Lake Victoria basin with high temperatures. Sub basins 5, 10, 11, 12, 20, 23 and 26 provide the third highest water yields mainly from percolation and surface flow.

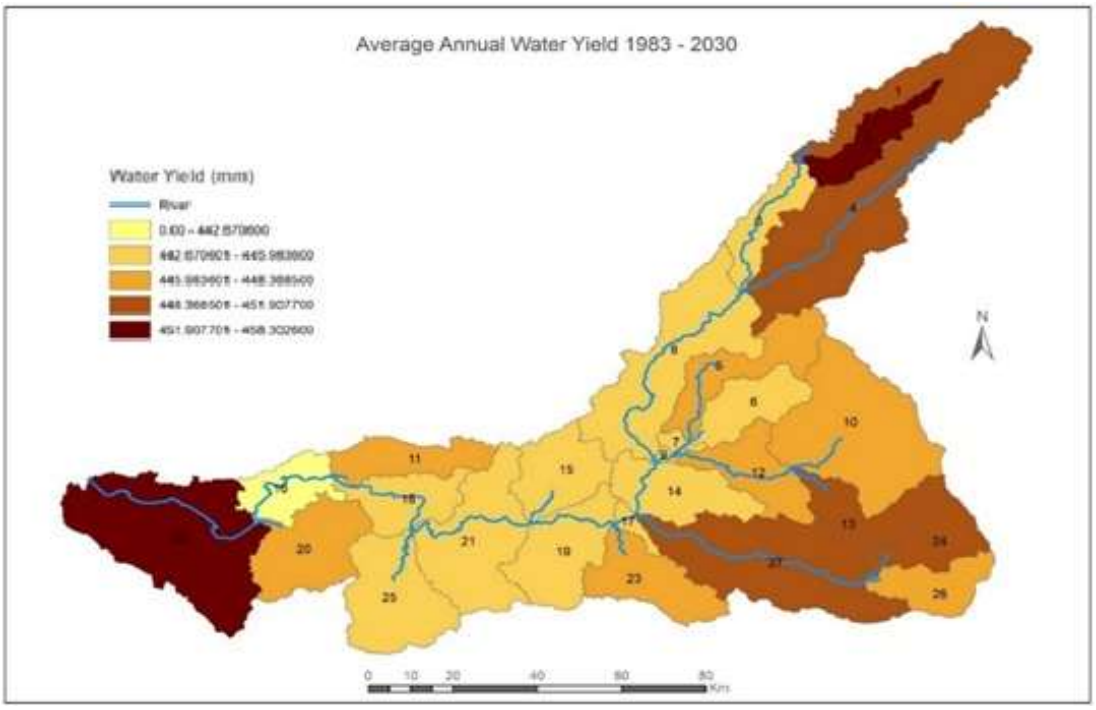

Figure 5.13: Sub basins Average Annual Water Yield (Source: SWAT Output)

The middle and lower reaches of the basin have majority of the sub basins such as sub basins 3, 6, 7, 8, 9, 14, 15, 17, 18, 19, 21 and 25 fall in the middle and lower reaches of the basin and provide the second lowest water yields after sub basin 16. The lower yields attributed to high evapotranspiration since the lower reaches of the basin are hot. Abstraction of water for irrigation and low or absence of rainfall result in low water yields especially in the ranches and conservation areas.

5.6 Mara River Basin Hydrography

Precipitation is the main source of water that exists in the Mara River basin as surface flow, lateral flow, percolation, surface water and ground water as well as those that

leave as water vapour into the atmosphere. This section depicts the existing 10-year moving average trends in precipitation and the other basin characteristics related to precipitation including the actual evapotranspiration, potential evapotranspiration, surface flow, ground water, percolation and water yield. Figure 5.14 shows a 10-year moving average trends in Precipitation and Evapotranspiration (ET) together with their linear trend lines. Moving average method is preferred because it removes the noise and outliers in the values used and therefore gives accurate trends in any two variables compared. Figure 5.14 shows a gently declining trend in both precipitation and evapotranspiration in the basin with variations across the years indicating values below and above the averages thereof. Although the variations differ, the trend lines are similar in that, a decrease in precipitation results in an almost equal decrease in evapotranspiration.

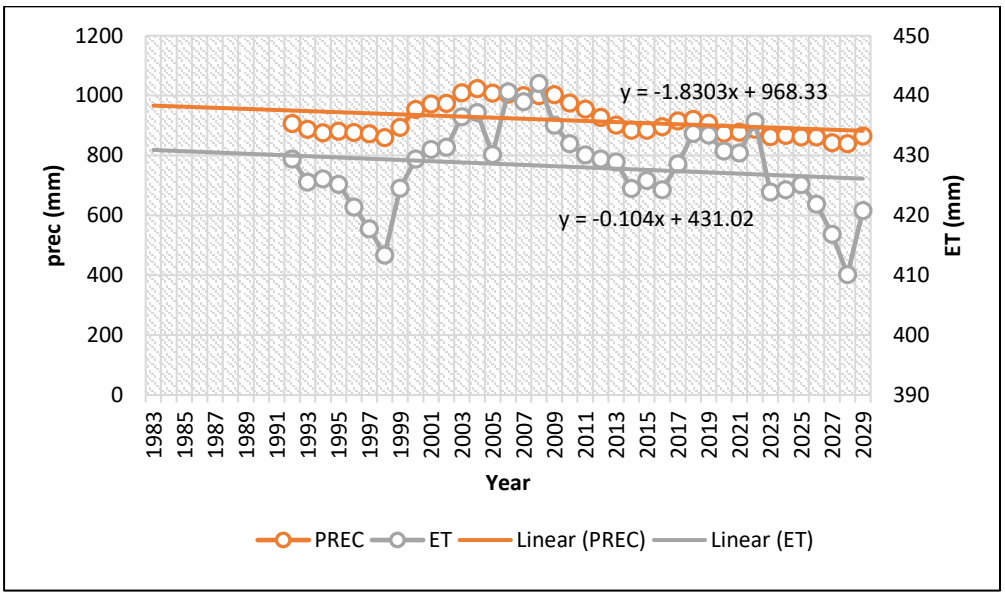

Figure 5.14: Annual Trends in Precipitation and Actual Evapotranspiration

The driest period was observed between 1992 and 1998, when both precipitation and evapotranspiration were below average. The driest year was 1998 and recorded the least amount of precipitation and evapotranspiration of 900mm and 435mm respectively. These dry years resulted in a generally degraded environment with negative implications on livelihoods and wildlife. The basin witnessed gradual rise in rainfall amounts between 1999 and 2004, recording the highest average of 1023mm in 2004 before levelling off and remaining almost the same in magnitude up to 2009. From 2009 to the present and beyond, as projected to 2030, the basin has and will witness gradual

decrease in precipitation, Specifically, between 2009 and 2012 and 2017 and 2019, the declining precipitation stood above the average values of precipitation while the other years had values below average. The basin therefore faces many predicaments in future in view of declining trends in precipitation that will influence the flow volumes and general environmental quality with implications on biodiversity and livelihoods.

The evapotranspiration curve show sharp change with change in precipitation. This is because, decrease in rainfall over time results in degraded vegetation cover in the Mara and therefore less vegetation cover to promote evapotranspiration. Such conditions discourage formation of rainfall in a basin. The low levels and declining trends in evapotranspiration into the future are an indication of deforestation and therefore, poor rainfall formation over the basin with adverse implications on the environmental, ecological and economic functions of Mara River basin. In general, Mara basin has witnessed gradual decline in precipitation and evapotranspiration over the study period, a situation which is expected to continue as further supported by the linear trend equations exhibiting a negative slope. These conditions support the fact that, land cover and land use change in the Mara have significant impact on rainfall and evapotranspiration with reduction in water yields. The general decrease in forestland, shrub land and grassland are resulting in reduced rainfall and evapotranspiration in the Mara River basin, with implications on water availability for livelihoods and environmental functions.

Surface flow is one of the components of precipitation in the basin in that, it is almost impossible to witness surface flow without rainfall in the basin, save for flows from springs and other underground sources. This explains the near similarity in their trends as indicated in Figure 5.15. Surface flow increases with precipitation and vice versa. From 1991 to 1999, both precipitation and surface flow were below average with steady reduction between 1991 and 1998 before they registered sharp increase to 2000. The sharp increase in the two indicated good increase in precipitation between 1998 and 2000, a period followed by gradual increase in precipitation to 2004 and surface flow to 2005.

Between 2004 and 2008, precipitation had gradual decrease while surface flow did not have specific trend. From 2009 to 2014/2015 both variables recorded sharp reduction

that crossed the mean trend lines with majority of the period under study indicating values below average (Figure 5.15). The projected values show a continuation in declining trends in both the precipitation and surface flow up to 2028 before taking a slow upward trend that is hardly above the mean trend lines. The trends in the two show a wanting condition that is a threat to continued provision of the basin's ecological and economic functions since the decrease in precipitation and surface flow over time would mean low Mara discharge, which with time, may turn the Mara into a seasonal river. Given that, the Mara River is the only source of surface water, during dry periods, the danger cannot be overemphasized.

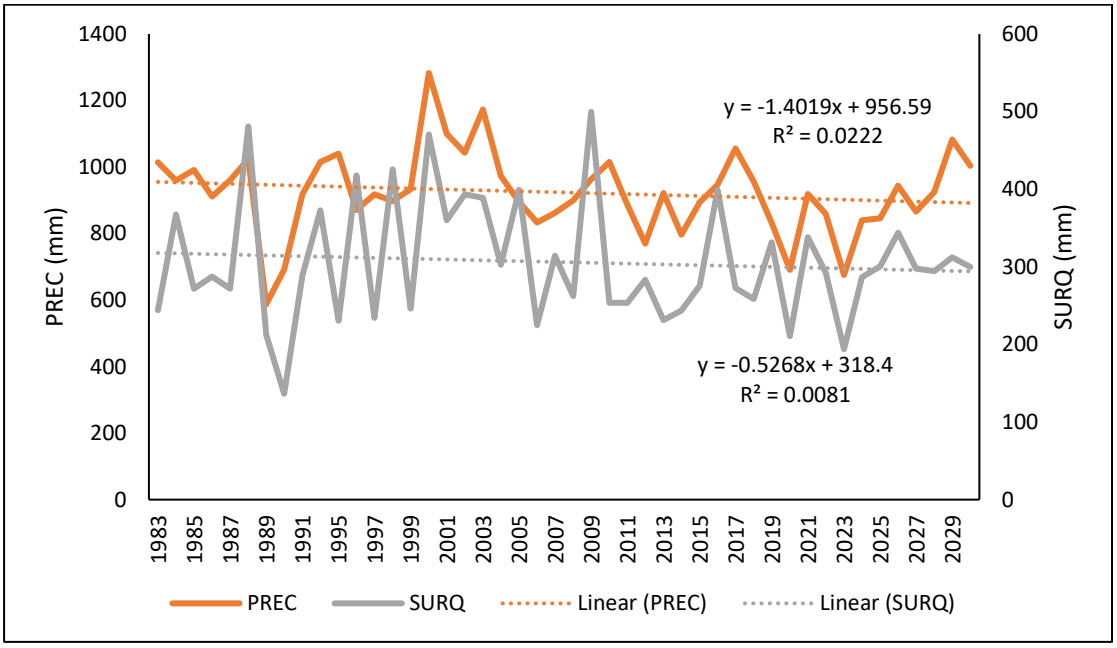

Figure 5.15: Annual Trends in Precipitation and Surface Flow

The precipitation and ground water curves show some association in that, increases in precipitation cause increases in groundwater and vice versa. This should be under normal circumstances, a situation that is lacking in the Mara basin due to much human indulgence in the basin's landscape. The rainfall was below average up to 1998 but with a slight decline before acquiring a gentle rise from 1999 to 2004 and then maintaining almost the same level to 2009 (Figure 5.16). From 2009 to the end of the study period, the rainfall continued in the gently declining trend. The ground water also exhibited the same trend as that of precipitation between 1998 and 2004, a decline in the trend with both curves falling below the mean values.

The year 2004 had the highest amounts of both precipitation and ground water with ground water. Ground water showed quite a sharp rise between 1998 and 2003 of about 50mm. It would be observed that a small change in precipitation resulted in more change in ground water. Between 2004 and 2009, both values were above average meaning that, this period witnessed more rainfall. The years after 2009 indicate declining trends in precipitation and ground water amounts, which are reflected in reduced flow volumes. Reduction in ground water volumes could be due to use of boreholes or reduction in precipitation or both. The time lag between the time water percolates and the time it adds to the river system makes the two curves not to be similar like the case in Figure 5.15.

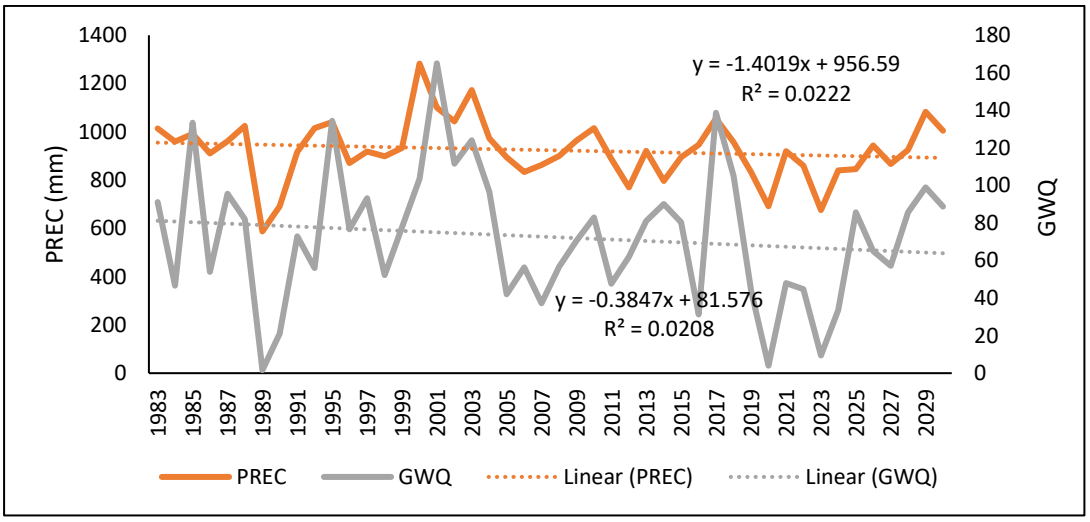

Figure 5.16: Annual Trends in Precipitation and Ground water

The first few drops from rainfall that reaches the surface when it rains get absorbed by the dry soil (percolation) until the top soil is saturated then it starts draining off as overland flow, surface runoff or surface flow. Hard surfaces like rocky areas do not absorb but enable the droplets to collect very fast forming overland flow. The curve for percolation is similar to that of ground water because it is the percolation that reach deep to form the ground water, the same time lag mentioned above (Figure 5.17). Much abstraction of ground water may interfere with the percolated water the same way it does with ground water.

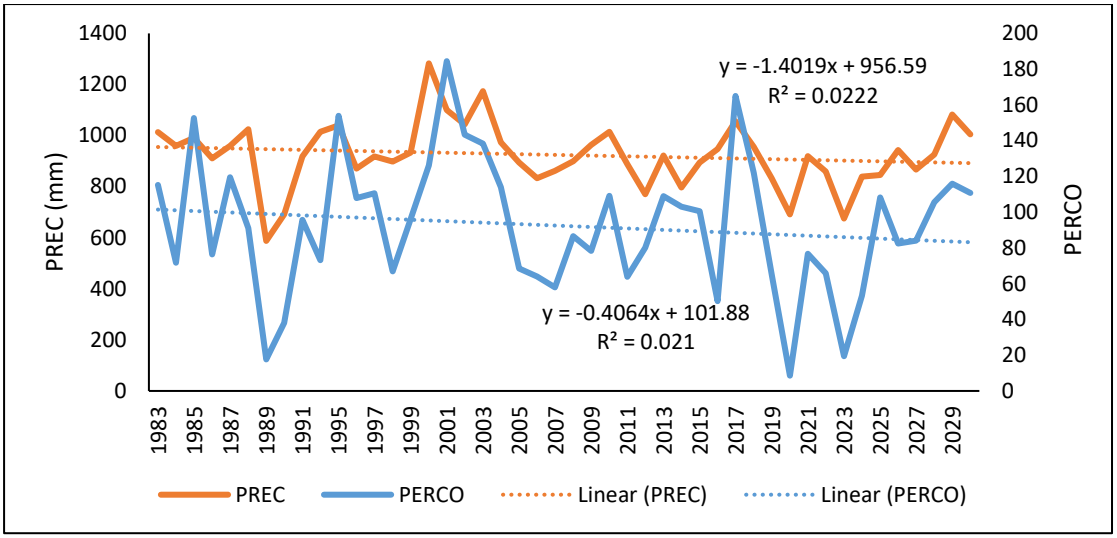

Figure 5.17: Annual Trends in Precipitation and Percolation

Years with higher levels of percolation or ground water than the precipitation simply indicate that, there existed good storages of percolation or ground water. These storages are likely to have had a boost from subsequent precipitation giving them the high levels. In summary therefore, the ten-year moving average trends show that, the basin is facing a declining trend in percolation just as precipitation is declining. This situation is impacting the water yields in the basin and therefore implications on sustainable utilization of the Mara water resources.

The 10-year moving average curves show similar trends for precipitation and water yield in which, the precipitation values stood higher than the water yield in the basin throughout the study period. It portrays the same characteristics as those of precipitation and surface flow because the surface flow adds directly to the flow volumes. Both precipitation and water yields curves showed declining trends (Figure 5.18). Just like in Figure 5.17, Water yields had a gradual decline between 1992 and 1998, which followed the precipitation curve. This period was among the driest in the basin. Between 1998 and 2004, there was sharp increase in water yields mainly due to increased precipitation that saw the curves cross the trends lines to stand above it.

The trends, though still positive tended to slow down between 2000 and 2004 before witnessing a gentle decline from 2004 to 2008, a period of four years, followed by a one rise in 2009 before facing a sharp decline from 2009 to 2014/2015. Another slight increase was noted between 2015 and 2018 followed by a general decline, which was

intermittent in nature with future trends indicating below average rainfall values and water yields in the basin. This means an environment not conducive for many economic activities including supporting the ecosystems and ecosystem services. Thus, the variations in the water yields and precipitation were almost similar with 1995 recording the lowest water yield mean of 425mm with 1998 recording lowest rainfall of 875mm respectively. The year 2005 recorded the highest water yields of about 545-mm. with the lowest water yields projected to be in 2027/2028 of 380mm. In the entire period of study, all the annual values were below average except the periods between 2000 and 2012 and, again between 2012 and 2017 and in 2019.

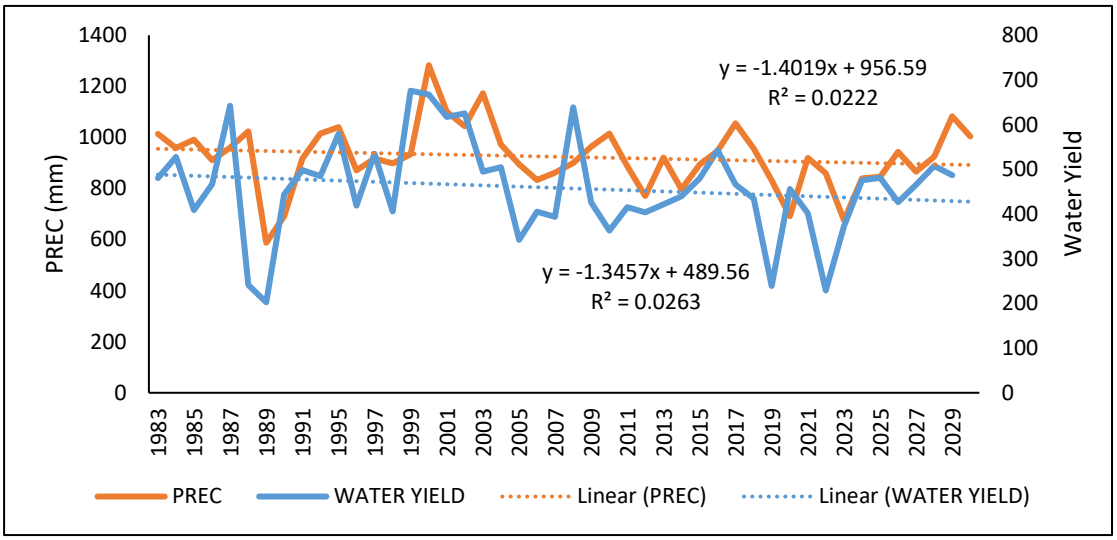

Figure 5.18: Annual Trends in Precipitation and Water yield

The projected precipitation and water yield scenarios to 2030 portray a water deficient basin with both precipitation and water yields being below the average values.

5.7 Simulation of River Flow under different Land Cover, Land Use and Climate Scenarios in the Mara Basin

The results of the analyses of the intertwining effects under varying land cover, land use and climate scenarios on the river flow volumes are discussed in terms of ten-year moving averages in water yields and the predictor variables of precipitation, surface flow, ground water, percolation and evapotranspiration and through scatter plots of the same predictors with the water yields. Thus, the third objective: 'Simulation of River Flow under different Land Cover/Land Use and Climate Scenarios in the Mara Basin'

was addressed here. Variations in surface flow, ground water, percolation and evapotranspiration informed on the differences in land cover and land use scenarios and therefore the implications of these predictor variables on the water yields were actually implications attributed to differences in land cover and land use scenarios. Equally, simulating river flows under changing precipitation and evapotranspiration and land cover/land use scenarios gave impacts of climate change on water yields. Evapotranspiration explained the changes in temperature and therefore the implications of temperature on water yields.

5.7.1 Water Yields and Precipitation

The trends in the ten-year moving averages for water yields and precipitation, as follow same pattern in that, an increase in precipitation results in an increase in water yields while a decrease leads to a decrease in the same. Precipitation is the most critical contributor to the water yields in the basin, feeding the river system mainly through these other variables under consideration. These variables are also known as predictors for they can be used to predict variations in water yields in the basin, hence very important in the process of hydrological cycle. Between 1994 and 2000, both precipitation and water yield were below the trend lines, gradually increasing to attain the maximum level in 2003 when precipitation was 1027.467 mm and water yields, 550.83m^3. For the next six years, the values did not change much, reaching 1002.568mm and 536.696m^3 in 2009 before crossing the trend lines in 2012 (Figure 5.19). The negative values in the trend line equations indicate decreases in both.

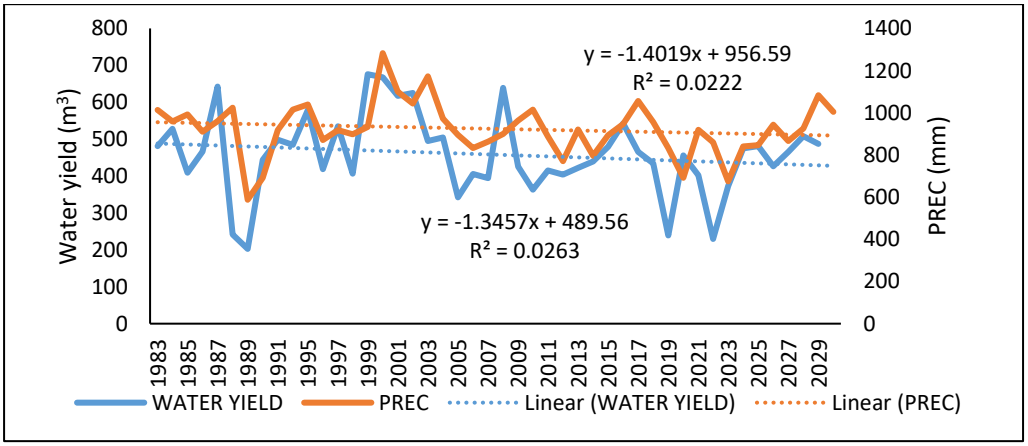

Figure 5.19: Water Yield and Precipitation

The basin experienced good amount of rainfall between 2002 and 2010, thus, the higher values of precipitation and water yields compared with the other years (Figure 5.19). From 2012 to the present, both precipitation and water yields have been on the lower side of the trend lines, indicating that the rains have gradually decreased in the basin and will continues to become less and less with time resulting in equally low water yields, as per the projections to 2030. The years beyond 2029 are likely to register slight increases in precipitation and therefore water yields that would mainly revolve around the trend line, unless corrective measures are taken to stop the trends. The R^2 of 0.2912 for water yields and 0.2849 for precipitation indicate that decrease in the two variables from one year to another is however not significant statistically, which will definitely become significant if deforestation and other degradation including drought occurrences continue.

5.7.2 Water yield and Surface flow

The results of the 10-year moving averages of water yields and surface flow give similar curves and trend lines in that, a decrease in surface flow results in a decrease in water yield and vice versa. The two trend lines show decreasing trends for the entire period of study as indicated by the negative trend line equations. Like in the case observed on Figure 5.19, the R-square (R^2) of 0.2912 and 0.2237 for water yields and surface flow indicate none significant change statistically, in-between the years (Figure 5.20). The volume of change from one year to the next in either the surface flow or water yields was not large enough to be distinguished from another year.

The observation is that, the water yields were higher than the surface flow in any given year because water yields receive from other sources including percolation and ground water while some water that would have added to surface flow percolate into the soil. The year 1991 had the lowest water yield and surface flow, a condition necessitated by severe drought in the basin. The period between 2001 and 2010 recorded the highest water yields and the highest surface flows, meaning that the years had high amounts of rainfall and recharge from ground water and percolation reservoirs. The years showing declining trends in water yields and surface flows may be due to reduced rainfall in the basin and abstraction of water by the various users.

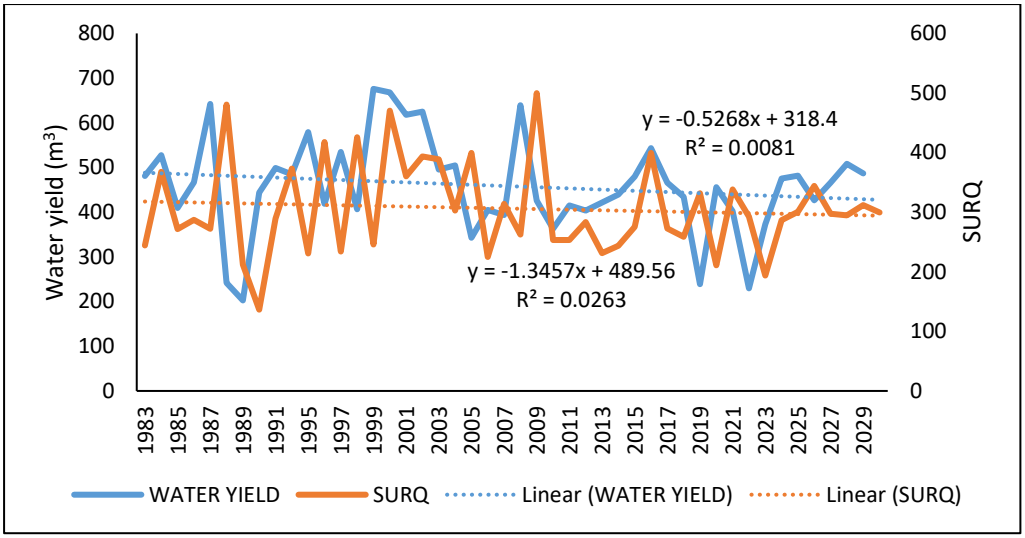

Figure 5.20: Water Yield and Surface Flow

High temperatures under reducing rainfall scenarios promote evapotranspiration that leaves the soils and the general environment dry. Such conditions result in loss of pasture, crop failure and loss of surface water especially in the Mara with negative impacts on livelihoods and biodiversity. Surface flow is influenced by the nature of ground cover in that, well-protected surfaces promote infiltration while bare surfaces increase overland flows. This is contrary to the situation in the Mara where forestland, shrub land and grassland are all reducing while surface flow is also decreasing instead of increasing. This is a situation attributed to reduction in rainfall due to the deforestation and climate variability and change implications.

5.7.3 Relationship in the Water Yields and Ground Water

The ten-year moving averages for water yields and ground water exhibit similarity in their variability and trends over the study period such that, an increase in ground water results in an increase in water yields and vice versa. Importantly, both the ground water is also on the decline in the basin as shown by the negative trend line equation, a situation expected to go beyond the projected year, 2030 due to increased human interventions on the landscape and climate related issues. The decline in ground water will be accelerating at a higher rate in future compared to the decline in water yields as indicated by the widening gap in the two trend lines (Figure 5.21).

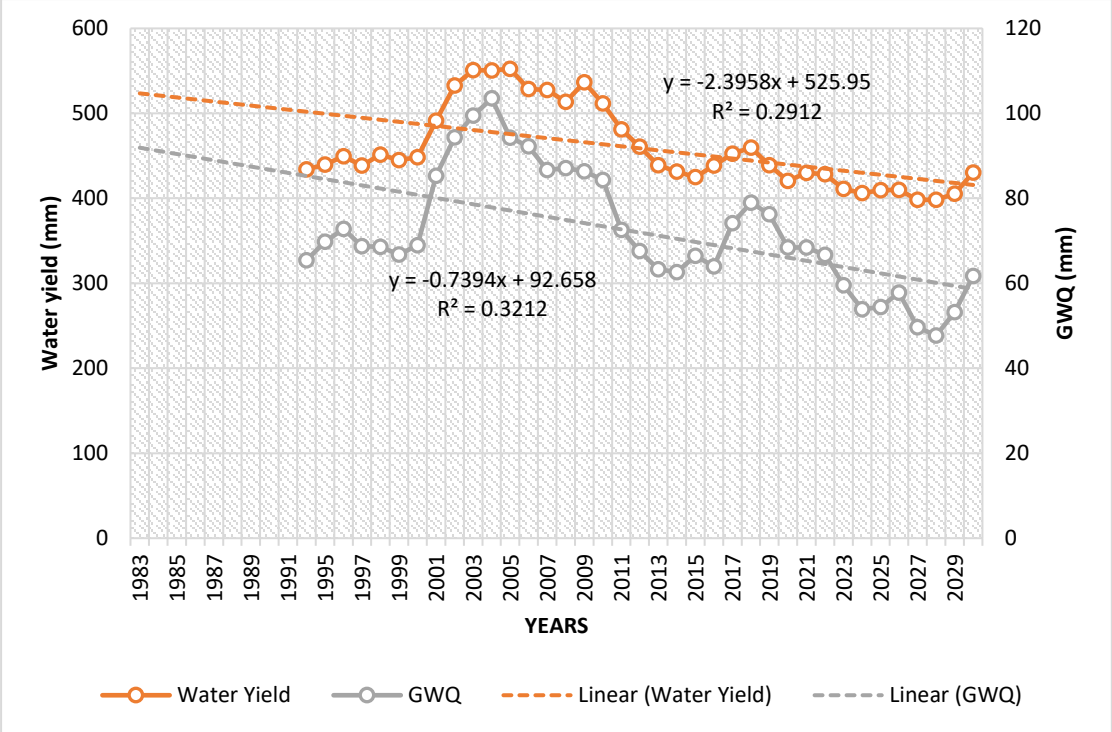

Figure 5.21: Water Yield and Ground Water

This could be because of increased/continued removal of ground cover (especially deforestation), which results in more runoff than infiltration and therefore less water reaching the under-ground reservoirs. Deforestation also reduces volume and rate of evapotranspiration and this reduces the amount of moisture in the atmosphere, resulting in less or poor rain formation, hence reduction in ground water and water yields over time. Just like in the case of surface flow and water yield, the ground water volumes are lower than the water yields throughout the study period. Under normal cases, water yields would be higher than ground water due to additions from percolation, surface flow and direct raindrops. The low ground water values could also be due to abstraction of ground water through boreholes and other avenues to fulfill the needs of the various water users in the basin, a case that would render the basin water deficient if not controlled.

R^2 of 0.3212 and 0.2912 indicate that ground water has moderately changed/reduced in its annual values compared with the water yields. The results on land cover and land use classification indicated that deforestation is still ongoing and therefore the trends in ground water and water yields simply confirm the impacts of land cover and land use change on the Mara hydrography. The lowest water yields and ground water were

before 1994, highest water yields between 2002 and 2004 while highest ground water was in 2003. The period between 2004 and 2011 show gradual reduction above the mean values after which, the values are generally below the average values to 2030 with 2027 to 2029 recording among the least. All these are indication of worsening implications of land cover, land use and climate change scenarios on rainfall and water yields in the Mara River basin.

5.7.4 Relationship in the Water Yields and Percolation

The annual trends in water yield and percolation have similar curve meaning that they follow the same pattern. The pattern witnessed here is that similar to those of those of surface flow and ground water with water yields (Figures 5.20 and 5.21). Years of low percolation resulted in low water yields with the water yields being much above the percolation values since it receives from other sources like surface flow and ground water (Figure 5.22). Up to 2000, both the water yields and percolation were at their lowest (about 360m^3); the same pattern was observed in rainfall, surface flow and ground water (both being below average). From 2000 to 2003 water yields increased from 470 to 550m^3 (maximum), a value that was almost the same up to 2005 before starting to decline, reaching its mean value in 2012.

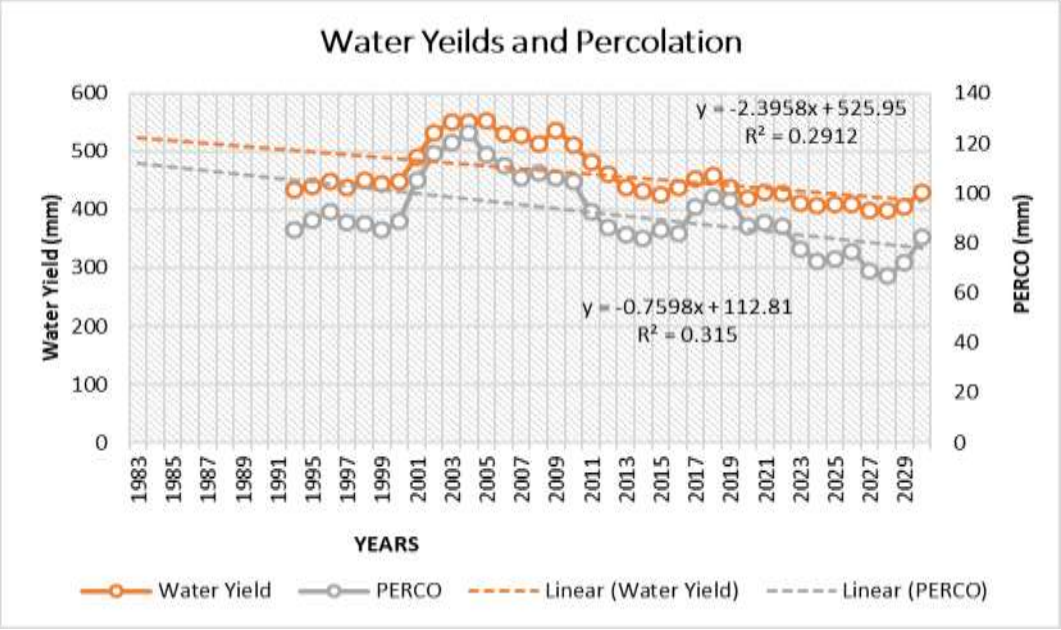

Figure 5.22: Water Yield and Percolation

From 2012 up to 2030, water yields were generally below the trend lines, except for 2017, 2018 and the projected 2030. Percolation was also above average between 2001

and 2010 and from 2017 to 2019. Most of the projections are below the mean, meaning that most years will have even lesser percolation with intensified deforestation and general removal of surface cover including grass and shrubs. The minimum percolation values were before 1995 with the lowest of all due in 2028 while the highest percolation was in 2004, around the time of maximum precipitation and water yields. Reduction in percolation is also because of decreasing trends in rainfall in the basin.

The declining trends in water yields and percolation as shown by the negative equations are a worrying scenario especially that, the projected values are tending to be below the trend lines, meaning less and less percolation and water yields in the basin in future. This is because, percolation, just like surface flow and ground water is influenced by ground cover. Unprotected soil due to deforestation and reduction in grassland and shrub land as witnessed in the Mara basin result in increased surface flows as opposed to percolation and therefore we expect less percolation and less addition to water yields from percolation. The gradient of the percolation trend line is becoming steeper with time, meaning that, it will reduce further with time as long as the surface cover removal including deforestation will still be going on, which would always result in reduced water yields in the basin. The R^2 of 0.315 means that variations in percolation is moderately affecting variations in the water yields. In other words, decrease in percolation is causing moderate reduction in water yields. This situation will become worse with continued removal of ground cover with increased

5.7.5 Relationship in the Water Yields and Actual Evapotranspiration

Comparing the trends in water yields and evapotranspiration between 1983 and 2030 like in the foregoing cases, the trends in evapotranspiration were in fact linear, following the trend line of the same. The two trend lines are expected to level off by 2021. The R^2 of 0.0266, for evapotranspiration trend line, which is also negative in its equation, indicates that variations in evapotranspiration have no direct cause on the variations on water yields. Of course, from land cover and land use point of view, and from variations in temperatures, evapotranspiration affects water yields. In the case of land cover and land use, less amount of water vapour is taken into the soil when the vegetation cover is removed, resulting in low formation of precipitation and therefore less water yields in the end (Figure 5.23).

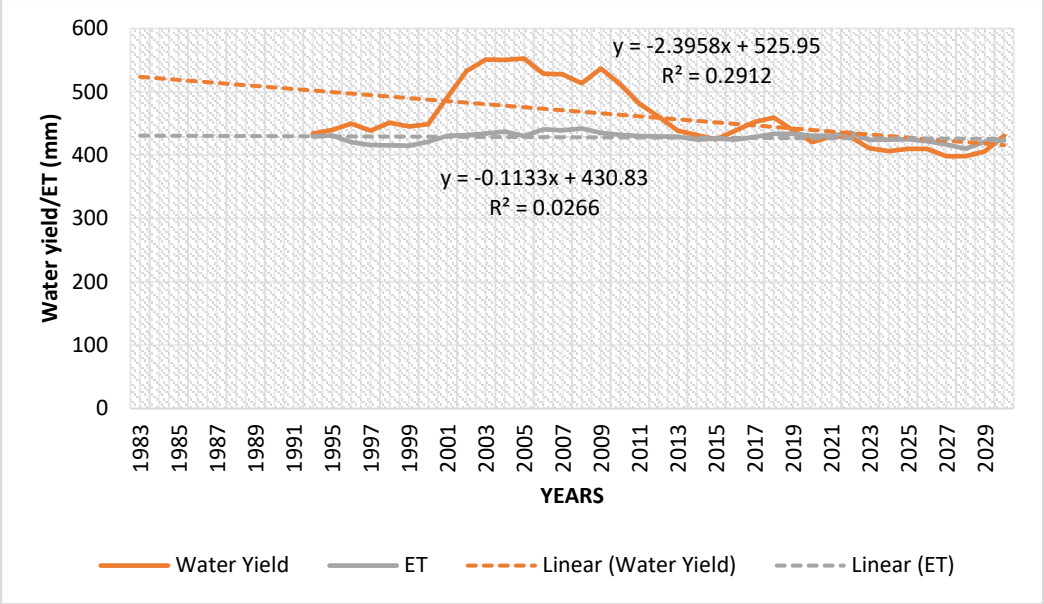

Figure 5.23: Water Yield and Actual Evapotranspiration

When temperatures increase with increased degradation and presence of greenhouse gases for example, evapotranspiration rates are increased and in the presence of large water bodies encourage rain formation, which would result in increased water yields. The case in the Mara is however, the opposite because the basin is largely a marginal area with few large water bodies, high temperatures do not necessary reflect high evapotranspiration (see for example Figure 5.23). Evapotranspiration parse is actually not a good measure of variations in water yields since the amount of water evaporating from a given water body and plants is minimal over a short period. In this study therefore, actual evapotranspiration was used as an attribute of land cover and land use in measuring the impacts on water yields.

5.7.6 Water Yields Parameters and Their Relationships

The results of the correlation matrix analysis of the SWAT model output data of precipitation, surface flow, lateral flow, ground water, percolation, surface water, evapotranspiration and potential evapotranspiration (predictor variables) and water yield (dependent variable) are presented and discussed. The aim was to give an in-depth understanding on how the above subcomponents of precipitation predict river discharge variations and attribute the same to changes in land cover, precipitation and temperature. Secondly, the data was from global weather and therefore we wanted to see how it compared with the results from the observed sources (discussed in section

5.3). The results of the model are contained in the correlation matrix (Table 5.7 and Appendix VII).

The Correlation Matrix indicate that there was strong positive correlation between water yield, precipitation, surface flow, ground water and percolation with r values of 0.830, 0.822, 0.701 and 0.701 respectively and P values in each case of less than 0.05. This means, precipitation, surface flow, ground water and percolation have strong positive correlation with water yields that are significantly significant. Importantly, variations in these predictor variables cause significant variations in the water yields in the Mara River Basin. An increase in any of them, for example precipitation, results in an increase in the water yields and reverse is the case with a decrease in any. Land use practices that lead to reduction in precipitation amounts and reliability such as deforestation and abstraction of ground water through boreholes would result in reduced water yields in the basin. Actual Evapotranspiration had an r of 0.265 and a P value of 0.072, implying that there is either a weak or no correlation between water yields and actual evapotranspiration in the Mara basin. In addition, based on the P value, the relationships are not significant statistically.

Table 5.8: Correlation Matrix of SWAT Output Predictors and Water Yield (1983-2030)

	Prec	Surq	Latq	Gwq	Perco	Sw	Et	Pet	Water Yield
Prec	1								
Surq	0.533537	1							
Latq	0.181793	0.026936	1						
Gwq	0.760762	0.171595	0.181499	1					
Perco	0.765351	0.174356	0.200187	0.987338	1				
Sw	0.653872	0.266628	0.399709	0.444063	0.490622	1			
Et	0.581082	-0.0727	0.215938	0.534862	0.522664	0.549317	1		
Pet	-0.44722	-0.11796	-0.1731	-0.50124	-0.51434	-0.38003	-0.15798	1	
Water Yield	0.829934	0.822188	0.130274	0.700572	0.700724	0.464768	0.264575	-0.373	1

However, when the potential evapotranspiration was considered against the water yields, a weak negative correlation coefficient of -0.373 was observed with a P value of less than 0.05. Potential Evapotranspiration being the total water budget required to escape into the atmosphere, this situation implies that, the higher the potential evapotranspiration the lower the water yields. As regards the surface water, the coefficient of correlation recorded r of 0.485 and a P that is less than 0.05, indicating that, surface water has a mild influence on water yields in the Mara River basin and therefore fail as a predictor in variations in water yields.

5.7.7 Model Suitability in Predicting Variations in Water Yields

The results of the analysis of the model of precipitation, surface flow, percolation, ground water, evapotranspiration, potential evapotranspiration and lateral flow for suitability of predicting the water yields were affirmative. Model summary, (Table 5.8), which is also known as the power of the model, contains the power of the regression model for predicting dependent variable, which is water yields in this case. The power of regression model is measured by the coefficient of determination (R^2), which values lie between -1 and 1 such that, the closure the power to either -1 or 1, the higher the percentage of the dependent variable that is explained by the predictor variables in the model.

Table 5.9: Model Summary

Model Summary[b]

Model	R	R Square	Adjusted R Square	Std. Error of the Estimate	Durbin-Watson
1	1.000[a]	1.000	1.000	1.45582	1.957

a. Predictors: (Constant), Actual Evapotranspiration, Surface flow, Lateral flow, Percolation, Surface Water, Rainfall, Ground water

b. Dependent Variable: Water yield

The R Square and Adjusted R Square have coefficient of determination (R^2) of 1.000. It means that, when other potential predictor variables are considered, the predictors in the model would still explain about 100% of the variations in the water yields (Table 5.9). This implies that, the model is good enough for predicting water yields in the Mara River basin. The significance of the model for the prediction was given by the analysis of variance (ANOVA). Analysis of variance is an integral part of the multiple

regression exercise and good in working out differences amongst more than two sample means at the same time. Table 5.10 has an F of 35923.18 with a P of 0.000. This indicates that the model made of precipitation, surface flow, lateral flow, ground water, percolation, actual evapotranspiration and surface water is statistically significant in predicting water yield in the Mara River Basin.

Table 5.10: Analysis of Variance (ANOVA) of Predictor Variables

ANOVA[a]

Model		Sum of Squares	df	Mean Square	F	Sig.
1	Regression	532953.476	7	76136.211	35923.18	.000[b]
	Residual	82.657	39	2.119		
	Total	533036.134	46			

5.7.8 Effect of Each Predictor Variable on Water Yields Variability

This subsection gives the effect of each independent variable of rainfall, surface flow, lateral flow, percolation, ground water, actual evapotranspiration and surface water on the water yields in the Mara as contained in the Coefficients of the Predictors Model (Table 5.11). The coefficients of the model indicate the association and significant levels of each variable to variations in the water yields. Regression Coefficients corresponding to the predictor variables give the predictors that are statistically significant in predicting the expected outcomes. As indicated on the table, the surface flow, ground water, percolation and actual evapotranspiration have t values of 231.936, 25.112, 15.778 and 4.990 with P values of 0.000 respectively.

Table 5.11: The Coefficients of the Predictors in the Model

Coefficients[a]

Model		Unstandardized Coefficients		Standardized Coefficients	t	Sig.	95.0% Confidence Interval for B	
		B	Std. Error	Beta			Lower Bound	Upper Bound
1	(Constant)	.382	3.720		.103	.919	-7.143	7.906
	Rainfall	-.004	.005	-.004	-.819	.418	-.013	.005
	Surface flow	1.000	.004	.727	231.936	.000	.992	1.009
	Lateral flow	-.001	.009	.000	-.129	.898	-.020	.018
	Ground water	1.046	.042	.352	25.112	.000	.962	1.130
	Percolation	.629	.040	.221	15.778	.000	.548	.709
	Surface Water	.001	.009	.000	.124	.902	-.017	.019
	Actual Evapotranspiration	.047	.009	.016	4.990	.000	.028	.066

a. Dependent Variable: Water yield

The t values of 231.936, 25.112, 15.778 and 4.990 and Ps of 0.000 explain that, the coefficients corresponding to these predictors are statistically significant and therefore, may be used for predicting water yields in the Mara River basin. On the other hand, the t values of -0.819, -0.129 and 0.124 with P values of 0.418, 0.898 and 0.902 for rainfall, lateral flow and surface water respectively indicate that rainfall, lateral flow and surface water are statistically not significant in predicting the water yields in the Mara. Importantly, the correlation coefficients model show that surface flow is very significant in predicting water yields with ground water and percolation following at a distance. Actual Evapotranspiration may also be used to assess variations in water yield specifically during droughts. The coefficients model specifies that, rainfall is not a good predictor of water yield variations. This is because it gives its water to surface flow, percolation, ground water, among others before the water can reach the streams. Surface flow is an attribute of the amount of rainfall and surface cover while percolation are influenced by ground cover and soil type.

In tropical areas, surface flow will increase with deforestation and torrential rainfall while in subtropical and marginal areas it will be dependent on the magnitude of rainfall. Good ground cover enhances percolation and therefore good ground water reservoir, which add to water yields in the Mara basin. Evapotranspiration influences water yields mainly through improved rain formation and this requires good forest cover to provide avenue for evapotranspiration. The situation in the Mara is that of deforestation and degradation that discourages formation of good amount of rainfall hence the observed decline in both rainfall and water yield. These conditions have negative impacts on the many systems in the Mara River basin.

5.8 Partial Scatter Plots of Water Yield and Predictor Variables

The results of partial regression plot of the predictor variables in the model (precipitation, surface flow, lateral flow, ground water, percolation, surface water and actual evapotranspiration) with water yield are presented and discussed, for a deeper understanding on their contribute to the water yields in the Mara River basin. These are plots showing the line of best fit and the deviations thereof, between the dependent variable and each of the independent (predictor) variables, Figures 5.24-5.29. These are derivatives of hydrological cycle, which is a critical process to the availability of both surface and ground water resources. The hydrological cycle is influenced by

anthropogenic factors and variations in climatic conditions especially accumulation of greenhouse gases in the atmosphere, resulting in global warming and therefore climate change. precipitation is top on the list of components of the hydrological cycle that affect the water resources in the Mara since it has direct input into the availability of water resources in the basin.

(i) Water Yields and Precipitation

From the partial regression scatter plot of precipitation against water yields (Figure 5.24), the coefficient of determination, $R^2 = 0.689$. This is a strong positive correlation, since it indicates that 68.9% variations in water yield is explained by precipitation while other predictors explain 31.1% of the variations. The 68.9% contribution of precipitation to variations in water yield is a significant input by rainfall to the water yields.

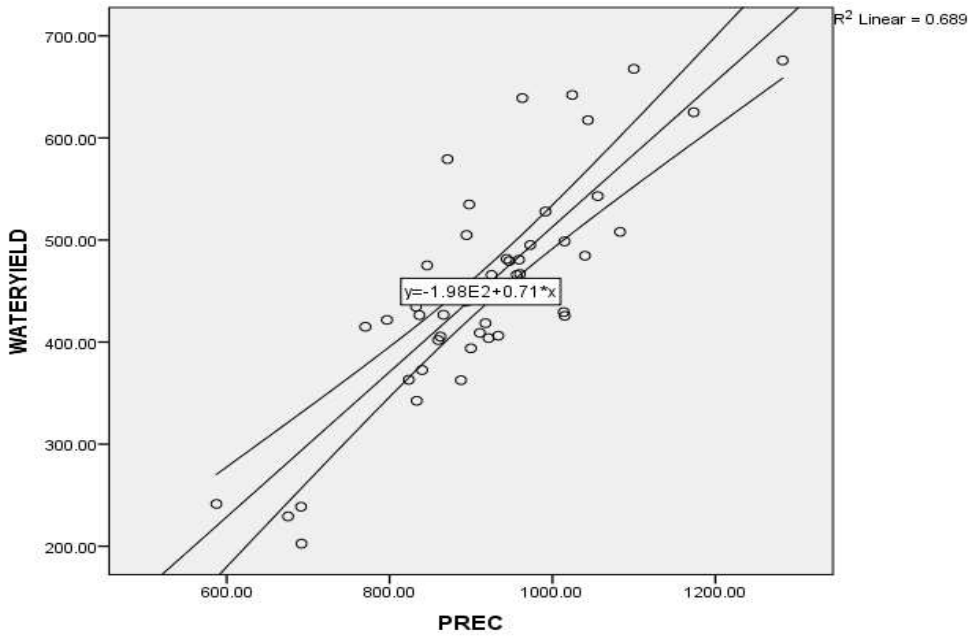

Figure 5.24: Scatter plot of Precipitation and Water Yield.

This is the opposite of the results contained in Table 5.11, which by comparing contribution of each predictor variable, namely- precipitation, surface flow, lateral flow, percolation, ground water, evapotranspiration (predictor in the model) with water yields variations indicated that, precipitation is not in any way significant statistically in the variations in the water yields. Activities that reduce precipitation amounts and distribution (such as deforestation and climate change implications) in the basin will

impact negatively on percolation, surface flow and ground water, among others. This will lead to reduced atmospheric and soil moisture hence, dry soils with serious implications on microorganisms, livelihoods, biodiversity and environmental quality.

(ii) Correlation between Water Yields and Surface Flow

The scatter plot of surface flow and water yield has a perfect positive correlation with the coefficient of determination (R^2) of 0.999, which implies that, approximately 99.9% of the variation in water yield is explained by surface flow, leaving a mere 0.1% explained by the other predictors including these in this model. This indicates that an increase in surface flow volumes results in an increase in water yields almost one on one while the opposite is the case when surface flow decreases like during droughts. In essence, surface flow explains 99.9% variations in water yield compared to 68.9% from precipitation (Figure 5.24).

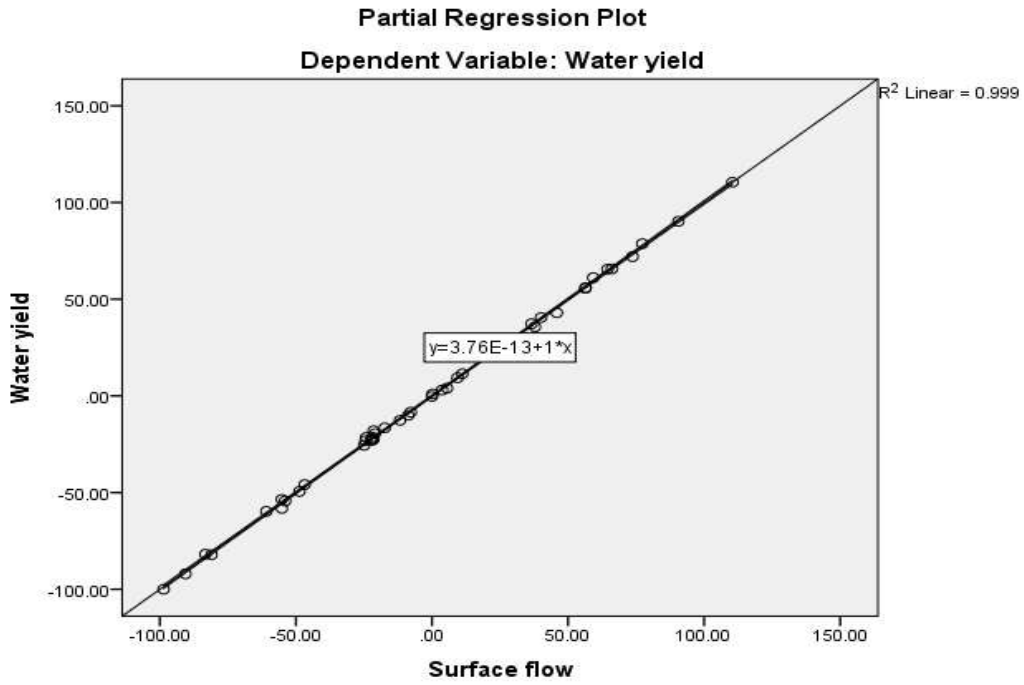

Figure 5.25: Scatter plot of Surface flow and Water Yield.

This situation however, is contrary to the results of the Correlation matrix in Table 5.8 and Appendix VII, which stated that surface flow and precipitation explain 82.2% and 83% variations in water yield respectively. In the study area, precipitation (specifically rainfall) is the main source of surface flow. It means that, activities that reduce precipitation such as deforestation, situations that are still ongoing in the Mara would

definitely cause reduction or failure in precipitation and therefore reduction in surface flow. This would have serious implications on the river flow volumes or water yields with extremely low base flows and very high peak flows due to droughts followed by periods of excessive rains, cases already witnessed.

(iii) Water Yields and Ground Water

The scatter plot of water yield against ground water (Figure 5.26) indicate a strong positive correlation. This is supported by the coefficient of determination, $R^2 = 0.942$, implying that approximately 94.2% variations in water yield are explained by groundwater while only 5.8% is explained by other factors. Reduction in ground water in the Mara basin will result in a reduction in water yield. For example, excessive abstraction of ground water for domestic, urban and industrial uses through channels such as boreholes would reduce the available ground water and therefore, the amount of water yield and degraded underground conditions.

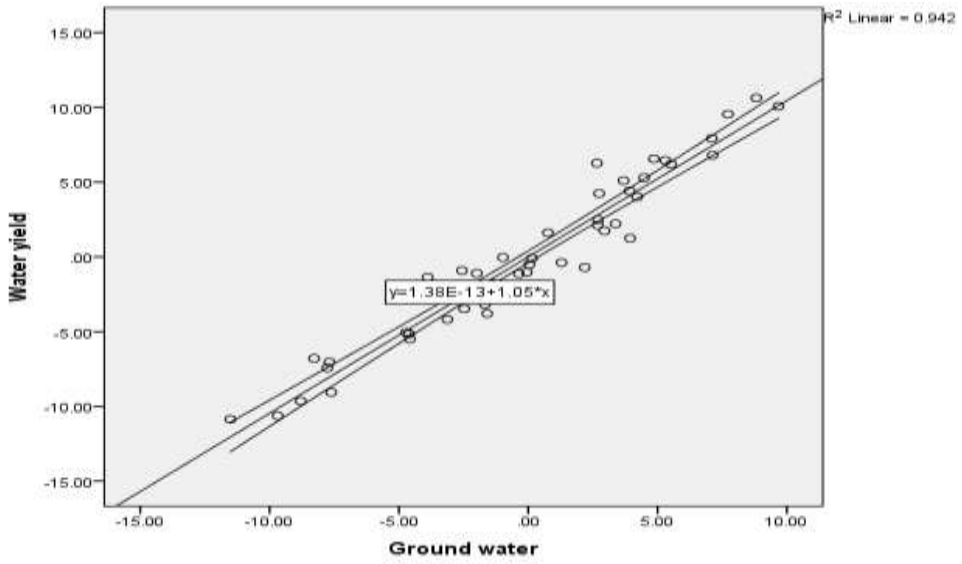

Figure 5.26: Scatter Plot for Ground Water and Water Yield

Such reductions in ground water would interfere with the water balance equation leading not only to the reduced water yield but also to reduced soil moisture content which with time, may lead to collapse in the various economic sectors, especially agriculture. Thus, ground water is only next to surface flow in order of their contributions to the Mara River flow volumes.

(vi) Water Yields and Percolation

The scatter plot of water yield against percolation also gave a strong positive correlation coefficient with a coefficient of determination, $R^2 = 0.865$ in linearity hence accounting for 86.5% variations in water yields. The other predictors explain a mere 13.5% of the variations, thus, the outliers observed on the diagram. During precipitation, the water percolates into the soil, experiences a time lag before the percolated water finds its way, and adds to the water yields. The period between the time it precipitates and the time-percolated water reaches the stream (time lag) results in the outliers as seen on Figure 5.27. Notably, activities resulting in removal of vegetation cover and hardening of the surfaces including building of pavements would increase surface run-off with increased erosion and environmental degradation not only in the Mara basin but also in any given environment or watershed

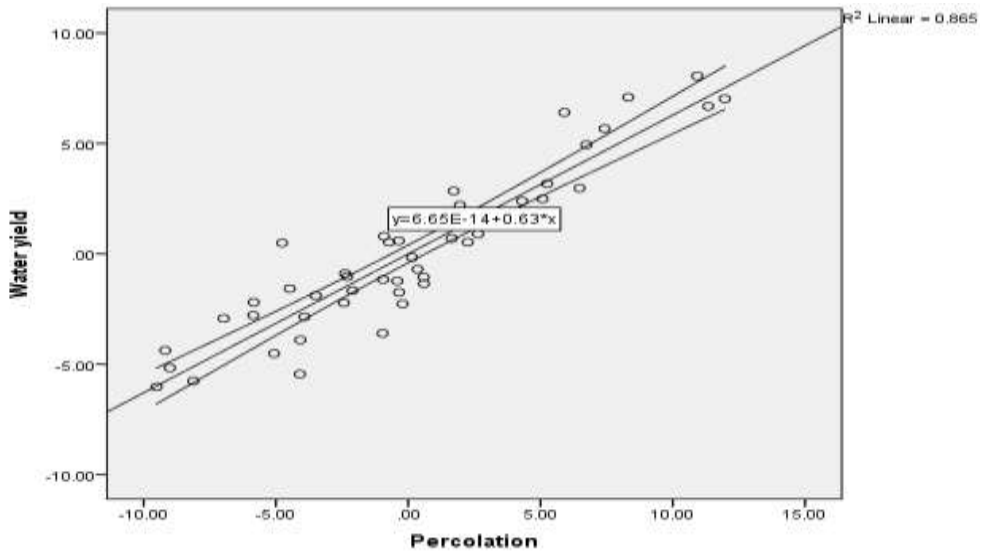

Figure 5.27: Scatter Plot for Percolation and Water Yield

(v) Water Yields and Actual Evapotranspiration

Regression plot of actual evapotranspiration and water yield had R^2 of 0.390, meaning a weak or no association between the two. Going by the value of P = 0.072, which is more than the significance level of 0.05, it is clear that, there is no correlation between the actual evapotranspiration and water yield, this supports the result contained on Figure 5.23. The scatter plot (Figure 5.28) shows the deviations from the line of good fit with many points as outliers and therefore supports the facts in the correlation matrix (Table 5.8.). Since evapotranspiration removes water from the surface and the soils, it

is important to note that, severe evapotranspiration would reflect negatively on the water balance with implications on the soil and atmospheric moisture.

Increased temperatures in marginal area like the Mara basin may results in evapotranspiration that may leave environment very dry that may not support agriculture and other economic activities including pastoralism and conservation areas. In the presence of large water bodies and good forest cover, evapotranspiration enhances formation of precipitation thereby keeping the environment moist. Looking at evapotranspiration differently, it is the link between the terrestrial and atmospheric systems, since it brings about the process of hydrological cycle, without which, there would be no precipitation forming. Figure 5.28 indicates that Evapotranspiration contribute very little to the variations in water yields, meaning that the variations are due to other variables, especially human uses in the various sectors of the economy.

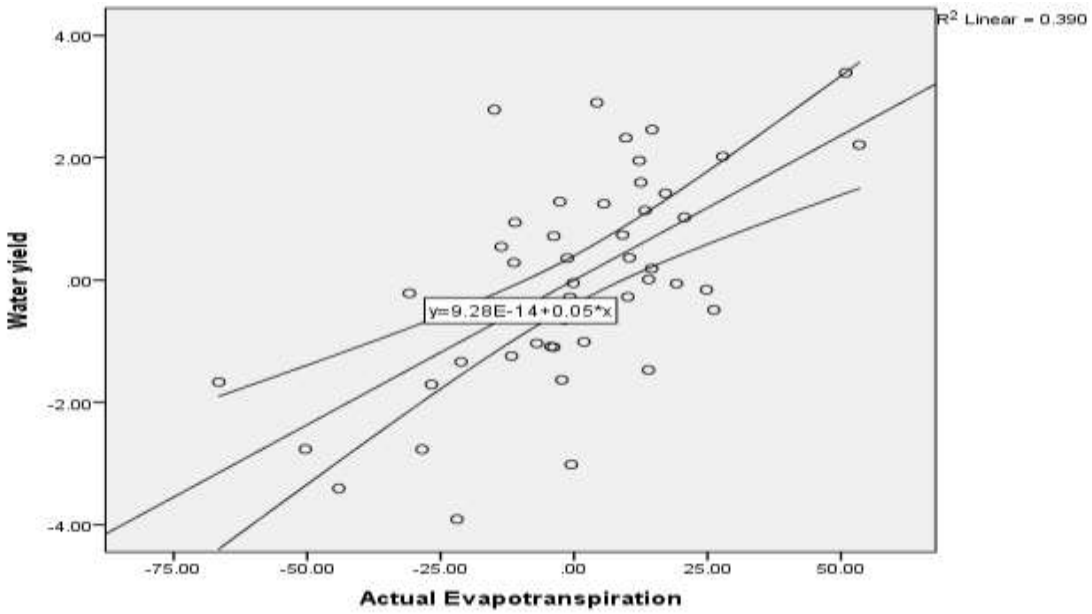

Figure 5.28: Scatter Plot for Actual Evapotranspiration and Water Yield

(vi) Water Yields and Potential Evapotranspiration

The coefficient of determination R^2 between Potential Evapotranspiration and the water yield was 0.139 (Figure 5.29). It is less than 0.3, and therefore no correlation between Potential Evapotranspiration and water yields. The curve actually gives a relationship but on a declining trend from the rest. When two linear variables are regressed, the relationships that exist ($R^{2)}$ has less value compared to results from correlation matrix. (Table 5.8). Correlation Matrix for potential evapotranspiration and water yield gives r

values of -0.373 and a P value of 0.010, meaning a weak negative correlation but somehow significant at 0.010 level because high temperatures as witnessed in the Mara basin and the larger Lake Victoria basin results in conventional rains that, when realized, results in some increase in water yield. Importantly, the scatter plot results for surface flow, groundwater, percolation and precipitation with water yield have coefficients of determination (R^2) of 0.999, 0.942, 0.865, 0.689 in that order, accounting for 99.9%, 94.2%, 86.5% and 68.9% variations in the water yields in the Mara River basin.

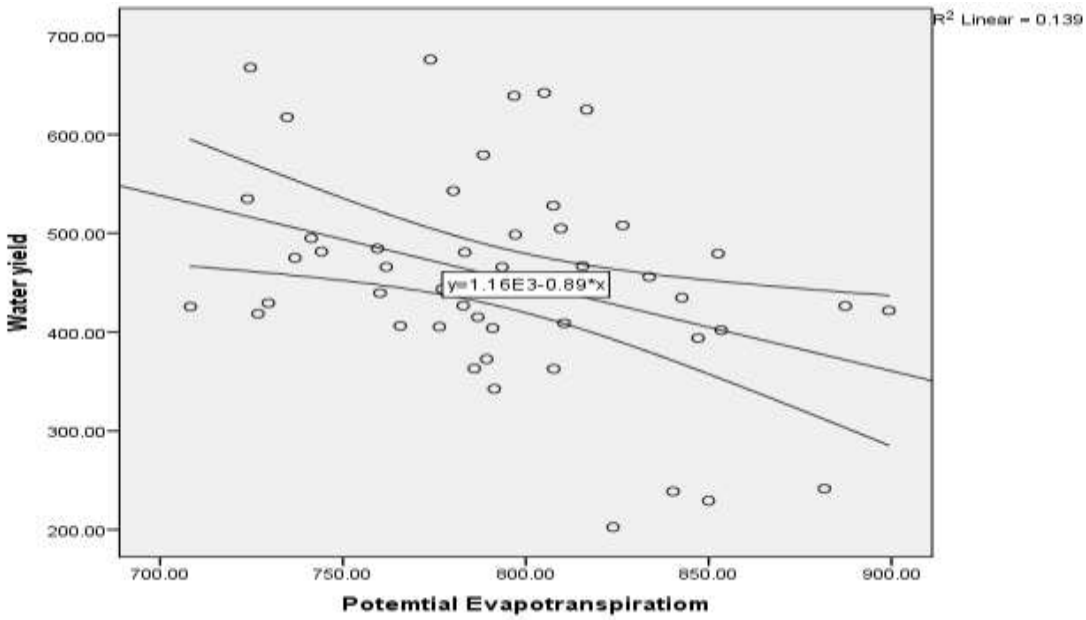

Figure 5.29: Scatter Plot for Potential Evapotranspiration and Water Yield

On the other hand, scatter plot of actual evapotranspiration and potential evapotranspiration with water yields have no significance association and therefore not good predictors in the variations in water yields. These three predictors of surface flow, ground water and percolation have higher coefficient of determination than precipitation because precipitation majorly adds to the water yields through these predictor variables with only a small percentage gadding to the water yields directly from raindrops. The declining trends in forestland, shrub land and grassland in impacting the Mara River flow volumes through reduced precipitation, ground water, percolation and evapotranspiration. Evapotranspiration is the linkage between the terrestrial and atmospheric system in that it take moisture to the atmosphere, initiating the process and sustaining the hydrological cycle.

Deforestation and removal of vegetation cover reduces the leaf coverage available for aiding evapotranspiration, a condition that results in less moisture released into the atmosphere. The outcome would be reduced precipitation that is also unevenly distributed. Equally, reduced forest cover results in less or no infiltration of precipitation into the soil but instead, drains off as surface flow that minimizes the ground water reservoirs. Removal of forest cover leads to accumulation of greenhouse gases in the atmosphere, adding to global warming process and climate change implications, especially high temperatures and reduced precipitation that is unreliable and characteristically erratic, as being witnessed in the Mara River Basin. This study therefore rejects the third objective 'There is no significant relationship between the simulated river flow and changes in land cover/land use and climate in the Mara River Basin.

5.9 River Flow Sensitivity Indices under different Land Cover, Land Use and Climate Scenarios in the Mara Basin.

The results of the Multiple Linear Regression Model showing the degree of association in the predictor variables of land cover, land use and climate with river discharge (dependent variable) are presented and discussed in this section. The results are in terms of the nature of the association of the model in relation to water yields; the strength of the association thereof and, how each of the predictor variables contribute to the observed variations in the water yields or discharge.

5.9.1 Water Yield Parameters and the Water Balance Equation

Forestland and built-up area were used to indicate human interventions on land and therefore, discharge while rainfall and temperature gave the different climate scenarios that impact the discharge. The observations from the correlation matrix (Table 5.12), the association between forest cover and discharge had an r of -0.670 and a P of 0.108. The -0.670 indicated a strong negative correlation between forest cover and discharge and this means that, the higher the forest cover, the lesser the discharge and vice versa. P of 0.108 is more than the level at which the significance level is tested ($\alpha = 0.05$), meaning that, the association between discharge and forest cover is not of statistical significance.

Given that forestland, rainfall, surface flow, ground water, percolation and evapotranspiration are all on the decrease, this scenario in the forest cover and discharge can be explained by reduction in evapotranspiration due to deforestation, resulting in reduced rainfall and finally, discharge. The results relating to built-up area and discharge dynamics gave an r of -0.316 and a P of 0.302. In essence, an r of -0.316 means a weak negative correlation between built-up area and discharge and the P of 0.302, which is more than 0.05, indicates the significance of the correlation. It means that, variations in built-up area have very little to do with the variations in discharge in the basin, there is no statistical significance in their relationship. This could be due to the small percentage of built-up areas in the basin because built-up areas including pavements increase runoffs and therefore should add to water yields. The contribution of changes in forest cover, shrub land and grassland and evapotranspiration to discharge is further explained in sub section 5.7.2.

Table 5.12: Correlation Model of the Study Variables

		Discharge	Forest Cover	Builtup	Rainfall	Temperature
Pearson Correlation	Discharge	1.000	-.670	-.316	.936	.061
	Forest cover	-.670	1.000	.153	-.773	-.482
	Builtup	-.316	.153	1.000	-.471	.322
	Rainfall	.936	-.773	-.471	1.000	-.045
	Temperature	.061	-.482	.322	-.045	1.000
Sig. (1-tailed)	Discharge	.	.108	.302	.010	.461
	Forest cover	.108	.	.403	.063	.206
	Builtup	.302	.403	.	.212	.299
	Rainfall	.010	.063	.212	.	.471
	Temperature	.461	.206	.299	.471	.
N	Discharge	5	5	5	5	5
	Forest cover	5	5	5	5	5
	Builtup	5	5	5	5	5
	Rainfall	5	5	5	5	5
	Temperature	5	5	5	5	5

The r of 0.936 for rainfall indicates a very strong positive correlation between rainfall and discharge in the Mara basin. This indicates that, 93.6% variations in discharge is explained by variations in rainfall. The P of 0.010 is less than 0.05, the level of significance and in essence, gives statistically significant correlation. Temperature has an r of 0.061, which means that 6.1% the variations in discharge is explained by temperature while 93.9% is attributed to other factors, mainly rainfall. The r of 0.061 indicate lack of correlation between discharge and temperature that is supported by a P of 0.461 that is more than α of 0.05. From the forest cover, built-up area, rainfall, temperature and discharge model, rainfall is the best predictor in the variations in discharge, surface flow, ground water and percolation are attributes of rainfall. The other predictor variables, including land cover/use, slope, soils and temperature explain a mere 6.4% in the variations.

5.9.2 Model Suitability in Predicting River Flow Volumes

The results on the suitability of the correlation model comprising forest cover, built-up area, rainfall, and temperature and discharge are in the model summary (power of model). The strengths are measured by the coefficient of determination, (R^2) whose values range from -1 to +1 such that, values greater than +0.5 indicate strong positive correlation, values equal to or less than +0.3 indicate either a weak positive correlation or no correlation. Equally, values less than -0.5 indicate strong negative correlation while values equal to or greater than -0.3 indicate weak negative correlation or no correlation at all. From Table 5.13, the R Squared and R Squared change, (R^2) = 1.000, which means that the model comprising forest cover, built-up area, rainfall and temperature is a perfect predictor model for variations in discharge with 100% variations in discharge explained by the model.

Table 5.13: Model Summary of the Predictor Variables

Model Summary[b]

Model	R	R Square	Adjusted R Square	Std. Error of the Estimate	Change Statistics					Durbin-Watson
					R Square Change	F Change	df1	df2	Sig. F Change	
1	1.000[a]	1.000	.	.	1.000	.	4	0	.	1.242

a. Predictors: (Constant), Temperature, Rainfall, Built_Up, Forest_Cover

b. Dependent Variable: Discharge

In a situation like this, the null hypothesis (H_0): 'Changes in land cover, land use and climate are not a good measure of river flow conditions in the Mara Basin" is rejected and the alternative accepted. The model in question is a perfect one for predicting variations in river discharge in the Mara River basin. In such a case, there would be no need for an adjusted R^2, which apportion the contribution of the potential predictors not considered in the model. Equally, the analysis of variance (ANOVA) has residual of 0.000, implying that, the values estimated by the model are equal to the actual values of the time series. Such a perfect predictor model leaves no error margin in the terms, therefore no F, and Sig. values on Table 5.14.

Table 5.14: Analysis of Variance (ANOVA) of the Predictor Variables

ANOVA[a]

Model		Sum of Squares	df	Mean Square	F	Sig.
1	Regression	34625.299	4	8656.325	.	.[b]
	Residual	.000	0	.		
	Total	34625.299	4			

a. Dependent Variable: Discharge

b. Predictors: (Constant), Temperature, Rainfall, Builtup, Forest Cover

5.9.2.1 Effect of Each Predictor Variable on Flow Variability

The results of each variable's ability to predict the variations in discharge are indicated on Table 5.14 (the coefficients of the predictors in the model). At 95% confidence, the lower and upper limits are the same, as also indicated by the standard error of zero (0) and partial correlation of 1.000 for each. Therefore, the need for t and sig. values to determine the strength and significance of the correlation does not arise. In this model, the estimated values in discharge variability are equal to the actual values of the time series.

Table 5.15: The Coefficients of the Predictors in the Model

Coefficients[a]

Model		Unstandardized Coefficients		Standardized Coefficients	t	Sig.	95.0% Confidence Interval for B		Correlations			Collinearity Statistics	
		B	Std. Error	Beta			Lower Bound	Upper Bound	Zero-order	Partial	Part	Tolerance	VIF
1	(Constant)	-2804.064	.000		.	.	-2804.064	-2804.064					
	Forest_Cover	.012	.000	.872	.	.	.012	.012	-.670	1.000	.316	.131	7.628
	Built_Up	.054	.000	.206	.	.	.054	.054	-.316	1.000	.168	.665	1.503
	Rainfall	1.457	.000	1.729	.	.	1.457	1.457	.936	1.000	.674	.152	6.590
	Temperature	38.415	.000	.492	.	.	38.415	38.415	.881	1.000	.285	.335	2.988

a. Dependent Variable: Discharge

5.9.3 Effect of Land Cover and Land Use Scenarios on Water Yields and Evapotranspiration Rates

The hydrological responses to land cover and land use change scenarios were derived from comparisons between the SWAT model results of the annual values of evapotranspiration and water yield with the 2016-land cover and land use followed by the 2011, 2003, 1995 and 1984 land cover and land use scenarios.

Table 5.16: Changes in average Water Yields and ET under different land use scenarios

Land Cover/Use Scenarios	Years	Annual Water Yield (mm & %)	Annual ET (mm & %)	Annual Rainfall (mm & %)
Land cover/use in 2016	2016	479.37 (24.33%)	431.75 (-1.00%)	946.87 (6.26%)
F+S+G (0.01+1.11+1.98)% to C 2.5%	2011	362.73 (-72.34%)	436.07 (-6.73%)	887.64 (-32.20%)
S+G 0.18+1.33)% to C & F (0.83+2.19)%	2003	625.13 (22.48%)	465.42 (-0.97%)	1173.46 (11.38%)
F+S+G (0.85+2.19+2.2)% to C (3.07)%	1995	484.59 (0.81%)	469.94 (4.87%)	1039.94 (7.78%)
F & S (0.44+1.65) to C&G (2.46+3.34)%	1984	480.71	447.04	959.01

Key: F = Forestland; S = Shrub land; G = Grassland and C = Cropland

The results of change in annual water yield and evapotranspiration according to various land cover and land use scenarios are summarized in Table 5.16. Notably, forestland, shrub land, grassland and cropland are the cover types analyzed. The land cover/land

use values are contained on Table 5.1 on page 128 while water yield, evapotranspiration and rainfall values from the SWAT model are in Appendix III. Table 5.16 indicates the changes in land cover/use, the annual rainfall, water yields and evapotranspiration over the study period in Mara. It is apparent that evapotranspiration decreased all through except between 1984 and 1995, albeit with different percentages, based presumably, on the composition of land cover and land use categories. This general decline in evapotranspiration is confirmed in the 10-year moving average trends in precipitation and evapotranspiration (Figure 5.14 on page 168). Rainfall and water yields increased except during the period between 2003 and 2011. This period is also the one that had indicated increase in forest cover. In 1995, the forest cover had decreased by 0.44%, shrub land 1.65% while grassland and cropland increased by 3.34 and 2.46% respectively. During this period, water yield increased by 0.8% evapotranspiration by 4.87% and rainfall by 7.78%.

By 2003, cropland increased by 2.19% while forestland, shrub land and grassland each decreased by 0.85, 0.18 and 1.33% respectively. This combination brought about an increase in water yield of 22.48%, a decrease in evapotranspiration of 0.97% with an increase in rainfall of 11.38%. Forests, shrubs and grass cover increase evapotranspiration rates with forest cover being the main reason for increased evapotranspiration due to the broad leaves and canopy interception and the deep roots. The leaves intercept raindrops in their canopy, which is later redirected into the atmosphere as water vapour. The ground water sucked by the roots, move upwards through capillary action through the stems and released through the leaves into the atmosphere through evapotranspiration process.

The decrease in forest cover, shrubs and grass cover in the Mara would result in reduction in evapotranspiration as witnessed in the basin presently. Between 2003 and 2011, the forest cover increased for the first and only time by 0.83% and resulted in a one-time decrease in water yield of 72.34%. During the same period, rainfall and evapotranspiration decreased before increasing over the 2011 to 2016 period except for evapotranspiration, when forest cover decreased. This finding is in agreement with Homdee *et al.,* (2010) who reported in their study on the impacts of land cover changes on hydrologic responses of Chi River in Thailand that, expansion of forest cover aimed at replacing farmland resulted in a decline in the annual river flow. This study reveals

that water yields have slight increase while evapotranspiration declines with reduction in forest cover, shrub land and grassland over the study period and the trends are projected to continue if no steps to mitigate or terminate the trend are taken. Notably, the changes in forest cover resulted in small changes in water yields in the Mara. From Table 5.16 and Figures 5.10 and 5.29, it is evidently clear that all the land use scenarios have resulted in significant reduction in the base and average flows over the whole period of study.

This agrees with the study by Mango *et al.,* (2011) in a study in the upper Mara River basin when they reported that land use dynamics affected base flow and seasonal average flows. Further, part of results could be explained from the findings by Homdee *et al.,* (2010), who reported that, a decrease in the area under forest by as much as 50%, which accounted for 10% of the catchment, resulted in a relatively small change in the water yields. Wilk, (2001) had also found a similar scenario and reported that, large decreases in forest cover in the Nam Pong catchment had no significant effect on river flows in the catchment. It should however be noted that, deforestation could shorten both the amount and timing of water yield during the rainy seasons. Reduction in forest cover results in minor decrease in annual evapotranspiration, which can behave differently with seasons probably because cropland has a lower rate of evapotranspiration compared to forestland. Reduced base and average flows is a challenge to water availability to the ecological and socio-economic environment in the Mara River basin.

5.9.4: A Log Plot of the Water Yields and Key Predictors in Water Balance

The results of a log linearity plot of the same coefficients of SWAT model annual values analysis (Figure 5.30) further explains the relationships in the water yields variability. as a function of water balance computation in the Mara River basin. From the log linearity plot, the relationship between surface flow, ground water, surface water and potential evapotranspiration and the water yield variability show both positive and negative or inverse correlations except for the potential evapotranspiration, which has an inverse and a weak association (Table 5.8, page 181) and Figures 5.24-5.29, for scatter plots respectively.

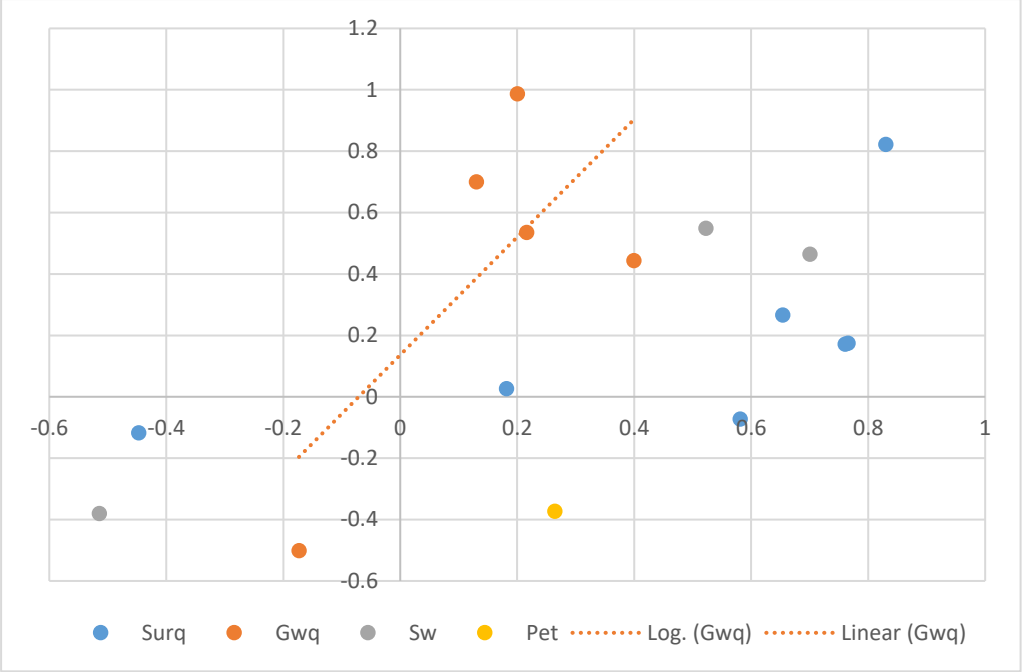

Figure 5.30: SWAT Model Water Yield Variables relationships

From the log plot, ground water gives a much stronger positive correlation than surface flow with the water yields, as indicated by the gradients of their slopes. Surface water that for real, has zero association with water yields has a gradient almost the same as that of surface flow, albeit with half performance that of surface flow as seen from the distribution of the dots in the compartments two and four. Surface water retains water that should have added to the yields in the river but it can perform this during flooding thus, the relationship in the log plot. Potential Evapotranspiration is negative, meaning that, it behaves inversely with the water yields. Being the total water budget that should leave a surface into the atmosphere, any changes in land cover and land use that lessen evapotranspiration results in less rainfall.

The decrease in rainfall adds to the potential evapotranspiration's implications that reduce surface flow, ground water, percolation and therefore, water yields. Surface flow, ground water, percolation, and evapotranspiration are a function of land cover and land use practices. Evapotranspiration is a natural phenomenon that has witnessed change in amounts and rates in the Mara due to human interventions on the landscape. The inverse correlation of potential evapotranspiration and the other variables mean that when potential evapotranspiration is low, the conditions are manageable and vice versa. High potential evapotranspiration puts much water demand in the water balance,

a situation that is not good for a basin like Mara that is water deficient. Increased evapotranspiration in the basin leads to an increase in each of the predictor variables of precipitation, surface flow, ground water and percolation, and therefore more water yields.

According to land cover and land use analysis results Mara River has faced many land use changes, which are still ongoing and have resulted in the reduction in forest cover, grassland, shrub land with huge increases in cropland and somewhat fast growth in urbanization. The environment is generally degraded and this is affecting rainfall, surface flow, percolation, ground water and evapotranspiration rates thus, the declining water yields in the basin with implications for the various stakeholders. In the breath of the ongoing discussion, changes in the land cover, land use and climate scenarios adversely impacting the Mara River flow volumes to the detriment of the many stakeholders in the basin and beyond, including the Nile system, a situation that must be reversed.

CHAPTER SIX: SUMMARY, CONCLUSIONS AND RECOMMENDATIONS

6.1 Summary of Findings

The results of forestland, grassland, shrub land, and rainfall and temperature analysis with the water yields revealed that, there was a strong association between land cover, land use and climate change and the hydrological regimes, which varied with time and space. In other words, spatio-temporal variations in land cover/use dynamics and in the rainfall and air temperature are causing significant variations in water yields in the Mara basin that are summarized under the following subsections based on the specific objectives.

6.1.1 Nature, Extent and Rate of Change in Land Cover and Land Use.

The land cover and land use analysis results established that, forest cover, grassland and shrub land decreased throughout the study period (1984 to 2016) at the expense of cropland and built-up areas, which increased in their extent over the same period as population increased with more demand for land for their social and economic wellbeing. Deforestation is still taking place in the Mara, especially on the Kenyan side in spite of the initiatives by the respective governments; the East African Community, Lake Victoria Basin Commission Secretariat; Lake Victoria Basin Commission and the Nile Basin Initiative, which is a Subsidiary Action Program of the Nile Equatorial Lakes.

Hotspots of change are around Musoma town and goldmines in Tarime of Tanzania, Bomet and its environs and Keringet area of Nakuru County. Deforestation in the Mara is adding to global warming and climate related implications witnessed in reduced rainfall, rise in air temperature and reduction in river flows, a situation characterized by increased low base flows and high peak flows during dry and rainy seasons respectively.

6.1.2 Spatio Temporal Variations in Rainfall, Air Temperature and River Flows.

The results from the analysis of the simulated maximum and minimum air temperature over the study period revealed gradual increase in air temperature in which, both night

and day time became warmer by about 0.5 and 0.6^0C respectively. The mean annual maximum and minimum air temperature did not record any significant change while the mean monthly maximum and minimum temperatures indicated significant change in the months of January, June September, October and November for maximum and in January, April, July and September for minimum temperature when tested at $\alpha = 0.05$. The basin has two rainy seasons, main one from March to May and the short rains from September to November.

The results of the analysis of rainfall patterns established that, the rains are bimodal, on a decline and are characterized by shifts such that, the usually dry months: December, January and February (DJF) and June, July and August (JJA) are becoming relatively wetter while the usually wet months such as March, April and May (MAM) and September, October and November (SON) are becoming relatively dry. The results of the analysis of annual cycles of mean monthly and annual rainfall trends showed temporal variations within the year and over longer-term periods. The mean monthly rainfall indicated seasonal variation in rainfall with none of the mean monthly and annual values indicating significant change at $\alpha = 0.05$ between 1983 and 2014 with same projection to 2030.

The results of river discharge trends analysis revealed declining trends as well over the study period. The mean annual trends revealed variability, with values in either side of trend line. 1990 had the least, 202.37m^3, 2006 had the highest, 675.91m^3 while 2023 is projected to reduce to around 229.28m^3 with 2030 recording 486.87m^3. The years beyond 2030 are projected to record even lower values with worse implications on the sectors that require consistent water supply in quality and quantity. The consequences of the downward trends in river flow volumes cannot be overemphasized given that, the Mara River is a lifeline to Maasai Mara –Serengeti Conservancies and the only available surface water in the basin during dry periods.

6.1.3 SWAT Hydrological Model

SWAT Model was found suitable in determining the third and fourth objectives of this study. It compared well, the values of the observed and simulated variables. For example, when observed and simulated rainfall were compared using t-test on a two-sample statistic assuming unequal variances at 2 degrees of freedom, critical value was

found to be 2.000995, calculated value was 0.698085 while table value was 4.303. Since the calculated value was less than table value it meant that, there existed no significant difference in the mean of the observed and simulated rainfall. In the power of the model of land cover, land use and climate scenarios in which, this study modelled varying forestland, built-up area, rainfall and temperature scenarios, the coefficient of determination had an R Squared and R Squared change of 1.000 and this revealed that, about 100% variations in river flow was explained by variations in rainfall. Based on the above, the following two sub sections outline outcomes of the third and fourth objectives.

6.1.3.1 River Flow Simulations under different Land Cover/Use and Climate Scenarios.

This study established that, there exists a significant relationship between the simulated river flows and changes in land cover, land use and climate in the Mara River Basin. The simulated model of forestland, built-up areas, rainfall and air temperature and river flow gave an R Squared and R Squared Change of 1.000. The model of forestland, built-up area, rainfall and temperature is perfect for predicting variations in river flow in the Mara River Basin, with 100% variations explained by the variables in the model. The same model gave an r of 0.939 and P of 0.010 for rainfall, meaning that, 93% variations in river flow is explained by variations in rainfall. Thus, variations in rainfall is significant in predicting variations in river flow in the Mara than variations in temperature (r of 0.061 and a P of 0.461) and forest cover (r of -0.670 and a P of 0.108). In essence, forest cover has inverse effect on river flows in that, when forestland increases, the flow should be on the decline due to increased infiltration and vice versa. Reduction in forest cover, in normal cases, should result in increased flows due to reduced ground cover and therefore reduced infiltration. The position of this study is that, reduction in forest cover is resulting in reduced rainfall due to reduced evapotranspiration rates and therefore, reduced flow volumes. Specifically, reduction in vegetation cover leads to accumulation of greenhouse gases in the atmosphere, heating the atmosphere instead of it being cooled to allow for rain formation. High temperatures especially during dry seasons are resulting in marked reduction in river flow volumes, although direct influence on the flow volumes are minimal.

6.1.3.2 River Flow Sensitivity Indices under different Land Cover and Land Use and Climate Scenarios

The results on the analysis of the generated river flow sensitivity indices under different land cover, land use and climate scenarios established that: Changes in land cover, land use and climate are a good measure of river flow conditions in the Mara Basin. The model of land cover, land use, rainfall and temperature with river flow gave a perfect prediction tool that explained about 100% variations in river flow volumes to be because of changes in land cover, land use and climate. Therefore, changes in land cover, land use and climate are a good measure of river flow conditions in the Mara river basin.

Variations in river flow were most sensitive to changes in rainfall than to changes in land cover, land use and temperature. About 93.6% variations in discharge is explained by variations in rainfall. The results of the analysis of land use changes with water yields and evapotranspiration revealed that, a significant reduction in forest cover, grassland and shrubs resulted in small change in river flow volumes. This position notwithstanding, changes in land cover and land use are very important due to their role in the science of infiltration, ground recharge and evapotranspiration process.

6.2 Conclusions

i. The overall objective was to determine the impact of land cover, land use and climate change on the hydrological regimes of the transboundary Mara River basin. This study has demonstrated that, using SWAT, which is a physically based model, in large and poorly gauged basins with varying land cover, land uses, soils, topography and climate like the Mara basin can yield useful results, especially with proper calibration of the model. The SWAT modeling exercise produced fair results in the present study and therefore, proved suitable for the analysis and evaluation of trends in the response of the Mara River basin to future land cover, land use and climate scenarios.

ii. The climate of the Mara river basin is changing, and will progressively become warmer and drier, if the trends of change in the main cover types including forest cover, rangelands, temperature and rainfall, were to continue. Any further conversion of forestland to either farmland or pasture land is likely to result in more

reduction in base flows and increased peak flows during dry and rainy seasons respectively. These changes would worsen the already unbearable challenges experienced in increased incidences of droughts and floods that have more often than not, resulted in loss of livestock, livelihoods and human life.

iii. Although river flows are most sensitive to variations in rainfall than the other variables, the long-term impacts of deforestation on the Mara River flows will be more critical than variations in rainfall parse. This is because of reduced evapotranspiration rate and infiltration that would leave both the soil and atmosphere dry throughout when conditions worsen. The Evapotranspiration is the link between the earth system and the atmospheric system, initiates and keeps the hydrological cycle in place. Land uses that reduce its rate of releasing moisture to the atmosphere would therefore promote instances of droughts and degraded environment in the Mara River basin.

6.3 Recommendations

From matters arising on study findings as well as challenges encountered therein, the author wishes to make the following general recommendations to policy makers and researchers in environmental issues particularly hydraulic sector.

6.3.1 Recommendations to Policy Makers

i. This study has provided useful methods and information that inform medium and long term planning of water resources management in the Mara in particular and in Kenya generally. These details should form part of the mainstream economic development strategies and integrated in the implementation of the National Water Master Plan 2030.

ii. SWAT hydrological model has shown its potential in modelling water yields in the Mara basin under different land cover/use and climate scenarios. Other hydrological models such as the USGS Geo Streamflow Model should be used to ascertain their suitability.

iii. Results of this study have shown that a combination of both land cover, land use and climate change leads to reduced water yields in the transboundary Mara basin and, in essence this region. Concerted efforts must be made to conserve this critical system.

6.3.2 Recommendations to Researchers

i. The climate change implications are already taking their toll in the Mara River Basin. Future researchers should carry out further investigations on this through climate modelling, using models like PRECIS RCM to complement the hydrological modelling results.

ii. SWAT hydrological model has shown its potential in modelling water yields in the Mara basin under different land cover/use and climate scenarios. Other hydrological models such as the USGS Geospatial Streamflow Model should be used to ascertain their suitability in a basin like Mara.

iii. Environmental degradation and encroachment on fragile ecosystems are still ongoing in the Mara despite the findings and recommendation from past studies to assist policy makers on formulating sustainable conservation policies. There is need to establish whether such recommendations are never used by the policy makers with a view to finding how best to link the Policy Makers and the Research world.

6.3.3 Recommendations to the Various Institutions and Organizations

i. NEMA as the body entrusted with environmental protection needs to be more robust in role as a watchdog in implementing environmental policies and regulations based on advances in science and technology for equitable and sustainable utilization of the meager resources.

ii. Where Acts such as Forest Conservation Act, Water Act, Mining Act, and others appear to contradict, the affected institutions ought to come together under the direction of NEMA, to ratify changes that may promote environmental equity and aesthetic values.

6.3.4 Recommendations to the Governments of Kenya and Tanzania

i. Globally, the governments have recognized the challenge of sustainability in natural resources utilization and the fact that, no single government can work alone in this area. It is imperative that, governments of Kenya and Tanzania work together on matters pertaining to the conservation of the transboundary Mara resources, especially through the framework of the East African Commission or Secretariat.

ii. The Governments should also encourage Companies, Local Communities and Non-governmental Organizations in their respective jurisdiction to participation on matters of policy formulation and implementation in conservation and utilization. Organizations like Kenya Forest Working Group, Conservation for Nature, among others should get a lot of support from the government to fulfill their mandate.

REFERENCES

Abbaspour, K C, M Framarzi, S Ghasemi, and H Yang (2009). "Assessing the Impact of Climate Change on Water Resources in Iran." *Water Resour. Res* 45 (2009).

Ahrens C. D., (2009): Meteorology Today, an introduction to weather, climate and the Environment, Ninth Edition, *Brooks/Cole 10 Davis Drive, Belmont CA94002, USA, 439-499*

Akhtar, M, N Ahmad, and M J Booij (2009). "Use of Regional Climate Model Simulations as Input for Hydrological Models for the Hindukush-Karakorum-Himalaya Region." *Hyrol Earth Systems Sci* 13 (2009): 1075-1089.

Akotsi, E N, J N Gachanja, D M Mugwe, and J Ojema, (2004). *Forest Cover Mapping: The Five Water Towers.* DRSRS_MENR Technical Report, Nairobi: Government of Kenya, 2004.

Anderson, R. J., Hardy, E. E., Roach, J. T., and Witmer, R. E., (1976). A Land Use And Land Cover Classification System For Use With Remote Sensor Data. United States Geological Survey. Washington DC, United States Government Printing Office.

Anyah, R. O. and Qiu, W. (2011). Characteristic of 20th and 21st century precipitation and temperature patterns and changes over the Greater Horn of Africa, Int. J. Climatology, 31, doi:10.1002/joc.2270, in press.

Arnold, J G, R Srinivasan, R S Muttiah, and J R Williams, (1998). "Large Area Hydrologic Modelling and Assessment Part 1: MOdel Development." *J. AM. Water Resour. Assoc* 34 (1) (1998): 73-89.

Arnold, J G, J R Kiniry, R Srinivasan, J R Williams, E B Haney, and S L Neitsch (2009). *Soil and Water Assessment Tool Input/Output File Documentation Version 2009,.* Texas Water Resources Institite Technical Report, Grassland, Soil and Water Reseaech Labaratory - Agricultural Research Service, Blackland Research Centre - Texas Agrilife Research, September 2011.

Arnold, J. G., Moriasi, D. N., Gassman, P. W., Abbaspour, K. C., White, M. J., Srinivasan, R., Santhi, C., Harmel, R. D., Van Griensven, A., Van Liew, M. W., Kannan, N., Jha M. K. (2012). SWAT: MODEL USE, CALIBRATION, AND VALIDATION, Transactions of the ASABE, Vol. 55(4): 1491-1508 2012 American Society of Agricultural and Biological Engineers ISSN 2151-0032

Awotwi, A., Kumi, M., Jansson, P.E., Yeboah, F. and Nti I.K., (20015). "Predicting Hydrological Response to Climate Change in the White Volta Catchment, West Africa." *J Earth Sci Clim Change* 6, no. 1 (2015): 1-7.

Ayuyo, I O., (2012). *Geospatial Analysis of Land Use and Land Cover Change in the Mau Forest Complex of Kenya.* Nairobi: University of Nairobi, Kenya, 2012.

Bernstein, L., Bosch, P., Chen, Z., Christ, R. and Davidson, O., (2007) *Climate Change 2007.* Synthesis Report; Summary for Policy Makers, IPCC, 2007.

Blasone, (2007). Parameter Estimation and Uncertainty Assessment in Hydrological Modelling, PhD Thesis, Institute of Environment & Resources, Technical University of Denmark

Bosshard, T., Carambia, M., Goergen, K., Kotlarski, S., Krahe, P., Zappa, M. and Schar, C. (2013). Quantifying uncertainty sources in an ensemble of hydrological climate-impact projections, Water Resour. Res., 49, doi: 10.1029/2011WR011533

Brissette, F. P., Khalili, M. and Leconte, R. (2007). Efficient stochastic generation of multi-site synthetic precipitation data, Journal of Hydrology (2007) 345, 121–133

Bronstert, A. Niehoff, D. and Būrger G. (2002). Effects ofClimate and Land Use Change on Storm Runoff generation: Present knowledge and Modelling Capacities. Hydrol Process 16:509-529.

Burn, D. H., Hannaford, J., Hodgkins, G. A., Whitfield, P. H., Thorne, R., and Marsh, T. (2012). Reference hydrologic networks II. using reference hydrologic networks to assess climate-driven changes in streamflow. *Hydrol. Sci. J.* 57, 1580–1593. doi: 10.1080/02626667.2012.728705

Hyandy, C, B, Abeyou Worqul, Lawrence W. Martz and Alfred N. N. Muzuka (2018). The impact of future climate and land use/cover change on water resources in the Ndembera watershed and their mitigation and adaptation strategies.

Central Bureau of Statistics (CBS). 2006. Ministry of Planning and National Development. Kenya Facts and Figures, 2006 Edition. Nairobi: CBS

Chaves, J., Neill, C., Germer, S., Neto, S.G., Krusche, A. and Elsenbeer, H. (2008). "Land management impacts on runoff sources in small Amazon watersheds." *Hydrol. Proc.*, 2008: 1766-1775.

Chebana, F., Aissia, M. A. B., and Ouarda, T. B. M. J. (2017). Multivariate shift testing for hydrological variables, review, comparison and application. *J. Hydrol.* 548, 88–103. doi: 10.1016/j.jhydrol.2017.02.033.

Chen, Zhongsheng, Yaning Chen, and Baofu Li (2013). "Quantifying the effects of climate variability and human activities on runoff for Kaidu River Basin in arid region of northwest China." *Theoretical and applied climatology* 111, no. 3-4 (2013): 537-545.

Chen, X., Kumar, M. and Mcglynn, B.L., (2014). Variations in streamflow response to large hurricane-season storms in a Southeastern US watershed. J. Hydrometeorol. http://dx.doi.org/10.1175/JHM-D-14-0044.

Christensen, J.H., Hewitson, B., Busuioc, A., Chen, A., Gao, X., Held, I., Jones, R., Kolli, R.K., Kwon, W.T., Laprise, R., Magaña Rueda, V.L., Mearns, Menéndez, C.G., Räisänen, J., Rinke, A., Sarr, A. and Whetton, P. (2007): Regional Climate Projections. In: Climate Change 2007: The Physical Science Basis. Contribution of Working Group I to the Fourth Assessment Report of the Intergovernmental Panel on Climate Change [Solomon, S., D. Qin, M. Manning, Z. Chen, M. Marquis, K.B. Averyt, M. Tignor and H.L. Miller (eds.)]. Cambridge University Press, Cambridge, United Kingdom and New York, NY, USA, 847-871.

Coe, R. and Cooper P., (2011). "Assessing and Addressing Climate-indiced Risk in Subsaharan Rainfed Agriculture." *Experimental AGriculture* 47, no. 4 (2011): 963-984.

Cong, Z., Zhao, J., Yang, D., and Ni, G. (2010). Understanding the hydrological trends of river basins in China. *J. Hydrol.* 388, 350–356. doi: 10.1016/j.jhydrol.2010.05.013

Coppin, P. and Bauer, M., (1996). Digital Change Detection. In: Forest Ecosystems with Remote Sensing Imagery. Remote Sensing Reviews. Vol. 13. p. 207-234.

Dai, Erfu, Zhuo Wu, and Quansheng Ge (2016). "Predicting the responses of forest distribution and aboveground biomass to climate change under RCPs scenarios in southern China." *Global Change Biology*, 2016: 3642-3661.

Dams, J. (2007). "Predicting Land-Use Change and Its Impact on the Groundwater System in the Grote-Nete Catchment, Belgium." *Hydrogeol. J.*, 2007: 891-901.

Davey, C.A. and Pielke, R.A. Sr. (2005). “Microclimate Exposures of Surface-based Weather Stations - Implications for the Assessment of Long-term Temperature Trends.” Bulletin of the American Meteorological Society 86(4) 497–504

Davies, T. C. (1996). Chemistry and Pollution of Natural Waters in Western Kenya. Journal of African Earth Sciences 23(4): 547-563.

De Pauw (1984). Soils, physiography and agro ecological zones of Tanzania. A Consultant Report submitted to United Republic of Tanzania.

Dessu, S. B., & Mellesse, A. M., (2012). Modelling the rainfall–runoff process of the Mara River basin using the Soil and Water Assessment Tool. *Hydrological Processes*, 26(26), 4038-4049.

Dessu, S.B., Melesse, A.M., Bhat, M.G. and McClain M.E. (2014). Assessment of water resources availability in the Mara River Basin. *CATENA* 115(O) 104-114 doi: http://dx.doi.org/10.1016/j.catena. 2013.11.017.

Dong, J., Crow, W. T., Duan, Z., Wei, L., and Lu, Y. (2019). A double instrumental variable method for geophysical product error estimation. *Remote Sens. Environ.* 225, 217–228. doi: 10.1016/j.rse.2019.03.003

Douglas, E. M., Vogel, R. M., and Kroll, C. N. (2000). Trends in floods and low flows in the United States: impact of spatial correlation. *J. Hydrol.* 240, 90–105. doi: 10.1016/S0022-1694(00)00336-X

Duan, Z., Tuo, Y., Liu, J., Gao, H., Song, X., Zhang, Z., et al. (2019). Hydrological evaluation of open-access precipitation and air temperature datasets using SWAT in a poorly gauged basin in Ethiopia. *J. Hydrol.* 569, 612–626. doi: 10.1016/j.jhydrol.2018.12.026

Droogers, P., Mantel, S. and Kauffman, S. (2006): River Basin Mo changing land use practices from pastoral to sedentary farming and increased migration of farming communities onto wildlife dispersal areas to support Green Water Credit Assessments, (DRAFT): Sponsored by: IFAD, World Soil Informat, SEI–Stockholm Environment, Institute, Future Water Science for Solutions, 25.

DRSRS, KFWG and Royal Netherlands Embassy (2006), Changes in forest cover in Kenya's five water towers 2003 – 2005.

East African Community (EAC), 2013. Protocol for Environment and Natural Resources Management. East African Community Secretariat, Arusha, Tanzania.

FAO, (2005). Global Forest Resources Assessment 2005. Progress towards sustainable forest management. FAO forest paper 147 (online), Rome.

FAO, (2006). Global Forest Resources Assessment 2005; Progress towards Sustainable Forest Management, Food and Agriculture Organization of the United Nations Forestry Paper 147, Rome, 350.

FAO, (2008). Forests and Water; A Thematic Study Prepared in the Framework of the Global Forest Resources Assessment 2005; Forestry Paper 155, Rome, 92.

FAO, (2010). Global Forest Resources Assessment Main report, FAO Forestry Paper 163. Food and Agriculture Organization of the United Nations, Rome, 2010.

Faramarzi, M., Abbaspour, K. C., Schulin, R., and Yang, H. (2009). Modelling blue and green water resources availability in Iran. *Hydrological Processes: An International Journal*, *23*(3), 486-501.

Feng Wu, Jinyan Zhan, Hongbo Su, Haiming Yan, and Enjun Ma, (2015). Scenario-Based Impact Assessment of Land Use/Cover and Climate Changes on Watershed Hydrology in Heihe River Basin of Northwest China.

Foley, J.A., DeFries, R., Asner, G.P., Barford, C., Bonan, G., Carpenter, S.R., Chapin, F.S., Coe, M.T., Daily, G.C., Gibbs, H.K., Helkowski, J.H., Holloway, T., Howard, E.A., Kucharik, C.J., Monfreda, C., Patz, J.A., Prentice, C.,M Ramankutty, N. and Snyder, P.K., (2005). Global Consequences of Land Use. Science Vol. 309.570 DOI: 10. 1126/Science. 1111772.

Foody, G. M. (2001). Monitoring the magnitude of land cover change on the southern limits of the Sahara. Photogrammetric Engineering and Remote Sensing, 67(7), 841-847.

Forster, P., Ramaswamy, V., Artaxo, P., Berntsen, T.R., Betts, Fahey, D.W., Haywood, J., Lean, J., Lowe, D.C., Myhre, G., Nganga, J., Prinn, R., Raga, Schulz, G.M. and Van Dorland, R. (2007). Changes in Atmospheric Constituents and in Radiative Forcing. In: Climate Change 2007. The Physical Science Basis. Contribution of Working Group I to the Fourth Assessment Report of the Intergovernmental Panel on Climate Change [Solomon, S., D. Qin, M. Manning, Z. Chen, M. Marquis, K.B. Averyt, M.Tignor and H.L. Miller (eds.)]. Cambridge University Press, Cambridge, United Kingdom and New York, NY, US, 129-234.

Gao, H., Li, H., Duan, Z., Ren, Z., Meng, X., and Pan, X. (2018). Modelling glacier variation and its impact on water resource in the Urumqi Glacier no. 1 in Central Asia. *Sci. Tot. Environ.* 644, 1160–1170. doi: 10.1016/j.scitotenv.2018.07.004

Gassman P. W., Reyes, M. R., Green, C. H., and Arnold J. G., (2007). The Soil and Water Assessment Tool: Historical Development, Applications, and Future Research Directions. American Society of Agricultural and Biological Engineers, vol. 50 (4): 1211-1250.

Gathanju, D., (2009). "Special Report: Human pressures destroying Maasai Mara Wildlife". www.peopleand planet.net/…/special-report-human-pressures-destroying masai-mara-wildlife.html.

Gereta, E., Wolanski, E., Borner, M. and Serneels, S. (2002). Use of an ecohydrology model to predict the impact on the Serengeti ecosystem of deforestation, irrigation and the proposed Amala Weir water Diversion Project in Kenya. Ecohydrology and Hydrobiology Vol. 2 No 1-4, 135-142.

Githui, F.W., (2008). Assessing the Impacts of Environmental change on the Hydrology of the Nzoia Catchment in the Lake Victoria Basin, PhD Thesis, Vrije Universiteit – Brussels, 1-142

Glavan, M. and Pintar M. (2012). Strengths, Weaknesses Opportunities and Threats of Catchment Modelling With Soil and Water Assessment Tool (SWAT) Model, Water Resources Management and Modelling, Dr. Purna Nayak (Ed.), ISBN: 978-953-51-0246-5, InTech, Available from http:www.intechopen.com/books/water-resources-management-and–modeling/strengthsweaknesses-opportunities-and-threats-of–catchment-modeling-with-soil-and-water-assessment

GoK (2009). Report of the Prime Minister's Task Force on the Conservation of the Mau forest complex, available online: http://www.kws.go.ke/export/sites/kws/info/maurestoration/maupublications/Mau Forest Complex Report. Pdf, last access: 15 June 2009.

GoK, (2010). Rehabilitation of the Mau Forest Ecosystem Programme. Prepared by the Interim Co-ordinating Secretariat, Office of the Prime Minister, on Behave of the Government of Kenya, with Support from the United Nations Environment Programme, April 2010, 260

GoK, (2011). Agricultural Sector Development Support Programme. Ministry of Agriculture, September Sci Clim Change 6: 249. doi:10.4172/2157-7617.1000249, 2011.

Goldewijk, K., (2001). Estimating global land use change over the past 300 years: the HYDE database. Global Biogeochem. Cycles 15, 417-433.

Griensven, Van A., (2005): Sensitivity, Auto-Calibration, Uncertainty and Model Evaluation in SWAT2005 (DRAFT), a.vangriensven@unesco-ihe.org

Griensven, Van A., Ndomba, P. Yalew, S. and Kilonzo, F. (2012): Critical Review of SWAT Applications in the Upper Nile Basin Countries, Hydrol. Earth Syst. Sci., 16, 3371–3381

Hamed, K. H. (2007). Improved finite-sample Hurst exponent estimates using rescaled range analysis. *Water Resour. Res.* 43, 797–809. doi: 10.1029/2006WR005111

Hamed, K. H., and Ramachandra Rao, A. (1998). A modified Mann-Kendall trend test for auto-correlated data. *J. Hydrol.* 204, 182–196. doi: 10.1016/S0022-1694(97)00125-X

Helsel DR, Hirsch RM (2002) Hydrological analysis and interpretation: statistical methods in water resources. US Geological Survey, Reston, VA.

Herrero, M., Thornton P.K., Notenbaert A.M., Wood S., Msangi S., Freeman H.A., Bossio D., Dixon J., van de Steeg J., Lynam J., Parthasarathy Rao P., Macmillan S., Gerard B., McDermott J., Seré C., Rosegrant M.W. (2010). Smart investments in sustainable food production: revisiting mixed crop livestock systems. Science 327:822-825

Hoffman, C. M., (2007). Geospatial mapping and analysis of water availability-demand-use within the Mara River Basin. MSc Thesis. Florida International University, Miami, Florida, USA.

Homdee, T. Pongput, K. and Kanae, S. (2011). "Impacts of Land Cover Changes on Hydrologic Responses: A Case Study of Chi River Basin, Thailand Annual Journal of Hydraulic Engineering, JSCE, Vol.55, 2011, February

Hough, J. (1986). Management Alternatives for Increasing Dry Season Base Flow in The Miombo Woodlands of Southern Africa. Ambio 15(6), 341-346.

Houghton, J. T. (1995). Climatic Change 1994: Radiative Forcing of Climatic Change and an Evaluation of IPCC IS92 Emission Scenarios. Intergovernmental panel on climate change. Cambridge University Press, Cambridge, UK.

Houghton, R.A., House, J.I., Pongratz, P., van der Werf, G. R., DeFries, R.S., Hansen, M.C., Le Quéré, C., Ramankutty, N. (2012). Carbon emissions from land use and land-cover change. Biogeoscienes 9, 5125-5142

Hulme, M, Doherty, R. M., Ngara, T. New M. G. and Lister D., (2001). "African Climate change: 1990 - 2100." *Climate Research*, 2001: 145-168.

Humi, H., Tato, K. and Zeleke, G., (2005) "The implications of changes in population, land use and land management for surface runoff in the Upper Nile basin area of Ethiopia." *Mount. Res. Dev.*, 2005: 147-154.

IPCC, (2000). *IPCC Special report: Emissions" Scenarios, summary to policy makers: A special report of IPCC working group III;* Published for the Intergovernmental Panel on Climate Change, 27

IPCC, (2001). *Climate Change 2001. Impacts, Adaptations and Vulnerability. Contribution of Working Group II to the Third Assessment Report of the Intergovernmental Panel on Climate Change.* Cambridge, UK: Cambridge University Press, 2001.

IPCC, (2007). Climate Change, 2007: Synthesis Report. Contribution of Working Groups I, II and III to the Fourth Assessment Report of the Intergovernmental Panel on Climate Change [Core Writing Team, Pachauri, R.K and Reisinger, A. (Eds.). IPCC, Geneva, Switzerland.

IPCC, (2013). *Climate change 2013: the physical science basis: Working Group I contribution to the Fifth assessment report of the Intergovernmental Panel on Climate Change*. Cambridge University Press.

Jacobs, J.H., Angerer, J., Srinivasan, R., and Kaitho, R. (2007). Mitigating Economic Damage in Kenya's Upper Tana River Basin: An Application of Arc-View SWAT. Journal of Spatial Hydrology, Vol. 7, No. 1, Spring 2007, 23-46

Jayakrishnan, J., Srinivasan, R., Santhi, C., and Anald, J.G. (2005). Advances in the Application of the SWAT Model for Water Resources Management, Hydrological Processes.19, 749-762 (2005), Wiley Interscience, John Wiley and Sons Limited.

Jensen, J.R., (2005). Introductory Digital Image Processing: A Remote Sensing Perspective, Third Edition, Prentice-Hall, Englewood Cliffs, New Jersey.

Jianwei Liu, Can Zhang, Limin Kou and Qiang Zhou, (2017). Effects of Climate and Land Use Changes on Water Resources in the Taoer River.

Jones, R.G., Noguer, M., Hassle, G.G., Hudson, D., Wilson, S.S., Jenkins, G.J. and Mitchell, J.F.B., (2004). Generating High Resolution Climate Change Scenarios Using PREIS, Met Office Hadley Centre, Exeter, UK, 44pp, April 2004.

Kareiva, P., Watts, S., McDonald, R. and Boucher, T., **(**2007). Domesticated nature: shaping landscapes and ecosystem changing land use practices from pastoral to sedentary farming and increased migration of farming communities onto wildlife dispersal areas for human welfare. Science 316:1866–1869.

Kendall M. G. (1975). Rank Correlation Methods. London: Charles Griffin and Company Limited.

Kenya National Bureau of Statistics (KNBS) 2009. Ministry of Planning and National Development. Kenya Population and Housing Census, 2009 Edition. Nairobi: KNBS.

Kiangi, P.M.R., Kavishe, M.M. and Patnaik, J.K., (1981): Some Aspects of the Mean Tropospheric Motion Field in East Africa during the Long Rains Season. *Kenya J. of Sci. and Tech. (A), 2, 91-103.*

Kinyanjui, J.M., (2009). The effect of human encroachment on the forest cover, composition and structure in the western blocks of the Mau forest complex, PhD thesis, Egerton University, Kenya, 128.

KNMI, (2006). "Climate change in Africa, (2006). Changes in extreme weather under global warming, Royal Netherlands Institute of Meteorology." n.d.

Krause P., Boyle, D.P. and Base F., (2005). Comparison of Different Efficiency Criteria for Hydrological Model Assessment Advances in Geosciences, 5, 89-97.

Lamprey, R. H. and Reid, R. S. (2004). Expansion of Human Settlement in Kenya's Maasai Mara: What Future for Pastoralism and Wildlife. Journal of Biogeography 31: 997-1032.

Lambin, E.F., Turner, B.L, and Geist, H.J, (2001). The Causes of Land Use and Land Cover: moving beyond the Myth. Global Environmental change: Human and Policy Dimensions 11:261-269.

Lambin, E. F., Samuel, B. and Geist, H. J. (2003). Global Land-Use and Land-Cover Trends." Bulletin of the American Meteorological Society 86(4) 497–504.

Lambin, E.F. and Geist, H.J. (2006). Land Use and Land Cover Change: Local Processes and Global Impacts. The IGBP series 1619-2435. Berlin: Springer.

Le Treut, H., Somerville, R., Cubasch, U., Ding, Y., Mauritzen, C., Mokssit, A., Peterson T. and Prather, M. (2007): Historical Overview of Climate Change. In: Climate Change 2007: The Physical Science Basis. Contribution of Working Group I to the Fourth Assessment Report of the Intergovernmental Panel on Climate Change [Solomon, S., D. Qin, M. Manning, Z. Chen, M. Marquis, K.B. Averyt, M. Tignor and H.L. Miller (eds.)]. Cambridge University Press, Cambridge, United Kingdom and New York, NY, USA, 93-127.

Liersch, S. (2003). The Program pcpSTAT, User's Manual, Berlin, August 2003, 5.

Lillesand T.M. and Kiefer R.W. (1999). *Remote Sensing and Image Interpretation (4th edition).* John Wiley and Sons, Inc, New York.

Lin, Y. P., Hong, N. M. and Wung, P. J. (2007). Modeling and Assessing Land-Use and Hydrological Processes to Future Land-Use and Climate Change Scenarios in Watershed.

LUCID. (2004). *A Research Framework to Identify Root Causes of Land-Use Change Leading to Land Degradation and Changing Biodiversity.* Nairobi: LUCID Project Working Paper 48, 2004.

LVBC and WWF-ESARPO, (2010). Assessing Reserve Flows for the Mara River. Nairobi and Kisumu, Kenya.

Majule, A. E., (2010). "Towards sustainable management of natural resources in the Mara river basin in Northeast Tanzania". Institute of Resource Assessment, University of Dar es Salaam, Tanzania.

Malutta, S., and Kobiyama, M. (2011). "SWAT application to analyze the floods in Negrinho River Basin - Santa Catarina." *12th International Conference on Urban Drainage.* Porto Alegre, Brazil: Federal University of Santa Catarina, 2011. 1-8.

Mango, L.M., Melesse, A.M., McClain, M.E., Gann, D. and Setegn, S.G. (2010). "Land use and climate change Impacts on the hydrology of the Upper Mara River Basin, Kenya: Results of a modeling study to support better resource management." *Hydrol Earth Syst Sci*, 2010: 2245-2258.

Mango L.M., Melesse, A.M., McGann, D. and Setegn, S.G., (2011). Land use and climate change impacts on the hydrology of the upper Mara River Basin, Kenya: results of a modeling study to support better resource management. Hydrology and Earth System Sciences 15, 2245-2258. European Geosciences Union.

Mati, B.M., Mutie, S., Home1, P., Mtalo, F., and Gadain, H. (2005). "Land Use Changes in the Transboundary Mara Basin: A Threat to Pristine Wildlife Sanctuaries in East Africa" 8th International River Symposium, Brisbane, Australia, September 6-9, 2005.

Mati, B. M., Mutie, S., Gadain, H., Home, P., and Mtalo, F.: Impacts of land-use/cover changes on the hydrology of the transboundary Mara River, Kenya/Tanzania,

Lake. Reserv. Manage. 13, 169– 177, doi:10.1111/j.1440-1770.2008.00367.x, 2008.

McCarthy, J.J., Canziani, O.F., Leary, N.A., Dokken, D.J. and White, K.S. (Eds.) (2001). *Climate Change 2001: Impacts, Adaptation and Vulnerability.* Contribution of Working Group II to the Third assessment Report of the Intergovernmental Panel on Climate Change. Cambridge University Press, Cambridge, UK and New York, USA.

Melesse, A., McClain, M., Abira, M., Mutayoba, W. and Wang, X. M. (2008). Modeling the Impact of Land-Cover and Rainfall Regime Change Scenarios on the Flow of Mara River, Kenya ASCE-EWRI. World Environmental and Water Resources Congress, (doi 10.1061/40976(316)558).

Michael Case, (2006). Climate Change Impacts in the Amazon: Review of the Scientific Literature. WWF Climate Change Programme. For a living planet.

Michaletz, S. T., Cheng, D. and Kerkhoff, A. J. (2014). "Convergence of terrestrial plant production across global climate gradients." *Nature*, 2014: 39-43.

Miles, L., Grainger, A. and Phillips, O. (2004). The impact of global climate change on tropical biodiversity in Amazonia. Global Ecology and Biogeography 13:553-565.

Miller, K. and Yates, D. (2005). Climate Change and Water Resources: A Primer for Municipal Water Providers, jointly sponsored by AWWA and UCAR, 94.

Ministry of Planning and National Development (2002). Narok District Development Plan (2002-2008). Government Printers. Nairobi, Kenya.

Ministry of Planning and National Development (2002). Bomet District Development Plan (2002-2008). Government Printers. Nairobi, Kenya.

Ministry of Planning and National Development (2002). Nakuru District Development Plan. (2002-2008). Government Printers, Nairobi.

Ministry of Planning and National Development (2002). Trans Mara District Development Plan. (2002-2008). Government Printers, Nairobi.

Mirus, B.B., Loague, K., Cristea, N.C., Burges, S.J., Kampf S.K. (2011). A synthetic hydrologicresponse dataset, J. Hydrol. Process, (2011).

Mitchell, J.F.B., Johns, T.C., Eagles, M., Ingram W.J. and Davis R.A. (1999). Towards the Construction of Climate Change Scenarios. Climate Change, 41, 547-581, Kluwer academic publishers, Printed in the Netherlands.

Moriasi, D.N., Arnold, J.G. Van Liew, M.W., Bingner, R.L., Harnel, R.D. and Veith, T.L. (2007). Model Evaluation Guidelines for Systematic Quantification of Accuracy in Watershed Simulations, Transactions of the ASABE, 2007 American Society of Agricultural and Biological Engineers ISSN 0001-2351, Vol. 50(3): 885-900.

Mutie, S.M., Mati, B., Home, P. and Gadain, H., (2006). Evaluating land use change effects on river flow using geospatial stream flow model in Mara River Basin, Kenya. Centre for Remote Sensing of Land Surfaces, Bonn, 28-30, 2006.

Mutua, F.M. (1986). On the Identification of Optimum Flood Frequency Model. PhD. Thesis, University of Nairobi, 1-52.

Mwania, J. M., (2014). Runoff Modelling of the Mara River using Satellite observed soil moisture and Rainfall. MSc. Thesis. University of Twente.

Ndomba, P., Mtalo, F. and Killingtveit A. (2008). SWAT model application in a data scarce tropical complex catchment in Tanzania, Journal of Physics and Chemistry of the Earth, 33, 626– 632.

Neitsch, S.L., Arnold, J.G. Kiniry, J.R and Williams J.R., (2005). Soil and Water Assessment Tool-Theoretical Documentation-Version 2005, Grassland, Soil and Water research laboratory, agricultural research service and Blackland research Center, Texas agricultural Experiment station, temple, Tex.:USDA-ARS.

Neitsch S. L., Arnold, J. G., Kiniry, J. R. and Williams, J. R., (2011). Soil and Water Assessment Tool Theoretical Documentation Version 2009. Grassland Soil and Water Research Laboratory –Agriculture Research Service Blackland Research Centre – Texas AgriLife Research, 596.

NEMA, (2004). Land use and Environment: State of the Environment Report, Kenya 2004. National Environment Management Authority (NEMA).

Nepal, S., Wolfgang, A. F. and Arun, B. S. (2014). Upstream-downstream linkages of hydrological processes in the Himalayan region. Ecological Processes 2014, 3:19 http://www.ecologicalprocesses.com/content/3/1/19.

Nganga, J. K., (2006). Climate change impacts, vulnerability and adaptation assessment in East Africa, paper presented at the United Nations Framework Convention on Climate Change (UNFCCC) African Regional Workshop on adaptation, Accra, Ghana, 21–23 September 2006.

Nicks, A. D., (1974). Stochastic Generation of the Occurrence, Pattern, and Location of Maximum Amount of Daily Rainfall. In: Proc. Symp. Statistical Hydrology, Aug-Sept. 1971, Tucson, Arizona, U.S. Dept. Agri, Misc. Publ. No. 1275, 154-171.

Noe, S., (2003). "The Dynamics of Land-Use Change and their Impacts on Wildlife Corridor Between Kilimanjaro National Park and Amboseli National Park, Tanzania." *LUCID Working Paper 31*. Nairobi: ILRI, 2003.

Nyakwanda W., Ogallo L. A, and Okoola R. E (2009). The Atlantic-Indian Ocean Dipole and its influence on East African seasonal rainfall, *Journal of Meteorology and Related Sciences, Kenya Meteorological Society, J. Meteorol. Rel., 3 3-12.*

O'Keeffe J., Piet L., Erik de R., van Steveninck W D., Anne van D., and Peter van der S., (2007). "The Environmental Integrity of Water Resources", UNESCO-IHE, Institute for Water Education, Delft, the Netherlands (Includes case study on the Mara Basin).

Okoola, R. E. (1996). Space-Time Characteristics of the ITCZ over Equatorial Eastern Africa during Anomalous Years. *Phd Thesis, Department of Meteorology, University of Nairobi.*

Olang, L. O. and F¨urst, J., (2011). Effects of land cover change on flood peak discharges and runoff volumes: model estimates for the Nyando River Basin, Kenya, Hydrol. Process., 25, 80–89, 2011.

Omeny, P.A., Ogallo, L., Okoola, R., Hendon H. and Wheeler, M. (2008). East African Rainfall Variability Associated with the Madden-Julian Oscillation, *Journal of Kenya Meteorological Society, A Journal in Meteorology and Related Sciences, Volume 2, Numbers 1-2, October 2008,105-114.*

Omondi, P.A., (2010). Teleconnections between Decadal Rainfall Variability and Global Sea Surface Temperatures and Simulations of Future Climate Scenarios Over East Africa. PhD Thesis, University of Nairobi Kenya: 1-23.

Önöz, B., and Bayazit, M. (2003). The power of statistical tests for trend detection. *Turkish J. Eng. Environ. Sci.* 27, 247–251. doi: 10.3906/sag-1205-120

Opere, A.O, (1998). Space-Time characteristics of stream flow in Kenya. PhD Thesis, University of Nairobi Kenya: 1-23.

Oruma, S. K., Kitheka J. and Mwangi M. (2017): The Study of the Effects of Mau Catchment Degradation on the Flow of the Mara River, Kenya. Journal of Environmental and Earth Science. Vol. 7. No 2, 2017. Pages 79-91

Parry M., Rosenzweig, C. and Iglesias A. (1999). *Climate change and world food security: a new assessment.* Global Environmental Change, 9 (1999), S51-S67.

Participatory Ecological Land Use Management Association Kenya (PELUM-K). 2010. *Climate Change Mitigation and Biodiversity Conservation*. PELUM Kenya efforts. Thika, Kenya.

Piao, S., Friedlingstein, P., Ciais, P., N de Noblet-Ducoudre, Labat, D. and Zaehle, S. (2007). "Changes in climate and land use have a larger direct impact than rising CO2 on global river runoff trends." *Proc. Nat. Acad. Sci.*, 2007: 15242-15247.

Ponce, V. M. and Hawkins, R. H. (1996). Runoff curve number: Has it reached maturity? Journal of Hydrologic Engineering 1(1):11-19.

Reyers, B., O'Farrell, P. J., Cowling, R. M., Egoh, B. N., Le Maitre, D. C. and Vlok, J.H.J. (2009). Ecosystem services, land-cover change, and stakeholders: finding a sustainable foothold for a semiarid biodiversity hotspot. Ecology and Society 14(1): 38. [Online] URL: http://www.ecologyandsociety.org/vol14/iss1/art38

Rummukainen, M. (2010). State-of-the-art with regional climate models; Advanced Review, WIREs Climate Change 2010 I, 82-96

Rwigi S. K. (2014). Analysis of Potential Impacts of Climate Change and Deforestation on Surface Water Yields from the Mau Forest Complex Catchments in Kenya. PhD Thesis, University of Nairobi.

Salas J. D., (1993). Analysis and Modelling of Hydrologic Time Series. Handbook of Hydrology, maidment d.r., editor in chief, McGraw-Hill, Inc. 19.1-19.72.

Sang, (2005). Modelling the Impact of Changes in Landuse, Climate and Reservoir Storage on Flooding in the Nyando Basin, Msc Thesis, Jomo Kenyatta University of Science and Technology.

Sang, Y.-F., Wang, Z., and Liu, C. (2014). Comparison of the MK test and EMD method for trend identification in hydrological time series. *J. Hydrol.* 510, 293–298. doi: 10.1016/j.jhydrol.2013.12.039

Schneider, C., Laize, C.L. R., Acreman, M.C. and Flörke, M., (2013). Hydrol. Earth Syst. Sci., 17, 325–339, 2013 www.hydrol-earth-syst-sci.net/17/325/2013/ doi: 10.5194/hess-17-325-2013.

Schuol, J., Abbaspour, R. C., Srinivasan, R. and Yang, H. (2008). Estimation of Fresh Water Availability in the West African Sub-Continent Using the SWAT Hydrologic Model, Journal of hydrology (2008) 352, 30-39.

Serneels, S., Said, M.Y., and Lambin, E. F. (2001). Land cover changes around a major East African wildlife reserve: the Mara Ecosystem (Kenya). Int. J. Remote Sensing, 2001, vol. 22, no. 17, 3397–3420.

Serinaldi, F., Kilsby, C. G., and Lombardo, F. (2018). Untenable nonstationarity: an assessment of the fitness for purpose of trend tests in hydrology. *Adv. Water Resour.* 111, 132–155. doi: 10.1016/j.advwatres.2017.10.015

Setegn, S.G., Srinivasan R. and Dargahi, B. (2008). Hydrological Modelling in Lake Tana Basin, Ethiopia Using SWAT Model. Open Hydrology Journal, 2008, 2, 49-62.

Sexton, A. M., Sadeghi, A. M., Zhang, X., Srinivasan, R. and Shirmohammadi A. (2010). Using Nexrad and Rain Gauge Precipitation Data for Hydrologic Calibration of Swat in a Northeastern Watershed, Transactions of the ASABE Vol. 53(5): 1501-1510 2010, American Society of Agricultural and Biological Engineers ISSN 2151-0032.

Singh, A. (1989). Digital Change Detection Techniques Using Remotely Sensed Data. International Journal of Remote Sensing. Vol. 10, No. 6, p. 989-1003.

Survey of Kenya (SoK). 2003. National Atlas of Kenya, Fifth Edition. Nairobi: SoK.

Tracy, J. B. and Scott, N. M., (2013). Using the Soil and Water Assessment Tool (SWAT) to assess land use impact on water resources in an East African Watershed. Ecosystem Science and Management, University of Wyoming, 1000 East University Ave., Laramie, WY 82071, USA.

Turner, B. L, Skole, D. L. and Moss, R.H., (1993). Relating Land Use and Global Land Cover Change: A proposal for an IGBP-HDP core project. Report form the IGBP-HDP working group on Land Use and Land Cover Change. Joint Publication of the IGBP No. 24 and HDP No, 5. Swedish Academy of Sciences, Stockholm.

Turner, B.L.II., Skole, D., and Sanderson, (1995). Land Use and Land Cover Change. Science/Research Plan (IGBP report No, 35, HDP report No, 7) IGBP of the ICSC and HDP of the ISSS, Stockholm and Geneva.

UNEP, (2005). Africa: Atlas of our changing environment. Nairobi, Kenya.

UNEP, (2009). *Treaties and Ratification*, UNEP Ozone Secretariat, 2009, http://ozone.unep.org (accessed 2 September 2012).

UNEP (2009a). "Kenya: Atlas of Our Changing Environment." Division of Early Warning and Assessment (DEWA), United Nations Environment Programme (UNEP), P.O. Box 30552, Nairobi 00100, Kenya pp 1 - 48.

UNEP, (2009b). Climate Change Science Compendium 2009, edited by McMullen C.P. and Jabbour J.

UNEP/IVM (1998). Handbook on Methods for Climate Change Impact Assessment and Adaptation Strategies; Edited by J.F. Feenstra, I. Burton, J.B. Smith, R.S.J. Tol, Version 2.0, October, 1998, 464.

UNEP, KWS and KFWG, (2005). Maasai Mau Forest Status Report Forest: An Interim Report, November 2005.

UNESCO (2006). Water: a shared responsibility. The UN World Water Development Rept 2. UNESCO, Paris.

UNFCCC, (2005). Compendium on methods and tools to evaluate impacts of, and vulnerability and adaptation to, climate Change, Final draft report; UNFCCC Secretariat, Stratus Consulting Inc. January 2005, 155.

UNFCCC, (2011). United Nations Framework Convention on Climate Change (2011) Outcome of the Ad Hoc Working Group on Long-term Cooperative Action Under the Convention (Draft Decision [-/CP.17]).http://unfccc.int/meetings/ urban_nov_2011/meeting/6245.php.

United Republic of Tanzania. National Bureau of Statistics (NBS) Online (2003). Key Statistics by Regions of the United Republic of Tanzania. Accessed January 10, 2007 at URL http://www.nbs. go.tz/stregions.htm.

United Republic of Tanzania. National Bureau of Statistics (NBS) Online (2013). Key Statistics by Regions of the United Republic of Tanzania. Accessed January 10, 2015 at URL http://www.nbs. go.tz/stregions.htm.

U.S. Geological Survey, (1999). The Landsat Satellite System Link, USGS on the World Wide Web. URL: http://landsat7.usgs.gov/landsat_sat.html. University of Ilorin, Department of Geography. (1981) Ilorin Atlas; Ilorin University press

Veith, Van T.L. and Ghebremichael, L.T, (2009): How To: Applying and Interpreting the SWAT Auto Calibration Tools. In: Proceedings of the Soil and Water Assessment Tool International Conference, August 5-7, 2009, Boulder, Colorado. 26-33.

Vitousek, P. M., Mooney, H. A., Lubechenco, J. and Melillo, J. M. **(**1997). Human domination of earth's ecosystems. Science 277:494–499.

Wagesho, N. (2014). "Catchment dynamics and its impacts on runoff generation: Coupling watershed modelling and statistical analysis to detect catchment responses." *Int. J. Water Res. Environ. Eng* 6, no. 2 (February 2014): 73-87.

Wang, X., Yu, S., Huang, G. H. (2004). Land Allocation Based on Integrated GIS Optimization Modeling At a Watershed Level. Landscape Urban Plan. 66, 61–74.

Wang, S., Zuo, H., Yin, Y., Hu, C., Yin, J., Ma, X., et al. (2019). Interpreting rainfall anomalies using rainfall's nonnegative nature. *Geophys. Res. Lett.* 46, 426–434. doi: 10.1029/2018GL081190

Wasserstein, R. L., Schirm, A. L., and Lazar, N. A. (2019). Moving to a world beyond "p <0.05". *Am. Statist.* 73, 1–19. doi: 10.1080/00031305.2019.1583913

WRA – Water Resource Authority, Kenya (2008). Catchment Management Strategy Lake Victoria South Catchment Area, Water Resource Management Authority, Nairobi, Kenya, 2008.

Webster, P.J., Moore, A.M., Loschnigg, J.P., Lebden, R.R., (1999). Coupled Ocean-Atmospheric dynamics in the Indian Ocean during 1997-98. Nature 401, 356-360.

Wilby, R. and Miller, K. (2009).Technical Paper (3): Climate Models and Scenarios. Water Research foundation and sponsors (UKWIR, WERF and NCAR), 2.

Wilk, J., Anderson, L. and Plermkamon, V. (2001). "Hydrological impacts of forest conversion to agriculture in a large river basin in northeast Thailand," Hydrological Processes, vol. 15, no. 14, pp. 2729–2748, 2001.

Wilson, S., Hassel, D., Hein, D., Jones R. and Taylor, R. (2009). Installing and using the Hadley Centre regional climate modelling system, PRECIS; version 1.8.2, precis.metoffice.com, September 11, 2009, 167.

Wilson, C. O. and Weng, Q., (2011). Simulating the impacts of future land use and climate changes on surface water quality in the Des Plaines River watershed, Chicago Metropolitan Statistical Area, Illinois. Science of the Total Environment, 409(20), 4387-4405.

Winchell M., R. Srinivasan, M. Di Luzio, J. Arnold (2010). ArcSWAT Interface for SWAT 2009 User's Guide, Grassland Research and Extension Centre, Texas AgriLife research, 720 East Blackland Road-Temple, Texas 76502 490.

Winchell M., Srinivasan R., Di~Luzio M., and Arnold J. G. (2013). *Arc SWAT Interface for SWAT 2009: User's Guide.* Texas Agricultural Experiment Station (Texas) and USDA Agricultural Research Service (Texas), Temple, Texas.

WMO, (2009). Guide to Hydrological Practices, Volume II Management of Water Resources and Application of Hydrological Practices. WMO – No. 168 Sixth Edition 2009.

World Resources Institute, (1996). *World Resources: A Guide to Global Environment, 1996-1997.* World Resources Institute, United Nations Environment Programme and the World Bank, Oxford University Press, Oxford, UK.

World Wide Fund for Nature, (2002). *The Impact of Climate Change.* World Wide Fund for Nature Climate Change Programme. Washington DC, USA.

WREM International Inc., (2008). Mara River Basin Monograph, Mara River Basin Trans-boundary Integrated Water Resources Management and Development Project, Final Technical Report, Atlanta, December 2008, 446p.

Yang X. L., Ren L. L. and Jiao D. L., (2013). Estimation of daily actual evapotranspiration from ETM+ and MODIS data over the headwater of West Liao River Basin in semi-arid region, China. Journal of Hydrologic Engineering, 18(11): 1530–1538.

Yu, X., Lamačová, A., Duffy, C., Krám, P., Hruška, J., White, T., Bhatt, G., 2014. Modeling long-term water yield effects of forest management in a Norway spruce forest. Hydrol. Sci. J. http://dx.doi.org/10.1080/02626667.2014.897406

Yue, S., Pilon, P., Phinney, B., and Cavadias, G. (2002b). The influence of autocorrelation on the ability to detect trend in hydrological series. *Hydrol; Process.* 16, 1807–1829. doi: 10.1002/hyp.1095

Zang, C. F., Liu, J., van der Velde, M., and Kraxner, F.: Assessment of spatial and temporal patterns of green and blue water flows under natural conditions in inland river basins in Northwest China, Hydrol. Earth Syst. Sci., 16, 2859–2870, doi: 10.5194/hess-162859-2012, 2012.

Zeng, N., Neelin J. D., Lau K. M. and Tucker C. J. (1999). Enhancement of Interdecadal Climate Variability in the Sahel by Vegetation Interaction. Science 286:1537–40.

Zhang, A., Zhang, C., Fu, G., Wang, B., Bao, Z. and Zheng, H. (2012). Assessments of impacts of climate change and human activities on runoff with SWAT for the Huifa River Basin, Northeast China. *Water Resources Management*, *26*(8), 2199-2217.

Zheng, H., Chen, F., Ouyang, Z., Tu, N., Xu, Weihua, Wang, X., Miao, H., Li, X., Tian, Y. (2008). Impacts of Reforestation Approaches on Run-Off Control in The Hilly Red Soil Region of Southern China. Journal of Hydrology 356, 174-184.

Zhuo, Wu, Dai Erfu, Quansheng Ge, XI Weimin, and Xiaofan Wang (2017). "Modelling the integrated effects of land use and climate change scenarios on forest ecosystem aboveground biomass, a case study in Taihe County of China." *Geographical Sciences*, 2017: 205-222.

APPENDICES

APPENDIX I: RAINFALL DATA FROM WRA AND KMS.

(a) Bomet Water Supply

TSID 1200000883 - 9035265 BOMET WATER SUPPLY - Rainfall [mm]

Year	Jan	Feb	Mar	Apr	May	Jun	Jul	Aug	Sep	Oct	Nov	Dec	Mean	Min	Max	Sum
1965							57.2	0	48.7	107.725	169.825	101.75	80.867	0	169.825	485.2
1966	44.287	156.087	194.85	238.375	50.3	34.8	61.987	173.738	128.575	71.9	104.9	20.725	106.71	20.725	238.375	1280.525
1967	9.375	48.3	117	222.075	244.563	92.612	45.25	29	56.638	85.162	151.887	92.613	99.54	9.375	244.563	1194.475
1968	33.95	161.762	228.188	343.775	125.025	78.813	55.825	107.063	41.7	121.9	167.7	82.55	129.021	33.95	343.775	1548.25
1969	154.262	167.837	147.35	101.463	52.337	108.8	54.1	44.85	139.65	45.275	144.325	88.15	104.033	44.85	167.837	1248.4
1970	202.45	135.175	285.55	275.575	137.863	132.538	46	77.4	88.325	66.375	45.675	99.662	132.716	45.675	285.55	1592.588
1971	69.563	14	146.887	266.862	150.85	54.075	98.425	195.525	44.162	78.112	24.737	115.9	104.925	14	266.862	1259.1
1972	139.962	0											69.981	0	139.962	139.962
1973	148.6	145.475	4.125	170.5	164.438	74.863	0	70.9	150.6	59.2	156.9	63.35	100.746	0	170.5	1208.95
1974	47.05	95.9	0	271.85	68.863	1.088	272.3	50.3	68.988	79.012	31.8	36.8	85.329	0	272.3	1023.95
1975	78.55	30.85	191.512	328.462	149.725	56.3	90.5	46.6	92.2	124.8	25.9	57.2	106.05	25.9	328.462	1272.6
1976	76.6	48	112.6	166.5	94.912	74.887	95.113	126.325	103.963	131.9	0	140.025	97.569	0	166.5	1170.825
1977	168.8	73.675	106.35	269.25	167.075	76.525	139.7	87.3	18.7	81.313	240.688	125.05	129.535	18.7	269.25	1554.425
1978	91.75	186.738	305.962	197.213	110.887	74.863	26.837	0	105	47	112.762	7.237	105.521	0	305.962	1266.25
1979	89.425	169.275	130.438	277.275	179.087	107.5	48	69.925	4.275	28.3	106.512	167.55	114.797	4.275	277.275	1377.562
1980	95.813	33.325	143.4	200.4	190.413	125.15	35.862	25.763	59.713	103.488	153.938	77.775	103.753	25.763	200.4	1245.038
1981	76.5	40	211.6	288.188	223.913	124.263	125.137	73.8	129.213	67.787	70.625	1.275	119.358	1.275	288.188	1432.3
1982	54.313	58.088	28.9	229	125.7	65.9	47.9	69.963	143.137	154.313	302.638	226.45	125.525	28.9	302.638	1506.3
1983	34.838	0.262		162.2	50.2	104.5	31	78.6	122.3	160.613	92.287		83.68	0.262	162.2	836.8
1984	70.912	44.588	44.25	289.45	15.7	29.1	89.8	117.6	51.487	111.113	170.3	105.4	94.975	15.7	289.45	1139.7
1985	46.237	113.45	252.363	237.25	165.238	159.663	63.8	33.5	52.1	99.025	173.575	229.338	135.461	33.5	252.363	1625.538
1986	59.862	70.6	113.3	199.775	92.825	60.6	78.7	75.262	29.938	85.1	121.5	144.7	94.347	29.938	199.775	1132.162
1987	77.9	72.7	146.8	204.5	176.425	186.788	28.487	65.8	90.3	25.6	174.5	0	104.15	0	204.5	1249.8
1988	103.45	44.05	202.4	335.6	107	54.6	61.6	101.5	62.9	19.8	104.2	79	106.342	19.8	335.6	1276.1
1989	56.1	194	136.5	336.6	149.9	52.1	74.3	82	102.1	192.438	112.463	158	137.208	52.1	336.6	1646.5
1990	67.1	91.7	250	343.3	188.875	33.5	0.525	140.063	53.838	146.1	75.912	69.688	121.717	0.525	343.3	1460.6
1991	127.425	49.775	115.2	191.288	90.412	268.837	31.075	143.788	73.275	114.625	53	131.3	115.833	31.075	268.837	1390
1992	16.3	91.737	42.862	42.3	199.5	170.688	93.012	23.775	55.713	126.412	93.75	110.45	88.875	16.3	199.5	1066.5
1993	166	225.9	152.8	7	0							240	131.95	0	240	791.7
1994	25	137.9	365.1	244.9	206.8	186.15	41.15	93.9	0	55.538	312.763	65.9	144.592	0	365.1	1735.1
1995	75.6	81.4	279.788	269.813	210.125	106.25	61.525	118.4	128.6	148.4	90.5	109.9	140.025	61.525	279.788	1680.3
1996	183.225	233.913	200.137	213.525	134.8	104.8	0						152.914	0	233.913	1070.4
1997	0	0	0	0	0	0	0	0	0	0	0	0	0	0	0	0
1998	0	0	0	0	0	0	0	0	0	0	0	0	0	0	0	0
1999	0	0	0	0	0	0	0	0	0	0	0	0	0	0	0	0
2000	0	0	0	0	0	0	0	0	0	0	0	0	0	0	0	0
2001	0	0	0	0	0	0	0	0	0	0	0	0	0	0	0	0
2002	0	0	0	0	0	0	0	0	0	0	0	0	0	0	0	0
2003	0	0	0	0	0	0	0	0	0	0	0	0	0	0	0	0
2004	0	0	0	0	0	0	0	0	0	0	0	0	0	0	0	0
2005	0	0	0	0	0	0	0	0	0	0	0	0	0	0	0	0
2006	0	0	0	0	0	34.1	22.9	55.2	60.025	35.875	347.5	401.2	79.733	0	401.2	956.8
2007	205.512	148.137	176.25	145.2	190.7	68.3							155.683	68.3	205.512	934.1
2008																
2009																
2010																
2011																
2012																
2013																
2014										0	142.512	157.887	100.133	0	157.887	300.4
2015	25	32	31.3	215.225	146.575	156	44.05	49.412	70.637	222.563	524.438	179	141.35	25	524.438	1696.2
2016	315.4	47.3	77.275	204.325	222.6	100.2	24.8	29.6	102.8	77.4	98.7	0	108.367	0	315.4	1300.4
2017	13.488	123.412	61.5	127.125	180.975	65.237	83.963	70.7	52.3	201.8	97.037	34.112	92.637	13.488	201.8	1111.65
2018	75.75												75.75	75.75	75.75	75.75
Mean	72.312	74.829	116.338	173.094	108.286	74.986	49.554	60.18	60.282	76.185	111.529	86.51	88.674			
Min	0	0	0	0	0	0	0	0	0	0	0	0		0		
Max	315.4	233.913	365.1	343.775	244.563	268.837	272.3	195.525	150.6	222.563	524.438	401.2			524.438	
Sum	3326.35	3367.312	5002.537	7616.138	4764.6	3224.388	2130.825	2527.55	2531.85	3275.963	4795.75	3719.938				46283.2

(b) Narok Keekorok Game Lodge

TSID 1200000892 - 9135013 NAROK KEEKOROK GAME LODGE - Rainfall [mm]

Year	Jan	Feb	Mar	Apr	May	Jun	Jul	Aug	Sep	Oct	Nov	Dec	Mean	Min	Max	Sum
1965	85.6	66	0	110.9	145.212	64.188	0	21.9	0	55.675	9.525		50.818	0	145.212	559
1966	72.35	68.688	185.662	164.8	36.1	40.4	32.7	30.4	190.5	30	45.4	26.7	76.975	26.7	190.5	923.7
1967	42.9	54.3	85.1	231.475	143.125	73.75	51.25	18.3	9.363	61.138	71.8	158.5	83.417	9.363	231.475	1001
1968	0	38.375	2.925										13.767	0	38.375	41.3
1969									29	20.788	83.412	117.575	62.694	20.788	117.575	250.775
1970	223.4	89.325	145.863	70.137	119.3	55.9	24.987	53.375	71.238	47.813	68.787	79.588	87.476	24.987	223.4	1049.712
1971	76.612	54.2	37.5	196.375	127.725	39.9	73	242.3	25.4	39.8	15.9	150.9	89.968	15.9	242.3	1079.613
1972	60.5	129.7	63.3	22.637	49.087	141.975	36.3	75.9	65.6	104.6	123.9	84.938	79.87	22.637	141.975	958.437
1973	213.463	55.4	26.2	67.6	55.55	130.35	6.2	16.6	84.2	48.9	46.4	119.15	72.501	6.2	213.463	870.013
1974	70.35	99.925	130.962	243.512	58.313	112.588	189.2	33.4	122.5	19.2	42.4	50.6	97.746	19.2	243.512	1172.95
1975	64.5	41.5	127.6	107.1	100.9	105.6	143.3	57.1	147.613	47.787	1.2	104.5	87.392	1.2	147.613	1048.7
1976	67.2	85.912	58.388	118.9	86.575	138.025	79.9	69.425	59.575	35.2	140.725	85.35	85.431	35.2	140.725	1025.175
1977	142.55	57.075	59.85	246.712	131.738	78	83.9	50.75	27.85	29.4	141.6	74.125	93.629	27.85	246.712	1123.55
1978	90.975	191.65	195.35	93.225	46.275	50.9	12.2	89.637	78.762	27.2	21.4	288.9	98.873	12.2	288.9	1186.475
1979	119.275	117.525	120	129	64.9	39.8	49.2	47.3	14.9	1.8	46.912	85.188	69.65	1.8	129	835.8
1980	105.625	84.275	143.6	177.1	215.85	83.05	44.9	36.2	29.9	78.5	91.8	115.1	100.492	29.9	215.85	1205.9
1981	24.5	95	255.063	211.538	80.338	39.825	78.238	22.7	31.388	19.413	36.9	79.675	81.215	19.413	255.063	974.575
1982	51.175	74.85	66.387	115.112	32.088	44.513	32.487	51.013	44.8	22.6	304.875	124.025	80.327	22.6	304.875	963.925
1983	78.3	88.2	53.75	116.35	12.1	88.1	56.5	79.3	92.625	61.575	132.4	99.4	79.883	12.1	132.4	958.6
1984	56.9	40.563	41.638	152	18	21	37.3	96.325	23.95	47.825	87.2	133.5	63.017	18	152	756.2
1985	11.962	131.45	89.438	149.25	78.7	46.2	37.013	12.088	61.5	35.9	143.4	34.8	69.308	11.962	149.25	831.7
1986	96.2	105.3	86.575	194.425	39.2	63	40.3	22.7	14.8	46.7	61.5	188.4	79.925	14.8	194.425	959.1
1987	121.8	65.3	160	84.275	91.575	132.65	47.075	27.825	63.5	23.7	122.7	20.9	80.108	20.9	160	961.3
1988	144.7	16.4	194.2	260.2	108	15.4	0	99.2	67.838	82.963	63.6	106.7	96.6	0	260.2	1159.2
1989	138.1	144.1	124.7	119.6	175.1	75.2	53.15	62.85	52.1	32.6	54.8	244.875	106.431	32.6	244.875	1277.175
1990	119.425	130.625	230.188	229.287	149.025	42.775	23.1	108.412	32.087	41.5	100.1	82.3	107.402	23.1	230.188	1288.825
1991	39.138	33.263	68.4	107.1	210.7	110.137	10.262	16.987	7.712	212.863	41.438	50.2	75.683	7.712	212.863	908.2
1992		67.25	143.875	160.9	80.675	133.9	52.8	12.1	61.2	59.5	50	47.2	79.036	12.1	160.9	869.4
1993	97.6	82.775	36.225	51.8	74.213	105.188	10.7	35.1	12.6	16.7	20.85	25.95	47.475	10.7	105.188	569.7
1994	92.4	15.375	174.025	98.8	79.1	51.7	29.1	25.3	11.4	37.7	188.313	54.725	71.495	11.4	188.313	857.937
1995	60.263	128.1	37.9	109.2	159.7	88.6	43.8	61.7	50.162	48.237	47.2	97.625	77.707	37.9	159.7	932.487
1996	84.275	132	106.15	46.75	40.662	71.938		108.887	144.213	102.525	94.075	108.5	94.543	40.662	144.213	1039.975
1997	58.925	5.475	47.4	239.8	100.4	63.5	43.6	0					69.887	0	239.8	559.1
1998																
1999																
2000																
2001																
2002																
2003																
2004																
2005																
2006																
2007																
2008																
2009																
2010																
2011																
2012																
2013																
2014																
2015								0	19	20.7	255.8	134.8	86.06	0	255.8	430.3
2016	9.9	50.6	77.45	218.363	168.988	58.7	0	0			2.938	21.263	60.82	0	218.363	608.2
2017	0	30.2	22.7	0	6.8	57.1	0	52.237	7.063	81	36.42	1.1	24.552	0	81	294.62
2018	82.1												82.1	82.1	82.1	82.1
Mean	82.44	78.549	99.952	140.734	93.516	74.662	44.452	51.097	53.162	49.752	82.226	96.88	78.952			
Min	0	5.475	0	0	6.8	15.4	0	0	0	1.8	1.2	1.1		0		
Max	223.4	191.65	255.063	260.2	215.85	141.975	189.2	242.3	190.5	212.863	304.875	288.9			304.875	
Sum	2802.962	2670.675	3398.362	4644.225	3086.012	2463.85	1422.463	1737.312	1754.338	1641.8	2795.67	3197.05				31614.72

(c) Narosura Chief's Camp

TSID 200000670 - 9135021 NAROSURA CHIEF'S CAMP - Rainfall [mm]

Year	Jan	Feb	Mar	Apr	May	Jun	Jul	Aug	Sep	Oct	Nov	Dec	Mean	Min	Max	Sum
1998							22	25.2	21.8	5.8	70.9	2.9	24.767	2.9	70.9	148.6
1999	8.5	0	157.4	22.8	32.6	0	0	25.1	69.3	108.3	26.3	10.4	38.392	0	157.4	460.7
2000	0	4.5	9	27.4	19.6	0	0	14.6	0	14.6	135.2	24	20.742	0	135.2	248.9
2001	0												0	0	0	0
2002	27.5	32.7	98.6	141.688	206.512	0	0	0	17	0	40	0	47	0	206.512	564
2003	0	103.8	32.438	146.063	148.2	7.5	0	15.2	0	9.3	0	11	39.458	0	148.2	473.5
2004	0												0	0	0	0
2005	85.9	13	56.6	107.8	144.4	9	11.8	1.2	0	3.6	8.9	0	36.85	0	144.4	442.2
2006	32.2	47.975	120.925	210.5	43.5	0	7	12.2	19.2	14.238	204.863	212	77.05	0	212	924.6
2007	23.313	85.55	38.438	159.962	52.188	11.65	17	12.4	9.6	11.5	24.2	71.3	43.092	9.6	159.962	517.1
2008	56.8	100.8	197.4	94.6	1.8	0	9.4	5.3	15.4	49.8	92.4	0	51.975	0	197.4	623.7
2009	10.738	13.762	0	93.4	123.7	2.3	0	0	6.1	37.737	41.963	79.7	34.117	0	123.7	409.4
2010	98.4	57.362	975.513	169.125	322.875	671.125	96	215.625	120.25	136.375	59.75	12	244.533	12	975.513	2934.4
2011	44	99	171.125	16.625	38.75	25.2	19.1	49.9	46.2	25.8	237.5	58.8	69.333	16.625	237.5	832
2012	36.7	67.775	71.725	170.2	109.8	19.5	18	41.5	97.5	57.7	0	0	57.533	0	170.2	690.4
2013	0	0	72.7	189.5	0	0	7.1	5.6	0	7.6			28.25	0	189.5	282.5
2014			87	48.2	30	9.9	16.5	9.9	18.5	30.9	7.7	72.6	33.12	7.7	87	331.2
2015	28	20.2	15.4	143	33.1	42.9	34.7	4.4	0	55.8	258.9	0	53.033	0	258.9	636.4
2016	0	0	0	0	0	0	0	0	0	0	54.5		4.955	0	54.5	54.5
Mean	26.591	43.095	131.516	108.804	81.689	49.942	15.212	25.772	25.932	33.474	78.942	36.98	54.829			
Min	0	0	0	0	0	0	0	0	0	0	0	0		0		
Max	98.4	103.8	975.513	210.5	322.875	671.125	96	215.625	120.25	136.375	258.9	212			975.513	
Sum	452.05	646.425	2104.262	1740.862	1307.025	799.075	258.6	438.125	440.85	569.05	1263.075	554.7				10574.1

APPENDIX II: OBSERVED RIVER FLOW DATA

(a) Amara Gauging Station

Year	Jan	Feb	Mar	April	May	Jun	July	Aug	Sept	Oct	Nov	Dec	Total	Average
1983	6.78	13.84	13.04	572.47	343.89	167.94	108.11	220.1	310.76	79.32	56.22	51.05	1943.5	161.96
1984	10.3	14.57	11.24	397.57	227.2	134.07	106.54	209.8	285.25	94.85	54.9	52.7	1598.97	133.2492
1985	3.26	13.11	14.84	747.38	460.57	201.8	109.67	230.39	336.27	63.79	57.54	49.4	2288.02	190.6683
1986	17.34	13.11	7.64	47.75	227.2	66.34	103.41	189.21	234.23	125.9	52.25	55.99	1140.37	95.03083
1987	30.57	15.98	63.04	108.25	227.7	363.83	119.2	73.08	74.78	44.31	88.56	72.18	1281.48	106.79
1988	40	20.1	28.82	263.42	178.48	202.91	224.46	428.14	344.69	382.09	71.43	46.14	2230.68	185.89
1989	227.99	23.79	28.26	251.69	427.97	100.4	152.67	422.4	383.18	455.1	150.32	149.14	2772.91	231.0758
1990	415.98	78.66	200.56	1251.86	677.46	160.31	99.31	271.83	175	78.74	81.43	35.41	3526.55	293.8792
1991	24.75	20.19	26.65	84.05	98.14	462.48	147.7	369.13	181.09	67.83	37.13	20.94	1540.08	128.34
1992	37.94	9.64	7.96	62.98	159.91	227.3	398.49	524.18	587.46	250.88	133.46	64.94	2465.14	205.4283
1993	121.95	324.63	79.09	49.55	170.78	224.15	206.61	202.52	184.67	71.21	50.89	39.68	1725.73	143.8108
1994	30.18	16.18	29.15	36.11	181.64	383.2	228.73	374.47	369.75	65.1	95.48	111.88	1921.87	160.1558
1995	10.19	63.37	210.49	14.43	309.54	303.68	217.67	102.8	141.09	170.52	111.51	100.66	1755.95	146.3292
1996	18.35	38.19	108.35	115.03	437.45	201.21	108.84	238.64	185.59	132.55	58.32	89.43	1731.94	144.3292
1997	26.51	13	6.2	215.62	328.3	98.74	264.85	197.49	132.12	66.76	250.22	1493.17	3092.98	257.7483
1998	1332.4	26.29	90.97	263.42	546.59	432.86	222.33	156.34	165.7	64.11	156.3	810.48	4267.79	355.6492
1999	684.48	16.18	49.67	135.36	282.1	69.65	77.65	124.53	135.58	61.45	62.37	127.79	1826.81	152.2342
2000	36.55	6.06	8.36	7.3	17.6	26.56	54.48	92.72	105.45	196.36	153.19	126.79	831.42	69.285
2001	97.7	9.73	51.43	56.5	375.66	42.05	129.03	329.32	74.18	308.22	454.13	27.01	1954.96	162.9133
2002	243.72	38.91	94.49	105.7	733.71	57.53	64.42	142.49	138.86	26.89	55.85	102.5	1805.07	150.4225
2003	1117.6	18.76	57.35	111.17	2537.65	881.26	392.5	366.09	414.81	178.16	51.55	24.37	6151.27	512.6058
2004	16.93	13.18	8.35	147.18	604.14	58.55	48.61	125.33	116.72	133.43	44.45	24.55	1341.42	111.785
2005	17.13	15.25	6.77	37.82	86.07	84.54	105.85	422.28	438.4	151.13	67	10.41	1442.65	120.2208
2006	4.28	31.32	308.66	964.41	693.05	265.85	521.26	608.51	139.17	55.59	56.48	582.71	4231.29	352.6075
2007	671.19	16.39	63.33	150.99	155.33	447.15	257.25	794.73	524.87	687.45	45.96	316.85	4131.49	344.2908
2008	4.68	1.46	10.31	38.74	75.55	39.45	73.4	210.43	252.98	221.1	184.35	50.99	1163.44	96.95333
2009	9.87	55.62	250.49	205.43	162.95	51.49	18.78	25.77	31.25	41.07	33.7	96.48	982.9	81.90833
2010	278.16	109.77	490.66	372.12	591.38	64.3	169.65	256.3	566.2	399.26	206.81	86.24	3590.85	299.2375
2011	14.89	82.7	17.35	18.46	64.76	199.17	207.07	461.15	607.96	146.95	176.22	60.27	2056.95	171.4125
2012	52.69	96.23	254.01	542.05	830.1	268.99	315.09	316.64	535.03	131.96	145.63	34.3	3522.72	293.56
2013	90.48	75.21	138.59	515.1	891.6	186.56	200.14	284.41	309.53	242.21	145.34	202.6	3281.77	273.4808
2014	153.96	54.19	23.18	131.71	860.85	227.78	228.86	229.94	268.57	376.88	158.32	99.39	2813.62	234.4692
2015	350.69	107.53	27.35	323.4	876.23	207.17	214.5	175.47	227.61	46.14	1088.95	1108.93	4753.96	396.1642
2016	547.42	160.87	31.51	227.56	868.54	217.47	228.86	202.71	248.09	211.51	623.64	604.16	4172.32	347.695

(b) Nyangores Gauging Station

					NYANGORES FLOW									
Year	Jan	Feb	Mar	April	May	June	July	Aug	Sept	Oct	Nov	Dec	Total	Average
1983	107.78	12.5	64.75	897.715	542.64	236.97	8.59	336.4	567.23	292.7	177.9	1.9	3247.075	270.5896
1984	92.75	2.47	27.49	28.14	457.18	277.315	97.45	7.48	162.81	146.67	73.4	157.2	1530.355	127.5296
1985	45.03	22.53	102.01	1767.29	722.41	435.43	186.31	311.86	327.5	147.54	104.72	142.72	4315.35	359.6125
1986	146.38	180.36	18.58	62.13	191.95	84.4	93	132.11	194.01	156.74	58.81	94.06	1412.53	117.7108
1987	39.56	110.96	34.47	211.78	492.95	1237.16	214.95	86.36	98.64	58.94	125.04	1.47	2712.28	226.0233
1988	45.84	32.23	34.52	1106.52	1384.98	369.24	303.26	322.08	441.6	823.31	112.47	53.11	5029.16	419.0967
1989	34.17	27.54	28.01	318.95	551.64	176.24	193.1	721.62	876.9	505.94	230.76	613.95	4278.82	356.5683
1990	640.31	78.43	489.54	3307.16	1242.99	297.81	166.26	300	223.46	96	86.53	63.11	6991.6	582.6333
1991	147.78	36.08	30.52	139.47	241.67	483.19	248.28	260.99	212.46	131.34	50.22	84.89	2066.89	172.2408
1992	135.14	78.615	22.09	118.01	304.05	430.03	606.41	561.86	822.09	486.81	180.44	106.66	3852.205	321.0171
1993	122.5	802.47	161.42	39.18	168.49	456.61	427.345	411.425	517.275	309.075	115.33	95.775	3626.895	302.2413
1994	128.82	440.5425	91.755	78.595	236.27	341.3625	343.6675	486.6425	496.34	147.9525	147.885	101.2175	3041.05	253.4208
1995	90.7	108.6438	126.5875	117.395	249.06	226.115	259.99	449.0338	475.405	123.925	132.9125	2.04	2361.808	196.8173
1996	52.58	64.79	58.27	219.17	261.85	242.48	208.5	183.65	795.81	171.98	117.94	131.27	2508.29	209.0242
1997	48.82	15.62	10.65	186.51	648.38	209.75	311.48	246.19	155	75.87	923.66	1663.86	4495.79	374.6492
1998	2314.97	293.26	160.93	341.59	1103.99	605.45	952.28	309.51	275.85	430.05	241.28	82.91	7112.07	592.6725
1999	53.09	24.62	58.11	250.77	438.85	328.15	536.07	18.9	489.72	258.1	117.75	90.63	2664.76	222.0633
2000	49.92	34.14	28.68	400.4	46.57	50.85	119.85	135.97	169.16	177.96	219.16	184.08	1616.74	134.7283
2001	584.91	295.02	110.57	550.02	1022.2	502.58	530.39	412.52	220.58	191.41	827.29	198.6	5446.09	453.8408
2002	162.59	66.94	106.69	209.32	1502.83	148.88	130.61	347.42	256.5	101.42	187.68	36.49	3257.37	271.4475
2003	527.81	77.47	48.09	410.24	1326.86	616.32	253.78	659.37	691.29	239.15	111.11	53.98	5015.47	417.9558
2004	313	56.85	7.7	327.02	1150.88	140.86	161.63	223.99	180.88	216.09	165.61	91.84	3036.35	253.0292
2005	98.2	36.22	46.08	134.35	475.66	412.17	210.78	601.28	785.86	239.83	139.06	66.75	3246.24	270.52
2006	43.08	38.17	298.22	591.43	805.34	173.69	154.78	255.25	237.24	151.45	301.97	1001.9	4052.52	337.71
2007	14	528.35	158.16	354.85	472.77	656.69	314.83	908.76	722.93	294.99	189.41	75.69	4691.43	390.9525
2008	49.68	34.81	46.2	169.57	230.98	282.24	210.27	11.56	354.23	406.62	368.83	156.17	2321.16	193.43
2009	68.69	74.11	41.67	89.38	217.38	126.61	3.98	121.42	124.83	137.48	131.68	159.98	1297.21	108.1008
2010	572.9	250.44	405.5	700.29	798.38	391.06	253.58	330.32	605.23	831.39	343.76	151.38	5634.23	469.5192
2011	92.39	80.3	113.12	106.98	182.68	332.71	343.44	342.36	1266.49	250.48	506.71	1652.91	5270.57	439.2142
2012	357.6	98.11	128.9	79.77	534.36	479.34	719.94	435.25	949.76	395.65	859.36	248.47	5286.51	440.5425
2013	341.12	111.49	232.63	2072.05	2228.84	169.05	207.51	438.22	454.06	557.45	162.56	132.73	7107.71	592.3092
2014	96.43	67.97	77.53	88.95	74.48	260.83	151.16	253.23	290.28	343.66	276.73	199.41	2180.66	181.7217
2015	108.82	55.52	38.59	67.79	701.87	1066.46	184.21	130.73	211.22	130.42	1780.5	1745.25	6221.38	518.4483
2016	591.34	166.76	73.97	97.31	74.48	663.645	167.685	191.98	250.75	237.04	1028.615	972.33	4515.91	376.3254

(c) Mara Gauging Station

						MARA FLOW							
Year	Jan	Feb	Mar	Apr	May	June	July	Aug	Sept	Oct	Nov	Dec	Total	Average
1983	107.7764	12.50195	64.7498	0	589.7968	347.6723	8.5887	336.3954	567.2258	292.6973	177.7764	1.9026	2507.084	208.9236
1984	92.7457	2.4735	27.4869	28.1428	457.181	259.915	97.44705	7.4844	162.8079	146.6689	73.4464	157.1986	1512.998	126.0832
1985	45.0327	22.5304	102.0127	1767.2854	722.4127	435.4297	186.3054	311.8577	327.4956	147.543	104.7223	142.7207	2548.063	231.6421
1986	147.3793	180.3601	18.5761	62.1291	191.9492	84.4002	92.9895	132.1123	194.0106	156.7429	58.8123	94.0554	1413.517	117.7931
1987	39.5641	110.958	34.4651	211.7832	492.9487	1237.156	214.9538	86.3587	98.6421	58.9437	125.0399	1.4564	2712.27	226.0225
1988	45.8438	32.2306	34.5213	1106.524	1384.976	369.2359	303.2557	322.0809	441.5981	823.3058	112.4693	53.1089	5029.15	419.0959
1989	34.1669	27.5359	28.0143	318.0143	551.6352	176.2443	193.1007	721.6193	876.9039	505.9408	230.7574	613.9493	4277.882	356.4902
1990	640.3141	78.4311	489.5404	3307.159	1242.994	297.8051	166.2551	291.9975	223.4632	95.9983	86.5301	63.108	6983.596	581.9663
1991	147.7769	36.0788	30.5182	139.4743	241.6674	483.1992	248.2805	260.9974	212.4624	2.4735	48.8288	84.88175	1936.639	161.3866
1992	135.1374	0.5126	22.0951	118.0106	304.0458	430.0312	606.4106	561.8614	822.0934	486.8046	180.4382	106.6555	3774.096	314.508
1993	122.4978	802.4658	161.4187	39.1794	168.4868	456.6152	427.3456	411.4294	517.2779	244.6391	114.6335	95.76863	3561.758	296.8132
1994	86.59953	401.4892	91.7569	78.595	236.2663	443.3232	516.8781	486.6454	669.6857	365.7218	147.5359	48.90326	3573.4	297.7834
1995	50.70125	233.1378	75.01565	148.881	202.3766	342.9026	362.6885	335.1474	732.7495	268.8517	162.7394	2.0379	2917.229	243.1024
1996	52.5776	64.7863	58.2744	219.1669	261.8463	242.482	208.499	183.6493	795.8133	171.9816	177.9429	131.2692	2568.289	214.0241
1997	48.8249	15.6227	10.6541	186.5138	648.3843	209.7515	311.4846	246.1915	155.0006	75.8725	923.6471	1663.859	4495.807	374.6506
1998	1495.91	23.45	90.97	263.42	546.59	432.86	222.33	156.34	175.67	65.99	156.3	810.48	4440.31	370.0258
1999	684.48	45.541	49.67	135.36	282.1	69.65	77.65	124.53	135.58	61.45	62.37	145.9	1874.281	156.1901
2000	36.55	6.06	8.36	95.93	75.55	1230	154.9	92.72	105.45	196.36	153.19	126.79	2281.86	190.155
2001	97.7	134.98	127.908	56.5	375.66	105.97	129.03	329.32	205.45	308.22	454.13	27.01	2351.878	195.9898
2002	243.72	38.91	125.23	105.7	733.71	57.53	164.9087	142.49	138.86	26.89	55.85	102.5	1936.299	161.3582
2003	1117.6	111.05	57.35	111.17	2537.65	881.26	392.5	405.25	414.81	178.16	51.55	24.37	6282.72	523.56
2004	106.6	13.18	8.35	175.78	604.14	108	89.09	235.8	178.96	133.43	321	24.55	1998.88	166.5733
2005	17.13	15.25	6.77	37.82	86.07	84.54	105.85	422.28	438.4	151.13	612	10.41	1987.65	165.6375
2006	4.28	31.32	308.66	964.41	693.05	265.85	521.26	608.51	139.17	55.59	56.48	582.71	4231.29	352.6075
2007	205.56	528.35	158.16	354.85	472.77	656.69	314.83	908.76	722.93	294.99	189.41	89.04	4896.34	408.0283
2008	49.68	34.81	46.2	169.57	230.98	282.24	210.27	11.56	354.23	406.62	368.83	156.17	2321.16	193.43
2009	98.67	74.11	41.67	89.38	217.38	126.61	3.98	121.42	124.83	137.48	131.68	159.98	1327.19	110.5992
2010	192.0854	147.3973	138.4135	157.4533	351.0359	204.425	107.125	66.49	239.53	272.05	442.7578	91.0378	2409.801	200.8168
2011	285.5008	220.6845	235.157	225.5266	484.6917	641.908	839.391	1779.347	1044.29	888.074	753.8355	1565.59	8964	746.9997
2012	143.8	784.8639	1682.029	2262.26	581.68	806.54	571.66	492.2	849.08	504.1	742.68	610.78	10031.67	835.9727
2013	115.07	165.79	978.6324	1979.29	1630.21	865.91	730.7	1516.735	87.1511	546.75	550.68	784.01	9950.9	829.244
2014	1110.355	212.991	1264.789	670.318	553.267	524.55	910.854	1052.871	913.285	1036.071	789.395	866.191	9904.937	825.4114
2015	1097.585	197.82	1264.788	674	543.351	523.0169	902.6186	1023.282	915.3632	1088.969	787.98	822.172	9840.946	820.0788

APPENDIX III: ANNUAL TOTAL FROM SWAT OUTPUT.

PREC - Precipitation, SURQ –Surface flow, LARQ –Lateral flow, GWQ – Ground water, PERCO –Percolation, SW –Surface water, ET – Actual Evapotranspiration, PET Potential Evapotranspiration and, Water Yield is the flow through river channel.

YEAR	PREC	SURQ	LATQ	GWQ	PERCO	SW	ET	PET	WATER YIELD
1983	1013.87	244.06	90.63	91.16	115.28	520.66	452.59	729.6	429.37
1984	959.01	367.49	63.67	46.66	71.7	558.48	447.04	783.32	480.71
1985	991.48	271.77	115.06	133.44	152.67	590.15	479.26	807.51	527.92
1986	910.9	287.42	62.97	53.95	76.36	618.17	380.11	810.48	409.02
1987	960.16	271.92	94.4	95.56	119.49	583.37	470.04	815.54	466.72
1988	1024.28	480.75	73.2	82.04	91.03	543.39	415.49	805.03	642.11
1989	587.44	212.21	25.74	1.62	17.67	476.39	356.39	881.63	241.45
1990	691.81	136.42	43.51	21	38.12	489.56	424.43	823.88	202.54
1991	917.68	289.08	77.6	72.96	95.75	590.83	439.08	777.23	443.75
1992	1014.87	373.03	65.62	55.98	73.08	583.91	429.61	797.15	498.65
1993	823.51	265.12	55.47	39.7	63.27	564.39	414.34	785.92	363.11
1994	836.63	347.82	47.7	28.13	47.98	537.93	452.22	887.36	426.41
1995	1039.94	230.63	13.25	134.53	153.97	555.1	469.94	759.42	484.59
1996	871.16	417.7	80.36	76.71	107.83	510.39	342.32	788.4	579.24
1997	917.71	234.16	84.09	93.14	110.67	540.68	433.49	726.8	418.53
1998	897.83	425.7	53.15	52.22	66.9	522.91	371.97	723.88	534.81
1999	933.43	245.98	78.28	77.63	96.05	556.09	468.24	765.67	406.27
2000	1282.7	470.45	97.49	103.63	126.08	607.82	473.03	773.92	675.91
2001	1099.95	360.09	32.42	165.06	184.48	574.61	455.21	724.7	667.7
2002	1043.62	393.36	5.25	111.66	143.29	551.35	432.92	734.72	617.47
2003	1173.46	388.78	5.31	124.03	138.25	567.07	465.42	816.64	625.13
2004	972.77	302.9	88.61	96.63	113.91	577.37	459.1	741.34	495.02
2005	894.51	399.27	59.93	42.06	68.57	533.65	399.71	809.57	504.86
2006	833.35	224.84	57.3	56.39	64.11	511.19	447.18	791.37	342.49
2007	862.42	314.08	52.6	37.19	57.85	568.63	417	776.38	405.4
2008	899.88	262.3	70.3	56.72	86.59	516.87	402.24	847.1	393.9
2009	963.02	499.75	64.28	70.53	78.34	530.74	398.72	796.8	639.08
2010	1015.09	253.53	84.5	82.95	109.19	614	442.48	708.3	425.73
2011	887.64	253.53	57.87	47.62	63.79	517.77	436.07	807.63	362.73
2012	770.23	283.27	65.73	61.94	80.11	532.14	426.3	786.87	414.99
2013	921.51	231.36	86.95	81.08	109.01	595.15	460.44	790.91	403.95
2014	796.82	243.8	82.54	90.1	103.07	464.86	414.96	899.26	421.77
2015	893.87	275.38	78.2	80.38	100.57	565.33	412.95	760.13	439.57
2016	946.87	399.31	49.28	31.23	50.16	566.36	431.75	852.58	479.37
2017	1055.54	272.49	21.66	138.79	165	552.3	459.92	780.17	543
2018	956.18	258.7	95.09	105.18	122.08	602.88	453.11	761.84	465.84
2019	832.5	331.55	55.36	43.7	65.28	544.9	396.47	842.68	434.66
2020	691.29	210.69	22.6	3.98	8.56	476.72	415.4	840.28	238.77
2021	919.46	338.2	66.9	48.03	76.79	582.68	432.81	833.75	455.84
202	859.7	292.29	61.71	44.79	65.73	585.59	478.98	853.44	401.96
2023	675.33	193.92	24.23	9.41	19.47	438.49	342.65	849.98	229.28
2024	839.87	286.76	49.62	33.72	53.24	560.51	418.48	789.28	372.65
2025	846.09	300.44	84.5	85.61	108.23	551.69	421.94	736.89	475.09
2026	943.78	343.88	67.79	65.11	82.45	559.62	399.01	744.15	481.47
2027	866.21	297.62	68.77	57.13	84.06	567.24	409.68	782.87	426.71
2028	925.18	294.42	80.46	85.61	105.53	563.78	385.5	793.53	465.74
2029	1083.06	312.1	91.86	98.99	115.88	604.98	503.33	826.49	508
2030									

APPENDIX IV: OVERLAY CHANGE STATISTICS

Table 1: Changes in land use and land cover between 1984 and 1995

1984	1995	Area (Ha)	Parcentage
no change	no change	1,136,357.58	79.24390377
Grassland	Shrubland	111,158.55	7.751642259
Shrubland	Grassland	75,124.08	5.238778243
Cropland	Grassland	29,712.69	2.072014644
Cropland	Shrubland	21,354.84	1.489179916
Grassland	Cropland	14,376.78	1.002564854
Shrubland	Forestland	12,104.01	0.844073222
Shrubland	Cropland	8,495.73	0.592449791
Forestland	Shrubland	7,796.07	0.543658996
Cropland	Forestland	3,604.50	0.251359833
Shrubland	Wetland	3,482.91	0.242880753
Grassland	Wetland	2,466.09	0.171972803
Wetland	Shrubland	1,782.45	0.124299163
Forestland	Grassland	1,227.24	0.08558159
Grassland	Forestland	1,226.70	0.085543933
Forestland	Cropland	1,162.62	0.081075314
Wetland	Waterbody	611.73	0.042658996
Bareland	Grassland	307.35	0.021433054
Wetland	Grassland	306.45	0.021370293
Grassland	Bareland	304.29	0.021219665
Grassland	Waterbody	285.57	0.019914226
Shrubland	Waterbody	249.48	0.01739749
Waterbody	Wetland	142.65	0.009947699
Waterbody	Shrubland	54.99	0.003834728
Built up Area	Shrubland	39.87	0.002780335
Waterbody	Grassland	38.07	0.002654812
Shrubland	Bareland	37.80	0.002635983
Built up Area	Grassland	31.14	0.002171548
Waterbody	Forestland	26.01	0.001813808
Cropland	Wetland	23.58	0.001644351
Forestland	Wetland	20.61	0.001437238
Bareland	Shrubland	19.26	0.001343096
Built up Area	Bareland	14.58	0.001016736
Grassland	Built up Area	11.97	0.000834728
Shrubland	Built up Area	10.98	0.00076569
Cropland	Bareland	7.02	0.00048954
Wetland	Forestland	6.12	0.000426778
Wetland	Cropland	5.94	0.000414226
Cropland	Built up Area	5.85	0.00040795
Waterbody	Built up Area	2.16	0.000150628
Waterbody	Bareland	1.53	0.000106695
Wetland	Bareland	1.17	8.159E-05
Built up Area	Cropland	0.99	6.90377E-05
Totals		**1,434,000.00**	**100**

Table 2: Changes in land cover and land use between 1995 and 2003

1995	2003	Area (Ha)	Percentage
No change	No change	1,148,009.27	80.05643476
Shrubland	Grassland	73,654.86	5.136322185
Grassland	Shrubland	70,908.28	4.944789276
Cropland	Grassland	30,807.53	2.148363023
Cropland	Shrubland	28,160.69	1.96378616
Shrubland	Forestland	15,290.52	1.066284427
Wetland	Shrubland	14,352.29	1.000856892
Grassland	Cropland	12,420.12	0.866116863
Wetland	Grassland	9,527.74	0.664416935
Shrubland	Cropland	8,828.85	0.615680098
Forestland	Shrubland	5,552.34	0.387192394
Waterbody	Shrubland	4,862.21	0.33906596
Waterbody	Grassland	4,246.84	0.296153381
Grassland	Forestland	2,232.79	0.155703545
Cropland	Forestland	1,737.60	0.121171286
Shrubland	Wetland	964.49	0.067258743
Wetland	Waterbody	425.71	0.029687188
Waterbody	Wetland	344.20	0.024002813
Grassland	Bareland	305.63	0.021313226
Forestland	Grassland	250.47	0.017466418
Cropland	Built Up Land	182.63	0.012735797
Bareland	Grassland	158.92	0.011082623
Shrubland	Waterbody	139.87	0.009753726
Forestland	Cropland	128.84	0.008984364
Grassland	Waterbody	80.69	0.00562715
Waterbody	Cropland	79.14	0.005519057
Grassland	Wetland	59.36	0.004139293
Wetland	Cropland	57.90	0.004037559
Shrubland	Bareland	54.07	0.003770508
Grassland	Built Up Land	40.21	0.002804037
Waterbody	Forestland	21.52	0.001500573
Built Up Land	Cropland	21.43	0.001494215
Bareland	Shrubland	16.50	0.001150863
Built Up Land	Grassland	12.58	0.000877454
Bareland	Cropland	8.57	0.000597686
Bareland	Built Up Land	6.75	0.000470519
Built Up Land	Waterbody	6.66	0.00046416
Forestland	Waterbody	6.20	0.000432369
Wetland	Forestland	6.11	0.00042601
Waterbody	Built Up Land	5.29	0.000368785
Cropland	Bareland	5.01	0.00034971
Cropland	Wetland	4.38	0.000305201
Shrubland	Built Up Land	3.28	0.000228901
Wetland	Bareland	2.64	0.000184392
Waterbody	Bareland	2.55	0.000178034
Built Up Land	Shrubland	2.10	0.000146242
Built Up Land	Forestland	1.82	0.000127167
Bareland	Forestland	1.64	0.00011445
Forestland	Wetland	0.91	6.35836E-05
Totals		**1,434,000.00**	**100**

Table 3: Changes in land cover and land use between 2003 and 2011

2003	2011	Area (Ha)	Percentage
no change	no change	1,129,930.95	78.79574268
Grassland	Shrubland	65,151.63	4.543349372
Shrubland	Grassland	63,178.47	4.405751046
Cropland	Shrubland	36,122.31	2.51898954
Cropland	Grassland	35,117.10	2.448891213
Shrubland	Cropland	28,065.60	1.957154812
Grassland	Cropland	17,108.28	1.193046025
Shrubland	Wetland	13,517.01	0.942608787
Forestland	Shrubland	12,855.51	0.896479079
Shrubland	Forestland	6,909.66	0.481845188
Grassland	Wetland	4,149.18	0.289343096
Shrubland	Waterbody	4,126.59	0.287767782
Grassland	Waterbody	2,911.95	0.203064854
Cropland	Forestland	2,890.35	0.201558577
Forestland	Grassland	2,725.02	0.190029289
Grassland	Forestland	2,038.86	0.142179916
Wetland	Waterbody	1,882.35	0.13126569
Wetland	Shrubland	1,704.78	0.118882845
Forestland	Cropland	908.82	0.063376569
Bareland	Grassland	367.47	0.025625523
Forestland	Wetland	291.51	0.020328452
Built Up Land	Cropland	283.50	0.019769874
Cropland	Waterbody	281.61	0.019638075
Cropland	Wetland	239.49	0.016700837
Waterbody	Grassland	230.22	0.016054393
Waterbody	Wetland	208.17	0.014516736
Waterbody	Shrubland	180.63	0.012596234
Wetland	Grassland	149.40	0.01041841
Bareland	Cropland	123.57	0.008617155
Grassland	Bareland	91.89	0.00640795
Bareland	Shrubland	82.26	0.005736402
Built Up Land	Grassland	41.85	0.00291841
Waterbody	Cropland	31.95	0.002228033
Cropland	Built Up Land	14.04	0.000979079
Shrubland	Built Up Land	13.95	0.000972803
Built Up Land	Shrubland	11.88	0.000828452
Bareland	Waterbody	9.99	0.000696653
Wetland	Cropland	8.91	0.000621339
Waterbody	Bareland	7.02	0.00048954
Grassland	Built Up Land	6.21	0.000433054
Shrubland	Bareland	5.76	0.000401674
Built Up Land	Waterbody	3.78	0.000263598
Bareland	Built Up Land	3.78	0.000263598
Waterbody	Forestland	3.60	0.000251046
Forestland	Waterbody	2.88	0.000200837
Forestland	Built Up Land	2.88	0.000200837
Waterbody	Built Up Land	2.88	0.000200837
Built Up Land	Bareland	2.61	0.000182008
Wetland	Built Up Land	0.99	6.90377E-05
Forestland	Bareland	0.90	6.27615E-05
Total		**1,434,000.00**	**100**

Table 4: Changes in land cover and land use between 2011 and 2016

2011	2016	Area (Ha)	Percentage
no change	no change	1,169,812.56	81.57688703
Shrubland	Grassland	54,378.72	3.792100418
Grassland	Shrubland	50,865.93	3.547135983
Cropland	Grassland	40,756.68	2.842167364
Cropland	Shrubland	36,729.18	2.561309623
Shrubland	Cropland	22,149.90	1.544623431
Grassland	Cropland	20,107.80	1.402217573
Forestland	Shrubland	7,398.18	0.515912134
Shrubland	Forestland	6,269.49	0.437202929
Wetland	Shrubland	6,033.78	0.42076569
Cropland	Forestland	4,120.20	0.287322176
Shrubland	Wetland	2,845.17	0.19840795
Forestland	Grassland	2,715.84	0.189389121
Wetland	Grassland	2,524.32	0.176033473
Grassland	Forestland	2,471.13	0.172324268
Forestland	Cropland	2,026.35	0.141307531
Waterbody	Shrubland	371.34	0.025895397
Wetland	Forestland	243.09	0.016951883
Grassland	Bareland	206.28	0.014384937
Bareland	Grassland	206.10	0.014372385
Wetland	Waterbody	202.32	0.014108787
Waterbody	Grassland	188.28	0.013129707
Waterbody	Wetland	167.40	0.01167364
Bareland	Shrubland	135.18	0.009426778
Shrubland	Waterbody	125.37	0.008742678
Grassland	Waterbody	109.89	0.00766318
Built Up Land	Cropland	98.64	0.006878661
Built Up Land	Shrubland	85.05	0.005930962
Wetland	Cropland	84.60	0.005899582
Waterbody	Cropland	75.06	0.00523431
Grassland	Wetland	58.95	0.004110879
Cropland	Wetland	52.65	0.003671548
Bareland	Waterbody	48.06	0.003351464
Cropland	Waterbody	36.54	0.002548117
Built Up Land	Grassland	35.37	0.002466527
Cropland	Built Up Land	33.66	0.00234728
Bareland	Cropland	30.24	0.002108787
Forestland	Waterbody	27.81	0.001939331
Shrubland	Bareland	23.85	0.00166318
Waterbody	Forestland	18.09	0.001261506
Bareland	Forestland	17.64	0.001230126
Waterbody	Bareland	17.19	0.001198745
Built Up Land	Bareland	16.02	0.001117155
Cropland	Unclassified	12.87	0.00089749
Unclassified	Grassland	11.97	0.000834728
Cropland	Bareland	10.71	0.000746862
Bareland	Built Up Land	10.44	0.000728033
Unclassified	Cropland	7.83	0.000546025
Shrubland	Unclassified	6.48	0.000451883
Bareland	Wetland	6.12	0.000426778
Shrubland	Built Up Land	5.22	0.000364017
Grassland	Unclassified	3.51	0.00024477
Grassland	Built Up Land	2.70	0.000188285
Unclassified	Forestland	1.26	8.78661E-05
Unclassified	Shrubland	0.99	6.90377E-05
Total		**1,434,000.00**	**100**

APPENDIX V: CHI-SQUARE COMPUTATION

OBSERVED FREQUENCIES						
Land cover	**1984**	**1995**	**2003**	**2011**	**2016**	**Total**
Forestland	104260.95	97959.59	85809.19	97544.07	97414.11	**482987.82**
Shrub land	496599.12	448860.7	417567.8	414826.3	398843.9	**2176697.9**
Grassland	704169.81	728104.1	696560.8	677281.5	648828.3	**3454944.5**
Cropland	99529.74	134840.5	178864.6	210182.9	245872.7	**869290.39**
Wetland	17619.03	13189.24	36225.1	21637.53	28823.4	**117494.3**
Water body	9114.84	8667.93	17390.83	9479.7	10055.16	**54708.46**
Built-up area	407.25	565. 96	379.85	661.14	1249.11	**2697.35**
Bare land	1575.36	1589.94	989.66	1728.27	2149.47	**8032.54**
Total	**1,433,276.10**	**1433212**	**1433788**	**1433341**	**1433236**	**7166683.2**

Expected frequency for any cell = Row total of the cell X Column total of the cell / Grand total

EXPECTED FREQUENCIES						
Land cover	**1984**	**1995**	**2003**	**2011**	**2016**	**Total**
Forestland	96593.48	96589.2	96628	96597.88	96590.79	482999.35
Shrub land	435321.2	435301.7	435476.61	435341	435309.04	2176749.55
Grassland	690959.72	690929	691206.4	690991.17	690940.43	3455026.7
Cropland	173850.74	173843	173912.8	173858.65	173845.9	869311.09
Wetland	23497.87	23496.8	23506.26	23498.94	23497.21	117497.08
Water body	10941.23	10940.7	10945.1	10941.73	10940.92	54709.68
Built-up area	539.45	539.4	539.64	539.47	539.43	2697.39
Bare land	1606.44	1606.4	1607.01	1606.51	1606.4	8032.76
Total	**1433310.13**	**1433246**	**1433821.8**	**1433375.4**	**1433270.1**	**7167023.6**

$$\chi^2 = \frac{(O - E)^2}{E}$$

Where O = Observed frequency and E = Expected frequency

	E	**(O-E)**	**$(O-E)^2$**	**$(O-E)^2/E$**
104261	96593.48	7667.52	58790863	608.6
496599.1	435321.2	61277.9	37554981028	8625.8
704169.8	690959.7	13210.1	174506742	252.6
99529.74	173850.7	-74321	5523611041	31772.2
17619.03	23497.87	-5878.84	34560759.7	1470.8
9114.84	10941.23	-1826.39	3335700.4	304.9
407.25	539.45	-132.2	17476.84	32.4
1575.36	1606.44	-31.08	966	0.6
97959.5	96589.2	1370.3	1877722.09	19.4
448860.7	435301.7	13559	183846481	422.3
728104.1	690929	37175.1	1381988060	2000.2
134840.5	173843	-39002.5	1521195006	8750.4
13189.24	23496.8	-10307.6	106246618	4521.8
8667.93	10940.7	-2272.77	5165483.47	472.1
565.96	539.4	26.56	705.4	1.3
1589.94	1606.4	-16.46	270.9	0.17
85809.19	96628	-10818.8	117046433	1211.3
417567.8	435476.6	-17908.8	320725117	736.5
696560.8	691206.4	5354.4	28669599.4	41.5
178864.6	173912.8	4951.8	24520323.2	141
36225.1	23506.26	12718.84	161768891	6881.9
17390.83	10945.1	6445.73	41547435.2	3796
379.85	539.64	-159.79	25532.84	47.1
989.66	1607.01	-617.35	381121.02	237.2
97544.07	96597.88	946.19	895275.52	9.3
414826.3	435341	-20514.7	420852916	966.7
677281.5	690991.2	-13709.7	187955874	272
210182.9	173858.7	36324.2	1319447506	7589.2
21637.53	23498.94	-1861.41	3464847.19	147.4
9479.7	10941.73	-1462.03	2137531.72	195.4
661.14	539.47	121.67	14803.59	27.4
1728.27	1606.51	121.76	14825.5	9.2
97414.11	96590.79	823.32	677855.82	7.02
398843.9	435309	-36480.7	1330841472	3057.2
648828.3	690940.4	-42112.1	1773428966	2566.7
245872.7	173845.9	72026.8	5187859918	29841.7
28823.4	23497.21	5326.19	28368299.9	1207.3
10055.16	10940.92	-885.76	784570.78	71.7
1249.11	539.43	709.68	503645.7	933.7
2149.47	1606.4	543.07	294925.03	183.6
χ^2				**119433.6**

Degree of freedom = (R-1) X (C-1) = (8-1) X (5-1) = 7X4 = 28

The χ^2 critical value for 28 degrees of freedom at 5 per cent level of significance is 41.34 while calculated value is 119433.6. Since the calculated value is greater than critical, value the null hypothesis that 'land use practices have not significantly changed over the study period in the Mara River Basin' is rejected and the alternative is accepted. Thus, 'land use practices have significantly changed over the study period in the Mara River Basin'.

APPENDIX VI: WATERSHED TOPOGRAPHIC REPORT

(a) Elevation report for the watershed

Summary of the Sub Basins	Height (m)
Max. Elevation	3,056.00
Min. Elevation	1,123.00
Mean. Elevation	1,687.84
Std. Deviation	360.51

(b) Elevation report for all the 27 sub-basins

Sub Basin No.	Minimum Elevation (M)	Maximum Elevation (M)	Mean Elevation (M)	Standard Deviation (M)
1	1972.00	2955.00	2395.01	209.03
2	1972.00	2600.00	2251.20	121.93
3	1689.00	2314.00	1884.37	101.00
4	1689.00	3056.00	2175.04	345.00
5	1525.00	2280.00	1785.15	164.28
6	1525.00	2125.00	1717.53	102.30
7	1502.00	1668.00	1561.26	35.77
8	1494.00	2193.00	1682.27	109.24
9	1621.00	2351.00	1860.61	111.25
10	1123.00	1134.00	1125.87	2.40
11	1154.00	1877.00	1433.14	215.33
12	1621.00	2460.00	1942.31	154.04
13	1472.00	1891.00	1556.57	45.11
14	1375.00	1967.00	1494.72	107.84
15	1140.00	1659.00	1172.79	68.96
16	1436.00	1613.00	1505.95	35.79
17	1154.00	1663.00	1272.86	110.00
18	1375.00	1744.00	1513.31	78.11
19	1140.00	1800.00	1268.79	115.06
20	1198.00	1902.00	1438.03	124.83
21	1123.00	1643.00	1235.62	99.48
22	1436.00	2079.00	1612.32	87.72
23	1849.00	2554.00	2118.96	163.67
24	1198.00	1779.00	1406.88	85.46
25	1849.00	2550.00	2069.84	123.94
26	1472.00	2276.00	1788.89	167.32
27	1675.00	2379.00	2027.89	121.35

Source: SWAT output, 2018

APPENDIX VII: CORRELATION MATRIX

Correlations

		Rainfall	Surface flow	Lateral flow	Ground water	Percolation	Surface Water	Actual Evapotranspiration	Potemtial Evapotranspiratiom	Water yield
Rainfall	Pearson Correlation	1	.534**	.182	.761**	.765**	.654**	.581**	-.447**	.830**
	Sig. (2-tailed)		.000	.221	.000	.000	.000	.000	.002	.000
	N	47	47	47	47	47	47	47	47	47
Surface flow	Pearson Correlation	.534**	1	.027	.172	.174	.267	-.073	-.118	.822**
	Sig. (2-tailed)	.000		.857	.249	.241	.070	.627	.430	.000
	N	47	47	47	47	47	47	47	47	47
Lateral flow	Pearson Correlation	.182	.027	1	.181	.200	.400**	.216	-.173	.130
	Sig. (2-tailed)	.221	.857		.222	.177	.005	.145	.245	.383
	N	47	47	47	47	47	47	47	47	47
Ground water	Pearson Correlation	.761**	.172	.181	1	.987**	.444**	.535**	-.501**	.701**
	Sig. (2-tailed)	.000	.249	.222		.000	.002	.000	.000	.000
	N	47	47	47	47	47	47	47	47	47
Percolation	Pearson Correlation	.765**	.174	.200	.987**	1	.491**	.523**	-.514**	.701**
	Sig. (2-tailed)	.000	.241	.177	.000		.000	.000	.000	.000
	N	47	47	47	47	47	47	47	47	47
Surface Water	Pearson Correlation	.654**	.267	.400**	.444**	.491**	1	.549**	-.380**	.465**
	Sig. (2-tailed)	.000	.070	.005	.002	.000		.000	.008	.001
	N	47	47	47	47	47	47	47	47	47
Actual Evapotranspiration	Pearson Correlation	.581**	-.073	.216	.535**	.523**	.549**	1	-.158	.265
	Sig. (2-tailed)	.000	.627	.145	.000	.000	.000		.289	.072
	N	47	47	47	47	47	47	47	47	47
Potemtial Evapotranspiratiom	Pearson Correlation	-.447**	-.118	-.173	-.501**	-.514**	-.380**	-.158	1	-.373**
	Sig. (2-tailed)	.002	.430	.245	.000	.000	.008	.289		.010
	N	47	47	47	47	47	47	47	47	47
Water yield	Pearson Correlation	.830**	.822**	.130	.701**	.701**	.465**	.265	-.373**	1
	Sig. (2-tailed)	.000	.000	.383	.000	.000	.001	.072	.010	
	N	47	47	47	47	47	47	47	47	47

**. Correlation is significant at the 0.01 level (2-tailed).